UNIVERSITÀ DEGLI STUDI DELL'AQUILA

Department of Civil, Construction and Environmental Engineering

DOCTORAL THESIS

The seismic behaviour of Cross-Laminated Timber buildings: Evaluation of the behaviour factor for the revision of the Eurocode 8

Ph.D Course in Civil, Construction and Environmental Engineering

XXXIII° cycle

Candidate

Vincenzo Rinaldi

SSD

ICAR/09

Course Coordinator

Prof. Marcello Di Risio

Thesis Tutor

Prof. Massimo Fragiacomo

The seismic behaviour of Cross-Laminated Timber buildings: Evaluation of the behaviour factor for the revision of the Eurocode 8

Vincenzo Rinaldi

Prof. Massimo Fragiacomo

Reviewers:

Prof. Dr. Werner Seim *University of Kassel*
Assist. Prof. Dr. Iztok Ŝuŝterŝiĉ *InnoRenew CoE*

The seismic behaviour of Cross-Laminated Timber buildings: Evaluation of the behaviour factor for the revision of the Eurocode 8

Vincenzo Rinaldi
Candidate ID number: 255368

Department of Civil, Construction and Environmental Engineering- DICEAA
University of L'Aquila

Version: 10^{th} June 2021

Website: http://www.diceaa.univaq.it

When you spend time to do something that could save human lives,
you will understand that everything went well.

[Blank page]

Acknowledgements

At the end of my research period as a PhD student, several moments have flown away quickly by me. These three years have been rich in contents for a human and a professional growth.

First of all, I would like to express my sincere gratitude to my tutor, Massimo Fragiacomo, for providing his invaluable guidance and professionalism in all fields and for supporting me. I thank all the research team and all collaborators as Maurizio Follesa, Giovanni Rinaldin, Grabriele Tamagnone and Martina Sciomenta for their time and support. Special thanks go to Igor Gavrić for his valuable experience shared with me. I would thanks also his colleagues from the InnoRenew research institute, who kindly hosted me and allowed me to understand the passion of research. Many thanks to Daniele Casagrande for his scientific and human advice which I have fixed in my mind. Additional thanks are for the reviewers for their valuable comments and suggestions.

Last but not least, I would like to thank my family for the received support: parents, grandparents, sister and her husband with their lovely baby. I thank my friends, especially those who, despite the distance, had the desire to be in touch anytime. Special thank to my darling girlfriend Catia, daily witness and indirect protagonist.

Abstract

Over the last 15 years, the wood-based structural industry has achieved general growth around the world. This positive trend is due to many reasons: the awareness of the importance of sustainable development and the high structural performance of timber structures in seismic-prone areas. Several researches were conducted in these years, leading to a deeper knowledge of seismic timber design. In particular, the Cross-Laminated Timber (CLT) system was widely investigated, becoming a competitive choice in seismic areas compared to other structural materials. Starting from 2015, the revision process of the overall structural Eurocodes is leading to a significant change even in the section dedicated to timber buildings' seismic behaviour.

The aim of this thesis is to evaluate and to propose the behaviour factors of CLT structures designed with dissipative behaviours for the revision of EN 1998:2004 (Eurocode 8). The work combines the review process of Eurocode 8 and of EN 12512. The two norms are linked since Eurocode 8 defines the demand whereas the EN 12512 describes the metodology to estimate the capacity of dissipative joints. The results, which came from ongoing studies, have been obtained using the Eurocode 8 version-prEN 1998-1-2:2020 (EC8 draft) dated 30/04/2020.

The motivations of a new estimation of the q-factor for CLT buildings are highlighted within a critical review of the current Eurocode 8. In specific, the behaviour factor will be divided into three contributions due to the new material independent formulation, and new seismic design rules will be introduced in the EN 1998 for CLT buildings. The definition of the intrinsic q-factor component has been carried out via numerical investigations based on experimental results on traditional CLT connections analysed with the EN 12512 draft. A significant amount of analysis has been done to define the conservative values. At the beginning, static non-linear analyses have been performed on several 2D configurations, and subsequentially, dynamic non-linear analyses have been done on some of the previous configurations. The obtained outcomes propose conservative values of the q-factors for the moderate and high ductility classes. Moreover, a new finite element (FE) strategy has been developed, starting from a state-of-the-art for practice-oriented purpose. The FE model allows integrating into a linear-elastic model the non-linearities of the seismic behaviour of CLT buildings, often neglected.

Keywords: Eurocode 8, Cross-Laminated Timber, Seismic Desing, EN 12512, CLT connections, Linear-Elastic Design, Non-Linear static analysis, Non-Linear dynamic analysis, IDA, CLT buildings Modelling, behaviour

factor

Sommario

Negli ultimi 15 anni, l'industria delle costruzioni in legno ha avuto una crescita generale in tutto il mondo. Molte sono le ragioni associate a questa tendenza positiva: la consapevolezza dell'importanza dello sviluppo sostenibile e le elevate prestazioni strutturali degli edifici in legno in zona sismica. Molte ricerche intraprese negli ultimi anni hanno portato ad una maggiore conoscenza nella progettazione sismica delle strutture in legno. In particolare, il sistema a pannelli in legno lamellare a strati incrociati (CLT o X-Lam) è stato oggetto di studio approfondito, diventando una valida e competitiva alternativa ad altri materiali da costruzione. Nel 2015 è iniziato il processo di revisione degli Eurocodici strutturali che porterà modifiche significative soprattutto nel campo della progettazione sismica degli edifici in legno.

Il presente lavoro mira a valutare e proporre il fattore di comportamento di strutture in CLT progettate in campo dissipativo per la revisione dell'EN 1998:2004 (Eurocode 8). Il lavoro combina il processo di revisione dell' Eurocodice 8 e quello dell' EN 12512. Le due norme sono strettamente collegate dal momento che l'Eurocodice 8 definisce la domanda mentre l'EN 12512 descrive la metodologia per la valutazione della capacità delle connessioni dissipative. I risultati fanno parte di studi ancora in corso ottenuti utilizzando l'Eurocodice 8 versione-prEN 1998-1-2:2020 (bozza EC8) datata 30/04/2020.

Le motivazioni di una nuova stima del fattore di comportamento per gli edifici in CLT sono evidenziate tramite una revisione critica dell'attuale Eurocodice 8. In particolare, il fattore di comportamento sarà suddiviso nel prodotto di tre contributi secondo una nuova formulazione valida per tutti i materiali, e nuove regole di progettazione sismica per strutture in CLT saranno riportate nella EN 1998. Numerose analisi sono state eseguite per definire dei valori conservativi. All'inizio, sono state condotte delle analisi statiche non-lineari su svariate configurazioni 2D, e successivamente, delle analisi dinamiche non-lineari su alcune configurazioni. I risultati ottenuti hanno permesso di valutare dei valori conservativi del fattore di struttura per le classi di duttilità media e alta. Inoltre, una nuova strategia di modellazione agli elementi finiti (FE) è stata sviluppata partendo dallo stato dell'arte con lo scopo di fornire uno strumento di analisi ai professionisti. Il modello FE proposto permette di integrare all'interno di un modello lineare elastico le non-linearità del comportamento sismico di strutture in CLT, spesso trascurate.

Parole chiave: Eurocodice 8, Pannelli in Legno lamellare a strati

incrociati, Progettazione sismica, EN 12512, Connessioni per X-Lam, Progettazione elastica-lineare, Analisi statica non-lineare, Analisi dinamica non-lineare, IDA, Modellazione edifici in CLT, Fattore di comportamento

Table of contents

List of Figures

List of Tables

[Blank page]

Introduction and aims of the research

Chapter abstract

The introduction chapter shows the research activities carried out during the PhD program. The entire research deals with the seismic behaviour of Cross-Laminated Timber (CLT) structure for the revision process of the Eurocode 8 (EN 1998). The results are part of ongoing work with the aim of proposing design values for CLT structures. Three aspects are studied in details: the applications of the last draft of the European standard for cyclic tests of timber joints (EN 12512), the development of a linear-elastic FE strategy and the estimation of the q-factors for the revision of the Eurocode 8 (EN 1998).

1.1 Aims of the research

The wooden construction industry is in continue growing across Europe. The use of timber structures is becoming a valid alternative for strategic buildings such as schools and government offices due to the high seismic performance achievable by different timber-based structural systems.

However, the available European seismic code, Eurocode 8 (EN 1998:2004), provide few and interpretive requirements used by practitioners for seismic design. The current edition, enacted in 2004, needs a significant revision since the scientific and the products knowledge had a rapid and radical growth more than the other structural materials.

The thesis is focused on the seismic behaviour of Cross-Laminated-Timber (CLT) structures with the aims of:

- Apply the EN 12512 draft in combination with EN 1998 draft;
- Develop a linear-elastic finite-element model strategy to improve the existing approaches;
- Estimate the behaviour factors for revising the Eurocode 8 for the two ductile classes designed in moderate (DC2) and high (DC3) respecting new design rules.

1.2 Methodology and structure of the work

The reported work derives from several modifications carried out during the PhD program accompanied by various ongoing drafts for the revision of EN 12512 and EN 1998. The revisions are still in process, and changes are certainly possible. A research period was attained at the Institute InnoRenew CoE (SL) between 01/10/2019-1/01/2020 to continue the studies with Dr. Igor Gavrić.
The thesis is composed of four main chapters, excluding the introduction and the conclusions, described below.

The second chapter introduces the Eurocodes and their organisation. The Eurocode 8 (EN 1998:2004), and specifically the current section related to timber structures, is analysed. Without providing a fully detailed description, a critical review shows the current limits for the seismic design (often left to user interpretation).
The table of contents of the last draf of the prEN 1998-1-2:2020 (30/04/2020) is shown with the future main novelties. A description of Cross-Laminated timber structures' seismic design is provided at the end of the chapter with the motivations for a new estimation of the q-factor.

The third chapter is focused on the non-linear behaviour of the typical mechanical joints for CLT structures. After an initial overview of the available methods to estimate the yield displacement and the cycle loading protocols, the limits of the European Standard document (EN 12512:2001) for its use together with the current EN 1998:2004 (Eurocode 8) are reported. The chapter describes a proposed revision of the EN 12512 for ensuring a unique interpretation of the two future norms (now ambiguous).
The new methodology is applied to the experimental test collected by Gavrić to find the design values of CLT connections used to estimate the q-factor contributions.
An extensive section is dedicated to the numerical modelling and calibration for non-linear static and non-linear dynamic analyses.

The fourth chapter is dedicated to the modelling strategies available for CLT structures for object-oriented approach. The developed FE strategy implemented is based on the upgrade of existing work to include the non-linear behaviour provided by the presence of the vertical loads and the non-linear behaviour of the hold-downs into a linear elastic model. Analytical equations are implemented to calibrate the FE material properties based on 2D area elements to capture all deformation mechanisms of a CLT shearwall. The proposed model is validated on full-scaled experimental walls, and the improvement demonstrated within a numerical comparison. The chapter supports the more refined non-linear analysis carried out in the next chapter since the shearwalls' kinematics made in single- or multi-panels CLT wall are widely discussed.

The fifth chapter aims to estimate the q-factors for CLT structures designed in moderate (DC2) and high (DC3) ductility classes following the new material independent formulation for the revision Eurocode 8. The methodology and the approach implemented to estimate the q-factor contributions are based on attaining the limit states at the connections level. Once the non-linear finite element models validation using full-scale wall tests, a parametric non-linear static analysis (pushover) is carried out on several 2D configurations to investigate various scenarios proposing unique conservative values for both classes.
Afterwards, an addition parametric analysis is performed by varying the ductility of the connections to find the minimum ductility at the connections level to ensure the proposed q-factors.
Finally, the performance on some CLT configurations is verified through incremental dynamic analyses to check the safety in probabilistic terms, to estimate inter-storey drift limits, and to build CLT structures' fragility curves.

The concluding chapter summarizes the overall outcomes obtained in the following work providing an outlook for future researches.

[Blank page]

The structural Eurocodes

Chapter abstract

The following chapter explains the structure of the current structural Eurocodes, focusing on *Eurocode 8: Design of structures for earthquake resistance* (EN 1998).
The seismic requirements for timber buildings are reported in Part 1 (EN 1998-1), and six pages are dedicated to the seismic design of all structural system. After a critical review of the current edition (EN 1998-1:2004), the new draft table of contents is presented (prEN 1998-1-2:2020, dated 30/04/2020), showing the main features of the future thirty-six pages.
A dedicated section shows the seismic design of the Cross-Laminated Timber (CLT) system following the new draft rules. Lastly, the motivations for a new estimation of the behaviour factors are introduced.

2.1 Overview of structural Eurocodes

The Eurocodes (ECs) are the European standards for structural design. ECs define the general reference of the current national legislation and allow the professional to use standard calculation criteria that can also be adopted abroad.

These standards, in addition to providing specifications for the structural design of works made with various materials (reinforced concrete, steel, masonry, wood, aluminium), deal with the geotechnical aspects of the design, the resistance of the structures to the fire and seismic actions and finally actions on the structures in the execution phase on temporary structures.

The Eurocodes were developed by the European Committee for Standardisation upon the European Commission's request to provide a common approach to structural design that uniforms the safety level of buildings in Europe.

Each of the Eurocodes consists of a general part (EN), the same for all European states and a National Annex (NAD), which varies from one European state to another, which contains the parameter values (NDP) that are set by the national authorities in function of the specificities of each state.

By 2002, ten sections have been developed and published:

- Eurocode 0: Basis of structural design (EN 1990); It provides the basic indications to design with the semiprobabilistic method at limit states, the combinations, the safety factors to use in combinations of actions;
- Eurocode 1: Actions on structures (EN 1991); It gaves the information necessary to determine the calculation actions on the structures from the various types of loads (snow, wind, thermal loads deriving from a fire, ecc);
- Eurocode 2: Design of concrete structures (EN 1992);
- Eurocode 3: Design of steel structures (EN 1993);
- Eurocode 4: Design of composite steel and concrete structures (EN 1994);

- Eurocode 5: Design of timber structures (EN 1995);
- Eurocode 6: Design of masonry structures (EN 1996);
- Eurocode 7: Geotechnical design (EN 1997);
- Eurocode 8: Design of structures for earthquake resistance (EN 1998);
- Eurocode 9: Design of aluminium structures (EN 1999).

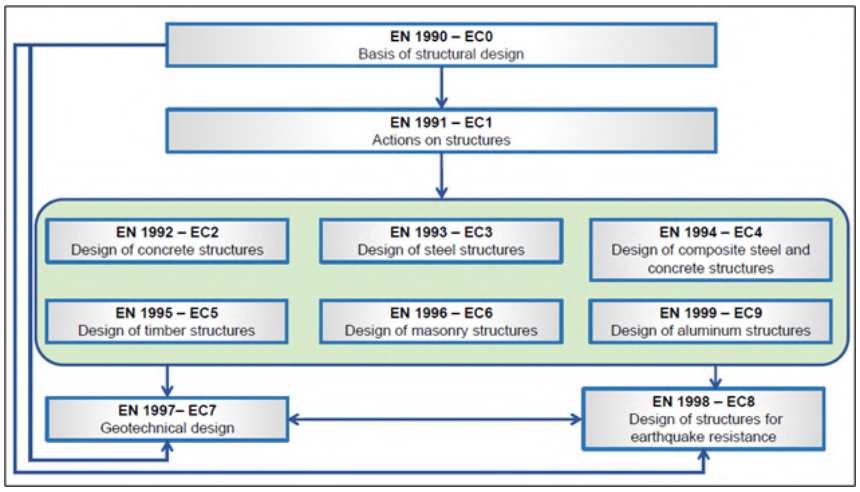

Figure 2.1. Organisation and interdependencies between the different European Codes.

2.2 Eurocode 8 (EN 1998)

Eurocode 8: Design of structures for earthquake resistance (abbreviated EN 1998 or, informally, EC8) contains all the seismic regulations, both for buildings and other civil engineering works, except special works such as nuclear power plants, offshore structures, and large dams. It connects to the other Eurocodes that treat the same works in the static field in a complementary way. It deals with timber buildings too. It is structured in parts:

- Part 1: General rules, seismic actions and rules for buildings;
- Part 2: Bridges;
- Part 3: Assessment and retrofitting of buildings;
- Part 4: Silos, tanks and pipelines;
- Part 5: Foundations, retaining structures and geotechnical aspects;
- Part 6: Towers, masts, and chimneys.

In particular, the Part 1 (EN 1998-1) establishes the necessary performance requirements applicable to buildings and civil engineering works in seismic areas and provides rules for the representation of seismic actions and their combination with other actions, with the aim of ensuring that in the event of an earthquake human lives are protected, the damage is limited. The main civil protection structures remain in operation. It is divided into 10 sections:

- Section 1 of EN 1998-1 contains the scope, normative references, assumptions, principles and application rules, terms and definitions, symbols and units;
- Section 2 of EN 1998-1 contains the basic performance requirements and compliance criteria applicable to buildings and civil engineering works in seismic regions;
- Section 3 of EN 1998-1 gives the rules for the representation of seismic actions and for their combination with other actions. Certain types of structures, dealt with in EN 1998-2 to EN 1998-6, need complementing rules which are given in those Parts;

- Section 4 of EN 1998-1 contains general design rules relevant specifically to buildings;
- Section 5: Specific rules for concrete buildings;
- Section 6: Specific rules for steel buildings;
- Section 7: Specific rules for composite steel-concrete buildings;
- Section 8: Specific rules for timber buildings;
- Section 9: Specific rules for masonry buildings;
- Section 10 contains the fundamental requirements and other relevant aspects of design and safety related to base isolation of structures and specifically to base isolation of buildings.

2.2.1 Section 8: Specific rules for timber buildings

Three different editions of the timber section have been released over the years (Follesa et al., 2018):

First release – 1988

It was based on Ceccotti and Lansen studies' and talks about the general principals of seismic design of timber structures. It deals with:

- General criteria;
- Materials;
- Structural types and ductility classes: Three ductility classes (non-dissipative, low dissipation and medium dissipation) and some types of structures were defined;
- Behaviour factors q: EC proposed a conservative value of q equal to 1.0 for three Ductility classes and each types of structures;
- Safety verifications, limits, suggestions of the values to adopt for the k_{mod} factor.

Second release – 1995

It represented a substantial improvement on the previous edition. In particular, the principal changes included:

- The introduction of new paragraphs and improvement of existing ones;
- The passage from 3 ductility classes to 4 with the new high ductility class;
- The introduction of structural solutions supported by graphic representations;
- Modification of behaviour factors q (equal between 1 and 3 according to ductility class);
- Limitation to the use of the behaviour factor provided in tabular form only for those dissipative zones that deformates plastically for at least three completely inverted cycles with a static ductility ratio of 4 for structures in the medium ductility class and 6 for those of high ductility without a reduction of more than 20% of their resistance;
- introduction of prescriptive ductility rules for dissipative zones, based on the diameter of the connections and the thickness of timber elements.

Last release – 2004 (current edition)

The most important innovations introduced were:

- Reduction in the number of structural systems;
- Introduction of some structural systems for timber roofs such as trusses;
- Decrease of ductility classes from 4 to 3;
- Introduction of different values of the behaviour factor ranging from 1.5 to 5;
- Elimination of graphic representations of the different structural systems;
- Modification of the partial safety coefficient values for the fundamental and accidental load combinations at the ultimate limit state in the case of dissipative and non-dissipative behaviour.

2.2.1.1 Review of the current edition EN 1998:2004

An extensive and complete overview of the current edition was led by Follesa ((Follesa et al., 2018), (Follesa, 2018)).

Currently, EN 1998-1-1:2004 Section 8 is the part dedicated to the seismic

design of timber buildings, and six pages compose it. The limitations are related to the doubts for the application of the Performance-Based Desing (PBD) (Ghobarah, 2001) for timber structures when Force-Based Design (FBD) is adopted. In specific:

- Unclear definition of the structural systems;
- Absence of a specific definition of the dissipative/brittle components;
- Absence of specific capacity desing rules;
- Absence of specific overstrength factors.

The structural systems are not clearly described (e.g. lack of explanatory drawings), there is not a clear reference to some structural systems such as the CLT (X-Lam) and Log House systems, the dissipative and non-dissipative zones are not unequivocally identified for each structural system, the capacity design rules for the hierarchy of resistances are not specified, and the overstrength factors are not present. Those aspects lead to an intepretation of the few rules.

2.3 The revision of Eurocode 8

2.3.1 General information

The revision process of the Eurocodes, and therefore of the Eurocode 8 (EC8), started in 2015 with the establishment of CEN (European Committee for Standardization) and will lead to a general modification of different sections. All information provided is valid until 1/01/21; changes are not excluded.

The prEN 1998:2020 will be divided into two parts: prEN 1998-1-1:2020 and prEN 1998-1-2:2020.
The prEN 1998-1-1:2020 (prEC8-1-1) ("Design of structures for earthquake resistance - Part 1-1: General rules and seismic action") contains general requirements for all types of structures for earthquake resistant design, including definition of the seismic action and the description of the methods of analysis and verification.
The prEN 1998-1-2:2020 (prEC8-1-2) ("Design of structures for earthquake resistance - Part 1-2: Rules for new buildings") defines the seismic rules for new buildings and temporary structures in seismic regions.

2.3.2 Behaviour factor according to prEN 1998-1-1:2020

The prEC8-1-1 provides a new definition of the q-factor valid for all structural material and based on the product of three components:

$$q = q_S \cdot q_R \cdot q_D \tag{2.1}$$

The behaviour factor is given by the product of the component that takes into account the overstrength introduced in the design q_S, the component that takes into account the overstrength due to the redistribution of the seismic action in redundant structures q_R and the component that consider the dissipative capacity q_D. Since q_S is fixed for all materials (material independent) and set to 1.5, the remaining components will define the basic values for the behaviour factor for all structural systems, in turn,

divided into three ductility classes: ductility class 1 (DC1, low-dissipative behaviour) where the factor q is equal to 1.5, ductility class 2 (DC2, moderate-dissipative behaviour) and ductility class 3 (DC3, high-dissipative behaviour).

A detailed description of the q-factor is reported in the dedicated chapter to estimate the q-factor for CLT buildings.

2.3.3 Overview of the Timber section

The modifications, led by the EC8 revision, will be mostly significative for the part dedicated to Timber structures since the scientific seismic improvement in the last years was higher than the other materials.
The CEN/TC250/SC8/WG3 "Timber" is the subgroup of the CEN/TC250/SC8 commissioned in the revision of the Eurocode 8 dedicated to the timber structures.
Section 13 will be dedicated to timber structures reported in prEC8-1-2 (unless changes). The current table of contents reports the following topics:

CHAPTER 13-SPECIFIC RULES FOR TIMBER BUILDINGS

1. Scope
2. Basis of design
    - Design concepts
    - Safety verifications
3. Materials
    - Mechanical properties of dissipative zones
    - Material properties
4. Structural types, behaviour factors, capacity design rules and limits of seismic action
    - Structural types
    - Behaviour factors
    - Capacity design rules common to all dissipative structural types
    - Limits of seismic action for design to DC1

5. Structural analysis
6. Verification of limit states
    - General
    - Limitation of interstorey drift at Significant Damage limit state
    - Non-linear static analysis
7. Rules for cross laminated timber structures
    - General rules
    - Design rules for DC2
    - Design rules for DC3
    - Detailing rules
8. Rules for light-frame structures
    - General rules
    - Design rules for DC2
    - Design rules for DC3
    - Detailing rules
9. Rules for log structures
    - General Rules
    - Design rules for DC2
    - Detailing rules
10. Rules for moment-resisting frames
    - General rules
    - Rules for DC2
    - Rules for DC3
    - Detailing rules
11. Rules for braced frame structures with dowel-type connections
    - General rules
    - Rules for DC2
    - Detailing rules

12. Rules for vertical cantilever structures
    - General rules
    - Design rules for DC2
    - Detailing rules
13. Rules for braced frame structures with carpentry connections and masonry infill
    - General rules
    - Design rules for DC2
    - Detailing rules
14. Rules for braced frame structures with carpentry connections
    - General rules
    - Detailing rules
15. Floor and roof diaphragms
    - General rules
    - Cross laminated timber floor and roof diaphragms
    - Light-frame floor and roof diaphragms
    - Timber-concrete composite floor and roof diaphragms
16. Transfer level. Design for DC2 and DC3
17. Checking of design and construction
18. – Annex L

The main novelties respecting the current EN 1998-1:2004 are:

- Variations in the general definitions and in design concepts;
- Update of the list of wood based materials and properties;
- Structural types definition with graphical descriptions;
- Dedicated chapters for each structural archetypes (e.g. CLT, light-frame, log structures, moment-resisting frames, braced frame structures, vertical cantilever structures);
- Re-definition of the ductility classes (DC1, non dissipative, DC2, moderate ductility and DC3, high ductility versus the current DCL, DCM and DCH);

- Definition of the behaviour factors specific for the structural archetypes and ductility class;
- New rules for the capacity design specific for the structural archetypes and ductility class;
- Definition of structural details;
- Definition of the dissipative and non-dissipative zones;
- Definition of the minimum ductility capacity of the dissipative zones;
- Definition of the overstrength factors;
- Prevision for the application of the non-linear static analysis.

As observable, the updating of the EN 1998 is substantial, passing from the current six to around thirty-six pages.

2.3.4 CLT buildings according to prEN 1998-1-2:2020

The seismic behaviour of Cross-laminated timber (CLT) buildings is the main topic of the work. This section introduces the technology and the design according to the prEN 1998-1-2:2020 (dated 30/04/2020).

2.3.4.1 CLT buildings: general information

CLT buildings are structures made of cross-laminated timber panels used as a primary shearwall system.

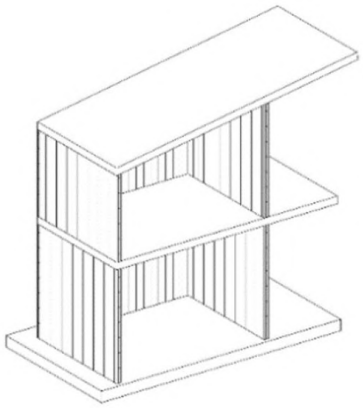

Figure 2.2. Cross laminated timber structures (from prEC8-1-2 "Structural types").

The CLT panels (Brandner et al., 2016) are made of boards placed side-by-side and arranged crosswise to each other at an angle of 90° and both used for walls and floors. CLT structures have a "box system" behaviour with a sufficient degree of hyperstaticity thanks to the mechanical connections used to connect panel-to-panel and panel-to-foundation.

Figures 2.3 show a typical CLT assembly, panels and connections, for single-panel (a) and multi-panel (b) structures. The design of innovative systems such as the "Pres-Lam" (Granello et al., 2020) are not reported.

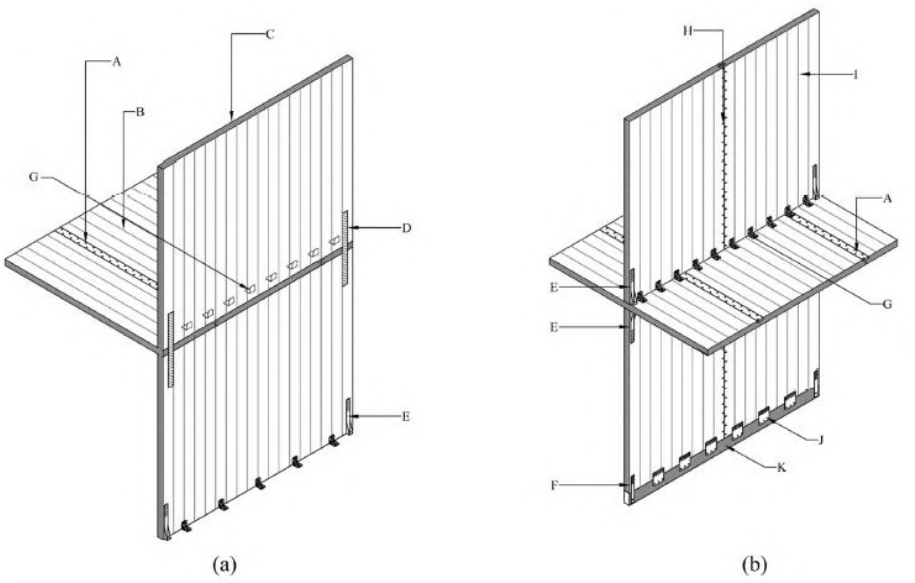

Key

A	Horizontal joint between cross laminated timber floor panels.
B	Cross laminated timber floor panel.
C	Single piece cross laminated timber wall panel.
D	Tie-down.
E	Hold-down.
F	Foundation tie-down.
G	Angle bracket.
H	Vertical cross laminated timber panel-to-cross laminated timber panel joint.
I	Cross laminated timber wall panel.
J	Shear plate.
K	Concrete base beam connected to the foundation and waterproof layer.

Figure 2.3. Exterior, single-panel (a) and interior, multi-panel (b) walls and floors in cross laminated timber structures (from prEC8-1-2 "General rules").

2.3.4.2 Seismic design of CLT buildings

The following section describes the seismic design of CLT buildings following the prEC8-1-2. Three ductility classes are available according to prEC8-1-2:

- Low-dissipative structural behaviour (DC1);
- Moderate-dissipative structural behaviour (DC2);
- High-dissipative structural behaviour (DC3).

The adoption of the ductility class is a choice of the engineer; however, the use of DC1 is limited for areas in which the maximum spectral acceleration Sa is lower than a specific value. The values of Sa_{lim} are reported in "Table 13.2" of prEC8-1-2 depending on the structural type. Currently for CLT Sa_{lim} is set to 4.0 m/sec^2.

Different design rules are provided based on the ductility class. As a general design concept, the DC1 class omits all capacity design rules at the local and global level simplifying the design process. DC2 and DC3 introduce the capacity design at the local and local/global levels, respectively.

For dissipative structures, the capacity design approach required that the strength and the ductility capacities be monitored simultaneously. For the sake of simplicity i) the design formulations and ii) the minimum ductility of the connections are briefly summarized and later recalled in the specific subsections.

i) Strength

The strength of the dissipative connections are assessing with:

$$F_{Rd,d} = k_{deg} k_{mod} \frac{F_{Rk,d}}{\gamma_M} \tag{2.2}$$

where:

$F_{Rd,d}$ is the design value of the strength of the dissipative zones;
k_{deg} is the strength reduction factor due to degradation under cyclic loading;
k_{mod} is the modification factor for duration of load and moisture content;
$F_{Rk,d}$ is the characteristic value of the strength of the dissipative zones;
γ_M is the material partial factor for accidental design situations.

The design strength of the non-dissipative components of DC2 and DC3 design and of all members of DC1 design should be calculated as:

$$F_{Rd,b} = k_{mod} \frac{F_{Rk,b}}{\gamma_M} \tag{2.3}$$

where:

$F_{Rd,b}$ is the design value of the strength of the non-dissipative components;

$F_{Rk,b}$ is the characteristic value of the strength of the non-dissipative components;

γ_M is the material partial factor for accidental design situations.

Meanwhile, non-dissipative connections or brittle components should be over-designed with the overstrength factor γ_{Rd} in case of a dissipative design approach. Following the capacity design and the hierarchy of resistance at the local level, the brittle part of the connections assembly should respect Equation 2.4 in which the γ_{Rd} is the overstrength factor:

$$\frac{\gamma_{Rd}}{k_{deg}} \cdot F_{Rd,d} \leq F_{Rd,b} \tag{2.4}$$

The values of the overstrength factors, reported in Table 2.1, are specific for the kind of failure mode: timber failures, metal plates failures, non-dissipative components at the wall and building level, e.g.

Capacity design at	**Brittle/non-dissipative failure mode**	**Overstrength factor γ_{Rd}**	**Formula No.**
Connection and 2D- or 3D- nailing plate level	Failure of the timber cross-section by shear, fracture in tension, etc. (EN 1995-1-1:2004, 6, and A2:2014), failure by block shear (EN 1995-1-1:2004, Annex A, and A2:2014), failure by plug shear, failure by splitting	1.6	2.4
	Tensile (1993-1-1:2005, 6.2.3) and shear (1993-1-1:2005, 6.2.6) failure of the steel plates (angle brackets, holddowns, tie-downs, etc.), tensile (1993-1-8:2005, 3.6) and pull-through failure of anchor bolts or screws	1.6	2.4
Wall and building level	Failure of the non-dissipative components at the wall and building level for each dissipative structural type, formation of a soft-storey mechanism as opposed to a global failure mechanism	1.6	2.5-2.7-2.8

Table 2.1. Values of the overstrength factors γ_{Rd} to be used in capacity design.

ii) Ductility

The dissipative sub-assembly/joints/2D-3D metal plates and connections should attain a ductility level not smaller than the values in Table 2.2 assessed with the EN 12512. These limits allow to guarantee the q-factor reported in the code[1].

[1] Approach valid for all structural type.

Structural type	Dissipative sub-assembly/joint/2D or 3D-nailing plate/connection	Type of ductility	μ DC2	μ DC3
a) Cross laminated timber structures	Shear wall*	Displacement	1.8	2.7
	Hold-downs, tie-downs, foundation tie-downs, angle brackets, shear plate	Displacement	1.8	1.8
	Screwed wall panel-to-panel joints	Displacement	-	3.5

*The values provided refer to the system ductility of the sub-assembly, taking into account the ductility of all the individual connections and components.

Table 2.2. Minimum required ductility μ as defined in EN 12512 of dissipative zones tested for CLT structures.

DC1: Low-dissipative structural behaviour

The dissipative capacity of the DC1 is limited due to the ineligible plasticity involved. DC1 class leads to adopting the behaviour factor components q_R and q_D equal to 1.0 while q_S is taken equal to 1.5. The design strength of all structural members should be calculated with Equation 2.3. No rules or specific level of ductility of the connections are required. The capacity design at the local level (e.g. metal plate-screws) is not necessary. However, the design strength should be the minimum value of all involved components. The general design should follow:

1. Evaluation the base-shear demand ($q = 1.5$);
2. Distribution of the base-shear demand along all shearwalls;
3. Assessing the demand V_{Ed} and M_{Ed} for each wall;
4. Design all components according to Equation 2.3.

As shown, the design process is straightforward, becoming a favourable choice in region/country with low seismic hazard.

DC2: Moderate-dissipative structural behaviour

The local ductility and the wall panels adopted rule the dissipative capacity of the DC2 class. The q-factor component q_R and q_D are greater than one thanks to the dissipative components which are:

- Shear connections between walls and the floor underneath, and between walls and foundation;
- The anchoring connections against uplift placed at wall ends and at wall openings.

The structural members and joints should be capacity designed, using Equation 2.5, are:

- All CLT wall and floor panels;
- Joints between adjacent floor panels or walls;
- Joints between floors and the supporting walls underneath;
- Joints between orthogonal walls and corners.

$$F_{Rd,b} \geq \frac{\gamma_{Rd}}{k_{deg}} \cdot \Omega_d \cdot F_{Ed,E} + F_{Ed,G} \tag{2.5}$$

where:

$F_{Rd,b}$	is the design strength of the non-dissipative joint or structural element;
γ_{Rd}	is the overstrength factor;
k_{deg}	is the strength reduction factor;
$F_{Ed,E}$	is the action effect in the non-dissipative joint or member due to the design seismic action;
$F_{Ed,G}$	is the action effect in the non-dissipative joint or member due to the non-seismic actions in the design seismic situation;
$\Omega_d = min(\Omega_{d,i})$	is the minimum value of all overstrength storeys ratio.

$$\Omega_{d,i} = min\left(\frac{\sum_{j=1}^{N_i}|V_{Rd,a,i,j}|}{\sum_{j=1}^{N_i}|V_{Ed,E,i,j}|}\,;\,\frac{\sum_{j=1}^{N_i}|M_{Rd,rock,i,j}|}{\sum_{j=1}^{N_i}|M_{Ed,E,i,j}|}\right) \tag{2.6}$$

in which:

$\Omega_{d,i}$ is the overstrength ratio at the ith storey;

$V_{Rd,a,i,j}$ is the design lateral strength related to shear connections of the jth shear-wall at the ith storey;

$M_{Rd,i,j}$ is the design rocking strength of the jth shear-wall at the ith storey including the stabilizing effect of the vertical load;

$V_{Ed,a,i,j}$ is the design global shear of the jth shear-wall at the ith storey due to the seismic action;

$M_{Ed,i,j}$ is the design rocking moment of the jth shear-wall at the ith storey due to the seismic action;

N_i is the number of shear-walls parallel to the seismic action at the ith storey.

The design steps of the entire structure that should be followed are:

1. Evaluation the base-shear demand ($q_{DC2} > 1.5$);
2. Distribution of the base-shear demand along all shearwalls;
3. Assessing the demand V_{Ed} and M_{Ed} for each wall;
4. Design the ductility (dissipative) components according to Equation 2.2 and the brittle components with Equation 2.3
5. Assessing the minimum overstrength ratio Ω_d;
6. Design the non-dissipative components with Equation 2.5.

The design steps demonstrate that the design process introduces the concept of capacity design at the local level (connections), promoting the ductility behaviour. For example, the metal plate's brittle failures and the anchoring system should prevent in shear-joints. On the other hand, the unique Ω_d factor guarantees the development of the ductile mechanisms (sliding and rocking) without remarkably overdesigning the structure.

DC3: High-dissipative structural behaviour

The high-dissipative capacity, in which q_R and q_D are grater than DC2, required that all shearwalls are multi-panel wall (also called segmented). The panels should have a length not smaller than $0.25h$ and greater than h, where h is the inter-storey height. The dissipative connections are:

- Shear connections between walls and the floor underneath, and between walls and foundation (still under discussion);
- The anchoring connections against uplift placed at wall ends and at wall openings;
- Shear connections between two adjacent panel of a wall.

Some considerations should be done regarding the shear connections associated with the sliding mechanism; The development of the primary dissipative mechanism of rocking, given by the plasticity of the vertical joints and the up-lift system, should prevail the sliding one in DC3 class. The reason can be simple explained considering a segmented CLT wall with high aspect ratio L/H and vertical load. Several studies demonstrated that under these conditions, the sliding deformation mechanism predominates the rocking one. In this situation, since the shear ductility of traditional angle-bracket shows a ductility level lower than 2.0, it is impossible to attained higher dissipative capacity. This conclusion leads to the need for overdesign the shear connections with capacity design rules to attain a rocking behaviour (Casagrande et al., 2019). The design theory for multi-panel shearwall follows (Casagrande et al., 2018) in which the uplift behaviour of angle-bracket is neglected. More recently, the same authors (Masroor et al., 2020) included the effect of the uplift behaviour of angle-brackets. However, during this study, it was observed that overdesigning the sliding strength leds to an indirect increasing of the rocking strength. Unless of further innovative shear connections or by using pre-drilled slotted holes in the vertical direction, it is difficult to reduce this phenomenon.

The structural members and joints which should be capacity designed are the same of DC2 class and they should respect Equation 2.5.

The design steps for DC3 structures are similar to the DC2. However, to attain a dissipative rocking mechanism as couple-panel behaviour (CP) (Nolet et al., 2019), the design strength of the anchoring system should respect:

$$F_{Rd,h} \geq \begin{cases} \gamma_{Rd} \cdot F_{Rd,c} \cdot \frac{K_{ser,anc}}{K_{ser,con}} & \text{if } K_{ser,anc} \geq n \cdot K_{ser,con} \\ max\left[\gamma_{Rd} \cdot F_{Rd,c} \cdot \frac{K_{ser,anc}}{K_{ser,con}} \; ; \; \gamma_{Rd} \cdot n_{vy} \cdot F_{Rd,c} - w \cdot b_{CLT}\right] & \text{if } K_{ser,anc} < n \cdot K_{ser,con} \end{cases} \tag{2.7}$$

where:

$F_{Rd,h}$ is the design strength of the anchoring 2D- or 3D-nailing plate against uplift;

γ_{Rd} is the overstrength factor;

$F_{Rd,c}$ is the design strength of the single timber-to-timber connection used in the vertical joint;

$K_{ser,anc}$ is the elastic stiffness of the anchoring 2D- or 3D-nailing plate against uplift;

$K_{ser,con}$ is the elastic stiffness of the single timber-to-timber connection used in the vertical joint;

n_{vy} is the number of fasteners used in the vertical joint;

b_{CLT} is the length of each single panel;

w are the non seismic actions in the seismic design situation per unit length applied on the segmented wall in the seismic design situation.

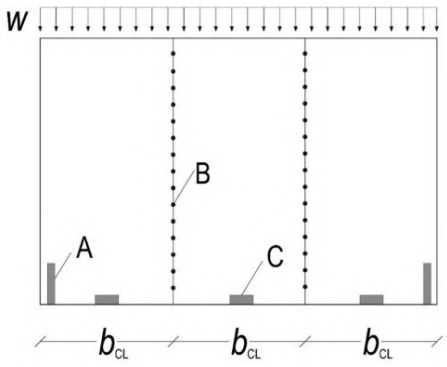

Key

A Anchoring 2D- or 3D-nailing plate against uplift (hold-down, tie-down, foundation tie-down).
B Single fastener connection in vertical joint.
C 2D- or 3D-nailing plate resisting shear (angle-bracket, shear plate).

Figure 2.4. Multi-panel CLT wall (from prEC8-1-2).

while, the design rocking strength $M_{Rd,rock}$ should be calculated as:

$$M_{Rd,rock} = b_{CLT} \cdot \left[F_{Rd,h} + F_{Rd,c} \cdot (m_{lp} - 1) \cdot n_{vy} + \frac{w \cdot m_{lp} \cdot b_{CLT}}{2} \right] \quad (2.8)$$

where:

$M_{Rd,rock}$ is the design rocking strength;

$F_{Rd,h}$ is the design strength of the anchoring 2D- or 3D-nailing plate against uplift;

$F_{Rd,c}$ is the design strength of the single timber-to-timber connection used in the vertical joint;

m_{lp} is the number of cross laminated timber panels in a segmented wall;

n_{vj} is the number of fasteners used in the vertical joint;

b_{CLT} is the length of each single panel;

w are the non seismic actions in the seismic design situation per unit length applied on the segmented wall in the seismic design situation.

An additional condition in terms of strength capacity should be satisfied respecting DC2 class. Equation 2.9 allows guaranteeing that the dissipative behaviour develops simultaneity along with the building height. No soft-storey is allowed.

$$\frac{max\left(\Omega_{d,i}\right)}{\Omega_d} \leq 1.25 \quad (2.9)$$

Following these concepts, the summarized design steps of the DC3 are:

1. Evaluation the base-shear demand ($q_{DC3} > q_{DC2} > 1.5$)
2. Distribution of the base-shear demand along all shearwalls;
3. Assessing the demand M_{Ed} for each wall;
4. Design the dissipative rocking mechanism respecting Equations 2.7 and 2.8;
5. Check and assessing Ω_d (Eq. 2.9);
6. Design the non-dissipative components with Eq. 2.5.

It is evident that an iterative approach is required between points 4 to 6 if

the up-lift strength of non-dissipative components such as the angle-bracket are taken into account in the design.

2.4 Estimation of the q-factor: motivation of the work

The aim of this work is to evaluate the behaviour factor (q-factor) of CLT buildings as a proposal for the revision process of Eurocode 8. The dissipative ductile classes DC2 and DC3 are investigated. The low-dissipative class DC1 is neglect since omits all capacity design concepts at the local and global levels.

Due to the novelties introduced for the new material independent formulation (§2.3.2) and the new seismic design rules for CLT structures (§2.3.4) based on the state-of-knowledge, the future tabulated values of the q-factors should be evaluated respecting both requirements. In fact, the q-factors depend on the design criteria in terms of safety verifications and the implemented capacity design rules.

[Blank page]

Behaviour of typical CLT connections

Chapter abstract

The mechanical characterisation of timber connections is a fundamental aspect of the seismic design of timber structures. Metal connections composed of mechanical fasteners are generally designed to locate ductile and dissipative mechanisms as timber has brittle behaviour. The worldwide standards propose different methodologies for defining the non-linear properties of connections in terms of ductility and energy assessment. In the European landscape, the reference standard for cyclic tests is EN 12512:2001, which is not currently well linked with the European seismic code EN 1998-1:2004 (Eurocode 8).

The following chapter analyses a proposal procedure developed by other authors to revise the EN 12512 in parallel with the update of Eurocode 8 (EC8) by standardising the EC8 requests with EN 12512 methodology for timber joints. The major modifications introduced in EN 12512 are a new methodology to estimate the ductility of connections based on oligo-cyclic degradation and the improvement of load protocol. The procedure was applied to experimental tests for typical Cross-Laminated Timber (CLT) connections to obtain the design parameters used to evaluate CLT's behaviour factor for the EC8 revision. The analysed connections were suddenly modelled through constitutive laws for static and dynamic non-linear finite element analyses.

3.1 Timber joints in seismic design

Timber joints are structural elements used to connect timber elements. The conventional classification of timber joints lists connections as carpentry joint, glued joints and mechanical joint (made with dowel-type fasteners or surface-type fasteners).

The following chapter focuses on the behaviour of traditional mechanical joints for Cross-Laminated Timber (CLT) structures made with dowel-type fasteners. Figure 3.1 shows the typical connections adopted (hold-downs, angle-bracket, self-tapping screws/nails). Generally, they are made with an assembly of cylindric metal fasteners and two/three-dimensional steel plates connected with timber components.

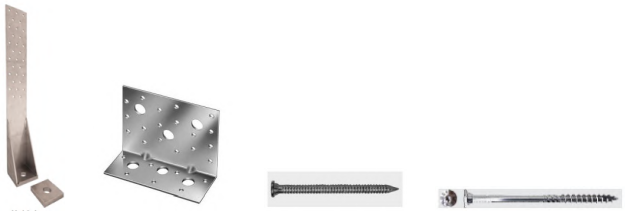

(a) (b) (c) (d)

Figure 3.1. (a) Hold-down, (b) Angle-bracket, (c) anular ringed nail, (d) self-drilling screw.

According to the most advanced worldwide codes, the dissipative concept should be considered in the seismic design following a Performance-Based Design methodology (Ghobarah, 2001). In the Johansen theory (Johansen, 1949), the ductile behaviour of connections made with cylindrical fasteners can be reached respecting geometrical and mechanical parameters[1]. Failures modes which guarantee the timber embedment and the plasticity of the fasteners are preferable due to the more energy dissipated ((Ceccotti et al., 2007), (Piazza et al., 2011)).

The energy and the ductile capacity of joints can be well understood and investigated by looking at its typical hysteretic behaviour (Figure 3.2). Considering a mechanical joint with metal fastners, the hysteretic behaviour shows four phenomena of interest:

[1] Fasteners diameters and length, spacing and distance between fasteners and timber's edges.

1. Impairment of the strength;
2. Reloading/Unloading stiffness degradation;
3. Pinching effect.

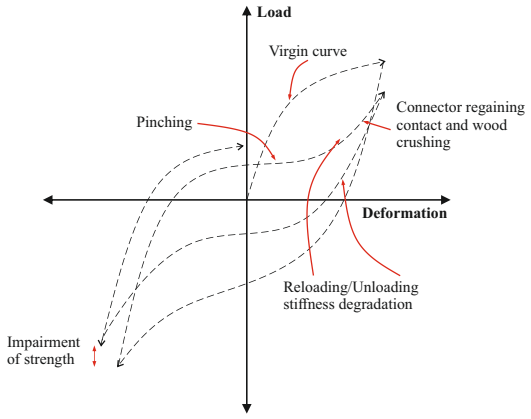

Figure 3.2. Typical hysteretic behaviour of steel-to-timber joint.

The impairment of the strength and re/un-loading degradation are related to the metal fasteners instead of the timber since virgin wood is compressed when the cyclic amplitude increases. The strength and the reloading degradation, generally, depend on the quality of the metal fasteners assuming a rigid metal plate behaviour.

The pinching effect is related to the wood embedment phenomenon in which during the reloading and unloading only the fastener provides a strength contribution.

Through a cyclic test, several aspects can be investigated, providing data useful for the seismic design of timber connections such as the determination of the ductility, the impairment of strength and the energy dissipation capacity.
However, the codes and the scientific community do not provide a unique/recognized cyclic test procedure and method to calculate the parameters of interest. Especially for ductility (a measure of plastic deformation), the debate is ongoing. Even if the definition of the ductility is straightforwards as the ratio between the ultimate δ_u and yield slip amplitude δ_y (Equation 3.1), different methods are available to define δ_y and δ_u.

$$\mu = \frac{\delta_u}{\delta_y} \tag{3.1}$$

A comparison of different Standard methods was led by Muñoz et al. (2008) finding that different methods give spread results for the yielding and the stiffness parameters.

3.2 Overview of the standard protocols and methods

The following section reports a brief overview of two aspects of interest for the characterization of the connection's behaviour: the evaluation of the yield point and the loading protocols for the cyclic test.

3.2.1 Estimation of the yield slip

The idea of using in the worldwide the same or comparable approaches for the estimation of the yield slip is fundamental, especially to compare different studies or connections system (traditional or innovative) as it was demonstrated by Muñoz et al. (2008). Different approaches are available:

- ASTM E2126 ($EEEP$) (ASTM, 2019);
- ASTM D5764 ($5\% \cdot \varnothing$) (International, 1995);
- Karacabeyli & Ceccotti (Karacabeyli and Ceccotti, 1996) ($K\&C$);
- CEN (European Committee for Standardization, 2001) (CEN);
- Yasumura & Kawai (Yasumura and Kawai, 1998) ($Y\&K$);
- Commonwealth Scientific and Industrial Research Organization ($CSIRO$).

In North-America ASTM E2126 ($EEEP$) (ASTM, 2019), ASTM D5764 ($5\% \cdot \varnothing$) (International, 1995), Karacabeyli & Ceccotti (Karacabeyli and Ceccotti, 1996) ($K\&C$) are commonly used.
$EEEP$, specific for the analysis of shearwalls, adopt the equivalent energy elasto-plastic curve (EEEP). $5\% \cdot \varnothing$ method use the 5% diameter offset line parallel to a secant curve passing through the 40% of the maximum strength. The $K\&C$ method adopt the slip associated with the 50% of the maximum strength.

In Europe (more details are reported in the dedicated section), the yield point is defined with two possible approaches ("Method a" and "Method b") depending on the shape of the backbone curve based on a bi-linearization (CEN) (European Committee for Standardization, 2001). In case of two well-defined linear parts "Method a" is suggested. In "Method b", the elastic part is defined with the stiffness passing through the 10% and 40%

of the maximum load. The post elastic line is tangent to the experimental curve with 1/6 of the elastic stiffness. The yield point is the intersection of the elastic and post-elastic branches.

In Japan, Yasumura & Kawai (Yasumura and Kawai, 1998) ($Y\&K$) developed a bi-linear curve. The first branch is defined with the stiffness passing trough the 10% and 40% of the maximum load. The second branch is a line tangent to the experimental curve with a secant stiffness of the 40% and 90% of the maximum capacity. The intersection of the two lines gives the coordinates of the yield point.

In Australia, the Commonwealth Scientific and Industrial Research Organization ($CSIRO$) (CSIRO and Organization, 1996) defines the yield point as the deformation corresponding to 1.25 times 40% of the maximum capacity.

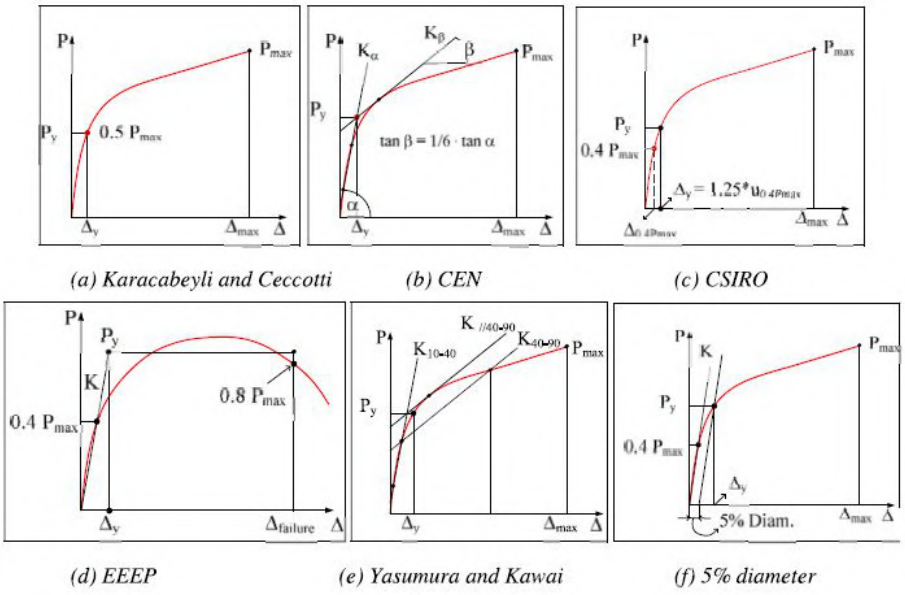

Figure 3.3. Most widespread methods to define the yield point (Muñoz et al., 2008).

3.2.2 Cycle loading protocols

The cycle test consists of applying a displacement history to a joint to investigate the hysteretic behaviour. The velocity, the amplitude and the frequency of the cycles depend on the standard document. The most commons loading protocols used for cycle testing of timber joints are:

- ASTM-CUREE of ASTM E2126 (also called CUREE test protocol) (ASTM, 2019);
- ISO 16670 (ISO/TC 165, 2003);
- EN 12512 (European Committee for Standardization, 2001).

The CUREE test protocol (Figure 3.4a) consists of two displacement patterns: the first pattern with six cycles at small amplitudes (of equal amplitude) while the remaining patterns are based group of three cycles with incremental amplitude. The first cycle of each group has a higher amplitude than the remaining two (-25%). The amplitude of the cycles is listed in the reference documents and adopt the ultimate displacement as reference slip amplitude.

The ISO 16670 (Figure 3.4b) loading schedule is based on two displacement patterns: the first pattern consists of five single fully reversed cycles at displacements of 1.25%, 2.5%, 5%, 7.5%, and 10% of the ultimate displacement while the second pattern consists of three fully reversed cycles with incremental amplitude at displacements of 20%, 40%, 60%, 80%, 100%, and 12% of the ultimate displacement.

The EN 12512 follows two possible procedures based on the yield displacement: "complete" and "short". The first one (Figure 3.4c) is based on the execution of groups of three complete cycles at the same slip with increasing amplitude while the second one (Figure 3.4d) implements a single group of three complete cycles at a pre-determined ductility.

As observable in Figure 3.4, the protocols adopt different displacement patterns which could give different results for the same connections/shearwall.

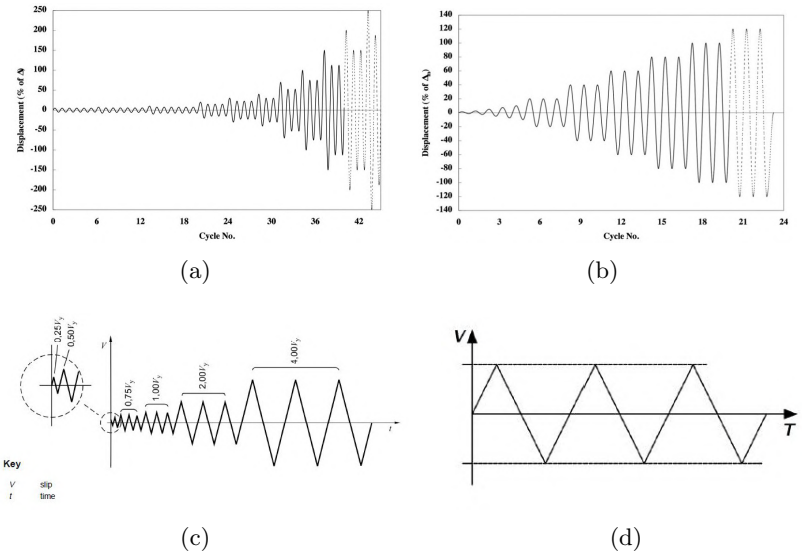

Figure 3.4. Loading test protocols: ASTM-CUREE (a), ISO 16670 (b), EN12512 "complete" (c) and "short" procedures (d).

3.3 Current EN 12512:2001 and EN 1998-1:2004

The current EN 12512:2001 (European Committee for Standardization, 2001) is the European standard reference document for estimating the ductility, the impairment of strength and energy dissipation properties for timber joints made with mechanical fasteners under cyclic loading. The EN 1998-1:2004 (Code, 2004) is the structural Eurocode dedicated to the seismic design of structures.

The two documents are strictly connected since in the seismic design of timber structures, the dissipative zones are located into the timber-to-steel connections through the yielding of the metal fasteners and the embedment of the timber fibres. Due to the seismic cyclic demand caused by the earthquake motion, dissipative connections should guarantee adequate low-cycle fatigue and ductility to ensure energy dissipation. Meanwhile, non-dissipative connections or brittle components should be over-designed with the overstrength factors in a dissipative design approach.

EN 12512:2001 is not well linked with all requirements of the EN 1998-1:2004 (EC8-1). In particular, section §8.8.3 (EC8-1) asks to check simultaneity ductility and the strength's impairment:

"In order to ensure that the given values of the behaviour factor may be used, the dissipative zones shall be able to deform plastically for at least three fully reverse cycles at a static ductility ratio of 4 for ductility class medium (DCM) structures and at a static ductillity ratio of 6 for ductility class high structures (DCH), without more than 20% reduction of their resistance."

The same inscription is reported in the Italian building code (NTC18) (Norme Tecniche, 2018) at section §7.7.3.1. This assumption is unique only for timber material since steel and reinforced concrete evaluate the impairment of the strength in different ways.

The "*reduction of their resistance*" has an ambiguous interpretation. It is not clear if the reduction of resistance is related to the difference between the first and the third cycle at a specific slip level which is in agreement with the "Short procedure" (as interpreted by Germano et al. (2015) and Casagrande et al. (2020)) or if it refers to the softening branch at the first envelope curve. No explanation of §8.8.3 section is reported in EN 12512:2001.

The impairment of the strength (or reduction of resistance) (Figure 3.5) is a measure of cyclic degradation described as: *"reduction in the load when attaining a given joint slip from the first to the third cycle of the same amplitude"* (§3.8 of EN 12512:2001) Equation 3.2:

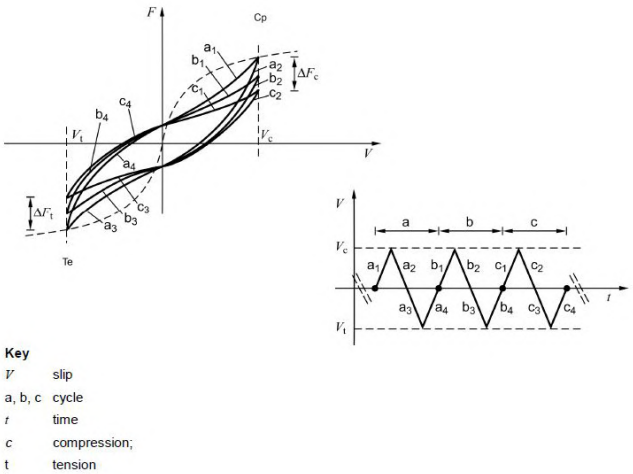

Figure 3.5. Definition of impairment of strength.

$$\Delta F_c = \Delta F_{1-3} = F_1(\delta) - F_3(\delta) \tag{3.2}$$

Besides, the impairment of the strength is related to the loading test procedure. EN 12512:2001 gives two different procedures, based on a displacement control test, ruled by the previous estimation of the yielding slip: "Complete procedure" and "Short procedure". The first one (Figure 3.4c) provides the execution of three complete cycles at the same slip with increasing amplitude. The second one (Figure 3.4d) implements a single group of three complete cycles at a pre-determined ductility. Both methods allow calculating the impairment of strength. However, it is well known that strength degradation is influenced by the number and the shape of the cycles performed. "Complete procedure" exhibit higher reduction than the "Short procedure" giving for the same connections different results. The test operator can select, based on its experience, the desired procedure becoming a limit of a real standard procedure.

According to EN 12512:2001 the definition of the ductility (Equation 3.1) is unique except the estimation of the δ_y and δ_u. The ultimate slip is the minimum between the failure, the slip related to the 20% degradation of the maximum capacity and 30mm. For the estimation of δ_y there are two possible methods. "Method a" (Figure 3.6a) is used when the yield point could be found with the intersection of two lines able to reproduce the elastic and post elastic branch. "Method b" (Figure 3.6b) is used when the yield point in well-not defined: the yield point is estimated by the intersection of a secant line passing through the 10% and 40% of the maximum capacity and a tangent line with a slope equal to 1/6 of the elastic one. As for the loading protocol, the methodology for the definition of the yield point is not unique.

An other important consideration is that the current EN 12512 disaggregate the ductility to the impairment of the strength. As an example, respecting the EN 12512, a simple fastener could show excellent behaviour in a monotonic test with an adequate ductility and strength, demonstrating a proper behaviour for seismic design. However, if the fastener shows a marked strength

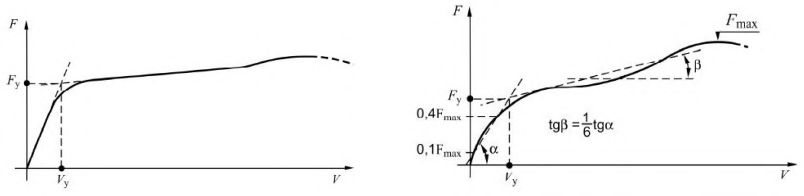

(a) (b)

Figure 3.6. Definition of yield values for a load-slip curve: (a) With two well-defined linear parts, (b) without two well-defined linear parts.

impairment under cyclic test without an adequate ductility, the fastener should be used with a propper maximum ductility or at least for non-dissipative zones.

In summary, the current EN 12512:2001 has the following limits when used with EN 1998-1:2004 (and/or NTC18):

- No rules in how apply EN 12512:2001 within §8.8.3 of EN 1998-1: 2004;
- Discutible choice of the loading protocol procedure;
- Discutible choice of the yielding values;
- Ductility and impairment of the strength are independent;
- No distinction between structural typology;
- No distinction between the effectively achievable ductilities of different joints.

In these years (∼2020), in conjunction with the revision of the EN 1998-1:2004, it is proposed a methodology developed by Casagrande et al. (2020) for the revision of the EN 12512:2001 which allows correlating the ductility to the strength impairment and by giving defined information about the methodology required. The new method, for the determination of the seismic capacity of dissipative timber connections, aims to joint the design and the testing standards' requirements. The method was used by the authors to different types of mechanical connections subjected to cyclic tests based on an experimental company.

Meanwhile, the "Working Group 1 of CEN TC124" (Sigrist et al., 2020) worked for the development of a Technical Specification (TS 12512) to link the current EN 12512:2001 to the requirements of the EN 1998-1:2004 (EC8), the next section reports the proposed procedure for the update of the EC8.

3.4 Prevision of EN 12512 and EN 1998

EN 1998 (EC8) and EN 12512 as shown before are strictly related. EC8 defines the seismic design requirements (demand) whereas EN 12512 define the properties of the timber connections (capacity). In the following sections, the proposal novelties for both documents are introduced.

3.4.1 Proposal Draft for EN 12512

Casagrande et al. (2020) is a proposal approach for the revision of the EN 12512. The novelties proposed are:

- Correlation between the impairment of the strength and ductility;
- Definition of a new loading test protocol.

3.4.1.1 Impairment of the strength and ductility

An additional deformation limit is adopted to correlate the impairment of timber connections' strength and ductility capacity.
The ultimate slip (Equation 3.3) is ruled by the minimum of the currents requirement (failure slip, slip related to a degradation of the 20% of the maximum capacity and 30mm) and the degradation displacement ($\delta_{\varphi_{imp}}$) related to a specific limit of the strength impairment factor φ_{imp}.

$$\delta_u = min\,[\,[\delta_f,\, \delta_{80\%F_{max}},\, 30mm],\, \delta_{\varphi_{imp}}\,] \tag{3.3}$$

Defined the impairment function (Equation 3.4) as the ratio between the strength reduction (Equation 3.2) and the strength at the 1st cycle for a specific amplitude slip, the impariment factor φ_{imp} is taken as a percentage of a tollerable cycle degradation (Figure 3.7) reported in prEC8-1-2.

$$\varphi_{imp}(\delta) = \frac{F_1(\delta) - F_3(\delta)}{F_1(\delta)} \leq \varphi_{imp} \tag{3.4}$$

Similar to ANSI/AISC 341-10[2] (ANSI, 2010), condition 3.5 is also introduced in order to avoid a large discrepancy between monotonic and cycle test. The strength reduction factor k_{deg} (Figure 3.8) is analitically

[2]It is adopted for the estimate of the low-cycle fatigue strength of steel beams-to-column joints.

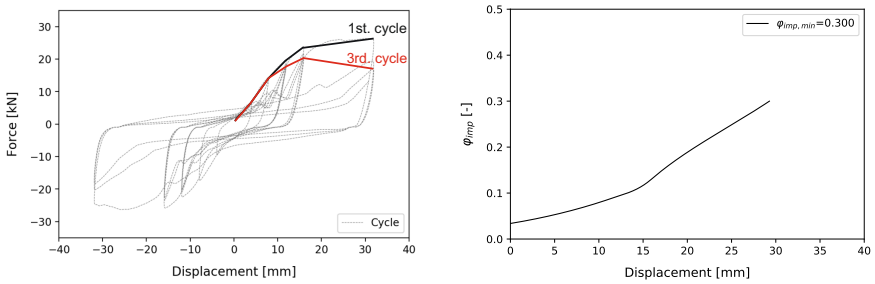

(a) (b)

Figure 3.7. Impariment of the strength: (a) 1st and 3rd test envelope, (b) impairment function (Casagrande et al., 2020).

defined as the ratio of the ultimate load at the 1st envelope curve in the cycle test and the maximumn nominal strength (F_N) of a monotonic test.

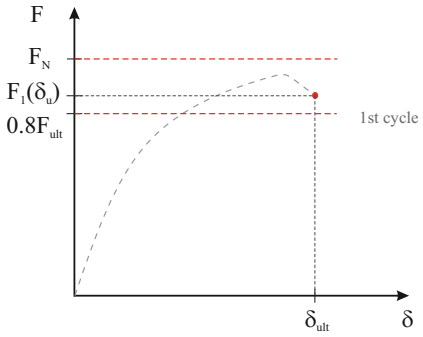

Figure 3.8. k_{deg} limits: ultimate load at the 1st envelope curve and the nominal strength.

$$k_{deg} = 1 \geq \frac{F_1(\delta_u)}{F_N} \geq 0.8 \tag{3.5}$$

If this condition is not satisfied, the ultimate degradation displacement is reduced until the inequality is respected.

3.4.1.2 Definition of a new loading test protocol

The new loading protocol is based on the improvement of the current "Complete procedure". Two aspects are at the base of the modification: more cycles with small increasing amplitude steps and groups of three fully reverse cycles at the same amplitude. The use of more cycles is in accordance with other loading standards (e.g. ASTM-CUREE and ISO 16670), whereas the slip amplitude of cycle groups allows calculating the impairment of the strength between the first and the third envelope curve[3].

[3]Conversely to ASTM-CUREE where the cycles of the groups have different amplitudes.

Table 3.1 compare the cycle patterns of the current EN 12512 and the new proposal.

EN 12512:2001	**N. of cycles**	1	1	3	3	3	3	3	3	3
	Step $[\delta_{y,m}]$	0.25	0.5	0.75	1.0	2.0	4.0	6.0	...	(+2.0)
New proposal	**N. of cycles**	1	1	3	3	3	3	3	3	3
	Step $[\delta_{y,m}]$	0.25	0.5	0.75	1.0	2.0	3.0	4.0	...	(+1.0)

Table 3.1. Current and new proposal loading procedure.

3.4.1.3 Summary

In summary, the EN 12512 proposal specifies the following steps for its usage with the future verision of EN 1998 (EC8):

1. Perform a monotonic test according to EN 26891:1991;
2. Estimate the nominal strength F_N as the maximum load capacity and calculate through "Method b" the yield slip $\delta_{y,m}$ respecting EN 12512;
3. Perform a cyclic test with the new proposal complete loading procedure (Table 3.1) and draw the 1st and the 3rd envelopes curves;
4. Estimate the ultimate displacement with equation 3.3 applying equation 3.2 with an impairment factor φ_{imp} equal to 0.3 (defined in EC8);
5. Estimate the yield displacement δ_y within "Method b";
6. Check equation 3.5 and if the verification is not respect, the ultimate displacement should be reduced;
7. Calculate the ductility ratio (Equation 3.1) and comparing the value with the EC8 limits.

3.4.2 Proposal Draft for EN 1998

The new draft of EC8 defines safety verification for new buildings at the ULS (Ultimate limit state) in terms of strength and ductility. The dissipative components' should follow the hierarchy rules by protecting failure modes and ensuring a minimum level of ductility.

3.4.2.1 Safety verifications

Strength verification

The strength of the dissipative zones should be calculated with Equation 3.6:

$$F_{Rd,d} = k_{deg} k_{mod} \frac{F_{Rk,d}}{\gamma_M} \tag{3.6}$$

where:

$F_{Rd,d}$ is the design value of the strength of the dissipative zones;

k_{deg} is the strength reduction factor due to degradation under cyclic loading;

k_{mod} is the modification factor for duration of load and moisture content;

$F_{Rk,d}$ is the characteristic value of the strength of the dissipative zones;

γ_M is the material partial factor for accidental design situations.

The design strength of the non-dissipative components should be calculated with Equation (3.7).

$$F_{Rd,b} = k_{mod} \frac{F_{Rk,b}}{\gamma_M} \tag{3.7}$$

where:

$F_{Rd,b}$ is the design value of the strength of the non-dissipative components;

$F_{Rk,b}$ is the characteristic value of the strength of the non-dissipative components;

γ_M is the material partial factor for accidental design situations.

Meanwhile, non-dissipative connections or brittle components should be over-designed with the overstrength factor γ_{Rd} in case of a dissipative

design approach. The capacity design at the local level, the brittle part of the connections assembly should respect Equation (3.8):

$$\frac{\gamma_{Rd}}{k_{deg}} \cdot F_{Rd,d} \leq F_{Rd,b} \tag{3.8}$$

The draft document of EN 1998-1-2 defines the mechanical properties of the dissipative zones as:

"The mechanical properties of dissipative zones should be determined by tests in accordance with EN 12512; they should correspond to a strength impairment factor φ_{imp} not greater than 0.3 and a strength reduction factor k_{deg} not smaller than 0.8. Testing conditions should represent the design intent (for example type of dissipative zone, loading conditions, restraints). The loading should consist in three reversed cyclic loads at each equal target deformation, these target deformation being progressively increased."

A correct and well definition of how calculate the two factors is reported also in the EC8 to avoid understanding errors:

"The strength impairment factor φ_{imp} in a cyclic test performed in accordance with EN 12512 is the ratio of the reduction $\Delta F_{1-3} = F_1 - F_3$ of resistance of the tested component from the first to the third cycle at equal applied deformation δ and the resistance F_1 at the first cycle. The strength reduction factor k_{deg} is the ratio of the resistance at the first cycle at the ultimate deformation δ_u determined according to EN 12512 to the maximum resistance in monotonic tests according to EN 26891."

Ductility verification

Together with the limitation of the impairment of the strength, connections should guarantee an adequate level of ductility. As shown in Table 3.2, the minimum values are specific for the structural system and the level (e.g. wall level and connection level) for moderate and high ductility classes. The limits ensure the attainment of the tabulated values of the behaviour factors (q-factors) for various structural systems.

Structural type	Dissipative sub-assembly/joint/2D or 3D-nailing plate/connection	Type of ductility	μ DC2	μ DC3
a) Cross laminated timber structures	Shear wall*	Displacement	1.8	2.7
	Hold-downs, tie-downs, foundation tie-downs, angle brackets, shear plate	Displacement	1.8	1.8
	Screwed wall panel-to-panel joints	Displacement	-	3.5
b) Light-frame structures	Shear wall*	Displacement	2.2	3.5
	Connection (nail/screw/staple)	Displacement	3.5	5.5
c) Log structure	Shear wall*	Displacement	1.4	-
d) Moment-resisting frames	Portal Frame*	Displacement	2.0	3.0
	Beam-column joint	Rotational	4.0	7.0
e) Braced frame structures with dowel type connections	Braced Frame*	Displacement	1.4	-
f) Vertical cantilever structures	Shear wall*	Displacement	2.0	-
g) Braced frame structures with carpentry connections and masonry infill	Shear wall*	Displacement	1.4	-

*The values provided refer to the system ductility of the sub-assembly, taking into account the ductility of all the individual connections and components.

Table 3.2. Minimum required ductility μ as defined in EN 12512 of dissipative zones tested.

3.4.2.2 Draft EC8-Annex L: Rules for non-linear analyisis

The revision of the EC8 will introduce the possibility of performing a displacement-based analysis for timber buildings for the first time. Nowadays for timber structures, non-linear analysis is mainly used by researchers instead of practitioners due to the lack of recognized analytical formulations and/or experimental curves provided by producers. Engineers used a linear analysis in which the strength and the stiffness of timber and connections elements are the unique information required (force-based approach). The verifications of the ductile and brittle mechanisms are based on the comparison between the capacity and the demand.
In displacement-based approach, the control is carried out by monitoring the deformation level for the ductility components and the strength demand for brittle ones at each step of the non-linear analysis.

"Annex L" gives information about the dissipative components for non-linear analyses defining:

- Linearization of the load-deformation curve;
- Definition of the Limit State at the connection level (or local level).

The construction of a force-deformation relationship is a tri-linear approximation based on the mean force-deformation relationship (joint, connection, 2D and 3D nailing plates, etc.). The tri-linear curve could follow two different approaches: an "experimental approach" (preferable) and an "analytical

approach" in case experimental tests are not available. The analytical procedure is introduced since currently, designers have problems to find experimental data. It is aspected that connections' producers will provide experimental data or the direct approximated tri-linear curve in the next future.

The Limit State definition at the local level will give a methodology to check the damage at the local (connections) and global (structure) levels'.

3.4.2.2.1 Linearization of the load-deformation curve

The following section shows the linearising methodology of the dissipative timber components following the two approaches. The EN 12512 is used to estimate the coordinates of the yield point (F_y; δ_y) while the maximum and the ultimate points composing the tri-linear curve the curves are constructed geometrically.

Experimental approach

The "Experimental approach" can be applied in case of experimental results following EN 12512 accounting the strength impairment factor φ_{imp}. The tri-linear curve was initially proposed by Gavric (Gavric et al., 2015a) and overcomes the limitation of using bi-linear with hardening law of the EN 12512 in the non-linear analysis (overestimating the maximum strength capacity). The residual strength at zero slip (F_0), get through the secant stiffness the passing through the 10 and 40 per cent of the maximum load capacity, is neglected avoiding practical and numerical problems in the tri-linear relationship.

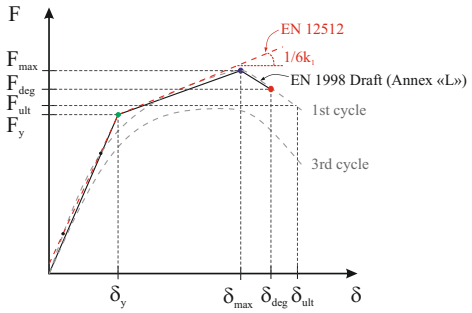

Figure 3.9. Construction of the tri-linear curve from experimental test.

Two possible curves (Figure 3.10a-b) with or without degradation are achievable depending on the ultimate displacement δ_u position.

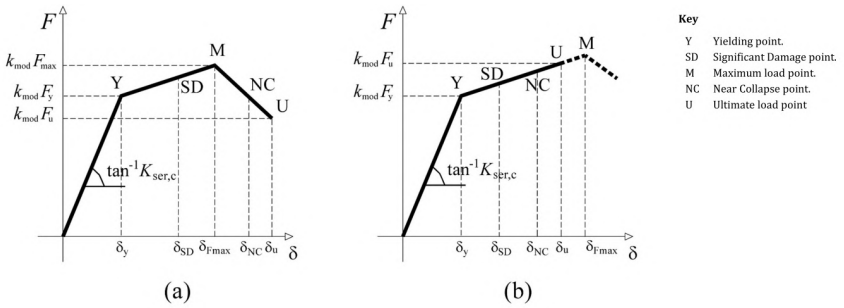

Figure 3.10. Derivation of the trilinear (a) and bilinear (b) load-deformation mean curve of zones in timber structures from the experimental curves according to EN 12512.

The first branch should be obtained by connecting the origin with the yield point Y ($k_{mod} \cdot F_y$; δ_y). The yield deformation δ_y and the yield load F_y should be determined according to EN 12512. The slip modulus $K_{ser,c}$ should be calculated as given by:

$$K_{ser,c} = \frac{k_{mod} \cdot F_y}{\delta_y} \tag{3.9}$$

The second branch should be obtained by connecting the yield load point Y with the maximum load point M ($k_{mod} \cdot F_{max}$; δ_{Fmax}) where F_{max} is the maximum load attained on the 1st cycle envelope load-deformation curve during the test, and δ_{Fmax} is the deformation attained at the maximum load F_{max}.

The third branch should be obtained by connecting the maximum load point M with the ultimate load point U ($k_{mod} \cdot F_u$; δ_u). The ultimate load F_u is the load attained on the 1st cycle envelope load-deformation curve corresponding to the ultimate deformation δ_u, which is determined according to EN 12512 assuming a limit value of the strength impairment factor φ_{imp} not greater than 0.30 and a limit value of the strength reduction factor due to degradation under cyclic loading k_{deg} not lower than 0.80.

When the ultimate deformation δ_u is smaller than the deformation related to the maximum load δ_{Fmax}, a bilinear curve should be used (Figure 3.10b).

"Analytical approach" should be used if experimental results are not available for the dissipative zones.
Only a tri-linearizaition with the softening branch is allowed instead "Experimental approach".

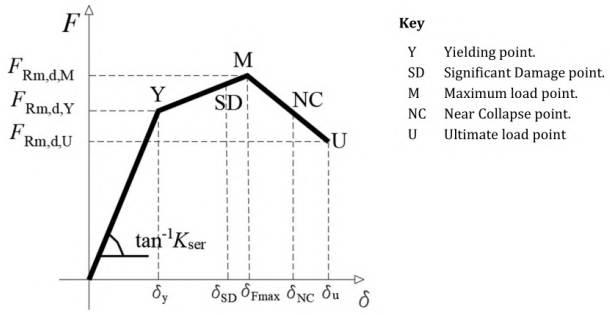

Figure 3.11. Trilinear load-deformation mean curve of dissipative zones in timber structures using analytical formulas.

The mean yield strength (Point Y) of the dissipative connection under seismic loading $F_{Rm,d,Y}$ may be calculated as:

$$F_{Rm,d,Y} = k_y \cdot k_{mean} \cdot k_{mod} \cdot F_{Rk,d} \tag{3.10}$$

k_y is the ratio between the yield strength and the maximum strength (Table 3.3);

k_{mean} is the ratio between the mean and the characteristic strength in static conditions (Table 3.3);

$F_{Rk,d}$ is the characteristic value of the strength of the dissipative connection in static conditions.

The yield deformation (Point Y) of the dissipative connection under seismic loading δ_y may be calculated as:

$$\delta_y = \frac{F_{Rm,d,Y}}{k_{ser}} \tag{3.11}$$

where k_{ser} is the slip modulus. The ultimate strength at the end of the softening branch (Point U) of the dissipative connection under seismic loading $F_{Rm,d,U}$ may be calculated using Formula 3.12.

$$F_{Rm,d,U} = k_{deg} \cdot k_{mean} \cdot k_{mod} \cdot F_{Rk,d} \tag{3.12}$$

The deformation at the end of the softening branch (Point U) of the dissipative connection under seismic loading δ_u may be calculated as given by:

$$\delta_u = \mu \cdot \delta_y \tag{3.13}$$

where μ is the ductility of the dissipative connection under seismic action.

The maximum strength (Point M) of the dissipative connection under seismic loading $F_{Rm,d,M}$ may be calculated:

$$F_{Rm,d,M} = k_{mean} \cdot k_{mod} \cdot F_{Rk,d} \tag{3.14}$$

The deformation at the maximum load (Point M) of the dissipative connection under seismic loading δ_{Fmax} may be calculated using:

$$\delta_{Fmax} = \delta_y + 0.5 \cdot (\delta_u - \delta_y) \tag{3.15}$$

The values of k_{mean} and k_y are tabulated values (Table 3.3) estimated based on the results of experimental tests available in literature ((Jorissen and Fragiacomo, 2011), (Gavric et al., 2015c), (Gavric et al., 2015a), (Izzi et al., 2016), (Jockwer and Jorissen, 2018)).

Type of dissipative connection/joint/subassembly	k_{mean}	k_y
High ductility semi-rigid beam-column joints with expanded tube fasteners and Densified Veneer Wood, Carpentry connections in log structures	1.20	0.90
Dissipative connections in cross laminated timber structures, Dissipative connections in light-frame structures, Shear walls in braced frame structures with carpentry connections and masonry infills, Moderate ductility semi-rigid beam-column joints, Dowel-type dissipative connections in braced frame structures, Base connections of vertical cantilever structures	1.35	0.90

Table 3.3. Values of the ratio k_{mean} between the mean and the characteristic strength of dissipative zones in static conditions, and of the ratio k_y between the yield and the maximum strength of dissipative zones.

3.4.2.2.2 Limit State at the connections level

Similar to the definition of the Limit States (LS) for a reinforced concrete beams[4], the estimation of the ultimate and the yield deformations defines directly the Yield (Y), the Significant Damage (SD) and the Near Collapse (NC) levels directly at the connections levels.

The SD (Equation 3.16) and the NC (Equation 3.17) are calculated as a percentage of the post-elastic range.

$$\delta_{SD} = \delta_y + \frac{0.5}{\gamma_{Rd,SD}} \cdot (\delta_u - \delta_y) \tag{3.16}$$

$$\delta_{NC} = \delta_y + \frac{1.0}{\gamma_{Rd,NC}} \cdot (\delta_u - \delta_y) \tag{3.17}$$

where:

δ_{SD} is the deformation at SD limit state;

δ_{NC} is the deformation at NC limit state;

$\gamma_{Rd,SD}$ is the partial factor on resistance at SD limit state.

$\gamma_{Rd,NC}$ is the partial factor on resistance at NC limit state.

For the Significant Damage LS, the SD point is located at the 50% of the post-elastic range while for the Near collapse LS, the NC point corresponds to the ultimate deformation of the connection.

The deformation limits will be used in the next chapter to define the "Displacement Domain" used for the definition of the limit state at the local (connection) and global (wall/structure) levels for the numerical models.

[4] In concrete structures, the chord rotation at the yielding θ_y and the ultimate θ_u deformations correspond respectively to the yielding and the near collapse. The significant damage is a fraction of the $3/4 \cdot \theta_u$.

3.4.2.3 Summary

In summary, the changes introduced during the revision process regarding the dissipative components are:

- Definition of the dissipative and non-dissipative connections for all structural systems;
- Well defined correlation between Eurocode 8 and the EN 12512;
- Correlation between the ductility and the impairment of the strength;
- Minimum values of ductility required for dissipative connections and ductility structural class;
- Capacity design rules at the connection level.

3.5 Implementation of EN 12512 Draft

In the following section, typical CLT connections listed in Table 3.4 are analyzed within the EN 12512 Draft. The mechanical connections were tested in CNR-Ivalsa Trees and Timber Insitute[5] in 2013 (Gavric et al. (2015b), Gavric et al. (2015c)) by Igor Gavrić. An extensive experimental programme made of monotonic and cyclic (EN 12512:2001) tests was carried out for different mechanical anchors in shear and tension (uplift).

These tests are still the most popular in the research field, becoming the main benchmark for numerical models[6].

The loading directions are defined as primary or secondary, depending on the type of connection (Figure 3.12).

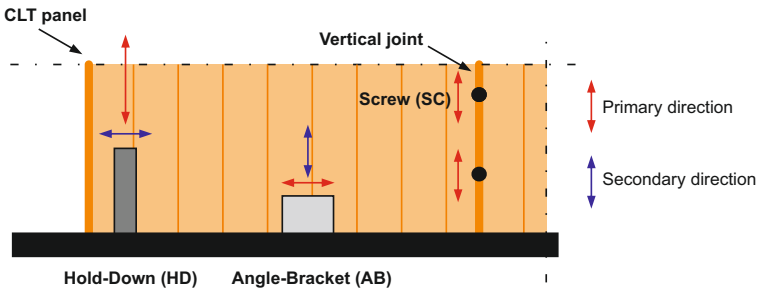

Figure 3.12. Definition of primary and secondary loading directions.

Generally, hold-downs are designed to resist to an uplift tension (primary direction) neglecting the shear behaviour (secondary direction) since does not provide a significant contribution ((Gavric and Popovski, 2014), (Gavric et al., 2015a)).

Angle-brackets and screws/nails are designed to work in the shear (primary direction). The only secondary component taken into account is the uplift tension of angle-brackets, which is significant in the evaluation of the wall capacity. In fact, the strength capacity in the two orotognal directions of an angle-brackets are comparable Gavric and Popovski (2014)(see also in next tables). Conversely, the ductility, the ultimate deformation and the hysteretic laws are very different. This assumption is supported by the results listed later in Table 3.5 and by other experimental investigations

[5] Now "Institute of BioEconomy (IBE)".

[6] See (Rinaldin et al., 2013), (Pozza et al., 2017), (Shahnewaz et al., 2018), (Franco et al., 2019), (Tamagnone et al., 2020).

((Tomasi and Smith, 2015), (D'Arenzo et al., 2019)).

The Half-Lap joint was taken into account against the "spline joint" (also collected in the Gavric et al. (2015b)) due to the capacity design requirement. As explained in §2.3.4.2 with Equation 2.7, the yield deformation of the hold-down should be greater than the yield deformation of the vertical joint multiply the overstrength factor γ_{Rd} which is (currently) fix to 1.6 to ensure the couple-panel behaviour for multi-panel walls. As reported in Gavric et al. (2015b), the yield deformation of the hold-down (WHT540), the half-lap joint and the spline-joint are respectively equal to 8.81mm, 2.55mm, 5.70mm. The spline-joint was excluded since $\gamma_{Rd} \cdot 5.70mm = 1.60 \cdot 9.12mm \geq 8.81mm$.

Metal connector		Properties	Test no.	Loading direction
Hold-down (HD)		WHT540 bolt ϕ 16 12 Anker-ϕ4x60mm	#1	Tension (Primary)
Angle-bracket (AB)		BMF 90x116x48x3 11 Anker-ϕ4x60mm	#2	Shear (Primary)
			#3	Tension (Secondary)
Half-Lap Joint (SC)		HBS ϕ8x80mm 2x2 screws	#4	Shear (Primary)

Table 3.4. Connections analyzed (Gavric et al. (2015c), Gavric et al. (2015b)).

3.5.1 Analyses and results

The method presented in section § 3.4.1.1 in combination with the methodology for the drawing of the post-elastic and softening branches (section §3.4.2.2.1) were applied to the experimental tests (section §3.5) used to investigate the behaviour of CLT structures in the following chapters.

Seven samples were analyzed for the hold-down, whereas six samples were taken into account for the half-lap joint and for the angle-bracket in both directions.
All data were analyzed with a dedicated tool developped in Python language (Rossum, 1995) based on an Akima interpolation [7](Akima, 1970) connecting the maximum strength a specific level of slip of the 1st and the 3rd envelope load-slip curves. The Akima interpolation approach was adopted since it allows a better approximation instead of the simplified linear one.

Figures 3.13, 3.14, 3.15 and 3.16 display the typical behaviour of the considered connections whereas Table 3.5 reports all parameters of interest. All linearization show an excellent with the 1st backbone curve. All connections show a reduction of the ductility, including the oligo-cycle fatigue as observable in the figures with the attainment of the impairment factor equal to 0.30. A reduction of the -9.16%, -15.71%, -2.62% was obtained from hold-down in tension, and the angle-bracket in tension and shear, respectively. The half-lap joint evinced a reduction of -37.78%.

[7]Piecewise cubic polynomials.

	Hold-down		**Angle Bracket**				**Half-Lap Joint**	
	Tension		**Tension**		**Shear**		**Shear**	
	Mean	**Dev.St.**	**Mean**	**Dev.St.**	**Mean**	**Dev.St.**	**Mean**	**Dev.St.**
$F_0\,[kN]$	0.58	0.16	0.32	0.04	0.25	0.02	0.08	0.04
$F_y\,[kN]$	40.56	2.79	19.16	0.50	23.95	1.12	2.84	0.27
$F_{max}\,[kN]$	48.37	2.58	23.54	1.01	27.92	1.37	5.34	0.85
$F_{ult}\,[kN]$	40.99	4.86	18.81	0.83	27.75	1.49	4.91	0.97
$F_{deg}\,[kN]$	45.19	5.77	21.88	2.00	27.78	1.43	4.99	0.68
$F_{design}\,[kN]$	48.04	2.39	23.54	1.01	27.75	1.14	4.91	0.79
$\delta_y\,[mm]$	8.75	1.49	7.10	0.66	12.83	1.00	2.47	0.37
$\delta_{max}\,[mm]$	20.05	3.15	18.35	1.59	28.70	2.01	25.03	1.84
$\delta_{ult}\,[mm]$	23.48	1.43	25.48	0.65	30.00	0.00	29.42	1.43
$\delta deg\,[mm]$	21.50	2.77	22.13	1.76	29.82	1.81	22.42	5.40
$\mu\,[-]$	2.74	0.45	3.61	0.32	2.35	0.18	12.11	1.65
$k_{deg}\,[-]$	1.09	0.14	0.83	0.08	1.08	0.06	1.04	0.14
$\mu_{deg}\,[-]$	2.51	0.51	3.12	0.17	2.29	0.14	8.79	1.30

Table 3.5. Connections results.

where:

F_0 is the strength at a zero deformation;

F_y is the yield strength;

F_{max} is the maximum strength capacity;

F_{ult} is the strength at the ultimate slip without the degradation effect;

F_{deg} is the strength at the ultimate slip with the degradation effect;

F_{design} is the design strength on the elasto-plastic curve accounting degradation;

δ_y is the yield deformation;

δ_{max} is the maximum deformation;

δ_{ult} is the ultimate deformation without the degradation effect;

δ_{deg} is the ultimate deformation with the degradation effect;

μ is the ductility without degradation;

k_{deg} is the degradation factor;

μ_{deg} is the ductility with the degradation effect.

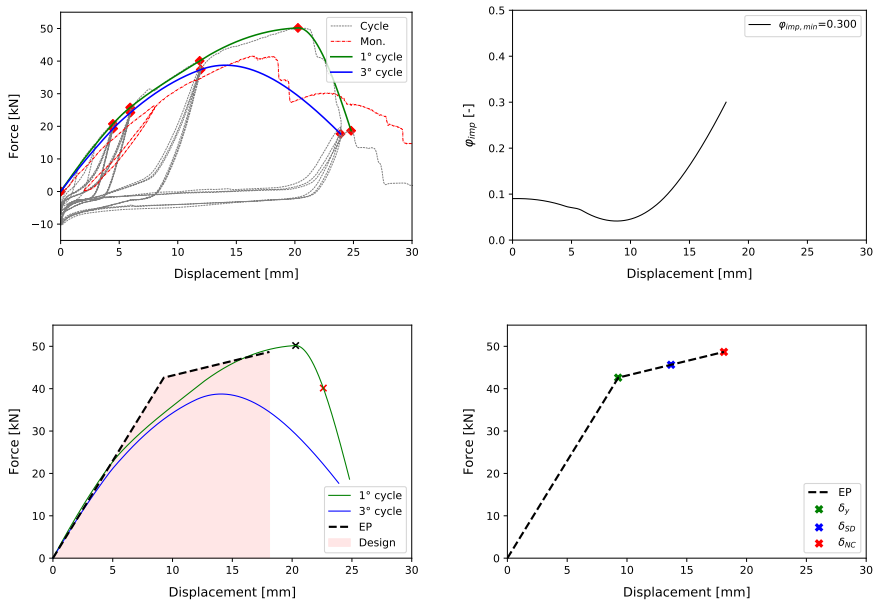

Figure 3.13. Sample #1.1: Hold-Down in tension.

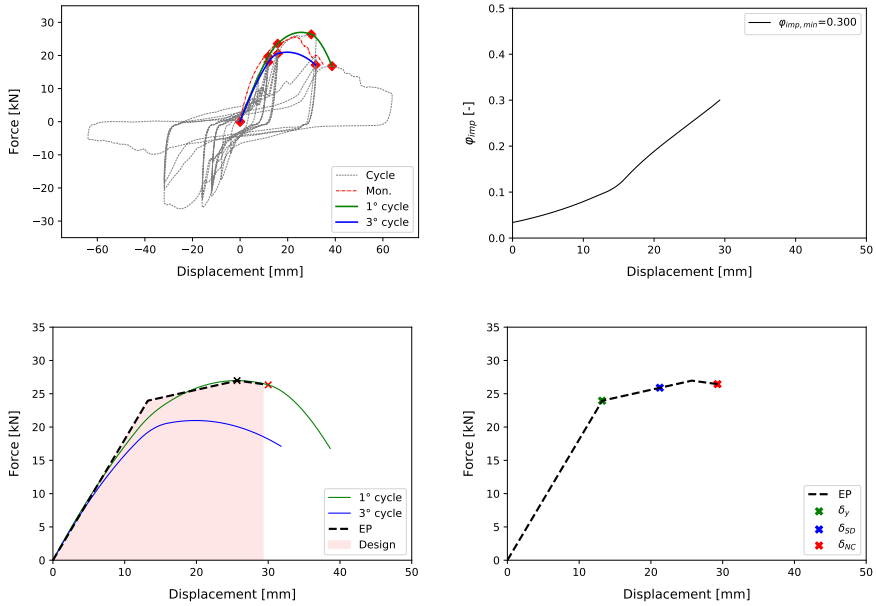

Figure 3.14. Sample #2.1: Angle-Bracket in shear.

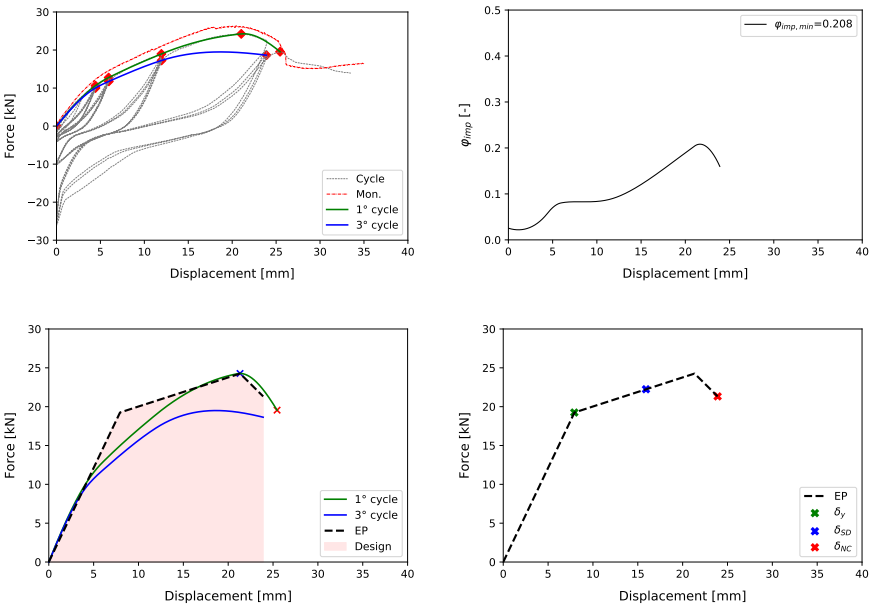

Figure 3.15. Sample #3.1: Angle-Bracket in tension.

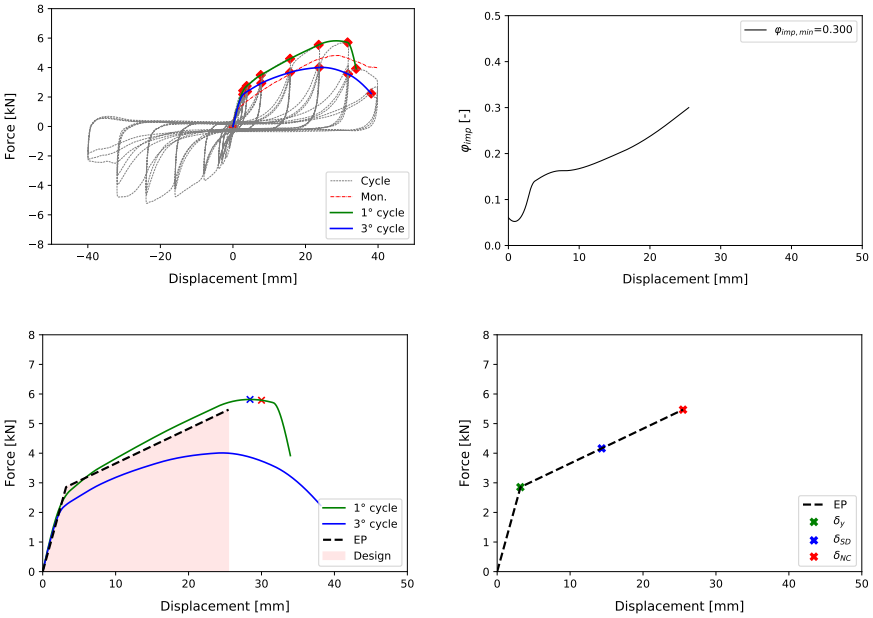

Figure 3.16. Sample #4.1: Half-Lap Joint in shear.

The characteristic strength required in Equation 3.6, is calculated in accordance with EN 14358 (CEN, 2006) within a log-normal distribution correct by a $k_s(n)$ factor to take into account the number of specimens n (Equation 3.18). The mean yield and failure slip values were adopted to define the limit states of the connections. In particular, the failure deformation accounts for the degradation effect respecting Equation 3.3.

$$\mu_{5\%,95\%} = \overline{\mu}_{50\%} - k_s(n) \cdot \overline{\sigma} \tag{3.18}$$

where:

$\mu_{5\%,95\%}$ is the characteristic values at the 5% or 95% modified by the number of specimens;

$\overline{\mu}_{50\%}$ is the log-normal average value;

$\overline{\sigma}$ is the log-normal distribution standard deviation;

$k_s(n)$ is the modification factor as in Table 3.6.

Num. of sp. n	3	5	10	15	20	30	50	100	500	∞
$k_s(n)$	3.15	2.46	2.10	1.99	1.93	1.87	1.81	1.76	1.69	1.64

Table 3.6. Modification factor for experimental test (EN 14358 (CEN, 2006)).

Metal connector	**Loading direction**	**Test**	$F_{5\%}$	$F_{95\%}$	$F_{95\%}/F_{5\%}$
Hold-Down	Tension	#1	42.60	54.07	1.27
Angle-Bracket	Shear	#2	25.15	30.57	1.22
	Tension	#3	21.24	26.06	1.23
Half-Lap Joint	Shear	#4	3.3	7.14	2.16

Table 3.7. Characteristic strength for connections accounting the limitated number of samples. ($k_s(6) = 2.388$ for all tests with a linear interpolation).

3.6 Non-linear numerical modelling of connections

Nowadays, nonlinear analysis of timber buildings is a field still limited to research purpose. Practitioners continue to use linear-elastic analysis based on the Force-Base Method (FBD) for the seismic design. The main reason is the difficult knowledge of the non-linear behaviour of connections and the absence of data given by the producers.
In order to perform a non-linear analysis to estimate the capacity of a CLT wall/building, is required an average behaviour of the timber connections. The following section, split into monotonic modelling and cycle modelling, is at the base of the non-linear analysis developed in the next chapter.

Over the last few years, many researchers worked on the characterization of the connection's behaviour proposing several empirical numerical models calibrated on experimental tests.

3.6.1 Monotonic modelling

3.6.1.1 Overview of the constitutive laws

In order to perform static non-linear analysis, there are several constitutive laws that can be implemented to fit the experimental curves both available for research and the practical scopes:

- Equivalent Energy Elastic-Plastic law (e.g. EEEP);
- Elastic-plastic with hardening branch (e.g. current EN 12512, etc.);
- Tri-linear curve with softening branch (e.g. proposal EN 12512: §3.4.1.1 - §3.4.2.2.1);
- Piecewise linear laws;
- Ad hoc-analytical laws (e.g. Foschi (1977), Dolan (1989), Richard et al. (2003), Folz and Filiatrault (2004)).

Due to the marked non-linear behaviour of timber connections, the skeleton curve (still to the maximum strength) provided by (Foschi, 1977) was widely adopted by other authors ((Dolan, 1989), (Richard et al., 2003), (Folz and Filiatrault, 2004)). During the CUREE Caltech wood frame

project (Reitherman and Hall, 2002) (1998-2002), Folz and Filiatrault (Folz and Filiatrault, 2004) provide the implementation of a one-dimensional hysteretic behaviour named in OpenSees framework "*uniaxialMaterial SAWSMaterial*"[8]. The model was originally made for wood shearwalls, but it could be extended to any level: micro-scale (screw/nail in wood), medium-scale (connection assembly) and large-scale (wall level).

3.6.1.2 Constitutive law adopted

The numerical model developed by Folz and Filiatrault (2004) was adopted for non-linear static analysis due to the excellent fit of the non-linear behaviour of timber components.

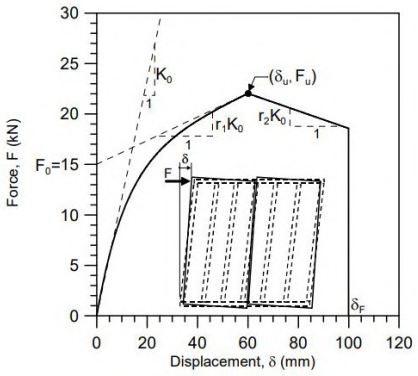

Figure 3.17. "*SAWSMaterial*" for monotonic analysis (Folz and Filiatrault, 2004).

The monotonic curve of the SAW model, reported in Figure 3.17, follows Equation 3.19.

$$F(\delta) = \begin{cases} sgn(\delta) \cdot (F_0 + r_1 K_0 |\delta|) \cdot \left[1 - e^{-K_0|\delta|/F_0}\right] & |\delta| \leq |\delta_u| \\ sgn(\delta) \cdot F_u + r_2 K_0 \left[\delta - sgn(\delta) \cdot \delta_u\right] & |\delta_u| < |\delta| \leq |\delta_f| \\ 0 & |\delta| > |\delta_f| \end{cases} \tag{3.19}$$

[8]SAWS is the acronym of the computer program: "Seismic Analysis of Woodframe Structures".

where:

δ is the deformation;

δ_u is the deformation at the maximun strength;

δ_f is the failure deformation;

F_0 is the intercept strength of for the asymtotic line to the envelope curve;

F_u is the maximum strength;

K_0 is the initial stiffness;

r_1 is stiffness ratio of the asymptotic line to the spring element envelope curve;

r_2 is the stiffness ratio of the descending branch of the spring element envelope curve.

A dedicated tool developed in Python language was used to find the optimal values for the parameters (δ_u , F_0 ,F_u , K_0 , r_1 , r_2) based on a fitting procedure. The 1st cycle envelope curve was taken into account. A mean curve was then defined based on the avarage of all parameters. The black lines in Figures 3.18 represent the mean numerical curves. Table 3.8 summarizes the parameters of all mechanical joints.

The numerical mean curves for all connections match very well the experimental results showing the goodness of the analytical formulation 3.19 and its validity for the implementation in non-linear static analyses.

The SAW model was used against the tri-linearization reported in §3.4.2.2 to get a more accurate behaviour of the complete non-linear response of the connections.

Metal connector	**Test**	F_0 **[N]**	F_u **[N]**	δ_u **[mm]**	K_0 **[N/mm]**	r_1	r_2
Hold-Down	#1	35775.80	47693.26	20.68	6587.87	0.0945	-0.4860
Angle-Bracket	#2	24727.00	27671.40	30.60	2667.80	0.0610	-0.2400
	#3	11220.10	23464.30	17.70	3963.70	0.1880	-0.2240
Half-Lap Joint	#4	2782.32	5263.64	23.52	2551.03	0.0423	-0.0477

Table 3.8. Numerical input data for non-linear static analyses.

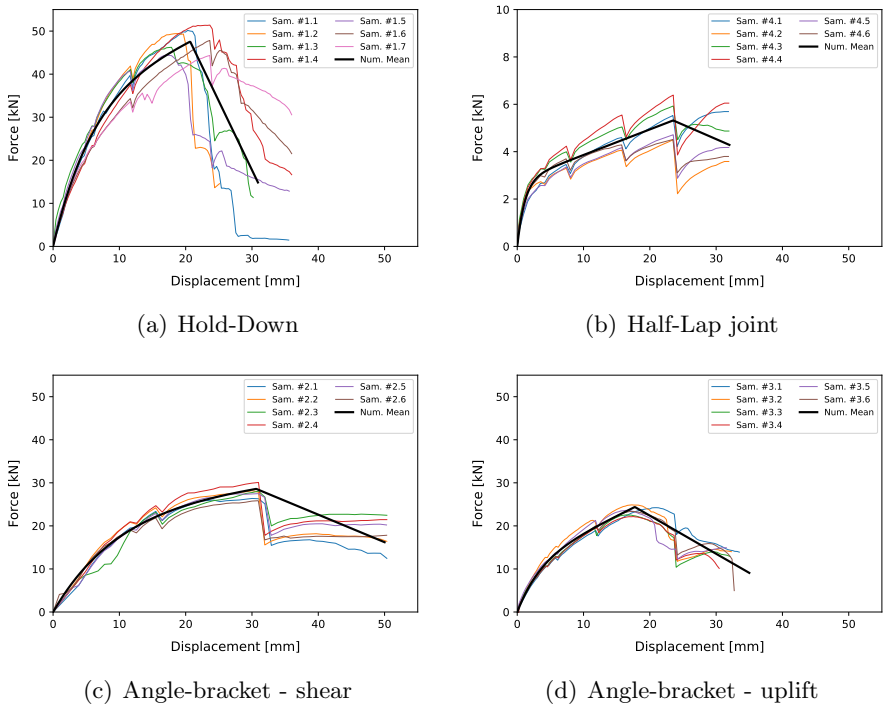

(a) Hold-Down

(b) Half-Lap joint

(c) Angle-bracket - shear

(d) Angle-bracket - uplift

Figure 3.18. Experimental and numerical comparison/calibration for non-linear static analyses.

3.6.2 Hysteretic modelling

3.6.2.1 Overview of the constitutive laws

The hysteretic behaviour of timber joints is a difficult challenging task due to the presence of all phenomena described in section § 3.1 (impairment of the strength, reloading/unloading stiffness degradation and pinching effect). The main hysteresis models developed for timber structures are:

- Foschi 1977 (Foschi, 1977);
- Kivell 1981 (Kivell et al., 1981);
- Stewart 1987 (Stewart, 1987);
- Dolan 1989 (Dolan, 1989);
- Ceccotti & Vingoli 1989 (Ceccotti and Vignoli, 1989);
- Blass 1994 (Blass et al., 1994);
- Richard & Yasumura (Richard et al., 2003);
- Folz & Filiatrault (Folz and Filiatrault, 2004);

- Rinaldin 2011 (Rinaldin et al., 2013);
- Pozza 2013 (Pozza, 2013a).

Foschi (Foschi, 1977) defined an analytical formulation to reproduce the hysteresis response of nailed joints including the pinching effect based on the properties of the connector and the embedment characteristics. Pinching, strength and stiffness degradations are taken into account. An application of the micro-scale model in a light frame 3D structure was carried out in (He et al., 2000).

Kivell (Kivell et al., 1981) developed a hysteretic piecewise linear model for moment-resisting nailed timber joints made with mild steel plates. The behaviour (based on the modified Takeda model) reproduce the pinching effect neglecting the strength and stiffness degradation.

Donal (Dolan, 1989) adopted the analytical formation defined by Foschi changing the softening branch law. The model reproduces the pinching behaviour neglecting strength and stiffness degradation. The hysteretic law was implemented to describe the cyclic behaviour of timber frame walls (White and Dolan, 1995) (nailed connections between the frame and the sheathing panel).

Ceccotti & Vingoli (Ceccotti and Vignoli, 1989) modelled moment-resisting joints for glulam and drift pins with a piecewise model neglecting the strength degradation. This model was the first one to be used for CLT connections (Ceccotti, 2008)[9] such as angle-brackets, hold-downs and screwed connections between adjacent panel calibrated with experimental results.

Richard and Yasumura (Richard et al., 2003) adopt the same analytical formulation of Foschi for the monotonic load changing the softening behaviour. Pinching, strength, stiffness degradation are taken into account. The model was used for the dynamic response of shearwalls.

Folz & Filiatrault (Folz and Filiatrault, 2004) during the CUREE-Caltech Wood framed Project implements an analytical model with 10 parameters in which the skeleton curve until the maximum strength capacity follows the Foschi model. The hysteretic law allows reproducing the pinching

[9]Modelled by using DRAIN-3DX in combination with purposely developed subroutines.

and the stiffness re-loading degradation.

Rinaldin (Rinaldin et al., 2013) introduce a piecewise law specific to the behaviour of CLT connections. Two types of laws were implemented: symmetrical and asymmetrical. The model allows reproducing the pinching, and the strength/stiffness degradation. Ad hoc-subroutines were developed in Abaqus permit to consider a bi-directional behaviour (tension and shear) of CLT connections by coupling the effect with a circular strength demand.

Pozza (Pozza, 2013a) proposed a simplified hysteresis model as a combination in series/parallel of uni-directional springs which reproduce the behaviour of steel connectors and the wood behaviour.

The numerical models presented before were specifically developed for timber joints/walls. However, another possible strategy to reproduce the hysteretic behaviour of timber joints/shearwall is the use of hysteretic models developed for different purposes. As an example, simplified bi-linear models or hysteretic models can be implemented, accepting some approximations. Moreover, in literature, several models incorporate the stiffness/strength degradation and the pinching effect, such as the Elwood model (Elwood and Moehle, 2006).

The hysteretic model developed by Elwood was originally implemented to reproduce the pinched load-deformation response of reinforced concrete elements under cyclic loading. In addition, unloading stiffness degradation, reloading stiffness degradation, strength degradation can be taken into account. All these aspects lead to the widespread use of this hysteretic model also in timber structures ((Rahmanishamsi et al., 2017), (Pozza et al., 2017), (Franco et al., 2019), (Lukacs et al., 2019), (Shahnewaz et al., 2020)).

3.6.2.2 Constitutive law adopted

In this thesis, several hysteretic laws were studied, such as Folz and Filiatrault (2004) and the "hysteretic law". Finally, the Elwood model was taken into account in the cycle and time-history analyses thanks to the numerical stability and the excellent fit of the experimental results. In the OpenSees platform (McKenna, 2011) the model is called "*uniaxialMaterial Pinching4*". The behaviour is a piecewise linear law.

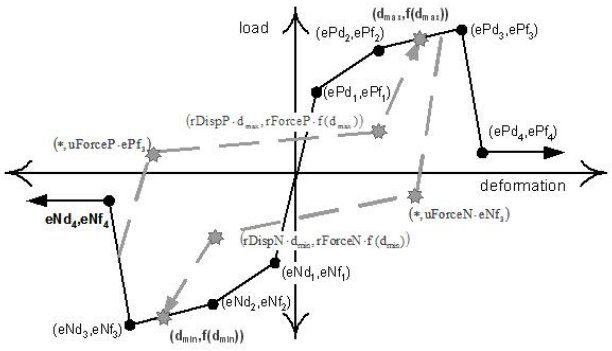

Figure 3.19. "*Pinching4Material*" for cyclic analyses ((Elwood and Moehle, 2006), (McKenna, 2011)).

To characterize the overall behaviour are required 38 parameters (22 are specific for the cycle response) (Mazzoni et al., 2006). Sixteen parameters define the backbone curves in the positive and negative branches. Additional thirteen parameters were used to characterize the pinched (rDispP, rForceP, uForceN, etc.) and unloading/reloading (gDi, gE and Damage) behaviour. More information about the damage model is available in the command language manual (Mazzoni et al., 2006).

Four experimental tests with average behaviour were taken into account. In particular, the calibration of the hysteretic parameters was based on sample #1.4 for the hold-down's tension behaviour, #3.1 and #2.5 respectively for the tension/shear behaviours of the angle-bracket and test #4.3 for the half-lap joint. The floating points were defined manually whereas the hysteretic parameters were evaluated by "MultiCal" tool (Chisari et al., 2017) within a multi-objective optimization managed by genetic algorithms (Non-dominated Sorting Genetic Algorithm II, NSGA-II)[10]. The optimization process adopted minimized the stress and the energy histories (Equations

[10]For more information see the manual.

3.20-3.21) between the numerical and the experimental test.

$$\omega_F = \frac{\sqrt{\sum_{i=1}^{T}\left(F_i^{num} - F_i^{exp}\right)^2}}{\sqrt{\sum_{i=1}^{T}\left(F_i^{exp}\right)^2}} \tag{3.20}$$

$$\omega_E = \frac{\sqrt{\sum_{i=1}^{T}\left(E_i^{num} - E_i^{exp}\right)^2}}{\sqrt{\sum_{i=1}^{T}\left(E_i^{exp}\right)^2}} \tag{3.21}$$

The results show an excellent fit for all connections and loading directions. The coefficient of determination (R^2) demonstrates excellent outcomes. Lower values of R^2 (totally acceptable, 95.85%) is for the angle-bracket in tension. The reason is associate with the discrepancy between the experimental and numerical response in compression starting from the 60% of the cyclic loading test.

	Hold Down	**Angle Bracket**		**Half-Lap Joint**
	Tension	**Tension**	**Shear**	**Shear**
ePf1 [kN]	7.95	4.71	3.33	0.76
ePf2 [kN]	34.29	15.24	20.09	3.05
ePf3 [kN]	52.07	24.17	29.50	5.90
ePf4 [kN]	31.17	15.67	22.07	5.00
ePd1 [mm]	1.00	1.00	0.50	0.20
ePd2 [mm]	10.00	8.00	12.00	2.50
ePd3 [mm]	23.65	20.98	30.28	23.55
ePd4 [mm]	30.00	30.00	50.00	40.00
eNf1 [kN]	-7.95	-4.71	-3.33	-0.76
eNf2 [kN]	-34.29	-15.24	-20.09	-3.05
eNf3 [kN]	-52.07	-24.17	-29.50	-5.90
eNf4 [kN]	-31.17	-15.67	-22.07	-5.00
eNd1 [mm]	-1.00	-1.00	-0.50	-0.20
eNd2 [mm]	-10.00	-8.00	-12.00	-2.50
eNd3 [mm]	-23.65	-20.98	-30.28	-23.55
eNd4 [mm]	-30.00	-30.00	-50.00	-40.00
rDispP	0.72	0.63	0.55	0.55
rForceP	0.18	0.1	0.32	0.15
uForceP	0.03	-0.04	0	0.06
rDispN	-0.72	-0.63	0.55	0.55
rForceN	0.18	0.1	0.32	0.15
uForceN	0.03	0.04	0	0.06
gD1	0.86	0.86	0.99	0.83
gD2	0	0	0	0
gD3	0	0	0	0
gD4	0	0	0	0
gDLim	0.04	0.08	0.15	0.15
gE	1	1	1	1
Damage	energy	energy	energy	energy

Table 3.9. Numerical input data for non-linear cyclic analyses.

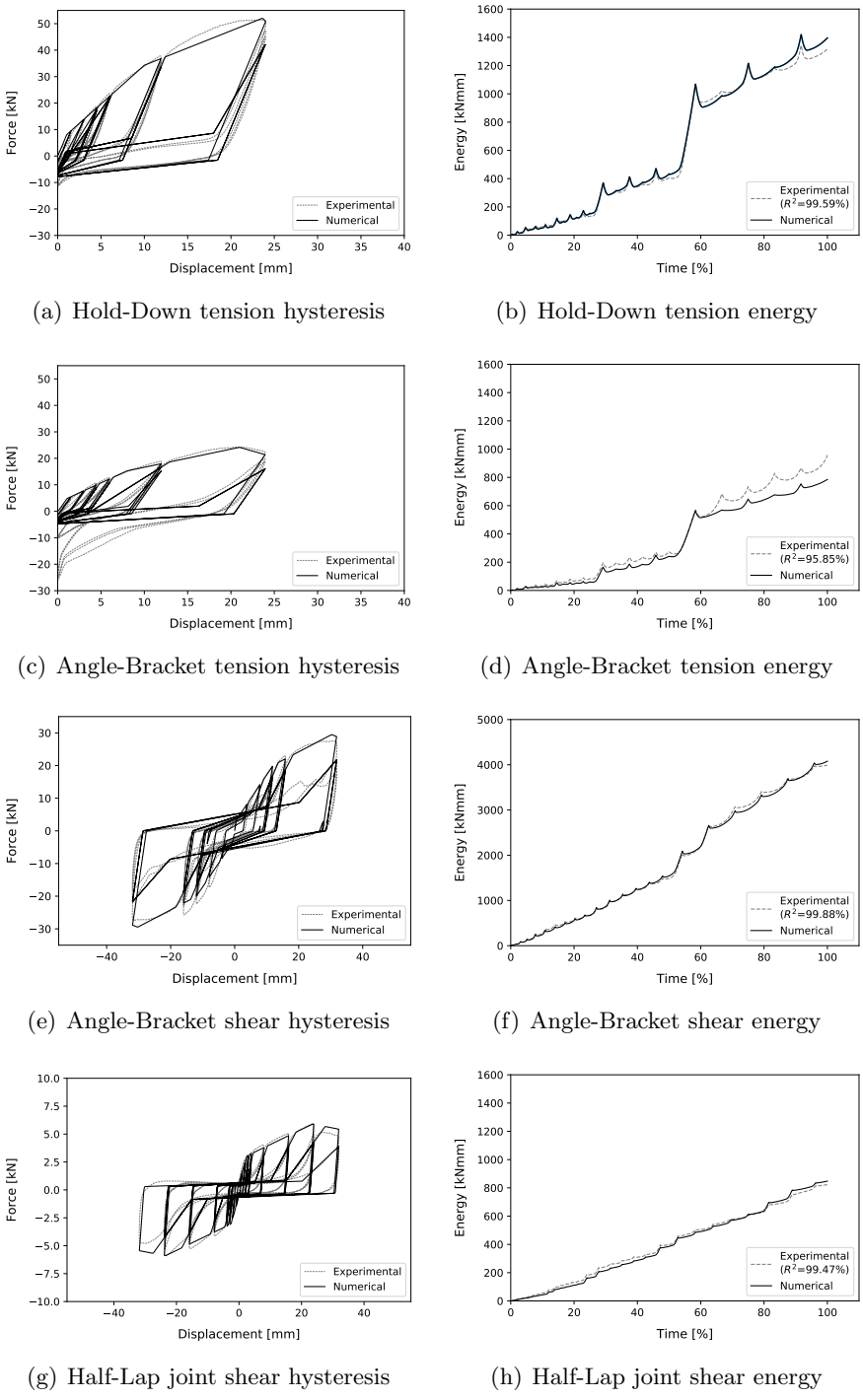

(a) Hold-Down tension hysteresis

(b) Hold-Down tension energy

(c) Angle-Bracket tension hysteresis

(d) Angle-Bracket tension energy

(e) Angle-Bracket shear hysteresis

(f) Angle-Bracket shear energy

(g) Half-Lap joint shear hysteresis

(h) Half-Lap joint shear energy

Figure 3.20. Experimental and numerical comparison/calibration for non-linear cyclic analyses.

3.6.3 Limit States and numerical modelling

As shown in section §3.4.2.2, the limit states at the connections level were defined monitoring the deformation level of the dissipative components. The following section aims to correlate the experimental evidence (especially

for bi-directional actions) with the numerical modelling for timber joints.

3.6.3.1 Bi-directional loading and dispacement domains

Looking at the kinematic mechanisms of a CLT shearwall (sliding and rocking), hold-downs and angle-brackets are subjected simultaneously to both tension and shear forces. Considering only one-loading direction in the design and in the modelling processes leads to underestimating the overall strength and the working ratio of the connections (Izzi et al., 2018a).
As analyzed in (D'Arenzo et al., 2019), the interaction between the two orthogonal directions could be included within a capacity domain. It is possible to define different shapes of domains for multiple loading directions, which were studied in (Gavric and Popovski, 2014): rectangular, triangular and circular. A circular domain gives an optimal compromise (Izzi et al., 2018b) however, currently, the usage is limited to the check of the strength capacity during the design or the verification phases. The domain is built starting from the yielding strength capacity in the two orthogonal directions by using:

$$\left(\frac{F_n}{R_n}\right)^2 + \left(\frac{F_v}{R_v}\right)^2 \leq 1 \tag{3.22}$$

where:

F_v , F_n Are the force at the i-th step respectively in the shear and tension directions;

R_v , R_n Are respectively the yielding strength in shear and tension.

The methodology is followed by the codes (e.g. (Code, 1995)) and European technical assessment for X-Lam connections (e.g. (EOTA, 2007)) and for nails (e.g. (EOTA, 2016), (EOTA, 2018)).

In this work, only the angle-brackets were considered with a circular domain since, as described before, the strength in the two orthogonal directions (shear and tension) are comparable ((Gavric and Popovski, 2014), (Flatscher et al., 2015), (Casagrande et al., 2016a)) (Figure 3.12).
Hold-downs were assumed with a uni-dimensional domain in the primary direction since they are stronger than the secondary direction (shear) (Figure

3.12).
The screws used for the vertical joint between adjacent panels (half-lap joint), as for hold-downs, had a uni-dimensional domain neglecting the in-plane separation between adjacent panels due to the bottom (angle brackets) and top (screws between vertical wall and overneath floor) of restrains (Figure 3.12).

The use of a circular domain for push-over and dynamic analyses, following the definition of the limit states at the local level, requires to switch from a strength to a displacement domain.
The domains were explicitly determined once the yield (Y), the significant damage (SD) and the near-collapse (NC) deformations in the corresponding loading directions defined following section §3.4.2.2.2.
The displacement domains of the CLT connections used in the parametric analisys in the next chapter were defined with the equations presented in Table 3.10 and displayed in Figure 3.21 with the values of section §3.5.

Limit State	**Disp. Domain**	**Hold-Down**	**Angle-Bracket**	**Half-Lap joint**
Y	DOM 1	$\frac{\delta_n}{\delta_{n,Y}} \leq 1$	$\left(\frac{\delta_n}{\delta_{n,Y}}\right)^2 + \left(\frac{\delta_v}{\delta_{v,Y}}\right)^2 \leq 1$	$\frac{\delta_v}{\delta_{v,Y}} \leq 1$
SD	DOM 2	$\frac{\delta_n}{\delta_{n,SD}} \leq 1$	$\left(\frac{\delta_n}{\delta_{n,SD}}\right)^2 + \left(\frac{\delta_v}{\delta_{v,SD}}\right)^2 \leq 1$	$\frac{\delta_v}{\delta_{v,SD}} \leq 1$
NC	DOM 3	$\frac{\delta_n}{\delta_{n,NC}} \leq 1$	$\left(\frac{\delta_n}{\delta_{n,NC}}\right)^2 + \left(\frac{\delta_v}{\delta_{v,NC}}\right)^2 \leq 1$	$\frac{\delta_v}{\delta_{v,NC}} \leq 1$

Table 3.10. Displacement domains for typical CLT connections.

where:

δ_v , δ_n Are the deformation at the i-th step respectively in the shear and tension directions;

$\delta_{v,Y}$, $\delta_{n,Y}$ Are respectively the yield strain in the shear and tension directions;

$\delta_{v,SD}$, $\delta_{n,SD}$ Are respectively the significant damage strain in the shear and tension directions;

$\delta_{v,NC}$, $\delta_{n,NC}$ Are respectively the near collapse strain in the shear and tension directions.

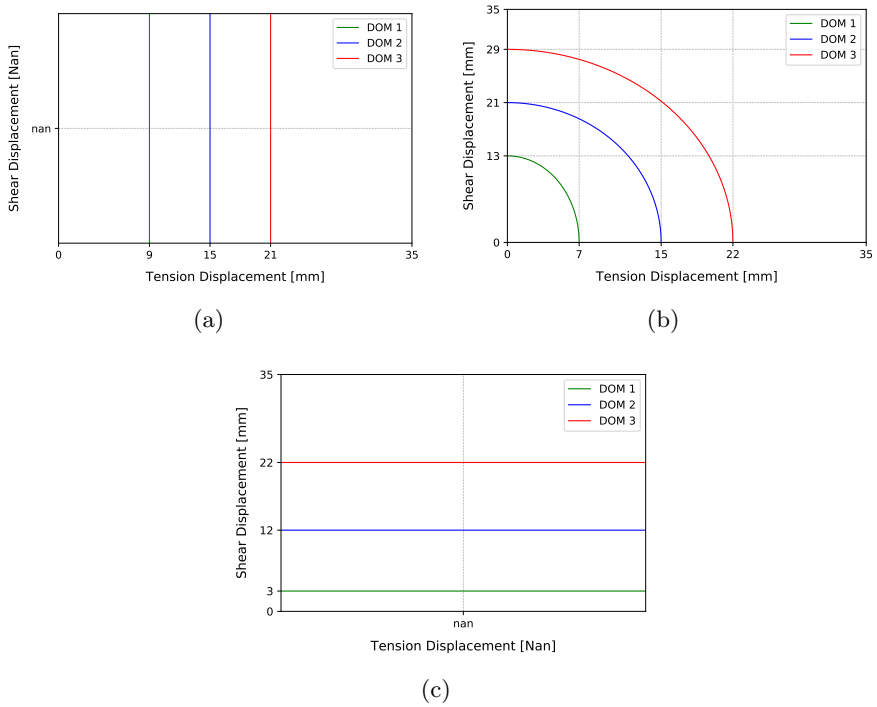

Figure 3.21. Avarage displacement domains for the analyzed connections: (a) Hold-Down, (b) Angle-Bracket, (c) Half-Lap Joint.

3.6.3.2 Numerical modelling of uni/bi-directional loading

The numerical modelling of CLT connections is a simple challenge if a uni-directional behaviour is considered for all connections. On the other hand, bi-directional behaviour is still now an open topic.

Rinaldin (Rinaldin et al., 2013) was the first who introduce a numerical interaction between the two orthogonal directions applying Equation 3.22. If the force point (F_n, F_v) is inside the domain, the two orthogonal hysteretic behaviour are independent. If the force point (F_n, F_v) exceed the limit, these values reduce the corresponding virgin backbone curves considering F_n, F_v as elastic strengths keeping constant the deformation points. Finally, when the ultimate displacement in one direction is reached, the entire spring is broken.

In OpenSees framework (McKenna, 2011), Hummel and Seim (2019a) considered the bi-directional behaviour by reducing the strengths in both directions with an α factor calibrated with a backanalysis at the wall level

($\alpha = 0.15$)[11]. The factor was used to modify the strength and the stiffness of the connections.

Except for the Rinaldin model, no ad hoc numerical constitutive laws are available in the literature to consider a coupled effect in two orthogonal directions. Generally, in the case of bi-directional behaviour of connections, the two laws are always independent. This effect leads to possible wrong outcomes since, as an example, angle-brackets could fail in tension while the shear contribution continues to work during the numerical analysis.

3.6.3.2.1 Implemented strategy

OpenSees framework (McKenna, 2011) was used in the next chapters due to the flexibility of the modelization, and as for all structural programs, the numerical coupling between multiple loading directions is impossible to define in an inelastic spring-element made of more behaviours.

In this PhD thesis, the connections were modelled as described in Table 3.11. The non-linear springs composing the zero-length and the two-node link elements have the parameters reported in Tables 3.8-3.9. Additionals parallel friction elements ("*Flat Slider Bearing Element*") (gap behaviour) with high compressive stiffness of 100 kN/mm connect the same nodes of the hold-downs and angle-brackets. A Coulomb friction law was assumed with coefficients equal to 0.35, 0.30 and 0.10 for timber-to-concrete, timber-to-timber and timber-to-steel contact, respectively (Petersen, 2013). A high initial elastic stiffness in local shear was assumed to equal 1000 N/mm (Hummel and Seim, 2019a).

The circular/uni-dimensional displacement domains (Figure 3.22) were used to control in post-processing phase at each time-step if the connections reached the yield (Y), the significant damage (SD) and the near-collapse (NC) limits with a uni/bi-directional action (tension/shear or tension+shear). Once one connection reaches the near-collapse, the wall/structure analysis was stopped accepting one failure. This strategy was followed since it is impossible to remove the collapsed connections during the analysis, and the

[11] $Q_{mod} = Q \cdot (1 - \alpha)$ where Q_{mod} is the modified quantities of strength and stiffness (called generically Q) with a rectangular domain.

Metal Connector	Behaviour	Disp. Domain	Finite Element
Hold-Down	Uni-directional	Uni-dimensional	Zero-Length + Friction
Angle-Bracket	Bi-directional	Bi-dimensional	Zero-Length + Friction
Half-Lap Joint	Uni-directional	Uni-dimensional	Two-node link

Table 3.11. Finite element modelling of metal connectors.

remaining load steps, after the failure of one connection (attainment of NC), have no physical sense. In fact, it could happen that during a non-linear analysis, only one of the two directions reaches the failure since the zero-length element with a bi-directional spring has a not-coupled behaviour.

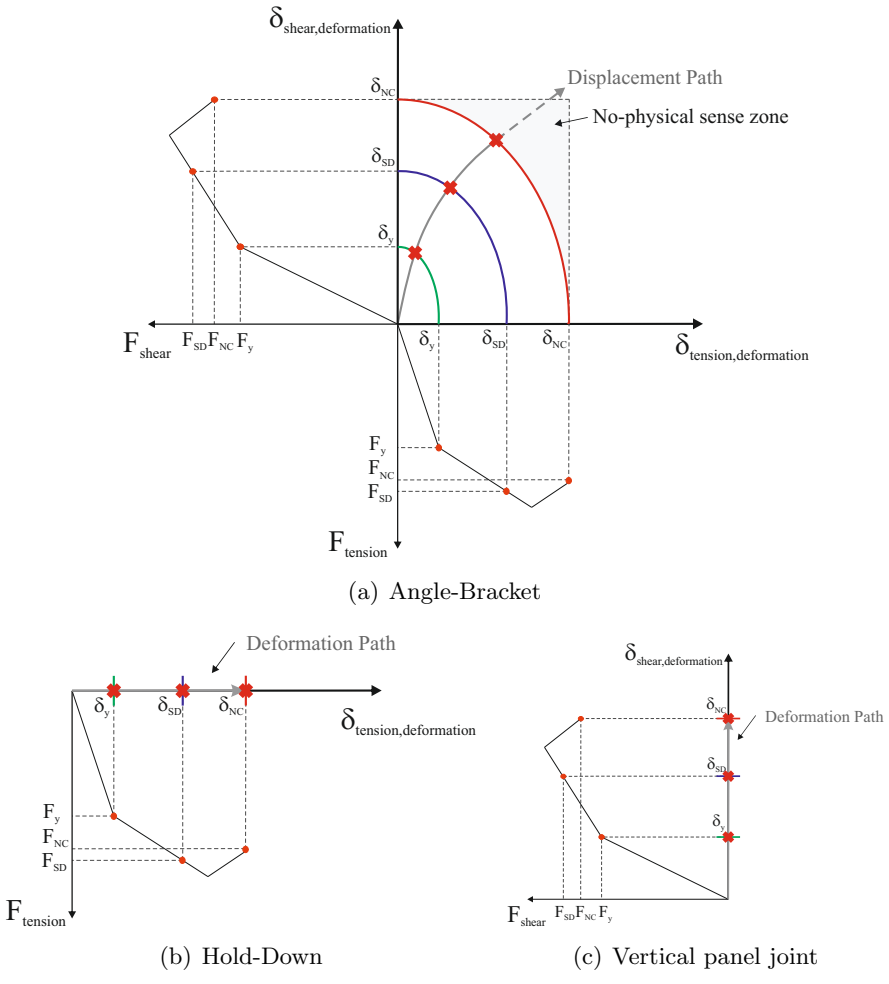

(a) Angle-Bracket

(b) Hold-Down

(c) Vertical panel joint

Figure 3.22. Displacement domains and numerical strategy for non-linear analyses.

Future studies will improve the philosophy of removing failure connections

by means of a multi-collapse analysis, as it is generally done for masonry structures.

In case of only uni-directional behaviour of the connections, such as neglecting the angle-bracket's uplift behaviour, the numerical problem is simplified since it is possible to define a minimum/maximum range deformation in which the strength became zero if these limits are attained.

[Blank page]

Practice-oriented FE model for seismic analysis of CLT buildings

---

Chapter abstract

A strong point of CLT buildings is the ability to withstand the seismic actions; however, it is not too easy to model a CLT structure due to the marked non-linear behaviour in seismic design.
In common practice, the Force-Based design method is the most common type of analysis used by engineers, requiring a suitable numerical model to capture all deformation mechanisms.

This chapter presents an upgrade of an existing practice-oriented FE design model for the seismic design of CLT structures. 2D elements are used both for the modelling of CLT panels and for mechanical connections, which are represented by a horizontal strip with a height smaller than the 7% of the height of the panel. Analytical equations for determining the elastic modulus of elasticity and the shear modulus of the horizontal strip are reported taking into account both rocking and sliding behaviour for single- and multi-panel CLT shearwalls. The validation of this proposal was carried out in terms of the shearwall lateral stiffness through the results of experimental tests on full-scale shearwalls published by other authors and through a comparison between a detailed non-linear model and the Christovasilis et al. strategy.

4.1 The in-plane behaviour of CLT shearwalls

In recent years, Cross-Laminated-Timber (CLT) buildings have been characterised by a fast-growing in the market of wood-based structural systems ((Hildebrandt et al., 2017), (Larasatie et al., 2020)). The possibility of using low-grade wooden boards (Sciomenta et al., 2019), lightness of structural panels and capacity of mechanical connections to dissipate seismic energy make CLT buildings a valuable alternative to other traditional structural types in seismic prone areas ((Pei et al., 2016), (Izzi et al., 2018a)).

Despite substantial research has been undertaken dealing with the seismic behaviour of CLT buildings, practice-oriented finite element (FE) modelling strategies for the seismic analysis of CLT structures are still at an early stage. If a general consensus has been achieved on the modelling of CLT panels, their interaction (e.g. contact between panels, contact with foundation, friction, non-linear behaviour of connections), still represent a key and challenging aspect in the development of practice-oriented linear-elastic FE models for the seismic analysis of CLT buildings.

Three main deformation contributions characterise the in-plane behaviour of single-and multi-panel CLT shearwalls, namely rocking, sliding and panel deformation. Sliding (Figure 4.1a) and rocking (Figure 4.1b) contributions are directly related to: i) the flexibility of mechanical connections (e.g. hold-down and angle-brackets) used to anchor the CLT panel to the foundation, ii) the panel aspect ratio and iii) the amount of vertical loads; the panel deformation conversely takes into account the shear and bending flexibility of the wooden elements. The major deformation contributions of single-panel shearwalls with no openings are commonly due to the rocking and sliding behaviour. A significant contribution of the CLT panel flexibility may be conversely observed in case of single-panel shearwalls with either door or window openings.

Two main rocking kinematic modes are observed in multi-panel shearwalls ((Nolet et al., 2019), (Casagrande et al., 2018)). In case of relative flexible

vertical joints, a coupled-panel behaviour with a significant slip along the vertical joint is generally observed (see Figure 4.2a) whereas a single-wall behaviour with a single centre of rotation is expected in case of relative stiff vertical joints (see Figure 4.2b).

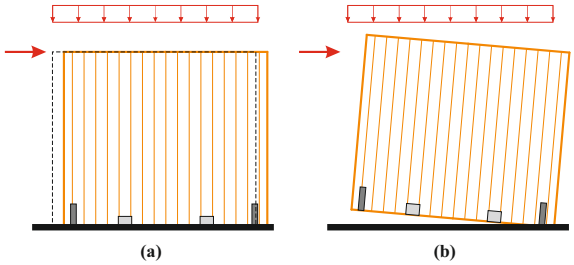

Figure 4.1. (a) Sliding and (b) rocking deformation contribution in a single-panel CLT shearwall.

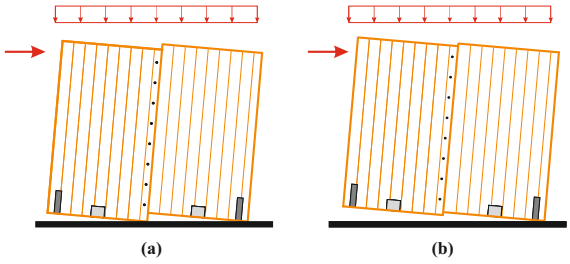

Figure 4.2. Rocking kinematic modes in a multi-panel CLT shearwall: (a) coupled panel - CP, (b) single-wall – SW.

Several analytical equations have been proposed for the determination of the lateral stiffness and the load-carrying capacity of single-panel CLT shearwalls (Lukacs et al., 2019). The main differences among the proposed equations regard the calculation of the panel length in contact with the foundation and the behaviour of mechanical anchors (hold-down and angle bracket) which may be characterised by either a uni- or a bi-directional behaviour. Analytical models for multi-panel CLT shearwalls were proposed by Gavric et al. (Gavric and Popovski, 2014), Tamagnone et al. (Tamagnone and Fragiacomo, 2018), Casagrande et al. (Casagrande et al., 2018) and Masroor et al. (Masroor et al., 2020) while Popovski et al. (Chen and Popovski, 2020) presented an analytical model for multi-panel balloon CLT shearwalls.

4.2 Overview of the practice-oriented modelling

A first modelling strategy for the seismic analysis of CLT buildings was developed within the SOFIE project (2006-2007) (Ceccotti et al., 2013), with the aim to predict the dynamic response of a 3- and a 7-storey CLT building in a shaking-table test. These models were adopted to perform non-linear dynamic analyses, taking into account the non-linear hysteretic behaviour of mechanical connections and the non-linear mutual interaction between the panels and between the panels and the foundation. Other authors proposed similar strategies for non-linear analyses of light-frame timber buildings (Follesa et al., 2010). However, it is noteworthy to mention that the complex implementation of these non-linear procedures and the need of input of several mechanical parameters have made these modelling strategies more suitable for research purposes rather than design practice (Izzi et al., 2018a).

Depending on how CLT panels are schematised, the practice-oriented FE modelling strategies of CLT shearwalls can be divided into two main categories, see Figure 4.3.

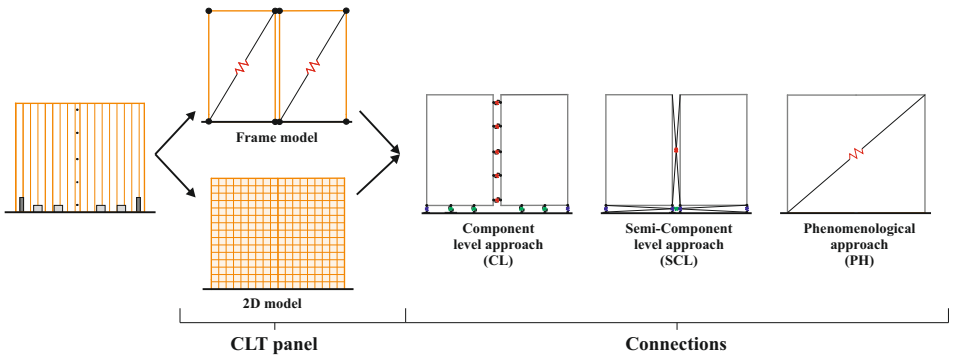

Figure 4.3. Modelling strategies for CLT panels and connections.

In a "Frame model" approach, two vertical and two horizontal frame 1D elements are used to create a hinged frame with the same width and height of the CLT panel whereas a diagonal hinged frame element is adopted to represent the lateral stiffness due to the bending and shear panel deformation (Pozza et al., 2015), (Mestar et al., 2020), (Rossi et al., 2016). According to a "2D model" approach either multi-layer or homogenous equivalent

orthotropic 2D elements are conversely used to represent the CLT panels (Rinaldin and Fragiacomo, 2016), (Sustersic et al., 2016), (Hummel and Seim, 2019b), (Christovasilis et al., 2020), (Demirci et al., 2018), (Franco et al., 2019), (Rinaldin et al., 2013), (Polastri et al., 2019). For both the two approaches the elastic properties (i.e. modulus of elasticity, shear modulus and Poisson ratio) of frame and 2D elements can be determined according to analytical equations proposed by (Bogensperger et al., 2010), (Blass and Fellmoser, 2004), (Flaig and Blass, 2013).

Three different approaches are commonly adopted for the modelling of connections. According to a "Component level – CL" approach, a link (spring) element is used to represent each single fastener (e.g. screw or nail in vertical joints) or mechanical anchor (hold-downs and angle-brackets), see (Mestar et al., 2020), (Rinaldin and Fragiacomo, 2016), (Sustersic et al., 2016), (Hummel and Seim, 2019b), (Demirci et al., 2018), (Franco et al., 2019), (Rinaldin et al., 2013), (Polastri et al., 2019). A "Semi-component Level – SCL" approach is adopted when a single link element models multiple connections or multiple mechanical anchors ((Rossi et al., 2016), (Christovasilis et al., 2020), (Ceccotti, 2008)). No spring elements are conversely adopted in the models where a "Phenomenological – PH" approach is used ((Pozza et al., 2015), (Sustersic et al., 2016)): the deformation contribution of connections and mechanical anchors is directly integrated into elastic properties of either frame or 2D elements used to model the CLT panels.

A "Frame model" was used by Ceccotti and Follesa (Ceccotti, 2008) for the modelling of CLT panels while spring elements were adopted according to a CL approach to model the interaction between the panels. An extensive comparison between the CL and PH approaches was carried out by Pozza et al. (2017), showing how the uplift forces on hold-down are generally overestimated in a PH than in a CL approach. Sustersic and Dujic (2012) introduced a detailed numerical model based on 2D elements for CLT panels and discrete springs with either uni- or bi-directional behaviour for connections and mechanical anchors (CL approach). A similar strategy was adopted by Rinaldin et al. (Rinaldin et al., 2013) while more recently

Mestar et al. (Mestar et al., 2020) proposed an equivalent frame model (EFM) for CLT walls with openings where the CL approach was used for the modelling of connections and mechanical anchors. Schickhofer and Ringhofer (2012) presented a frame model in which an equivalent two-degree of freedom spring (shear/rotation) is lumped at the shearwall base.

Follesa et al. (Follesa et al., 2013) developed a 3D building model for the seismic analysis of the 3-storey CLT building tested in the SOFIE project (Ceccotti et al., 2013); 2D elements were used to schematise CLT panels while symmetrical truss elements were implemented for angle-brackets at the bottom of shearwalls and the vertical joints between the CLT according to an SCL approach. Floor and roof panels were not explicitly modelled using a rigid in-plane constraint to simulate the diaphragm behaviour of the floor and roof elements. Christovasilis et al. (Christovasilis et al., 2020) adopted 2D elements to simulate both the flexibility of CLT panels. walls and floors, and the deformation contribution due to angle-brackets and vertical joints between the panels according to a PH approach. Both the models presented by Follesa et al. (Follesa et al., 2013) and Christovasilis et al. (Christovasilis et al., 2020) were validated through of the dynamic behaviour of low-amplitude shaking table tests (Ceccotti and Follesa, 2006), neglecting the deformation contribution due to the rocking behaviour.

The stabilising effect of the vertical load on the activation of the rocking behaviour of CLT shearwalls was taken into account in the frame model presented by Rossi et al. (Rossi et al., 2016) and Casagrande et al. (Casagrande et al., 2016b). The elastic properties of the frame models were established using analytical equations taking into account panel deformation, sliding and rocking behaviour through an iterative approach.

4.3 Proposal FE model strategy

The following section shows an upgrade of the existing practice-oriented FE design model presented by Christovasilis et al. (Christovasilis et al., 2020) to properly consider the rocking deformation contribution, given by the mechanical anchors and the vertical joints, and take into account the stabilising effect of the vertical load both for single- and multi-panel shearwalls. Many research showed that rocking represent a significant contribution in the lateral deflection of multi-storey CLT shearwall.

The upgrade is supported through the same modelling strategy presented by Christovasilis et al. (Christovasilis et al., 2020) adding some of the main features of the FE models presented by Casagrande et al. (Casagrande et al., 2016b) and Follesa et al. (Follesa et al., 2013). The strategy presented adopts 2D elements for modelling of both CLT panels and connections by using the analytical formulations proposed in (Casagrande et al., 2018), (Casagrande et al., 2016b) to properly take into account the rocking deformation contribution in the determination of the effective modulus of elasticity and shear modulus of the 2D elements.

4.3.1 Modelling strategy and kinematic modes

Single- and multi-panel CLT shearwall are modelled as in Figure 4.4. Orthotropic homogeneous 2D elements are adopted to reproduce: the floor of thickness s, the CLT panels of heigh H and the connections as an horizontal strip of height h at the bottom of the shearwall. All 2D elements have a thickness equal to the CLT panel t.

The vertical elastic modulus of the floor is assumed equal to the out-of plane compressibility (modulus of elasticity perpendicular to grain $E_{c,90}$) to account the deformability due to the rocking mechanism. The remaining moduli are assumed stiff to neglect the deformations in the other directions.

Effective modulus of elasticity along the vertical and horizontal direction, $E_{ef,2D,v}$ and $E_{ef,2D,h}$, are used to take into account the in-plane axial deformation contribution of the CLT panel whereas an effective in-plane

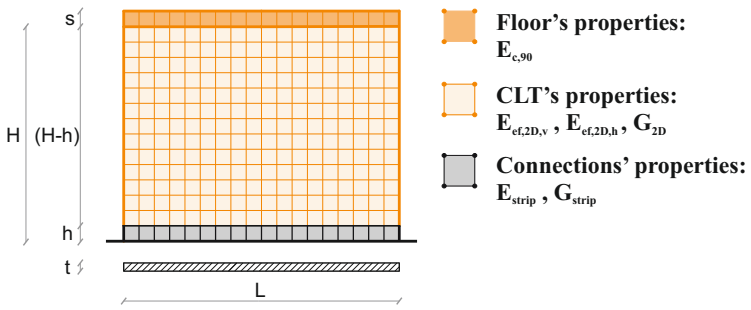

Figure 4.4. Modelling of CLT shearwalls by means of 2D elements and horizontal area strips.

shear modulus G_{2D} is defined to consider the influence of torsional deformation of laminations on the in-plane shear deformability of the panel. The analytical equations reported in (Bogensperger et al., 2010), (Blass and Fellmoser, 2004) or (Flaig and Blass, 2013) can be adopted for the determination of $E_{ef,2D,v}$, $E_{ef,2D,h}$ and G_{2D} depending on CLT panel layout. A null value of Poisson ratios is adopted according to (Christovasilis et al., 2020) and (Turesson et al., 2019) disaggregating the stress/deformation in the two orthogonal directions.

The equivalent modulus of elasticity along the vertical direction E_{strip} and shear modulus G_{strip} of the horizontal strip take into account the deformation contribution due to rocking and sliding behaviour of each shearwall, see Figure 4.5b. The height h of the base strip is assumed equal to or smaller than $0.07 \cdot H$ to reduce the error of accuracy due to the base strip's physical dimension. For CLT wall with H equal to 3m, the h is around 20cm.

E_{strip} and G_{strip} are calculated at different levels and depending on mechanical properties of the shearwall can assume different values at the different storeys.

In order to ensure a high level of ductility and energy dissipation in multi-panel shearwalls, a coupled panel behaviour (CP) with the yielding of the vertical joints is assumed at each storey. Therefore, the modelling strategy presented in this section should be adopted only if the multi-panel shearwalls are designed according to a capacity design approach such that the CP behaviour is ensured and the SW behaviour is avoided. Analytical expressions and design provisions for the design of a multi-panel CLT

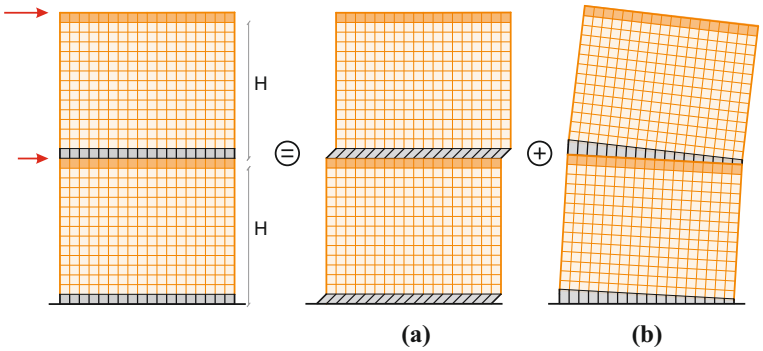

Figure 4.5. Multi-storey deformation: (a) sliding deformation, (b) rocking deformation.

shearwall characterised by a CP behaviour where all vertical joints yield are available in (Casagrande et al., 2019).

For single-panel shearwalls, a rigid rotation of shearwalls at each level due to the rocking mechanism which causes a linear increase of the lateral displacement of the upper stories (i.e. cantilever behaviour) is supposed, see Figure 4.6a. Due to the smaller size of panels in a multi- than a single-panel wall, it is assumed that in multi-panel shearwalls the panels do not significantly contribute to the out-of-plane bending of the floor panels which, for this reason, do not rotate ($\varphi = 0$, see Figure 4.6b). No rotation accumulation along the height of the buildings is hence supposed; no influence of the rocking behaviour at the upper stories is hence considered, according to a multi-panel shear-type behaviour.

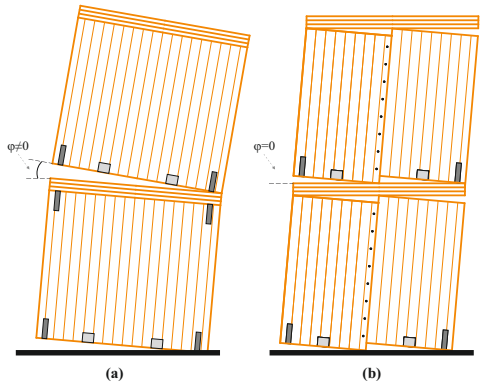

Figure 4.6. Kinematic modes for multi-story single-(a) and multi-panel (b) shearwalls.

It is noteworthy to mention that vertical strips made with equivalent

2D elements were used by Christovasilis et al. (Christovasilis et al., 2020) to properly model the deformation contribution due to vertical joints in multi-panels shearwalls; in the upgraded model presented in this paper, the deformation contribution of the vertical joint is conversely integrated into bottom horizontal strip. This choice was made in order that the deformation contribution of vertical joint is properly taken into account in the rocking deformation of the multi-panel CLT shearwalls. In (Christovasilis et al., 2020), in fact, the contribution of vertical joints was only related to the shear deformation of the panels.

In the upgraded model, the friction contribution is neglected as done in common practice and specified in (Izzi et al., 2018a) when the Force-Based Design (FBD) approach is adopted. In (Follesa et al., 2013) and (Sustersic and Dujic, 2012) an additional stiffness provided by the friction effect is included in the total stiffness of the angle bracket considering the yield displacement of the weak fastener of the shear-transferring connections and the total friction force assuming a friction coefficient equal to 0.4 for each wall.

4.3.2 Elastic lateral stiffness of single- and multi-panel CLT walls

The estimation of the elastic stiffness associated to the sliding and rocking mechanisms for single- and multi-panel CLT walls is based on the mechanical elastic behaviour under in-plane lateral loads.

4.3.2.1 Rocking stiffness

A secant rocking stiffness K_r evaluated at the 40% of the overturning moment capacity at the yielding of the hold-downs $M_{0.4HD,y}$ $(0.4 \cdot M_{HD,y})$, with the corresponding relative lateral top displacement $d_{0.4HD,y}$ is used in the proposal strategy.

$$K_r = \frac{M_{0.4HD,y}}{d_{0.4HD,y} \cdot H} \tag{4.1}$$

The effect of the activation/no-activation of the rocking mechanism is integrating by comparing the stabilising moment contribution M_{stab} due to the vertical loads and the overturning moment $M_{0.4HD,y}$. The stabilising moment contribution is directly defined once known the amount of the vertical load per unit length w and, the total length of the wall L in single-panel shearwalls, and the length/number b_{CLT}/m of each single-panel in multi-panel shearwalls. The overturning moment capacity at the yielding of the hold-downs $M_{HD,y}$ is estimated via kinematic relationships specific for the shearwalls type. A secant stiffness at 40% is considered as generally done for shearwall in ASTM (2019).

Since a secant rather than the initial lateral stiffness is adopted, a linear analysis can be conducted without considering the activation force of rocking through an iterative approach. The contribution of the activation force is in fact automatically included in the determination of the rocking capacity at $M_{HD,y}$ as shown in Figure 4.7 for both single- and multi-panel shearwalls. If $M_{0.4HD,y}$ is greater of M_{stab}, the secant stiffness K_r defines the rocking stiffness, on the contrary, the rocking is considered no-active. This approach allows accounting the only sliding deformation contribution into the G_{strip} if the vertical loads inhibit the rocking mechanism. As a

basic assumption for both shearwall types, the angle-brackets are assumed to work elastically along the tension direction.

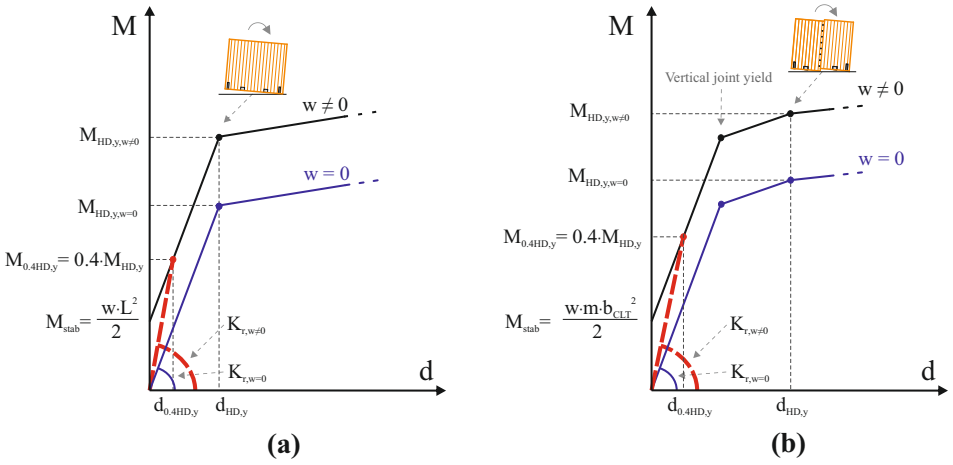

Figure 4.7. Secant stiffness due to the stabilising effect of the vertical load on a single- (a) and multi-panel (b) CLT shearwall.

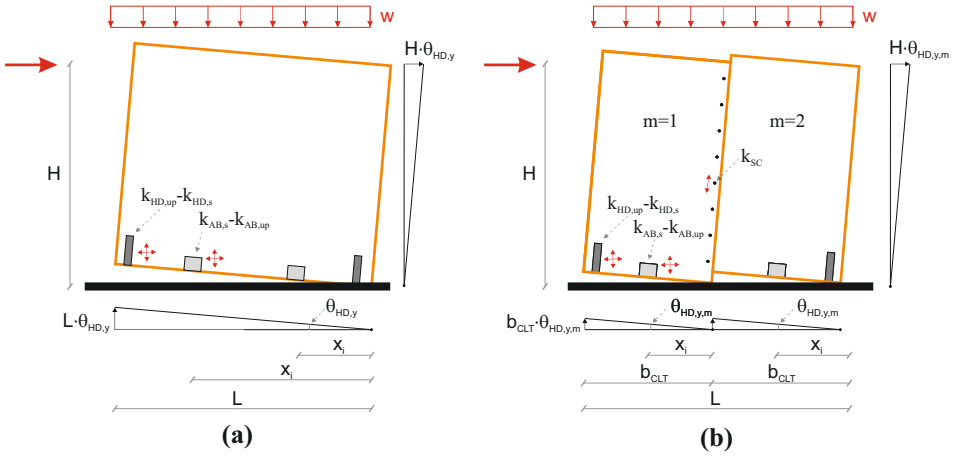

Figure 4.8. Rocking kinematic configurations used to determine the equivalent lateral stiffness of shearwalls at the yield condition of single- (a) and multi-panel (b) shearwalls.

Single-panel shearwall

In a single-panel shearwall, the overturning moment $M_{HD,y}$ related to the yielding of the hold-downs (Equation 4.2) is defined fixing the rotation $\theta_{HD,y}$ equal to the ratio between the yield displacement of hold-down along the vertical (tensile) direction and the distance between the centre of rotation and the position of the hold-down (approximable to L). The lateral top displacement corresponding to $M_{0.4HD,y}$ is evaluable with Equation 4.3.

$$M_{HD,y} = L \cdot \left[F_{y,HD,up} + \frac{u_{HD,y} \cdot k_{AB,up}}{L^2} \sum_{0}^{n_{AB}} x_i^2 + \frac{w \cdot L}{2} \right] \tag{4.2}$$

$$d_{0.4HD,y} = \frac{M_{0.4HD,y} - 0.5 \cdot w \cdot L^2}{L^2 \cdot k_{HD,up} + k_{AB,up} \cdot \sum_{0}^{n_{AB}} x_i^2} \cdot H \tag{4.3}$$

where:

$M_{HD,y}$	the overturning moment capacity at the hold-down yielding;
$d_{0.4HD,y}$	the lateral top displacement corresponding to $M_{0.4HD,y}$;
x_i	distance of the angle bracket i-th from the centre of rotation ;
$F_{y,HD,y}$	hold-down yield tensile strength;
$k_{HD,up}$	hold-down stiffness along vertical (tensile) direction;
$k_{AB,up}$	angle-bracket stiffness along vertical (tensile) direction;
$u_{HD,y}$	yield displacement of hold-down along vertical (tensile) direction;
n_{AB}	is the number of angle-brackets per each shearwall;
w	vertical load per unit length.

Multi-panel shearwall

According to Follesa et al. (2018) and as proposed into the new draft of Eurocode 8, in multi-panel CLT shearwall, all vertical joints should yield before hold-down and angle-brackets in order to maximise the ductility and energy dissipation as exhibit in a couple panel behaviour, see Figure 4.2b. Fixing the rotation $\theta_{HD,y,m}$ as the ratio of the yield tensile deformation of the hold-down and the length of each CLT panel b_{CLT}, the overturning capacity at the hold-down yielding is calculated with Equation 4.4. The multi-panel shearwall lateral displacement $d_{0.4HD,y}$ is estimated with Equation 4.5.

$$M_{HD,y} = b_{CLT} \cdot \left[F_{y,HD,up} \cdot \left(1 + \frac{1}{b_{CLT}^2} \frac{k_{AB,up}}{k_{HD,up}} \sum_0^{n_{AB}} x_i^2 \right) + (m-1) \cdot n_{SC} \cdot F_{y,SC} + \frac{w \cdot m \cdot b_{CLT}}{2} \right] \tag{4.4}$$

$$d_{0.4HD,y} = \frac{M_{0.4HD,y} - 0.5 \cdot w \cdot m \cdot b_{CLT}^2}{b_{CLT}^2 \cdot \left(k_{HD,up} + (m-1) \cdot n_{SC} \cdot k_{SC} + \frac{k_{AB,up}}{b_{CLT}^2} \sum_0^{n_{AB}} x_i^2 \right)} \cdot H \tag{4.5}$$

where:

$M_{HD,y}$	the overturning moment capacity at the hold-down yielding;
$d_{0.4HD,y}$	the lateral top displacement corresponding to $M_{0.4HD,y}$;
b_{CLT}	is the length of each CLT panel;
x_i	distance of the angle bracket i-th from the centre of rotation of the CLT panel;
m	is the number of panels;
n_{SC}	is the number of fasteners along the vertical joint;
$F_{y,HD,up}$	hold-down yield tensile strength;
$F_{y,SC}$	shear strength of each fastener;
$k_{HD,up}$	hold-down stiffness along vertical (tensile) direction;
$k_{AB,up}$	angle-bracket stiffness along vertical (tensile) direction;
k_{SC}	stiffness of each fastener along the vertical joint;
n_{AB}	is the number of angle-brackets per each shearwall;
w	vertical load per unit length.

4.3.2.2 Sliding stiffness

The lateral stiffness of the shearwalls related to sliding mechanism K_s is calculated according to Equation 4.6 considering the stiffness of angle-brackets and hold-down along the horizontal direction.

$$K_s = n_{AB} \cdot k_{AB,s} + n_{HD} \cdot k_{HD,s} \tag{4.6}$$

where:

n_{AB} is the number of angle-brackets per each shearwall;

n_{HD} is the number of hold-downs per each shearwall;

$k_{AB,up}$ angle-bracket stiffness along horizontal (shear) direction;

$k_{HD,up}$ hold-down stiffness along horizontal (shear) direction.

4.3.2.2.1 Friction contribution

Even if the friction contribution is not accounted in the proposed strategy due to the considerations in §4.3.1, Equation 4.7 shows the proper equation which could be implemented. If the friction contribution is taken into account, the addition K_f should be added to Equation 4.6.

$$K_f = \frac{\mu_k \cdot w \cdot L}{u_{AB,y,s}} \tag{4.7}$$

where:

μ_k coefficient of kinetic friction;

$u_{AB,y,s}$ yield displacement of angle-bracket along horizontal (shear) direction of the weakest connection.

This contribution leads to estimate the sliding stiffness as a function of the vertical load, the friction coefficient and the shear yielding deformation of the shear-transferring connection.

4.3.3 Analytical equations for the elastic properties of bottom horizontal strip 2D elements

The analytical equations adopted to define the modulus of elasticity E_{strip} and shear modulus G_{strip} of 2D elements representing the deformation contribution of mechanical anchors and vertical joints in the horizontal strip are presented.

For each single-panel wall, E_{strip} and G_{strip} are calculated by considering the rocking and sliding mechanical behaviour, respectively.
For multi-panel walls, since the accumulation of rotations along with the height of the wall was neglected and a shear-type behaviour was assumed, both rocking and sliding behaviour are integrated into the shear modulus

of the strip G_{strip}. The shear deformation of the horizontal strip does not in fact contribute to the rotation at the top of the shearwall and for this reason the lateral displacement of the upper storeys is not influenced by the accumulation of rotations by the lower storeys.

The values of modulus of elasticity and shear modulus of 2D elements of the strip are determined in order that the CLT shearwalls are characterised by the same rocking K_r and sliding K_s equivalent lateral elastic stiffness of the shearwall according to Equations 4.8-4.9-4.9-4.11.
For single-panel shearwalls:

$$G_{strip} = K_s \cdot \frac{h}{L \cdot t} \tag{4.8}$$

$$E_{strip} = \begin{cases} K_r \cdot \frac{12 \cdot h \cdot H^2}{L^3 \cdot t} \leq E_{ef,2D,v} & \text{if } M_{stab} = \frac{w \cdot L^2}{2} < M_{0.4HD,y} \\ E_{ef,2D,v} & \text{if } M_{stab} = \frac{w \cdot L^2}{2} \geq M_{0.4HD,y} \end{cases} \tag{4.9}$$

For multi-panel shearwalls:

$$G_{strip} = \begin{cases} \left(\frac{1}{K_s} + \frac{1}{K_r}\right)^{-1} \cdot \frac{h}{L \cdot t} \leq K_s \cdot \frac{h}{L \cdot t} & \text{if } M_{stab} = \frac{m \cdot w \cdot b_{CLT}^2}{2} < M_{0.4HD,y} \\ K_s \cdot \frac{h}{L \cdot t} & \text{if } M_{stab} = \frac{m \cdot w \cdot b_{CLT}^2}{2} \geq M_{0.4HD,y} \end{cases} \tag{4.10}$$

$$E_{strip} = E_{ef,2D,v} \tag{4.11}$$

where:

H is the height of the wall panel;

L is the length of the panel;

h is the the height of the base-strip;

t is the the thickness of the CLT panel.

4.4 Validation with experimental full-scale test

The validation of the modelling strategy presented in this section was carried out by comparing the values of the lateral stiffness of single- and multi-panel CLT shearwalls obtained from the experimental tests presented in (Gavric et al., 2015c) with those from finite element models.

Three wall panel configurations with dimensions equal to 2.95x2.95m were considered: single-panel walls (Test I – Figure 4.9a), two-panel walls with a half-lap vertical joint (Test II) and two-panel walls with spline vertical joint (Test III), see Figure 4.99b. All wall specimens were made of 5-layer CLT panels with a total thickness of 85mm (**17**-17-**17**-17-**17**). The mechanical properties in terms of elastic stiffness K_{el}, yield strength F_y, and yield displacement u_y of connections used in the experimental tests are reported in (Gavric et al., 2015a) and (Gavric et al., 2015b) and summarised in Table 4.2. For angle-brackets a bi-directional behaviour along vertical (tensile) and horizontal (shear) direction was assumed while uni-directional behaviour along the direction parallel to the vertical joints was adopted for half-lap/spline joints and along vertical (tensile) direction for hold-downs. The shear stiffness of the hold-downs is neglected due to the premature yielding slip that affects the shearwall's lateral response only at the early loading stages.

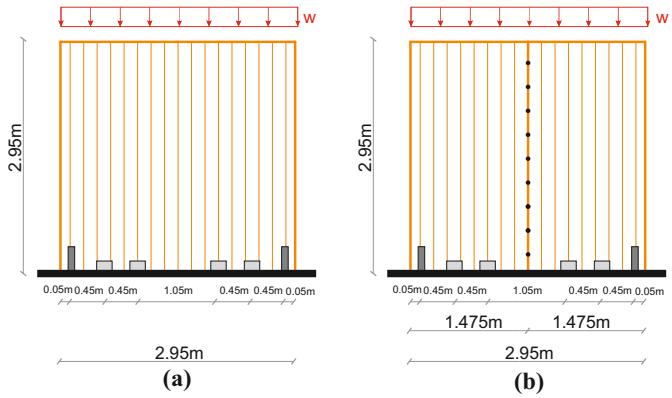

Figure 4.9. Experimental shearwall tests presented in (Gavric et al., 2015c): single- (a) and multi-panel (b) shearwalls.

The effective elastic moduli along the vertical $E_{ef,2D,v}$ and horizontal $E_{ef,2D,h}$ direction as well as the effective shear modulus G_{2D} of the 2D

	Hold-Down	Angle bracket		Screws Half-lap	Screws Spline
	Tension	Tension	Shear	Shear	Shear
F_y [kN]	40.44	19.24	23.01	3.24	4.85
F_{max} [kN]	48.33	23.47	26.85	5.25	7.33
F_{ult} [kN]	38.79	18.74	21.48	4.20	5.86
K_{el} [kN/mm]	4.59	2.65	1.96	1.27	0.85
K_{p1} [kN/mm]	0.68	0.41	0.23	0.10	0.09
K_{p2} [kN/mm]	-2.77	-0.86	-1.60	-0.13	-0.45
u_y [mm]	8.81	7.26	11.74	2.55	5.70
u_{max} [mm]	20.30	17.69	28.51	23.50	34.37
u_{ult} [mm]	23.75	23.19	31.86	31.55	37.66

Table 4.1. Mechanical parameters of hold-down, angle-brackets and screws in vertical joints ((Gavric et al., 2015a), (Gavric et al., 2015b)).

Shear wall	Test ID	Num. HD	Num. AB	Num. SC	Vert. Load [kN/m]
Single-panel	I.1	2	2	-	18.5
	I.2	2	4	-	18.5
	I.3	2	4	-	9.25
Multi-panel half-lap	II.3	2	4	10	18.5
Multi-panel Spline	III.2	2	4	2x10	18.5
	III.4	2	4	2x10	18.5
	III.5	2	4	2x10	18.5
	III.6	2	4	2x10	0

Table 4.2. Number of hold-down, angle-brackets, screws in the vertical joints and vertical load.

elements representing the CLT panels in the FE models were equal to 6748 MPa, 4622 MPa and 530 MPa and were calculated according to equations proposed in (Bogensperger et al., 2010) and (Blass and Fellmoser, 2004), assuming an elastic modulus of elasticity E_0 and shear modulus G_{mean} of wooden boards equal to 11000 MPa and 690 MPa, respectively. The modulus of elasticity E_{strip} and the shear modulus G_{strip} of the horizontal strip were calculated according to the analytical equations reported in the previous section, as shown in Table 4.3.

Test ID	G_{strip} [MPa]	E_{strip} [MPa]	$K_{proposal}$ [kN/mm]	K_{exp} [kN/mm]	Var. [%]
I.1	3.13	371.92	3.49	4.69	-25.62
I.2	6.25	253.61	5.49	4.78	14.95
I.3	6.25	128.70	4.62	4.97	-6.98
II.3	3.66	-	4.36	4.48	-2.66
III.2	3.10	-	3.77	3.5	7.83
III.4	3.10	-	3.77	3.13	20.57
III.5	3.10	-	3.77	3.77	0.10
III.6	2.11	-	2.67	2.82	-5.29

Table 4.3. Comparison in terms of lateral stiffness between experimental tests and FE models.

The values of the lateral stiffness obtained from the experimental tests

K_{exp} and from the finite element models $K_{proposal}$ are reported in Table 4.3. The values of $K_{proposal}$ were assessed by means of a linear-elastic analysis, as the ratio of a top horizontal force of 10 kN and the corresponding lateral displacement of the shearwall. The scatter of the experimental results of tests III.2-4-5 shows the intrinsic randomness of the experimental values, responsible for the same discrepancy of tests I.1-2. Therefore, the results show a reasonable accuracy of the modelling strategy, especially for the multi-panel configurations.

4.5 Validation and Comparison

This section aims to validate the New Proposal (NP) through a non-linear Target Model (TM) based on the component level approach and to perform a comparison with the Christovasilis et al. modelling strategy (CH). Two in-plane structural configurations made in single-/multi-panel walls are taken into account.

Two geometrical configurations composed of 3-storey seismic load resisting system (SLRS) with two CLT shearwalls are presented. The first configuration (see Figure 4.10) has shearwalls with aspect ratio L/H greater than one (shearwall-6m L/H=2.14 and shearwall-4m L/H=1.43) while the second configuration (see Figure 4.11) has shearwalls with aspect ratio L/H smaller than one (shearwall-2.8m L/H=1.0 and shearwall-2.4m L/H=0.86). The use of different wall aspect ratios was followed to investigate configurations in which the rocking mechanisms could be limited ($L/H > 1$) or substantial ($L/H \leq 1$). The two configurations of SLRS were designed as single-panel and multi-panels shearwall according to the provisions reported in the timber section of the draft document for the revision process of Eurocode 8 (Follesa et al., 2018). Each configuration was analysed in the presence and in the absence of the vertical loads to examine different scenarios.

The two shearwalls were made with 5-layer CLT panel with a total thickness of 100 mm. The shearwalls height was 2.8m with a floor thickness of 200mm for a total inter-storey height of 3m. The same mechanical anchors (hold-down -HD and angle-brackets -AB) and screws SC along the half-lap vertical joints presented in the previous section for the validation with the experimental tests were adopted. The number and layout of hold-down, angle-brackets and screws at each storey are reported in Tables 4.4 and 4.5. A uniform distributed loads equal to 18 kN/m and 6 kN/m were applied respectively at the inter-storeys and roof level for both shearwalls. The lateral design loads were distributed over the height of building either according to the seismic masses and stories height.

All modelling strategies adopt CLT panels modelled using 2D elements

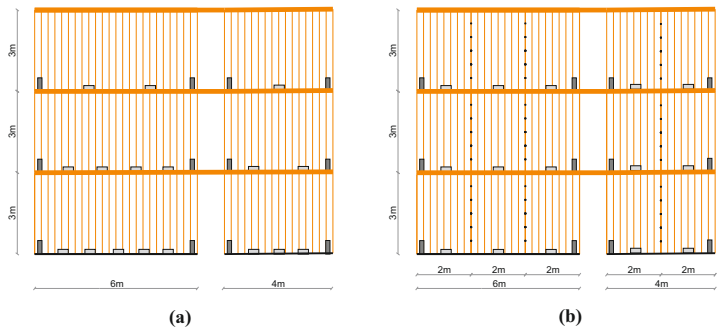

Figure 4.10. SLRS configuration 1 ($L/H > 1$): single- (a) and multi-panels (b) shearwalls.

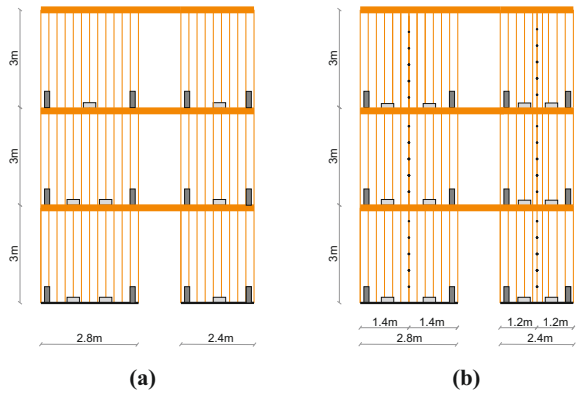

Figure 4.11. SLRS configuration 2 ($L/H \leq 1$): single- (a) and multi-panels (b) shearwalls.

characterised by the same effective moduli of elasticity and shear modulus used in the previous section.

In the TM (Figures 4.12a-4.12c, Figures 4.13a-4.13c), the mechanical anchors (hold-down, angle-bracket and screws) were modelled by means of non-linear links (spring) whose mechanical behaviour were described by the tri-linear curve reported in Table 4.1. A uni-directional behaviour along the vertical–tensile direction was assumed for the hold-downs while for angle-brackets a bi-directional behaviour were used. For the sake of simplicity, equivalents angle-brackets are lumped in the middle of each panel. The floor's compressibility was accounted with gap-elements assuming an elastic modulus $E_{c,90}$ equal to 370 MPa and calibrated with the mesh-size. The base contacts were assumed rigid. Rigid horizontal frames connect the two shearwalls in multi-panel configurations. Each single-panel is hinged at the top centre with the rigid frame while non-linear springs and contacts connect the downer frame to the panel bottom. In single-panel configurations,

kinematic constraints connect the shearwalls whereas floors were not explicitly modelled.

The values of the elastic moduli E_{strip}, the shear modulus G_{strip} and the shear modulus of vertical joint G_{sc} (the last one valid only for CH) of the CH and the NP at each storey and for each wall are reported in Tables 4.6-4.7 (Figures 4.13b-4.13d, Figures 4.13b-4.13d). The E_{strip} and G_{strip} moduli were calibrated for a base strip of 200 mm while G_{sc} for 50 mm with a length of 2.6 m. The floors were modelled in both models with an elastic modulus $E_{c,90}$ in the vertical direction equal to 370 MPa whereas the remaining moduli were equal to 110 GPa.

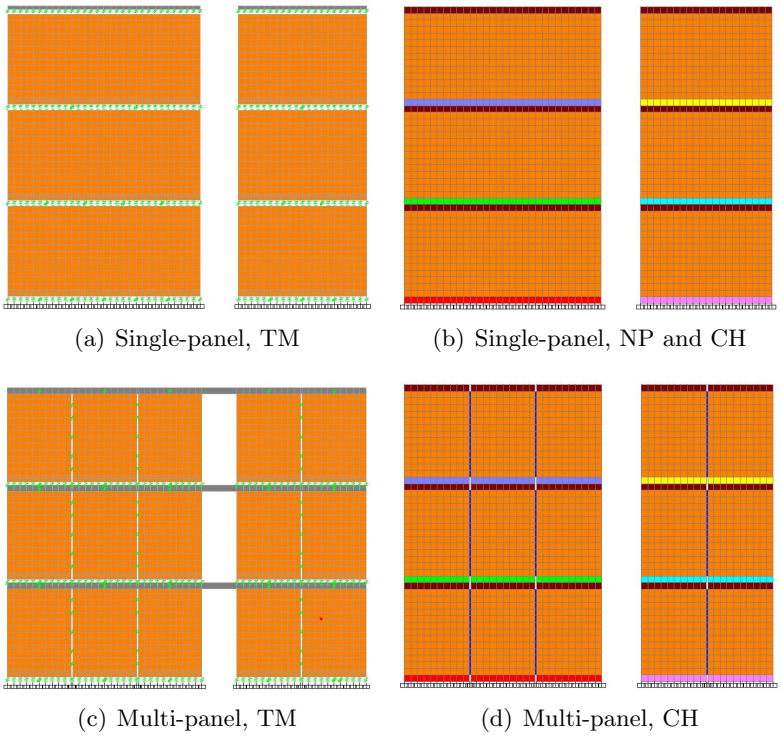

(a) Single-panel, TM (b) Single-panel, NP and CH

(c) Multi-panel, TM (d) Multi-panel, CH

Figure 4.12. FE models of configuration 1: $L/H > 1$

The comparison between the two models was performed in terms of lateral stiffness of the SRLS.

According to the CH and the NP, the SRLS lateral stiffness for the models was determined through a modal analysis from the values of the mass and the fundamental period of the SRLS at the first mode. The TM lateral

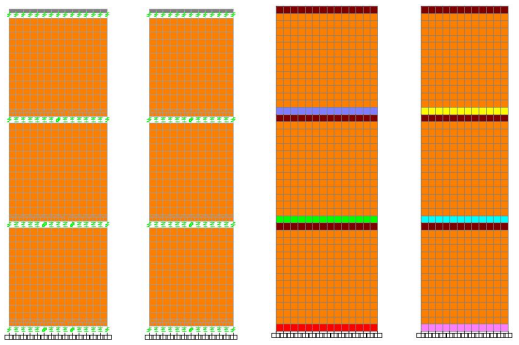

(a) Single-panel, TM (b) Single-panel, NP and CH

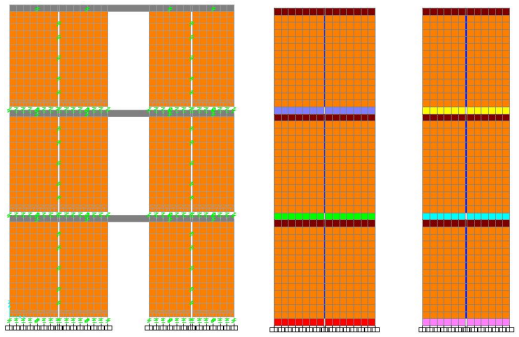

(c) Multi-panel, TM (d) Multi-panel, CH

Figure 4.13. FE models of configuration 2: $L/H \leq 1$

	Single-panel model		**Multi-panel model**	
Storey	shearwall-6m	shearwall-4m	shearwall-6m	shearwall -4m
1	2 HD 5 AB	2 HD 3 AB	2 HD 7 AB* 5 SC	2 HD 9 AB 5 SC
2	2 HD 4 AB	2 HD 2 AB	2 HD 5 AB* 5 SC	2 HD 7 AB 5 SC
3	2 HD 2 AB	2 HD 1 AB	2 HD 4 AB 5 SC	2 HD 3 AB 5 SC

*with double strength and stiffness of the standard values.

Table 4.4. SLRS configuration 1 ($L/H > 1$): layout of anchors.

stiffness was estimated as the secant line at the 40% of the maximum load on the pushover since non-linear behaviour of connections and gap elements are used. An elastoplastic curve was defined with the equivalent energy elastic-plastic (EEEP) bilinear idealisation method. The load profile was kept from the modal load path of the NP modal analysis.

	Single-panel model		Multi-panel model	
Storey	shearwall-3m	shearwall-2.4m	shearwall-2.8m	shearwall -2.4m
	2 HD	2 HD	2 HD	2 HD
1	2 AB	1 AB	3 AB*	5 AB
			5 SC	5 SC
	2 HD	2 HD	2 HD	2 HD
2	2 AB	1 AB	5 AB	4 AB
			5 SC	5 SC
	2 HD	2 HD	2 HD	2 HD
3	1 AB	1 AB	2 AB	2 AB
			5 SC	5 SC

*with double strength and stiffness of the standard values.

Table 4.5. SLRS configuration 2 ($L/H \leq 1$): layout of anchors.

		Christovasilis et al.				New Proposal			
		Single-panel model		Multi-panel model		Single-panel model		Multi-panel model	
Storey	Modulus	Shearwall L=6m [MPa]	Shearwall L=4m [MPa]	Shearwall L=6m [MPa]	Shearwall L=4m [MPa]	Shearwall L=6m [MPa]	Shearwall L=4m [MPa]	Shearwall L=6m [MPa]	Shearwall L=4m [MPa]
	G_{strip}	3.27	2.94	9.15	8.82	3.27	2.94	9.15-w 3.02-w/o	8.82-w 2.90-w/o
1	E_{strip}	-	-	-	-	6748-w 34.55-w/o	6748-w 41.45-w/o	-	-
	G_{sc}			1.22	1.22	-	-	-	-
	G_{strip}	2.61	1.96	6.53	6.86	2.61	1.96	5.52-w 2.51-w/o	5.27-w 2.52-w/o
2	E_{strip}	-	-	-	-	6748-w 31.08-w/o	6748-w 36.37-w/o	-	-
	G_{sc}			1.22	1.22	-	-	-	-
	G_{strip}	1.31	0.98	2.61	2.94	1.31	0.98	1.78-w 1.48-w/o	1.86-w 1.55-w/o
3	E_{strip}	-	-	-	-	65.57-w 24.25-w/o	64.95-w 31.52-w/o	-	-
	G_{sc}	-	-	1.22	1.22		-	-	-

-w with vertical loads, -w/o without vertical loads.

Table 4.6. SLRS configuration 1 ($L/H > 1$): Elastic and shear moduli of the horizontal stripes.

		Christovasilis et al.				New Proposal			
		Single-panel model		Multi-panel model		Single-panel model		Multi-panel model	
Storey	Modulus	Shearwall L=2.8m [MPa]	Shearwall L=2.4m [MPa]	Shearwall L=2.8m [MPa]	Shearwall L=2.4m [MPa]	Shearwall L=2.8m [MPa]	Shearwall L=2.4m [MPa]	Shearwall L=2.8m [MPa]	Shearwall L=2.4m [MPa]
	G_{strip}	2.80	1.63	8.40	8.17	2.80	1.63	7.83-w 2.02-w/o	6.38-w 1.72-w/o
1	E_{strip}	-	-	-	-	6748-w 51.96-w/o	6748-w 52.53-w/o	-	-
	G_{sc}	-	-	1.22	1.22	-	-	-	-
	G_{strip}	2.80	1.63	7.00	6.53	2.80	1.63	3.86-w 1.87-w/o	3.17-w 1.58-w/o
2	E_{strip}	-	-	-	-	1501.93-w 51.96-w/o	1281.73-w 52.53-w/o	-	-
	G_{sc}	-	-	1.22	1.22	-	-	-	-
	G_{strip}	1.40	1.63	2.80	3.27	1.40	1.63	1.45-w 1.23-w/o	1.41-w 1.19-w/o
3	E_{strip}	-	-	-	-	73.10-w 45.02-w/o	79.17-w 52.53-w/o	-	-
	G_{sc}	-	-	1.22	1.22	-	-	-	-

-w with vertical loads, -w/o without vertical loads.

Table 4.7. SLRS configuration 2 ($L/H \leq 1$): Elastic and shear moduli of the horizontal stripes

The results are summarised and compared in Table 4.8 whereas in Figures 4.14-4.15, the lateral stiffness of the SRLSs and the elasto-plastic curves of the TM are overlapped. The lateral stiffnesses of the SLRS of the TM were assumed as reference values.

Configuration	**Shearwalls**	**Model**	**With vertical loads**		**Without vertical loads**	
			K_e [kN/m]	Var. [%]	K_e [kN/m]	Var. [%]
"1" $L/H > 1$	Single-panel	Target Model	5110.56	-	2490.39	-
		Christovasilis et al.	5736.11	**+12.24**	5736.11	**+130.33**
		New Proposal	5631.21	**+10.19**	2739.00	**+9.98**
	Multi-panel	Target Model	8258.39	-	4843.28	-
		Christovasilis et al.	11698.29	**+41.65**	11698.29	**+141.54**
		New Proposal	10181.16	**+23.28**	6098.52	**+25.92**
"2" $L/H \leq 1$	Single-panel	Target Model	1923.37	-	671.23	-
		Christovasilis et al.	2345.18	**+21.93**	2345.18	**+249.39**
		New Proposal	2201.22	**+14.45**	717.40	**+6.88**
	Multi-panel	Target Model	2658.01	-	1734.64	-
		Christovasilis et al.	4292.07	**+61.48**	4292.07	**+147.43**
		New Proposal	3130.83	**+17.79**	1983.54	**+14.35**

Table 4.8. Comparison of the lateral stiffness of the SRLSs.

The scatter between TM and CH/NP underline that, as general aspect, the elastic models overestimate the lateral stiffness. The reasons are associated with the more accuracy given by the discrete springs combined with 2D elements which guarantee a more realistic force/deformation distribution. CH, due to the neglected effect of the rocking mechanism, predict better the configurations with the vertical loads. The results show minor errors for single-panel shearwalls instead of multi-panels shearwalls for configurations 1 with $L/H > 1$. The scatter between the models is highlighted especially for configurations with $L/H \leq 1$ without vertical loads showing a maximum error, for the specific case, of +249.39%. The NP limits the scatter up to +25.9% for all configurations/shearwalls type regardless of the vertical load's contribution. Due to the analytical formulations used and the marked non-linear behaviour of CLT SLRS, the NP can predict well the initial stage of lateral deformation with reduced errors in a conservative approach. Hence, the proposed model can be considered acceptable independently from the aspect ratio of the shearwalls and the amount of the vertical loads.

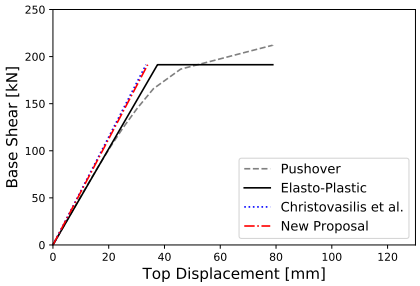

(a) Single-panel, With vertical loads

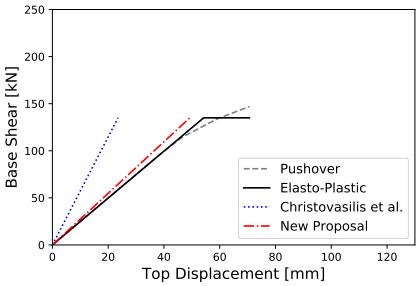

(b) Single-panel, Without vertical loads

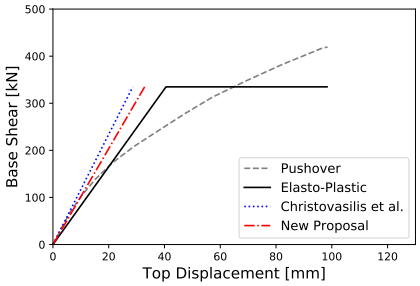

(c) Multi-panel, With vertical loads

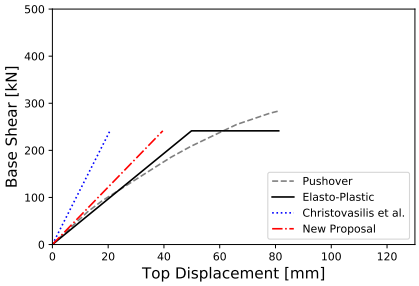

(d) Multi-panel, Without vertical loads

Figure 4.14. Configuration 1: $L/H > 1$

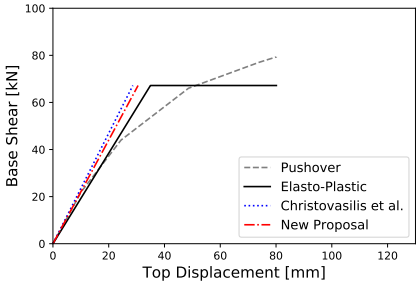

(a) Single-panel, With vertical loads

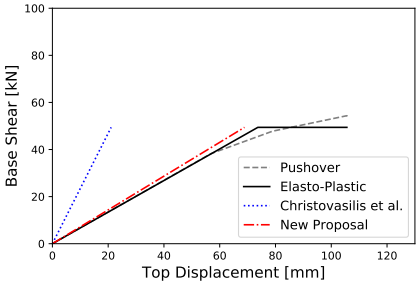

(b) Single-panel, Without vertical loads

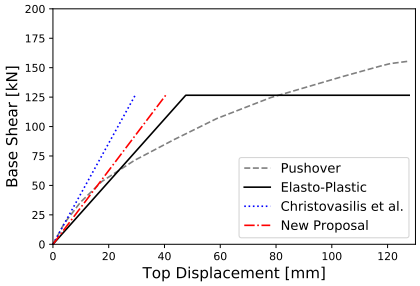

(c) Multi-panel, With vertical loads

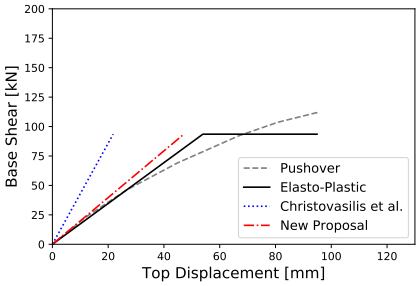

(d) Multi-panel, Without vertical loads

Figure 4.15. Configuration 2: $L/H \leq 1$

4.6 Discussion and Outlook

The experimental and numerical validation of the New Proposal FE model strategy, based on the upgrade of the Christovasilis et al. (Christovasilis et al., 2020), shows the potentiality of predicting into a linear-elastic model the main non-linearities of the lateral response of CLT shearwall. The finite element (FE) strategy has the following novelties:

- Use of only 2D area elements into a FE model;
- Applicability for single- and multi-panel CLT shearwalls;
- Inclusion of the vertical load contribution;
- Inclusion of the floor compressibility.

CLT panels, CLT floors thickness and timber connections (hold-downs, angle-bracket and vertical joint) are modelled with area elements with orthotropic material properties, facilitating the modelling phase and neglecting the use of discrete springs into FE model.

The strategy was implemented for single- and multi-panel CLT shearwalls as required in the next generation of Eurocode for the moderate (single-panel) and high (multi-panel) dissipative classes.

Analytical equations were implemented to account for the vertical load contribution into a linear-elastic method without an iterative process. A secant rocking stiffness passing through the 40% of the maximum overturning moment capacity includes the vertical load effect and checks the activation/no-activation of the overturning mechanism.

The use of 2D area elements was included to incorporate the floor's out-of-plane compressibility and its physical dimension into a FE model.

The New Proposal should allow a more refined distribution of the seismic base-shear along the shearwall of a 3D structure thanks to its predisposition for response-spectrum modal analysis. Future investigations are scheduled for its use in real buildings, whereas an application of the modelling strategy will be shown in an in-press paper (see List of Publications).

[Blank page]

Evaluation of the behaviour factor for CLT buildings

Chapter abstract

Cross-Laminated Timber structures (CLT) are becoming widely used around the world. The excellent properties of the CLT system allow having safety buildings in case of telluric events. However, few specific seismic design rules are available in worldwide standards, such as in the current structural Eurocode (EN 1998-1:2004).
The revision of the Eurocodes is going to define several aspects based on state-of-the-art knowledge, such as the design of CLT buildings.

The following chapter shows the procedure adopted to assess the q-factors for CLT buildings following the new seismic design rules provided in the last draft of the Eurocode 8 (prEN 1998:2020). Two dissipative classes designed in moderate (DC2) and high (DC3) ductility classes were investigated. A parametric numerical study based non-linear static analysis was carried out to get the q-factor contributions following the new material independent formulation. The structural performances of some CLT configurations designed into different ductility classes were analyzed with incremental dynamic analyses. The results show the excellent performances of the CLT as a seismic-resistant structural system, providing suggested values for the revision process.

5.1 The behaviour factor

The behaviour factor q (q-factor) is dimensionless number applicate in most seismic design codes. Eurocode 8 (Code, 2004) defines the behaviour factor (called "strength reduction factor R" in North American codes) as follows:

> § 3.2.2.5-(2): *The behaviour factor is an approximation of the ratio of the seismic forces that the structure would experience if its response was completely elastic with 5% viscous damping, to the seismic forces that may be used in the design, with a conventional linear analysis model, still ensurig a satisfactory response of the structure.*

The q-factor allows scaling the elastic response spectrum into a new design spectrum (inelastic response spectra) in which the seismic demand in the linear field is identified, taking into account the energy dissipation/overstrength capacities of a structural system into a non-linear field. The q-factor is defined as the ratio between the seismic action to maintain the structure in the elastic range F_E and the seismic design action F_d.

$$q = \frac{F_E}{F_d}$$

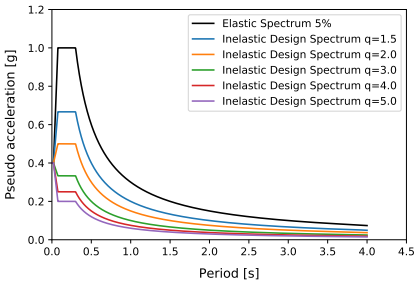

Figure 5.1. Reduction of the pseudo-elastic response spetrum with different behavior factors.

The q-factor can be divided into two main components: the coefficient q_0, which considers the intrinsic over-strength and the dissipative capacity, and a coefficient q_S which takes into account all the over-resistances introduced in the design phase.

$$q = q_0 \cdot q_S \tag{5.1}$$

The definition 5.1 is valid for any structure made with different structural materials. While q_0 component is specific for the structural materials, the structural typology and the dissipative energy capacity (strictly related to construction details), the q_S component depends on the design code (e.g. due to the material partial safety factors) and the designers' safety level.

Flowchart in Figure 5.2, proposed by Pozza (Pozza, 2013b) and integrated with the FEMA approach, summarize the available methods to estimate the q-factor:

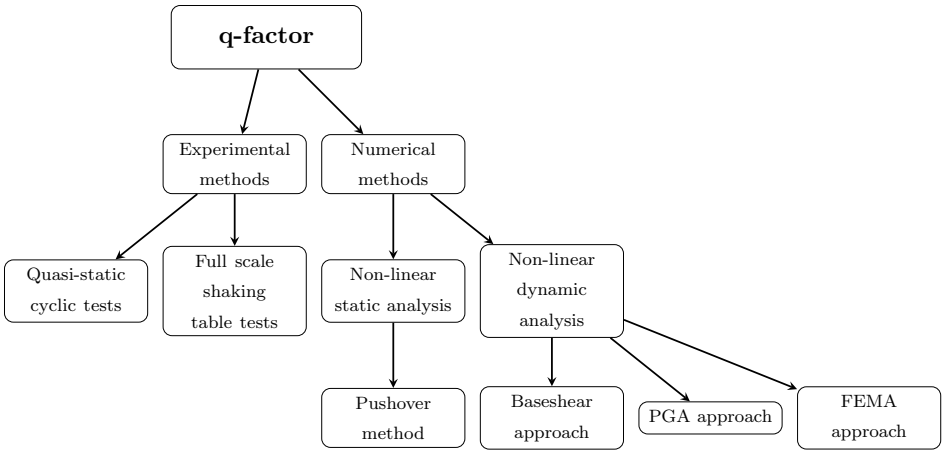

Figure 5.2. Methods for evaluating the behaviour factor (q-factor).

The experimental methods are the most realistic ones; however, they have few practical problems. The first problem is related to economic reasons, especially for full-scale shaking table test. The second problem is that the results are strongly dependent on the design methods, the connections used and the limited number of configuration which could be analyzed.
Numerical methods are widespread in the research community to overcome the limitations of the experimental methods. Generally, these types of analysis are always associated with experimental tests followed by non-linear numerical calibrations.

Currently, whereas in North America an accredited material independent method exist to estimate the q-factor (FEMA et al., 2009), in Europe no standard procedure is recognized. The most common approach adopted in

Europe to evaluate the q-factor is based on pushover methods (as used in Sanchez-Ricart and Plumier (2008)) however, no specific prescriptions are provided as an independent material method.
In the next generation of the Eurocodes, probably (not the future one), the estimation of the q-factor will be more sophisticated since will joint the structural capacity (in terms of strength and ductility) and the target probability of collapse (Žižmond and Dolšek, 2019) giving a consistency between Force-Based (FB) and Displacement-Based (DB) approaches.

5.1.1 Goals and method to evaluate the q-factor for CLT buildings

This work aims to evaluate the q-factor for CLT buildings according to the new draft of Eurocode 8 (EC8 draft) respecting the version-prEN 1998-1-1:2020 (prEC8-1-1) dated (20/02/2020) and the version-prEN 1998-1-2:2020 (prEC8-1-2) dated (30/04/2020). The estimation and the values of the q-factor contributions are subordinated to specific design rules. The main changes introduced in the new version of the EC8 section for timber structures are reported in §2.3.

The available values of the q-factor for CLT buildings present in literature does not follow the latest prescriptions of the new draft of EC8 in terms of design criteria and q-factor formulation. A new estimation of the q-factor is required for two ductility classes: DC2 (moderate ductility) and DC3 (high ductility).
A unique value of the q-factor is not allowed since the dissipative capacity, and the over-strength components are separated according to the new material independent formulation provided by the prEC8-1-1 (later shown).

In this chapter, the q-factors for CLT buildings designed in moderate and high ductility classes were estimated via numerical methods following the new EC8 draft's design prescriptions. In particular, a parametric study was carried out by analysing several 2D CLT configurations via non-linear static analysis (pushover method), and values of the q-factors were derived. Subsequently, the obtained values of the q-factors were verified on some

2D CLT configurations via non-linear dynamic analysis using Incremental Dynamic Analysis (IDA).

5.2 Behaviour factor for CLT buildings: Overview of the proposed values

The estimation of the behaviour factor for CLT buildings still now is a hot topic. Several experimental tests and sophisticated numerical analysis were carried out to estimate the q-factor by using different methods in the last years. Table 5.1 summarizes the main research carried out along the years in chronological order.

Looking at all results, the behaviour factor for CLT buildings varies ranges between 1.5 to 4.5. It is a generally shared vision that the q-factor increases with the structure's height and by using wall panels with a low aspect ratio L/H. Low values of the aspect ratio lead to promote the rocking instead of the sliding mechanism leading to more dissipative capacity.

The international regulatory landscape is still young, and different criteria are followed based on the country. In (Tannert et al., 2018) are compared different worldwide seismic design approaches and regulations which show the ongoing implementation in the national codes. Focusing on the European and North America codes, both do not explicitly describe the CLT structural system leading to a few seismic design rules. In particular, the Eurocode (EC8) (European Commitee for Standardization, 2004), the National Building Code of Canada (NBCC, 2015) and the American Society of Civil Engineers (ASCE, 2017) recommend the Force-Based Design method for seismic design of new structures. However, the use of this method depends on the choice of q-factor/R-factor.

More detailed analyses and experimental investigations have been carried out to improve the prescriptions of seismic codes in recent years. In particular, the evaluation of the q-factor was investigated since it is the base of the seismic analysis.

The first step to calculate the q-factor for codes improvement was carried out by Popovski and Karacabeyli (2014) (Popovski et al., 2014)

for the NBCC. The results were included in the CSA086 standard[1]. The study was based on non-linear numerical analyses by using SAPWood. Experimental data (Popovski et al., 2010) were adopted to calibrate the hysteretic response of CLT walls. The behaviour factor, reported in the CSA086, is divided into the overstrength R_0 and the ductility R_d components for the first time. Values of $R_0 = 1.5$ and $R_d = 2.0$ ($R = R_0 \cdot R_d = 3.0$) should adopt if the length-to-height ratio (or aspect ratio) is lower than one, ensuring the rocking behaviour or a combined rocking-sliding behaviour. Moreover, if the length-to-height ratio is greater than one or sliding is the predominant deformation mechanism, the behaviour factor should be $R = R_0 \cdot R_d \leq 1.3$.

Since the US code does not provide any rules for CLT buildings until 2016, the strength reduction factor suggested was 4.5 ((Pei et al., 2013), (Pei et al., 2016)) for ASCE 7. More recently, van de Lindt et al. (van de Lindt et al., 2020) examined the strength reduction factor for its inclusion in ASCE 7 and the International Building Code (IBC). The study follows the FEMA approach respecting the collapse margin ratio. The research suggests a fixed value of 3.0 for the walls with length-to-height equal to 2:1 or walls with mixed aspect ratio up to 4:1 and 4.0 for wall systems made with aspect ratio up to 4:1.

In Europe, the current version of Eurocode 8 (EN 1998:2004) does not explicitly provide the CLT system. No specific design rules are available, and CLT walls' design follows the traditional timber construction theory. More details are present in the next section.

[1] CSA O86 provides criteria for the structural design and evaluation of wood structures or structural elements.

Reference	year	Method	Approach	Analysis details	Configuration details	Value
(Ceccotti and Follesa, 2015)	2006	Experimental	PGA	Full scale shaking table test	3D structure. 3-storey.	3.40
(Ceccotti et al., 2006)	2006	Experimental	PGA	Full scale shaking table test	3D structure. 3-storey. Minimum value.	1.43
(Ceccotti, 2008)	2008	Numerical	PGA	Non-linear dynamic analysis	3D structure. 3-storey. Median value.	3.00
(Popovski and Karacabeyli, 2011)	2011	Numerical	FEMA P695	Non-linear dynamic analysis	2D structure.	3.00
(Ceccotti et al., 2013)	2013	Experimental	PGA	Full scale shaking table test	3D structure. 6-storey.	from 3.40 to 3.00
(Pei et al., 2013)	2013	Numerical	Pushover	Non-linear static and non-linear dynamic	3D structure. 6-storey.	4.50
(Popovski et al., 2014)	2014	Numerical		Non-linear dynamic analysis	3D structure. 6-storey.	$2 \cdot 1.5 = 3$
(Pozza et al., 2014)	2014	Numerical	PGA	Non-linear dynamic analysis	2D structure. Several configurations.	2.0 to 3.0
(Pozza et al., 2015)	2015	Numerical	PGA	Non-linear dynamic analysis	3D structure. 3-storey.	3.0 to 4.0
(Flatscher et al., 2015)	2015	Experimental	PGA	Full scale shaking table test	3D structure. 3-storey with large walls.	2.84
(Sustersic et al., 2016)	2016	Numerical	Pushover	Non-linear static analysis	3D structure. 4-storey. N2 method.	single panel: 2.1 multi-panel: 2.9
(Pozza et al., 2017)	2017	Numerical	PGA	Non-linear dynamic analysis	2D structure. Several configurations.	2.00
(Follesa et al., 2018)	2018			Summary of experimental and numerical background	Non-dissipative structures	1.50
					CLT structures with single panel	2.0
					CLT structures with multipanel wall connected with deformable vertical joint	3.0
(Hummel and Seim, 2019b)	2019	Numerical	Pushover	Non-linear static analysis	3D structure. Several configurations.	up to 3.0
(van de Lindt et al., 2020)	2020	Numerical	FEMA P695	Non-linear static and non-linear dynamic analysis	3D structure. Several configurations.	3.0 and 4.0

Table 5.1. State-of-the-art of q-factor for CLT buildings.

5.2.1 Behaviour factor for CLT buildings: EN 1998-1-1:2004

The current Eurocode 8 part 1 (EN 1998-1-1:2004) dedicates chapter 8 to the seismic design of timber structures. "Table 8.1" reports the behaviour factors for different structural systems. CLT buildings are not mentioned. The main reason for this lack is attributable to the newness of the CLT in 2004. A possible interpretation could be to classify CLT structures as *"DCM (medium capacity to dissipate energy), Glued wall panels with glued diaphragms"* assessing a q-factor equal to 2.0. However, CLT buildings could reach different dissipative capacity levels based on how they are made (Follesa et al., 2018). Multi-panels walls (or "segmented walls"), in which the rocking mechanism is guaranteed, allows dissipating more energy compared to single-panel walls thanks to the presence of dissipative ductile joints (if properly designed).

Design concept and ductility class	q	**Examples of structures**
Low capacity to dissipate energy - DCL	1.5	Cantilevers; Beams; Arches with two or three pinned joints; Trusses joined with connectors
Low capacity to dissipate energy - DCL	2	Glued wall panels with glued diaphragm, connected with nails and bolts; Trusses with doweled and bolted joints; Mixed structures consisting of timber framing (resisting the horizontal forces) and non-load bearing infill.
	2.5	Hyperstatic portal frames with doweled and bolted joints.
High capacity to dissipate energy - DCH	3	Nailed wall panels with glued diaphragms, connected with nails and bolts; Trusses with nailed joints.
	4	Hyperstatic portal frames with doweled and bolted joints.
	5	Nailed wall panels with nailed diiaphragms, connected with nails and bolts.

Table 5.2. Structural types and upper limit values of the behaviour factors for the three ductility classes ("Table 8.1" of EN 1998-1-1:2004).

Besides, no specific capacity design rules or seismic detailing are provided. The dissipative/brittle zones are not mentioned.

Over the last 15 years, the research allowed to enhance the knowledge

of several aspects of the CLT, such as timber panels quality, fire resistance, improvement of the timber-to-steel connections, and seismic design leading to a significant extension/modification of the future Eurocodes 5 and 8.

5.3 Behaviour factor according the New Draft of Eurocode 8

The new draft of Eurocode 8 (prEN 1998-1-1:2020) provides a new definition of the q-factor as:

> *Factor used for design purposes to reduce the forces obtained from a linear analysis, to account for the overstrength as well as for non-linear response of a structure, associated with the material, the structural system and the design procedures.*

The material indipendent formulation of the behaviour factor q is the product of three components:

$$q = q_S \cdot q_R \cdot q_D \tag{5.2}$$

where:

- q_S behaviour factor component accounting for overstrength due to all other source;
- q_R behaviour factor component accounting for overstrength due to the redistribution of seismic action effects in redundant structures;
- q_D behaviour factor component accounting for the deformation capacity and energy dissipation capacity.

Specifically, the behaviour factor is given by the product of the component that takes into account the overstrength introduced in the design q_S, the component that takes into account the overstrength due to the redistribution of the seismic action in redundant structures q_R and the component that consider the dissipative capacity q_D. Since q_S is fixed for all materials (material independent) and set to 1.5, the remaining components will define the basic values for the behaviour factor for all structural systems, in turn, divided into three ductility classes: ductility class 1 (DC1, low-dissipative behaviour) where the factor q is equal to 1.5, ductility class 2 (DC2, moderate-dissipative behaviour) and ductility class 3 (DC3, high-dissipative behaviour).

The q_R is estimated as the ratio α_u/α_1 (prEC8-1-2 5.3.2(6)) between the

value of the seismic action for which the formation of a number of plastic hinges such as to make the structure labile and the one for which the first element structural achieves plasticization. On the other side, an analytical formulation to calculate the q_D contribution is not available.

5.3.1 Approach implemented to estimate the q-factor for CLT buildings

The q-factor components' estimation is related to the definition of the seismic performance measured by level of damage within the limit states (LS). Two limits state are considered: the significant damage SD and the near-collapse NC. The prEC8-1-1 defines the SD and the NC limit state as:

- *LS of Significant Damage (SD) shall be defined as one in which the structure is significantly damaged, possibly with moderate permanent drifts, but retains its vertical-load bearing capacity; ancillary components, where present, are damaged (e.g., partitions and infills have not yet failed out-of-plane). The structure is expected to be repairable, but, in some cases, it may be uneconomic to repair;*
- *LS of Near Collapse (NC) shall be defined as one in which the structure is heavily damaged, with large permanent drifts, but retains its vertical load bearing capacity; most ancillary components, where present, have collapsed.*

The significant damage limit state SD was taken into account for the definition of the q_S-q_R-q_D components allowing an adeguate safety margin.

The deformation at the local level of each connection was used to identify the limit states SD and NC at the global level on the capacity curve (Figure 5.3)[2]. In this work, the yield point Y corresponds to the yield strength's attainment in one connection, and it is not necessarily associated with a specific limit state at the global level. The limit states at the connection level were identifined by implementing the rules of the prEC8-1-2-Annex L (§3.4.2.2). The displacement domains reported in §3.6.3 were

[2]This approach is currently adopted by other structural materials like concrete and steel. In concrete structures e.g., the chord rotation limits are checked for the ductile mechanisms.

adopted to achieve the limit states at the global level. Hold-downs and the screws in the vertical half-lap joint had a uni-directional behaviour whereas angle-brackets had a bi-directional behaviour (§3.6.3).

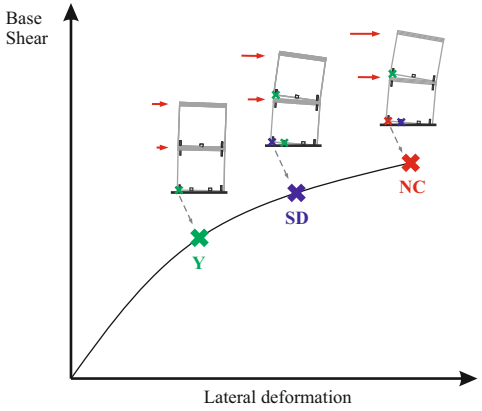

(a) Limits states: Local vs Global levels

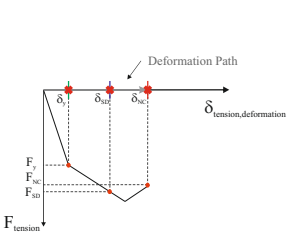

(b) Hold-Down

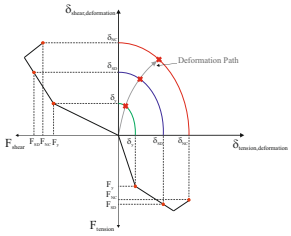

(c) Angle-Bracket

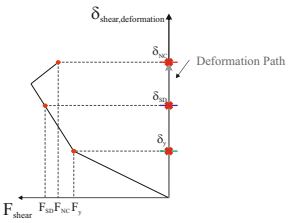

(d) Vertical panel joint

Figure 5.3. Definition of the limit states: first yield Y, Significant Damage SD, Near Collapse NC on the capacity curve (a), Displacement domain of hold-down (b), Displacement domain of angle-bracket (c), Displacement domain of the vertical panel joint (d).

According to prEC8-1-1, the elasto-plastic curve, representative of the capacity of a structure, has an hardening behaviour (Figure 5.4). The elasto-plastic equivalency is based on the investigations conducted by De Luca ((De Luca et al., 2013a), (De Luca et al., 2013b)) in order to optimize the current bilinear fit for static pushover curves. The new approach introduces a close fit on the initial stiffness and adopts the maximum strength capacity for energy balance method.

The initial stiffness (k^*) is identified by the straight line passing through the point where the first yield occurs (B), while the conventional yield value (d_y^*, F_y^*) is calculated through the equality of the area underneath by the capacity curve at the point of maximum capacity A following Equation 5.3.

The slope of the hardening branch is identified by connecting the points (d_y^*, F_y^*) and A.

$$d_y^* = \frac{2E^* - F_m^* d_m^*}{k^* d_m^* - F_m^*} \tag{5.3}$$

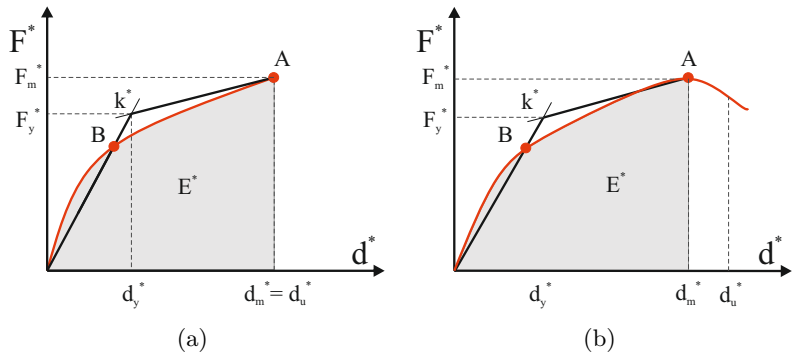

Figure 5.4. Elasto-plastic energy equivalence according the EC8 draft.

Following the design methodology of the SDOF (Figure 5.4), the components of the behaviour factor q for hardening systems can divided into:

$$q_S = \frac{V_1}{V_d} \qquad q_R = \frac{V_{SD}}{V_1} \qquad q_D = \frac{V_E}{V_{SD}} \tag{5.4}$$

$$q = q_S \cdot q_R \cdot q_D = \frac{V_1}{V_d} \cdot \frac{V_{SD}}{V_1} \cdot \frac{V_E}{V_{SD}} \tag{5.5}$$

In which V_d and V_1 correspond respectively to the seismic design and

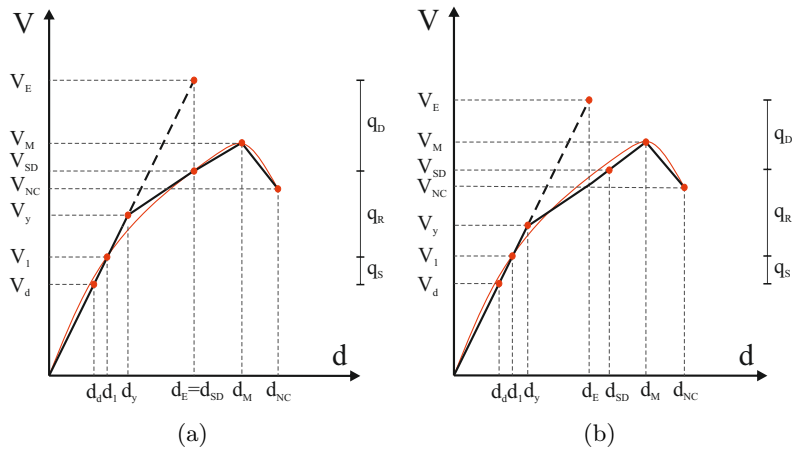

Figure 5.5. Capacity curve. Equal displacement rule (a), Equal energy rule (b).

the first plasticization base-shears. V_{SD} and V_{NC}, with their respective

displacements, define the attainment of the life-safety (significant damage, SD) and collapse (near-collapse, NC) limit states. Finally, V_E identifies the base-shear of an infinitely elastic linear response. In the absence of a softening branch, the near-collapse point coincides with the peak of the capacity curve (V_m, d_m).

Several methods are available to estimate V_E, thus the q-factor ((Cornell, 1996), (Miranda and Bertero, 1994)). In this work, V_E was calculated by respecting the equal energy rule (EE) and the equal displacement rule (ED) for hardening systems (Albanesi and Nuti, 2007):

Equal energy rule $T^* \leq T_0$ (EE):

$$d_E = \begin{cases} \sqrt{2 \cdot d_{SD} \cdot d_y - d_y^2} & for\ p = 0 \\ \sqrt{2 \cdot d_{SD} \cdot d_y - d_y^2 + d_{SD}^2 \cdot p - 2 \cdot d_{SD} \cdot d_y \cdot p + d_y^2 \cdot p} & for\ p \neq 0 \end{cases} \tag{5.6}$$

Equal displacement rule $T^* > T_0$ (ED):

$$d_E = d_{SD} \tag{5.7}$$

$$V_E = k^* \cdot d_E \tag{5.8}$$

where:

- d_E is the maximum elastic displacement at the SD limit state of the SDOF;
- d_{SD} is the maximum inelastic displacement at the SD limit state of the SDOF;
- d_y is the conventional yield displacement of the SDOF;
- p is the ratio between the post-elastic and the elastic stiffnesses;
- T_0 is the period corresponding to the peak of the (linear) response spectrum in acceleration;
- T^* is the period of the equivalent SDOF oscillator.

The period T^* of the equivalent SDOF with mode shape ϕ is calculated using Equation 5.9:

$$T^* = 2\pi\sqrt{\frac{m^*}{k^*}} \tag{5.9}$$

where:

$m^* = \sum m_i \phi_i$ is the mass of the SDOF;

k^* is the elastic stiffness of the SDOF.

Equations 5.6-5.7 were adopted to calculate the elastic displacement d_E thus the corresponding V_E (Equation 5.8) ((Gulkan and Sozen, 1974), (Albanesi et al., 2000)). It should be noted that if $p = 0$, Equation 5.6 is equivalent the "Newmark-Hall method" (Newmark and Hall, 1982).

5.3.1.1 General discussion

Timber structures, CLT structures in specific, show different capacity curves compared to other structural materials/systems (i.e. concrete and steel). In general, they are more similar to masonry structures in which cantilever shearwalls are identifiable, multi-failures are achievable, and the global yield is not-well defined. In particular, the capacity curves of CLT structures are characterized by:

- Not-well defined global yield point;
- Marked hardening behaviour;
- Not-well defined position of the global plastic mechanism;
- Absence of a post-elastic plateau.

Many researches show this typical behaviour via numerical analyses (Sustersic et al., 2016), (Yasumura et al., 2016) and through experimental tests (Popovski and Gavric, 2016), (Hummel and Seim, 2019b)).
These aspects are the results of problems highlighted in the definition of the yield point in timber connections, especially for hold-downs and angle-brackets in tension, and it is also pointed out when bi-linearization approach, including the hardening shape in the post-elastic branch, is included like in prEC8-1-1.

Therefore, the estimation of q_R and q_D contributions becomes challenging if hardening bi-linearization is used instead of typical elastic-perfectly plastic approaches.
In prEC8-1-1 the overstrength is divided into two components: q_S and

q_R. However, the analytical definition of the overstrength factor, generally called Ω, is the ratio between the ultimate load-bearing capacity (now identified at the SD LS) and the design base shear. The contribution of the overstrength effect was largely investigated for concrete and steel structures ((Rahgozar and Humar, 1998), (Mitchell et al., 2003)).

The overstrength is the product of the "design structural overstrength" Ω_D, the overstrength due to the "plastic redistribution" Ω_P and the overstrength due to the "structural hardening" Ω_H (Figure 5.6).

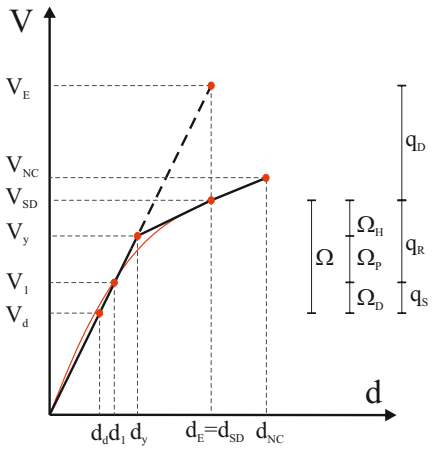

Figure 5.6. Adopted overstrength factors for CLT buildings: q_S and q_R.

$$\Omega = \Omega_D \cdot \Omega_P \cdot \Omega_H \tag{5.10}$$

These components depend on several aspects such as: (i) material effect due to higher yield strength compared to the nominal strength, (ii) strain hardening behaviour of the dissipative components, (iii) redistribution of the internal forces, (iv) material safety partial factors, (v) minimum structural requirements and (vi) contribution of the non-structural elements.

Whereas in steel and concrete structures, Ω_H could be negligible since Ω_P is predominant, in timber structures, there is not a well-defined distinction between the plastic and hardening overstrengths. The main reasons depend upon the non-linear behaviour of the connections and the in series global deformation mechanism that rules the CLT shearwalls' behaviour.

In the present work, the estimation of the q-factor follows the rigorous

definition of the q_R component by applying Elnashai and Mwafy (2002) for bi-linearization hardening systems. The q_R component is estimated as the product of Ω_P and Ω_H, whereas the q_S component coincides with Ω_D.
It was observed that the DC3 ductility class is mainly affected by hardening, while the DC2 ductility class shows lower values (later explain) leading to negligible difficulties in estimating the q_R as generally happen when elastic-perfectly plastic linearization is used.

On the other hand, due to the absence of an analytical definition of the q_D component, the approach proposed in Uang (1991), and applied in (Gerami et al., 2017), may be a possible strategy since the prEC8-1-1 defines the q_D as a mix of energy and displacement capacity. According to this approach, the q_R contribution is estimated as the ratio between V_y and V_1, whereas q_D as the ratio between V_E and V_y. This approach is acceptable if no yield plateau and no criteria of locally well-defined limit state are available.

However, in order to be consistent with the definition reported in the prEC8-1-2 (clause 5.3.2(6)) of the q_R contribution, the Elnashai and Mwafy (2002) method was adopted and the q_D contribution estimated in turn (see Equations 5.4).

It is encouraged the use of non-linear static analyses since different modelling strategies could be implemented, and the overstrength may be influenced (i.e. neglecting the bi-directional behaviour of angle-brackets). The numerical investigations presented in the following sections provide a detailed modelling strategy to calibrate the q-factors accounting for all dissipative components.

5.4 Estimation of the q-factor via non-linear static analysis (NLSA)

The following section introduces an extensive study to estimate the q-factor contributions for the moderate (DC2) and high ductility (DC3) classes by numerical non-linear static analysis. The low-ductility class (DC1) is neglected since no-capacity design rules should be respected and q_R-q_D are kept equal to 1.0 by default.

5.4.1 Parametic analysis

A parametric study was carried out to have a reasonable number of configurations useful to estimate the behaviour factor's contributions. Several 2D-CLT configurations with different structural geometry (building height, number of storeys, number of shearwalls, site conditions) were analyzed with a parametric study because no distinction is expected in the prEC8-1-2 between the number of storeys/wall aspect ratio. The parametric study was performed through non-linear static analyzes. Pushover analyses are less computationally expensive than non-linear dynamic ones, providing a direct and intuitive correlation between local damage and global damage. Besides, the adoption of 2D configurations simplifies the design process and the computational effort.

The non-dissipative components (i.e. the joint between the floor and the supporting walls underneath, the joints between orthogonal walls and corners), even if are non-dissipative, were neglected in the design and modelling stage to exclude their deformability into the q-factor.
The hierarchy of resistance was not monitored at the connections' level, although the design strengths came from experimental results.

The parametric analyses were conducted through an ad hoc program developed in Python language, which allows design and analysis of any structural configuration following the Eurocode 8 draft. It is to emphasize that the results are valid if the design rules are respected. The steps followed for each structural configuration are summarized in the flowchart shown in Figure 5.7 and commented later.

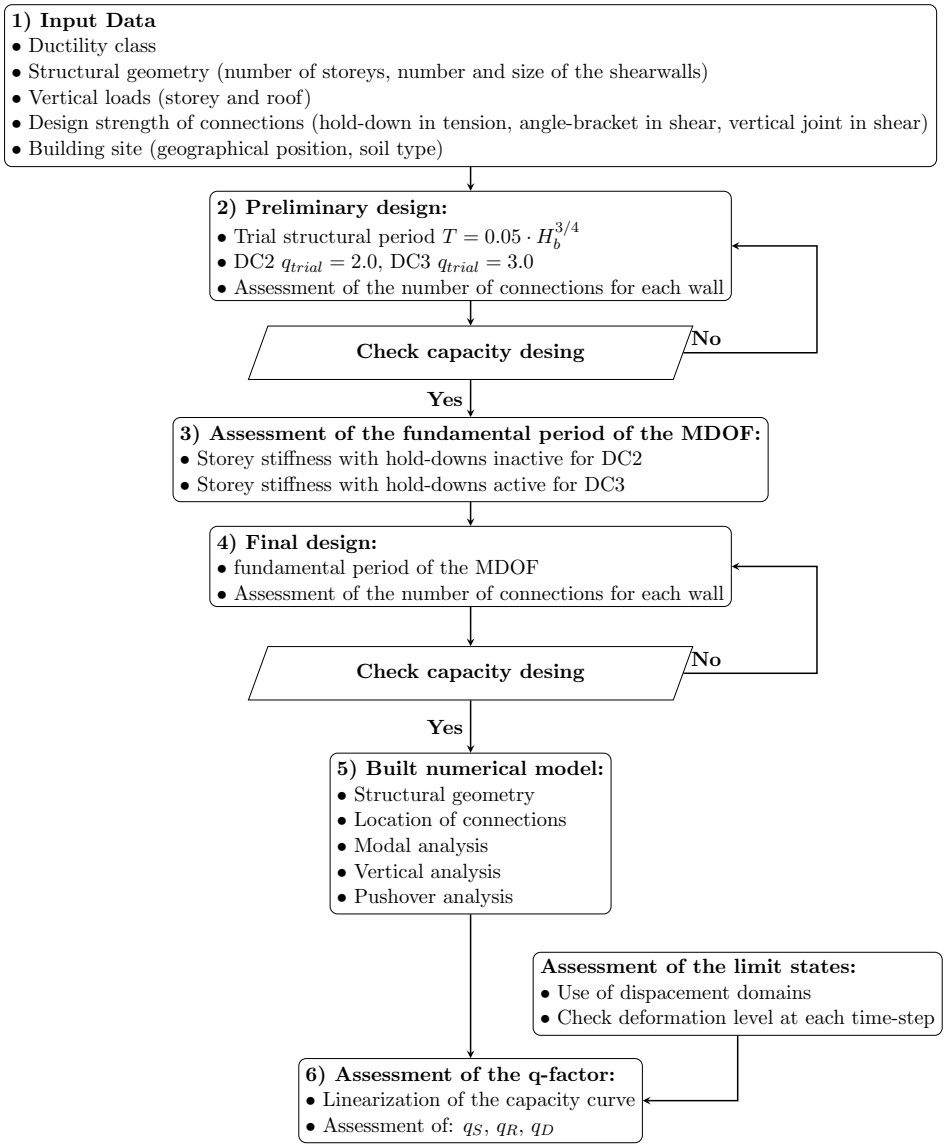

Figure 5.7. Flowchart for the estimation of the q-factor through NLSA.

1) Input Data

The first step to start the estimation of the q-factor for each configuration was the definition of the input data. After choosing the ductility class (DC2 or DC3), the structural geometry was required: the number of storeys, number and size (L/H) of the shearwalls are assumed to be reasonable with the engineering judgment. In the case of DC3 walls, the length of each wall panel was evaluated considering two vertical joints for walls with a total length greater than or equal to 5m and one vertical joint for walls with a smaller dimension. The inter-storey height was assumed to be the same for all levels and equal to 3.0m.

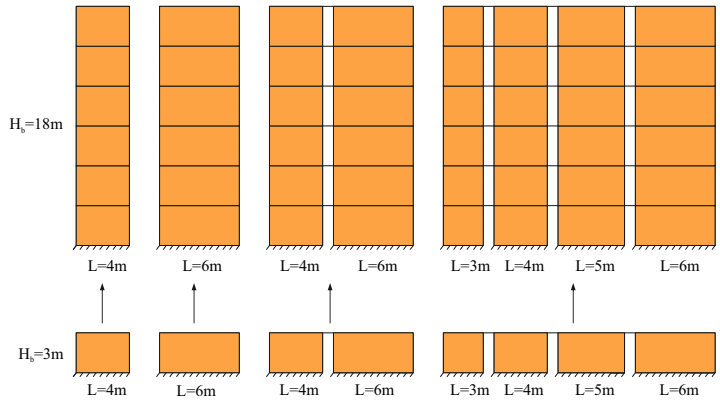

Figure 5.8. Example of different configurations from 1 to 6 storeys: [4], [6], [4,6], [3, 4, 5, 6].

The vertical loads (i.e. the seismic storey mass) were kept constant for all storeys and organised into storey-load and roof-load. The gravity loads/masses respect the load combination for seismic conditions ($w = G_{k1} + G_{k2} + \psi_{E,i} \cdot Q_{k,i}$) accounting the likelihood of the loads $Q_{k,i}$ with the combination coefficient $\psi_{E,i}$. The influence length of all shearwalls

	G_{k1} $[kN/m^2]$	G_{k2} $[kN/m^2]$	$\psi_{E,i} \cdot Q_k$ $[kN/m^2]$	w $[kN/m^2]$
Storey	1.0	2.0	$0.3 \cdot 2.0 = 0.6$	3.6
Roof	0.8	0.4	0.0	1.2

Table 5.3. Seismic loads/masses.

was assumed equal to 5m. The regularity in elevation was always respected since prEN 1998:2020-1-1 allows considering regular buildings those without abrupt changes of mass/stiffness from the base to at least one storey below the top storey.

The dissipative connections' design strengths were estimated from experimental data and adapted, as described in the §3.5, for design purpose.

The reference site was L'Aquila (Italy) where for a return period of $T_R = 475$ years, with a probability of exceeding of 10% in 50 years, the PGA on subsoil A-T1 is equal to 0.26g. The maximum spectral acceleration (new reference following the EC8 draft part 1) is 0.62g. L'Aquila is classifiable as a high-seismic risk area. Subsoil type A, B, and C were taken into account as a representable site condition scenario.

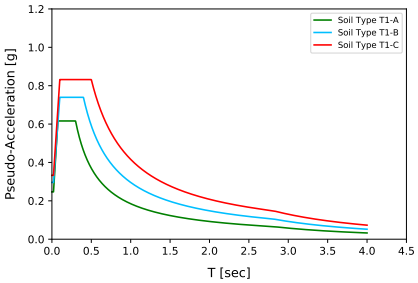

Figure 5.9. Elastic spectrum of L'Aquila: Soil Type A, B and C.

2) Preliminary design

Each configuration was designed through a linear-static analysis with a trial behaviour factor equal to 2.0 and 3.0, respectively for DC2 and DC3. CLT structures' design was an iterative process related to many non-linearities (described in the previous chapter) and the possible deformation mechanism which affects the correct estimation of the fundamental period. A first preliminary structure was design evaluating the base-shear demand through the simplified formulation of the fundamental period provided by the code[3]. The base-shear demand distribution along the building's height was proportional to the fundamental mode. Hold-downs were used as an uplift resisting system, while angle-brackets were designed for the sliding forces. For the DC3 class, an overstrength factor γ_{Rd} equal to 1.60, as reported in Table 2.1, was used to prevent the sliding mechanism to ensure the couple panel mechanism. An iterative loop controls that the capacity design at the wall and global levels satisfy all requirements.

3) Assessment of the fundamental period of the MDOF

An addition design process was carried out after step 2) to overcome the weakness of the fundamental period's formula. Since the fundamental period and the base-shear demand were strickly correlated, a new estimation was carried out on an MDOF (multi-degree-of-freedom oscillator) system based on the preliminary structure. Each level of the MDOF was characterized by a storey stiffness function of the number and the typology of the connections used in step 2). In particular, the storeys stiffness were calculated considering the sliding stiffness of the angle brackets in the DC2 structures (HD non-

[3] $T = 0.05 \cdot H_b^{3/4}$ where H_b is the height of the building, in [m], measured from the foundation or from the top of a rigid basement.

active) while the in-plane rocking stiffness for the DC3 structures (HD active).

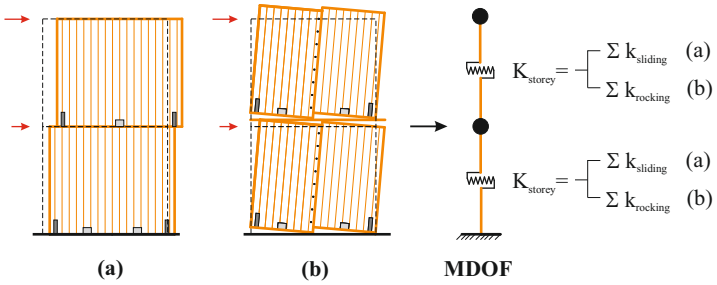

Figure 5.10. Definition of the MDOF system. Sliding storey stiffness for DC2 (a) and storey rocking stiffness for DC3 (b).

4) Final design

The design procedure and considerations of the Final design are the same as step 2) except for the fundamental period adopted. In a practical and conservative design, the design steps were rest at this stage since, since if the fundamental period of the structure is in the decreasing branch of the design spectrum, the seismic demand will decrease at each subsequent iteration.

5) Built numerical model

A dedicated tool was developed to generate the numerical model based on the structural geometry and location of the connections. The details of the numerical model are reported in the dedicated section. The numerical model was suddenly analyzed with a modal analysis to get the displacement modal vector (first mode) ϕ and the participant factor Γ. After the application of the vertical loads, two non-linear static analyses were carried out. The pushovers were force-controlled with invariant load profiles proportional to the first vibration mode and proportional to the floor masses.

6) Estimation of the q-factor

Once defined the capacity curves (for the two load paths) the yield (Y), the significant damage (SD) and the near-collapse (NC) points were identified by checking the connections' deformation level at each time-step using the procedure described in §5.3.1. Each pushover curve was linearized as in

Figure 5.5 with the corresponding equations. The estimation of the q-factor components was achieved with Equations 5.4.

The sample of configurations considered includes a total of 180 2D models for a total of 360 analyzes per class of ductility (Table 5.4).

Number of storeys:	From 1 to 6
Configurations: **([L. shearwall 1, L. shearwall n.])**	[4], [6], [4, 4], [6, 6], [4, 6], [3, 6, 6], [4, 5, 6], [4, 5, 5, 6], [3, 4, 5, 6], [4, 5, 6, 3, 4.5, 5, 6]
Storey load (G_{k1}, G_{k2}, $0.3 \cdot Q_k$): (floor influence length 5m)	3.6 kN/m^2
Roof load (G_{k1}, G_{k2}): (floor influence length 5m)	1.2 kN/m^2
Soil condition: (Topographic class T1)	A, B, C
Profilo di carico: Proportional to the first mode	1
Load Path: Proportional to the mass	1
Total number of analysis	360

Table 5.4. Matrix of the analyzed configurations.

5.4.2 Numerical model

The finite element numerical models were developed by using the OpenSees framework (McKenna, 2011). For models with moderate DC2 and high ductility DC3, the wooden panels are schematized as an assembly of four frames (*element elasticBeamColumn*), with linear transformation, subsequently defined as "frame-box". The deformability of the CLT wall is simulated using two horizontal elements with high axial and bending stiffness and two vertical elements with high axial stiffness and bending stiffness able to represent the shear and flexural deformability (even if estimated as a cantilever behaviour) of the panel, obtaining a shear-type behaviour. The modulus of inertia I_{wall} of the single vertical frame is evaluated according to the following equation:

$$I_{wall} = \frac{1}{2} \cdot \frac{K_{wall} \cdot H^3}{12 \cdot E} \tag{5.11}$$

where K_{wall} is calculated as the series stiffness proposed in (Casagrande et al., 2018) whose contributions of shear K_{SH} and bending K_B are estimated with Equations 5.12-5.13. H is the height of the wall. The elastic modulus E and the cross-section area of the vertical frame, fictitious values equal to $100GPa$ and $10e12mm^2$ are considered, respectively. The elastic equivalent moduli G_{eq} and E_{eq} of the CLT panels are calculated with (Flaig and Blass, 2013) and (Blass and Fellmoser, 2004), respectively.

$$K_{SH} = \frac{G_{eq} \cdot A_{CLT,wall}}{H} \tag{5.12}$$

$$K_B = \frac{3 \cdot E_{eq} J_{CLT,wall}}{H^3} \tag{5.13}$$

$$\frac{1}{K_{wall}} = \frac{1}{K_{SH}} + \frac{1}{K_B} \tag{5.14}$$

$A_{CLT,wall}$ and $J_{CLT,wall}$ are the area and inertia modulus of the cross-section of the CLT wall. Conventionally, a $120mm$ thick panel composed of 5 layers (**24**-24-**24**-24-**24**) made in C24 was used for all levels. The variability of the thickness of the walls in elevation is thus not considered. The frame-boxes are connected through zero-dimensional elements. The zero-dimensional elements (*element zeroLength*) are hold-downs (HD) modelled

in the only primary direction with unidirectional behaviour (uplift), angle-brackets (AB) with bidirectional behaviour (uplift and shear) and friction elements (*element flatSliderBearing*) located in the same nodes where the HDs and ABs are positioned. The Coulomb coefficient of friction was assumed to be 0.35 in the timber-to-concrete contact, 0.30 in the timber-to-timber contact and 0.1 in timber-to-steel contact as reported in (Petersen, 2013). The friction elements have a high compressive stiffness equal to 100 kN/mm, assuming a rigid contact for wall-to-floor and wall-to-foundation. The initial shear stiffness of the friction elements is set 1000 N/mm to avoid convergence problems.

In the case of the DC2 configuration, the horizontal structural elements (inter-floor slab and roof) are not explicitly modelled since a cantilever behaviour is attributed to the multi-storey shearwalls. In the case of configurations with multiple shearwalls in parallel, kinematic constraints (*EqualDOF*) are used to simulate a rigid diaphragm.

In the case of the DC3 model, the horizontal structural elements are elastic frames with high bending stiffness, representative of a rigid plane (shear-type behaviour in which rotations at the head of the walls are free). The floors are constrained to the lower walls through kinematic constraints placed on the central nodes of the lower segmented panels and to the upper walls through HD, AB and contacts. The lower and upper nodes of the adjacent segmented walls are connected through kinematic constraints that impose the same displacements in the horizontal direction. The vertical joints (half-lap) are modelled as links (*element twoNodeLink*) connecting the lower right node of the segmented $wall - j$ to the upper left node of the segmented $wall - (j + 1)$.

The connections (HD, AB and SC) are modelled with different constitutive laws depending on the type of analysis: SAWS material for non-linear static analysis and Pinching4 materials for cycle/dynamic analyses both available in the OpenSees library. In the case of a vertical joint, the material properties attributed to the link elements are obtained by multiplying the strength and stiffness of the single screw by the effective number. The parameters of the connections are reported in §3.6.1.2-§3.6.2.2.

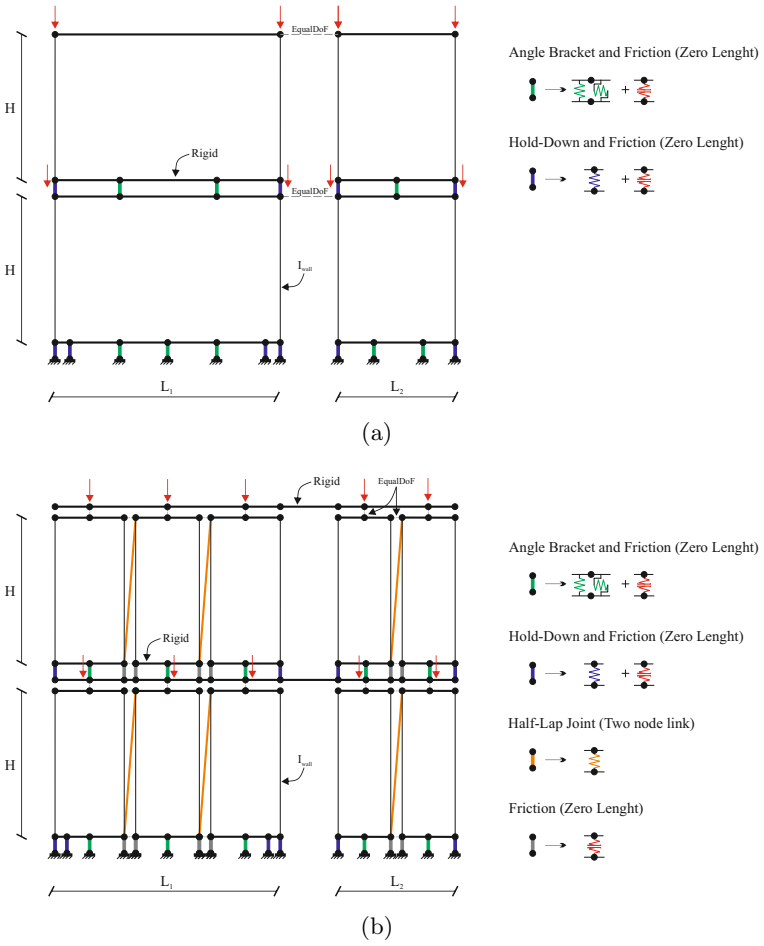

Figure 5.11. Numerical models: DC2 (a), DC3 (b).

5.4.2.1 Validation of the numerical model and limit states check

Two configurations of full-scale shearwalls reported in (Gavric et al., 2015c) were designed to validate the numerical models and the definition of the limit states. The first configuration (Figure 5.12a) made of the single-panel wall, due to the definition of the prEC8-1-2 is classifiable as DC2 class (moderate ductility) while the second configuration made of multi-panels (Figure 5.12b) as DC3 (high ductility). The walls aspect ratio L/H are equal to 1. A constant uniform vertical load of 18.5kN/m is applied at the top of the walls. Two hold-downs are placed at the corner of each wall. Four angle-brackets are located in the same position for both models (see Figure 5.12). Twenty screws are adopted in the vertical joint of test (b). The connections properties are described in §3.6.1.2-§3.6.2.2.

The numerical model's validation was carried out with different constitutive laws: SAWS material used for pushover analysis and Pinching4 materials for cycle/dynamic analyses.

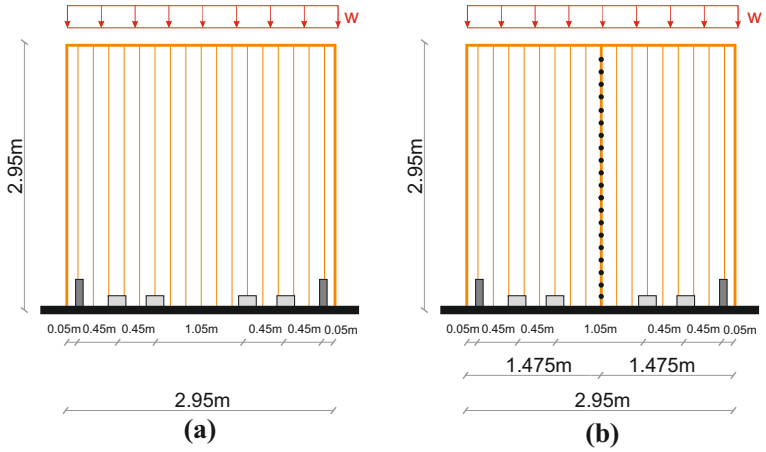

Figure 5.12. Wall panel test configurations (Gavric et al., 2015c): single-panel wall (classificable as DC2) (a), multi-panel wall (classificable as DC3) (b).

Figure 5.13 shows the finite element model (FE model) adopted for (Figure 5.13a) single-panel (Figure 5.13b) multi-panel walls in the deformed shape under a horizontal top load. It is evident the different deformation mechanisms. Both walls tests show a sliding deformation comparable due to the number and typology of shear connections adopted. The rocking behaviour is different due to a flexible vertical joint between the adjacent panels for Figure 5.13b).

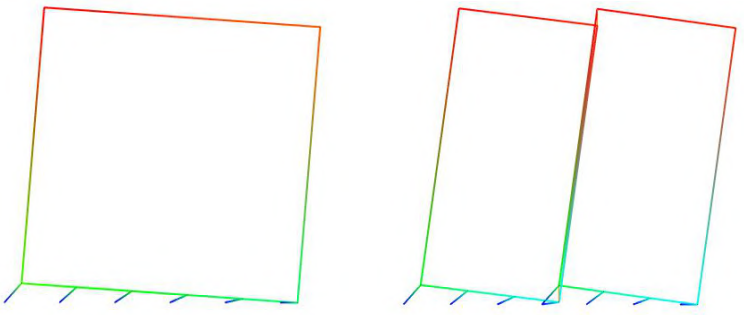

(a) (b)

Figure 5.13. FE model wall panel test: single-panel wall (a), multi-panel wall (b).

5.4.2.1.1 Monotonic-test validation

The monotonic test's validation was carried out following two steps: (i) application of the vertical load and (ii) application of horizontal incremental load on the top nodes of the frame-box.

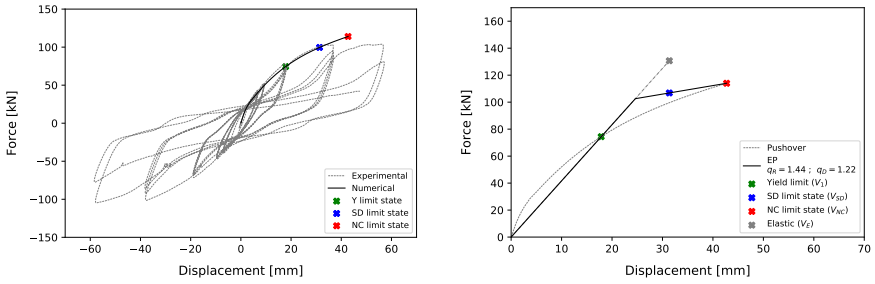

(a) (b)

Figure 5.14. Numerical model DC2: Hysteretic response (a), Energy (b).

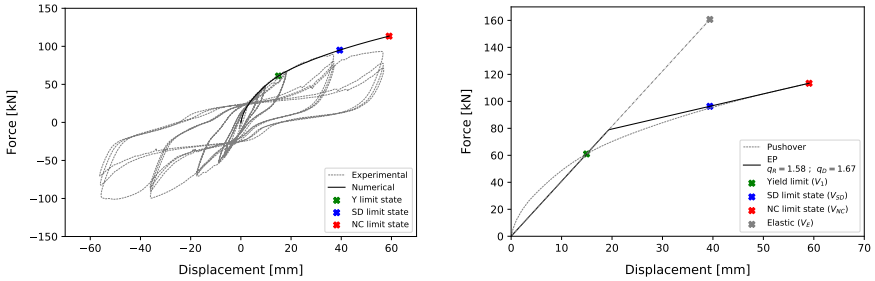

(a) (b)

Figure 5.15. Numerical model DC3: Hysteretic response (a), Energy (b).

The results show an excellent overlap of the monotonic numerical curve and the first cycle envelope curve for both configurations. Besides, the position of the limits state on the monotonic curve are reasonable. The absence of the degradation behaviour depends on the load-control analysis, which does not reproduce the strength's impairment. However, this phenomenon does not affect the overall behaviour significantly. In Table 5.5 are reported the corresponding values of base-shear, top displacement and q-factor contributions for DC2 and DC3 classes.

	V_1 [kN]	V_Y [kN]	V_{SD} [kN]	V_{NC} [kN]	V_E [kN]	d_1 [mm]	d_Y [mm]	d_{SD} [mm]	d_{NC} [mm]	q_R	q_D	q_0
DC2	74	103	107	114	131	18	25	31	43	1.44	1.22	1.76
DC3	61	79	96	113	161	15	19	39	59	1.58	1.67	2.64

Table 5.5. Results of wall panel test configurations.

5.4.2.1.2 Cycle-test validation: Pinching4 material

The validation for the cycle-test was carried out following two steps: (i) application of the vertical load and (ii) application of horizontal displacement history on the top nodes of the frame-box.

The experimental and numerical comparison (Figures 5.16-5.17) show a satisfying overlapping for the hysteretic response and the total energy involved during the cycle tests. Two considerations can be made.

In Figures 5.16-5.17 the singularity observable during the unloading path, especially for the DC2, at ±20mm is associated with the vertical load and the low re/un-loading stiffness of the connections. However, the modification of the overall response is limited and admissible.

The second consideration is the underestimation of the energy with the increasing of the displacement level. This effect could be acceptable due to the limited values of the R-squared coefficient for both models. Besides, the reduction of the dissipated energy depends on the neglected behaviour in shear of the hold-downs.

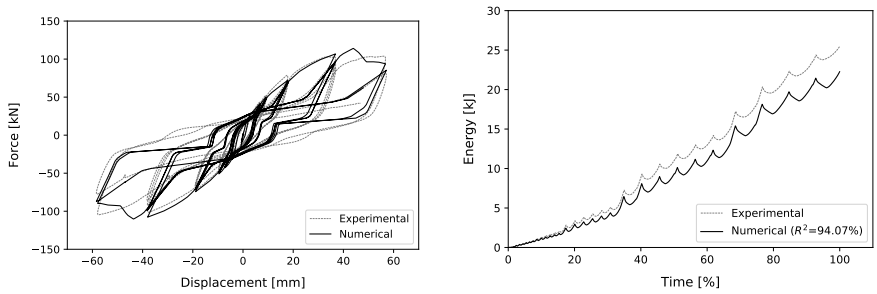

(a) (b)

Figure 5.16. Experimental and numerical comparison of DC2: hysteretic response (a), time-history energy (b).

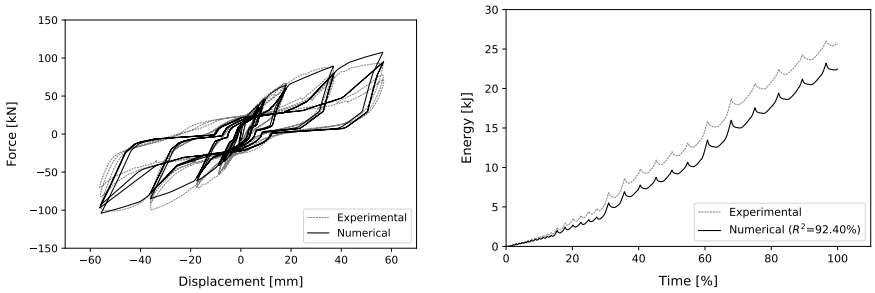

(a) (b)

Figure 5.17. Experimental and numerical comparison of DC3: hysteretic response (a), time-history energy (b).

5.4.3 Results: Comparison between DC2 and DC3

By way of example, a single configuration designed in DC2 and DC3 class is compared and analyzed. The remaining configurations show the same typical behaviour. The outcomes of each configuration are reported in Annex A.

The examinad configuration examined ("Model 173") is made of five storeys and four shearwalls (3m-4m-5m-6m) designed on soil type C. Figures 5.18 display the pushover curves (modal (a-c) and mass-proportional (b-d) load paths) while Figures 5.19 the corresponding deformed shapes. The overall seismic response is similar for the remaining configurations. A few considerations may be done on:

- Friction effect;
- Linearization of the capacity curve;
- Limit states;
- Maximum strength capacity.

Both ductility classes manifested a remarkable stiffness at the first loading phases due to the friction contribution. The friction influence the model's behaviour, mainly: the linearization curve and the estimation of the q_S contribution.

Some configurations required a modification of the linearization procedure present in section §5.3.1 and illustrated in Figure 5.20[4]. The reasons are

[4]It should be recalled that the limit states at the global level depend on deformation at the connections levels.

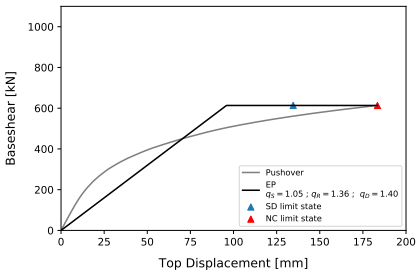

(a) DC2: Modal load path

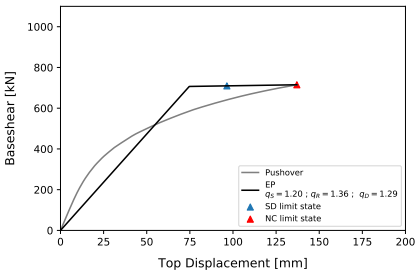

(b) DC2: Mass-proportional load path

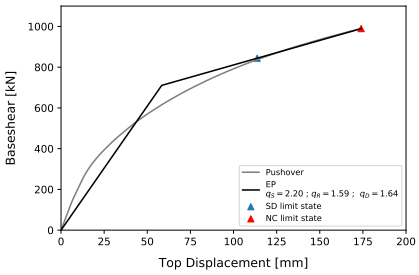

(c) DC3: Modal load path

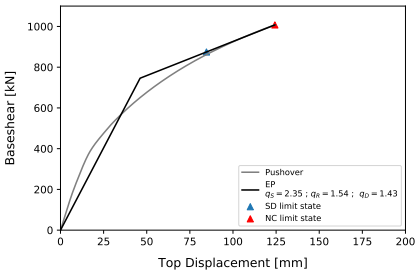

(d) DC3: Mass-proportional load path

Figure 5.18. Pushover curves: DC2 (a-b) and DC3 (c-d).

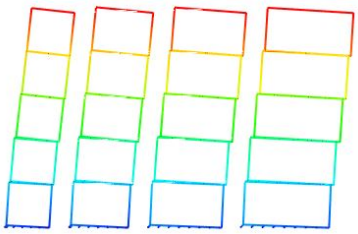

(a) DC2: Modal load path

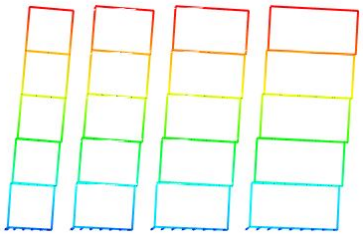

(b) DC2: Mass-proportional load path

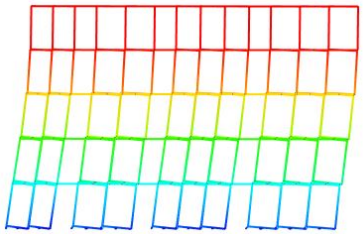

(c) DC3: Modal load path

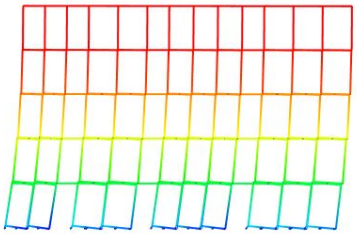

(d) DC3: Mass-proportional load path

Figure 5.19. Deformation shapes: DC2 (a-b) and DC3 (c-d).

the significant non-linearity manifested in the first loading phases and the connections' limited ductility. Due to the energy equivalence (Equation 5.3), the slope of the hardening branch could be negative (Figure 5.20(left)). The implemented solution was to adopt a plateau (non-hardening hardening curve) after the yielding point, by respecting the energy equivalence, if post-elastic stiffness was negative (Figure 5.20(right)). The effective yield point (d_1, V_1) is redefined through the intersection between the capacity and the elastic branch of the elastoplastic curve (from point B to $B^{\sim}$). The new conventional yield point (d_y, V_y) is shifted to the left (displacement reduction) in a conservative approach ($d_y^{\sim}$, $V_y^{\sim}$). DC2 class is mostly affected by this phenomenon due to the limited ductility of the connections (hold-downs and angle-brackets). On the contrary, in DC3 class, due to the premature yield slip value (in shear) of the half-lap joints, the yield point (d_1, V_1) is often located at the early stages of displacement, in this way avoiding problems of energy balance. Some discussions are ongoing within CEN/TC250/SC8 to address this issue by defining a secant stiffness when the current linearization procedure leads to negative stiffness values after the yielding point.

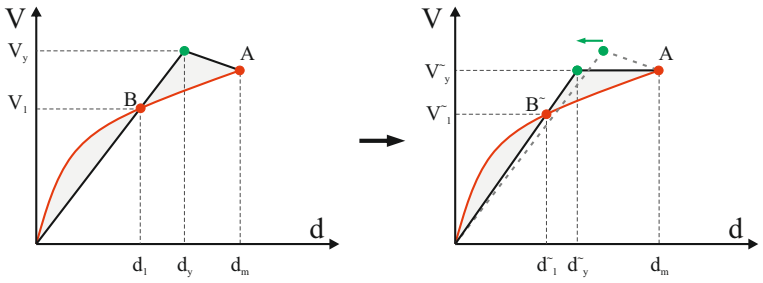

Figure 5.20. Modification of the linearization procedure.

The limit states (SD-NC) identified on the elastoplastic curve depends on the level of damage at the connections level. It is noteworthy that the significant damage limit state (SD) is located around the middle point of the post-elastic branch. This aspect guarantees a margin of safety before the attainment of the near-collapse limit state (NC).

DC2 and DC3 classes show different levels of maximum strength capacity for the same configuration. DC3 configurations present a higher maximum

strength capacity than DC2 leading to higher values of the q_S component. The q_S component is in genearal affected by several variables such as:

- The ratio between the capacity of the dissipative connection and the demand on the same connection;
- The ratio between the minimum capacity of the structure and the seismic demand (due to the minimum constructive details and site conditions);
- The modelling strategies adopted;
- The partial safety factors applied to the materials.

In addition the q_S factor also depends on: (i) the over-design, which is oftend preferred to time consuming optimization; (ii) the contribution in the tension of angle-brackets; and (iii) the respect of the capacity desing rules at the global level. All of these three aspects are strictly related.

The non-fully optimized design depends on the difficulties of its implementation in the design process. Future studies will investigate this important aspect.

In the design phase, the angle-brackets' tension stiffness and strength were neglected because of its complex implementation due to the need of a further iterative step. Evaluating the wall's overturning capacity (M_{Rd}), including the contribution to the uplift of angle-brackets, would in fact involve a new estimation of Equation 2.9 to be used in the design of the shear connections themselves and of all the non-dissipative components. This approach is not immediate. In addition, to promote the rocking instead of the sliding mechanism, angle-brackets with high shear capacity are required, which would inevitably introduce a greater tensile strength and stiffness, unless specific measures such as ovalized holes are taken. It is advisable to limit the number of angle-brackets on each wall and to place them near to the wall centre to obtain a symmetrical cyclic behaviour under in-plane loadings. It is desirable to develop innovative high strength shear connections which work only in shear.

Another issue is to comply the capacity desing rules at the global level, which is required to satisfy Equation 2.9. However, the storeys overstrength ratio $\Omega_{d,i}$ on the upper storeys (except the last one) tends to be significant due to the minimum number of connections adopted for practical reasons

(at least two hold-downs per wall and five screws on each vertical joint). The seismic demand in all other storeys where the ratio between capacity and demand tend to be unitary ($\Omega_{d,i}$) has then to be increased to ensure widespread plasticization. To avoid a considerable number of connections in DC3 (especially for angle brackets), the design strength adopted for HD and AB are 0.5 and 1.0 times the experimental strength for one- and two-story configurations, respectively, and 1.0 times for the rest. The DC2 class adopts the experimental strength since it is less influenced by the overdesigning phenomenon.

However, since the work aims to evaluate the intrinsic components, q_R and q_D, all overstrength introduced in the following analyses are neglibible. The q_S coefficient will be set to 1.5 for all structural materials according to the new Draft of EC8 (prEC8-1-1). For timber, this is approximately the ratio between the mean and the characteristic strength of the connections.

5.4.3.1 DC2 class

The results of DC2 class are shown in Table 5.6, whereas the trends and the relative contributions of the behaviour factor, sorted by load profiles, are shown in Figures 5.21.

The q_S contribution shows a wide dispersion of the results observed in the case of Figure 5.21a. The reasons for a standard deviation of 0.69 can be mainly attributed to the issues discussed in the previous section.

Regarding the remaining components, the values of q_R and q_D are an intrinsic property of the system and completley indipendent of the over-strengths introduced in the design phases. Unlike the q_R, which depends entirely upon the system and the structural configuration, the q_D value is evaluated following the criterion of equal displacement and energy for bilinear systems. In particular, it has been observed that q_0 ($q_R \cdot q_D$) tends to increase with the number of floors and is dependent on the size of the shearwalls of the structural configuration. Parametric analyses have shown that the behaviour factor is higher in structures composed of shearwalls where the L/H ratio is small due to the significant overturning mechanism that results in greater deformability of the panel. Conversely, structures characterized by higher L/H ratios, due to the dominant sliding mechanism,

tend to have lower behaviour factor values. Therefore, the behaviour factor q, in structures composed by shearwalls with both low and high L/H ratio, is governed by the collapse of the high L/H ratio walls.

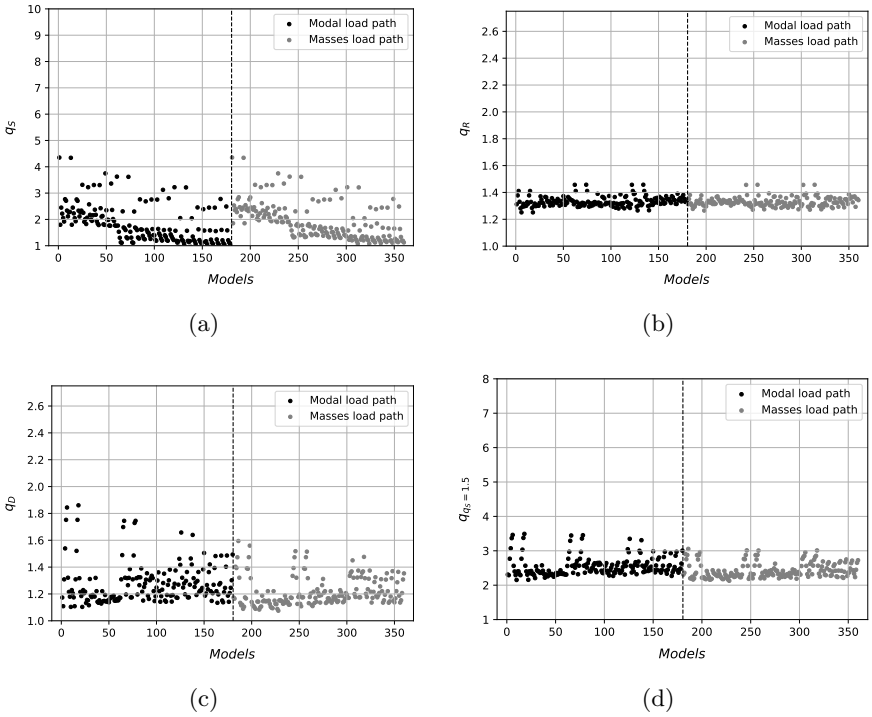

Figure 5.21. q-factor contributions for DC2: (a) q_S, (b) q_R, (c) q_D and (d) $q_{q_{s=1.5}}$.

	Mean	**Median**	**St. Dev.**	**5th-percentile**	**95th-percentile**
q_S	1.85	1.68	0.69	1.08	3.23
q_R	1.33	1.32	0.04	1.29	1.39
q_D	1.25	1.20	0.13	1.11	1.49
$q = 1.5 q_R q_D$	2.49	2.41	0.26	2.20	3.00

Table 5.6. Results for the moderate ductility class DC2.

Based on the results achieved and by adopting a conservative approach, it is possible to assume the 5th-percentile of the rounded results obtained for CLT structures in the moderate ductility class (DC2). In summary, the q_S is fixed and set to 1.5, and the proposed values of q_R and q_D are respectively 1.30 and 1.15 for a precautionary value of the behaviour factor equal to 2.24.

5.4.3.2 DC3 class

The results of DC3 class are shown in Table 5.7, whereas the trends and the relative contributions of the behaviour factor, sorted by load profiles, are shown in Figures 5.22.

The q_S component shows a dispersion of the results greater than DC2 ductility class with a deviation of 1.13 (Figure 5.22a).

Both q_R and q_D components are responsible for the more dissipative capacity than the DC2 ductility class. The q_R component exhibits values between 1.5 and 1.70 with a low standard deviation (0.05). The q_D component varies in a range between 1.4 to 1.6 with quite a higher standard deviation (0.07).

The intrinsic component q_0 ($q_R \cdot q_D$) remains quite constant for all configurations. In particular, unlike structures in DC2, no significant variation with the L/H ratio is observed. The motivation behind lies in the design of the walls with vertical joints. The vertical half-lap joint's yielding guaranteed the rocking mechanism (ductile) instead of the sliding one (less ductile). The ductility of the building tends to increase by using segmented walls with short panel size.

	Mean	**Median**	**St. Dev.**	**5th-percentile**	**95th-percentile**
q_S	3.52	3.31	1.13	2.10	5.55
q_R	1.58	1.58	0.05	1.49	1.67
q_D	1.51	1.52	0.07	1.40	1.61
$q = 1.5 q_R q_D$	3.57	3.54	0.23	3.25	3.94

Table 5.7. Results for the high ductility class DC3.

As reported in Table 5.7, the 5-th percentile values of the q_R and q_D for structures in high ductility class (DC3) are respectivally 1.49 and 1.40 with a more limited standard deviation in the case of q_R. Conservatively it is possible to assign as default values 1.50 for the q_R and 1.40 for the q_D by establishing a global behavior factor equal to 3.15 ($q_S = 1.5$).

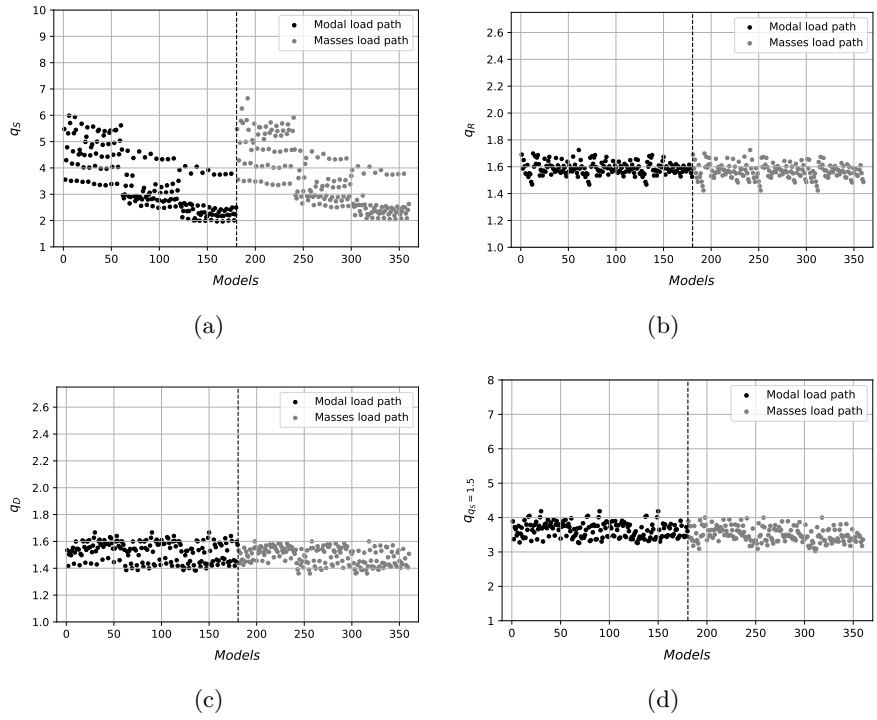

Figure 5.22. q-factor contributions for DC3: (a) q_S, (b) q_R, (c) q_D and (d) $q_{q_{s=1.5}}$.

5.4.3.3 General consideration of the results

The FE model described in §5.4.2 could be classifiable as a "component level model" and, as is already known, the findings are the results of design and modelling assumptions. The following points could be discussed:

- Two-dimensional instead of three-dimensional model;
- Use of frame elements instead of 2D area elements;
- Kinematic mechanisms and wall-to-slab iteration;
- Orthogonal walls iteration.

The model was conceived to perform a parametric study that could be easily managed with two-dimensional instead of three-dimensional models. The FE strategy could be extended without any difficulties for three-dimensional problems. In the following analysis, the spatial aspect is neglected for the sake of simplicity. However, it should be noted that, for irregular structures (in elevation and in plan), the q-factor is penalized with a reduction of 20% (as for all structural materials).

The use of frame elements instead of 2D area elements for the CLT panel allows for a huge reduction of the FE model matrix leading to lower analysis times. Due to the limited error observable in the validation, the strategy was assumed as reasonable.

The kinematic mechanisms are still a hot topic for the research field, and common consent is not available. The kinematic mechanisms depend on the shearwall size, the vertical loads, the connections' mechanical properties, and the dissipative and non-dissipative components. However, especially for the single-panel multi-storey shearwalls, it was observed that the kinematic assumption of cantilever behaviour is aspectable (Casagrande et al., 2021). Meanwhile, for multi-panel multi/single-storey shearwalls, the kinematic mechanisms become more complicated. The main reason is associated with the effect of the connections between the wall and the up-floor (Tamagnone et al., 2020) which modify the couple-panel (CP) behaviour. The used strategy neglect the connections between the wall and the up-floor (designed to be non-dissipative connections) in the form of a simplified strategy assuming a shear-type behaviour (see §4.3.1), providing to the achievment of the CP behaviour.

The orthogonal walls' contribution is neglected since it is dubious due to the infinite possible positions where they can be located in a 2D model. Future investigation will consider a 3D structure in which the effect will be include.

5.4.4 Local and Global limit state

Downstream the parametric analysis, the displacement corresponding to the SD LS defined by monitoring the connections' local deformations was correlated with the coefficient α_{SD} on the SDOF curve (Figure 5.4). α_{SD} is defined as the portion of the plastic part of the displacement of the equivalent SDOF oscillator that corresponds to the attainment of SD (Figure 5.23).

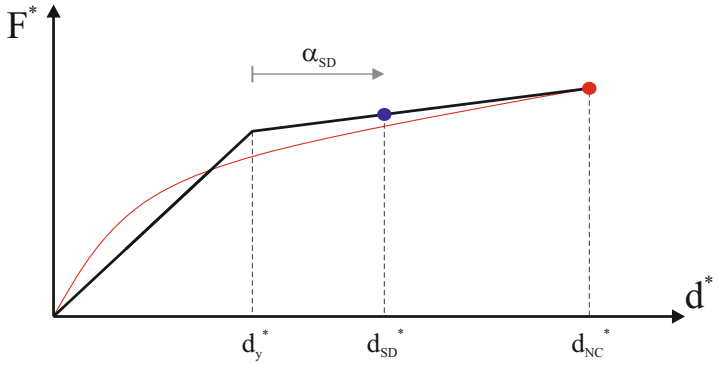

Figure 5.23. Definition of α_{SD}.

$$\alpha_{SD} = \frac{(d^*_{SD} - d^*_y)}{(d^*_{NC} - d^*_y)} \tag{5.15}$$

The results in Table 5.8 underline that for DC2 and DC3, the mean values of α_{SD} are 0.34 and 0.48, respectively. The main difference is related to the presence of the vertical half-lap joints in the DC3 class which allows anticipates the effective yield point (V_1, d_1) and therefore increases the post-elastic branch of the SDOF. As a preliminary investigation, the obtained values could be used to perform a displacement-based verification without monitoring the level of damage at the connections level. It is emphasized that these values are valid for the same modelling strategy and the connections adopted. However, the use of the local deformation attained at the connection level is encouraged instead of monitoring the global deformations even if additional studies are available.

		Mean	Median	St. Dev	5th-percentile	95th-percentile
DC2	α_{SD}	0.34	0.31	0.09	0.24	0.51
DC3	α_{SD}	0.48	0.47	0.04	0.45	0.56

Table 5.8. α_{SD} coefficient: correlation between local and global ductiliy.

5.4.5 Variation of the q-factor with connections ductility

The results reported in the previous sections are explicitly calibrated on specific experimental tests of the connections (Gavric et al. (2015c), Gavric et al. (2015b)). Since the global market of timber connections offers several products with different behaviour (especially in terms of ductility), the following section investigates the dependency of the q-factor on the connections ductility. The strength and the skeleton curves of the traditional timber-to-steel screw connections are reasonably similar to those used (see (Tomasi and Sartori, 2013) and (Schneider et al., 2015)). Therefore this study adopts the same connections by only varying the level of ductility.

Many combinations are analysed since there may be either two or three ductility components in DC2 or DC3 CLT walls assembly, respectively. The parametric analyses used four and eight scenarios with different connections' ductility, respectively, for DC2 and DC3. The yield point in the connections was fixed while the ductility was varied by assuming reasonable values. The failure deformation was directly defined as the product of the yield slip and ductility. The post-peak branch of the SAWS constitutive link was considered as a plateau. Furthermore, although the connections' failure deformation cannot exceed 30mm (according to EN 12512), in scenario 4, a higher deformation limit of the angle-bracket shear was adopted.

The comparison of the results was carried out through parametric analyses for the two ductility classes (DC2 and DC3) with a representative sample of configurations shown in Table 5.9. The deformability limits of all the connections, rounded to the millimetre, are summurized in Tables 5.10-5.11-5.12-5.13-5.14-5.15-5.16-5.17.

Number of storeys:	From 1 to 6
Configurations: **([L. shearwall 1, L. shearwall n.])**	[4], [6], [4, 6], [3, 6, 6], [3, 4, 5, 6]
Storey load (G_{k1}, G_{k2}, $0.3 \cdot Q_k$): (floor influence length 5m)	3.6 kN/m^2
Roof load (G_{k1}, G_{k2}): (floor influence length 5m)	1.2 kN/m^2
Soil condition: (Topographic class T1)	B
Profilo di carico: Proportional to the first mode	1
Load Path: Proportional to the mass	1
Total number of analysis	60

Table 5.9. Configuration summary for each ductility class.

	Hold-Down	**Angle-Bracket**		**Half-Lap Joint**
	tension	**shear**	**tension**	**shear**
$\mu = \delta_{NC}/\delta_Y$	1.5	1.5	1.5	3.0
δ_Y [mm]	9	13	7	3
δ_{SD} [mm]	11	16	9	6
δ_{NC} [mm]	14	20	11	9

Table 5.10. Configuration "1".

	Hold-Down	**Angle-Bracket**		**Half-Lap Joint**
	tension	**shear**	**tension**	**shear**
$\mu = \delta_{NC}/\delta_Y$	1.8	1.8	1.8	3.5
δ_Y [mm]	9	13	7	3
δ_{SD} [mm]	13	18	10	7
δ_{NC} [mm]	16	23	13	11

Table 5.11. Configuration "2".

	Hold-Down	**Angle-Bracket**		**Half-Lap Joint**
	tension	**shear**	**tension**	**shear**
$\mu = \delta_{NC}/\delta_Y$	2.0	2.0	2.0	4.0
δ_Y [mm]	9	13	7	3
δ_{SD} [mm]	14	20	11	8
δ_{NC} [mm]	18	26	14	12

Table 5.12. Configuration "3".

	Hold-Down	**Angle-Bracket**		**Half-Lap Joint**
	tension	**shear**	**tension**	**shear**
$\mu = \delta_{NC}/\delta_Y$	3.0	3.0	3.0	5.0
δ_Y [mm]	9	13	7	3
δ_{SD} [mm]	18	26	14	9
δ_{NC} [mm]	27	39	21	15

Table 5.13. Configuration "4".

Table 5.18 and Table 5.19 summarize the results, respectively, for the DC2 and DC3 class. The 5th-percentiles of the results are adopted as reference values in a conservative approach. The q_S component of DC2 shows an increase with the connections ductility, while it remains the

	Hold-Down	**Angle-Bracket**		**Half-Lap Joint**
	tension	**shear**	**tension**	**shear**
$\mu = \delta_{NC}/\delta_Y$	2.0	2.0	2.0	5.0
δ_Y [mm]	9	13	7	3
δ_{SD} [mm]	14	20	11	9
δ_{NC} [mm]	18	26	14	15

Table 5.14. Configuration "5".

	Hold-Down	**Angle-Bracket**		**Half-Lap Joint**
	tension	**shear**	**tension**	**shear**
$\mu = \delta_{NC}/\delta_Y$	3.0	3.0	3.0	8
δ_Y [mm]	9	13	7	3
δ_{SD} [mm]	18	26	14	14
δ_{NC} [mm]	27	39	21	24

Table 5.15. Configuration "6".

	Hold-Down	**Angle-Bracket**		**Half-Lap Joint**
	tension	**shear**	**tension**	**shear**
$\mu = \delta_{NC}/\delta_Y$	1.8	1.8	1.8	5.5
δ_Y [mm]	9	13	7	3
δ_{SD} [mm]	13	18	10	10
δ_{NC} [mm]	16	23	13	17

Table 5.16. Configuration "7".

	Hold-Down	**Angle-Bracket**		**Half-Lap Joint**
	tension	**shear**	**tension**	**shear**
$\mu = \delta_{NC}/\delta_Y$	1.5	1.5	1.5	5.0
δ_Y [mm]	9	13	7	3
δ_{SD} [mm]	11	16	9	9
δ_{NC} [mm]	14	20	11	15

Table 5.17. Configuration "8".

same for DC3 class. In DC2 configurations, due to the re-design of the elastoplastic curves (a phenomenon described in the previous section), the base-shear V_1 decreases in case of low-ductility connections. On the other side, in DC3, the half-lap joint yields before the other connections (hold-downs and angle-brackets) in all configurations; thus, the q_S does not change. The q_R factor remains almost constant for all configurations since the connections' skeleton curve is the same. The dissipative component q_D increases in both cases with the connections' ductility, as expected. While in DC2 the variation is not significant due to HD and AB's limited available ductility, careful consideration should be given to DC3 where screws/nails of the vertical joints govern the dissipative capacities. The ductility variation of the HDs and ABs does not substantially change the

		Conf. "1"	Conf. "2"	Conf. "3"	Conf. "4"
q_S	Mean:	1.34	1.41	1.67	1.70
	Median:	1.25	1.30	1.51	1.56
	St. Dev.:	0.47	0.51	0.57	0.58
	5th-perc.:	0.84	0.90	1.16	1.22
	95th-perc.:	2.39	2.49	3.02	2.97
q_R	Mean:	1.32	1.33	1.32	1.36
	Median:	1.32	1.33	1.32	1.35
	St. Dev.:	0.03	0.03	0.04	0.05
	5th-perc.:	1.28	1.28	1.28	1.30
	95th-perc.:	1.37	1.37	1.39	1.43
q_D	Mean:	1.14	1.16	1.28	1.45
	Median:	1.12	1.14	1.25	1.44
	St. Dev.:	0.08	0.08	0.13	0.11
	5th-perc.:	1.07	1.08	1.10	1.32
	95th-perc.:	1.33	1.35	1.51	1.768
$q = 1.5 q_R q_D$	Mean:	2.26	2.30	2.53	2.95
	Median:	2.23	2.27	2.48	2.91
	St. Dev.:	0.15	0.14	0.24	0.20
	5th-perc.:	2.12	2.14	2.24	2.73
	95th-perc.:	2.62	2.60	2.91	3.33

Table 5.18. Results of DC2 configurations.

		Conf. "1"	Conf. "2"	Conf. "3"	Conf. "4"	Conf. "5"	Conf. "6"	Conf. "7"	Conf. "8"
q_S	Mean:	3.30	3.30	3.30	3.30	3.30	3.30	3.30	3.30
	Median	3.06	3.08	3.08	3.08	3.08	3.08	3.08	3.08
	St. Dev.:	0.63	0.64	0.64	0.64	0.64	0.64	0.64	0.64
	5th-perc.:	2.58	2.57	2.57	2.57	2.57	2.57	2.57	2.57
	95th-perc.:	4.56	4.56	4.56	4.56	4.56	4.56	4.56	4.56
q_R	Mean:	1.41	1.43	1.45	1.48	1.48	1.63	1.51	1.48
	Median	1.41	1.43	1.45	1.47	1.47	1.64	1.51	1.47
	St. Dev.:	0.03	0.02	0.03	0.04	0.04	0.06	0.04	0.03
	5th-perc.:	1.35	1.39	1.41	1.42	1.42	1.53	1.44	1.42
	95th-perc.:	1.45	1.46	1.50	1.54	1.54	1.72	1.58	1.54
q_D	Mean:	1.12	1.19	1.27	1.34	1.34	1.59	1.40	1.34
	Median	1.11	1.18	1.27	1.35	1.35	1.61	1.42	1.35
	St. Dev.:	0.03	0.05	0.05	0.05	0.05	0.10	0.06	0.05
	5th-perc.:	1.08	1.12	1.21	1.27	1.27	1.45	1.32	1.27
	95th-perc.:	1.17	1.26	1.34	1.41	1.41	1.74	1.48	1.41
q_D	Mean:	2.36	2.55	2.77	2.97	2.97	3.90	3.17	2.97
	Median	2.36	2.54	2.75	2.95	2.95	3.89	3.13	2.95
	St. Dev.:	0.07	0.11	0.13	0.15	0.15	0.30	0.18	0.15
	5th-perc.:	2.24	2.38	2.57	2.76	2.76	3.51	2.89	2.76
	95th-perc.:	2.50	2.74	3.00	3.24	3.24	4.30	3.46	3.24

Table 5.19. Results of DC3 configurations.

result for a given half-lap joint ductility (see configurations 4 and 5).

Figures 5.24a-b show the 5th/50th/95th-percentiles of the behaviour factor q (y-axis) against the connections' ductility (x-axis) and the proposed q-factors of the previous section. In the case of DC2, accepting a median value (50th-percentiles) is possible to guarantee a q-factor equal to 2.24 with a minimum ductility of 1.5 for hold-downs and angle-brackets, respectively. The q-factor equal to 2.12 corresponds to the 5th-percentiles, which is lower

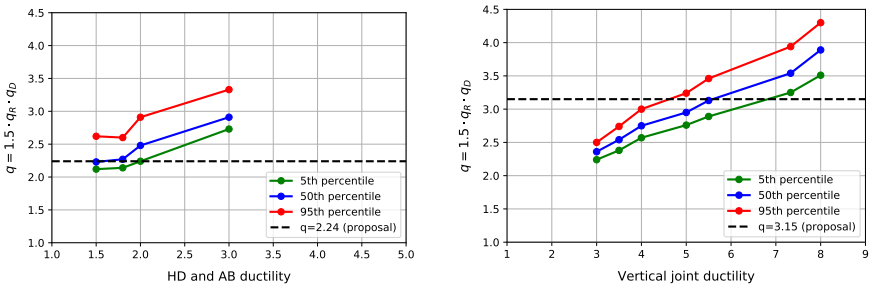

(a) DC2 (b) DC3

Figure 5.24. q-factor vs connections' ductility variation.

than the -5.36% of the 50th-percentiles. In DC3, to obtain an overall behaviour factor q equal to 3.15, the vertical joint connections' ductility could be of the order of 5.5 (configuration "7"). This value could be classified as moderate ductility ($4 \leq \mu \leq 6$) according to Smith et al. (2006).

The proposed values for both ductility classes are acceptable due to all uncertainties in the modelling not included.

5.4.5.1 General discussion

The parametric investigation allows estimating the minimum ductility level of the dissipative components. The proposed ductility values are the minimum capacity required to guarantee the attainment of the q-factors. Generally, the ductility level of the connections is greater than the proposed values (see (Jockwer and Jorissen, 2018), (Rossi et al., 2019)). However, these values ensure the proposed q-factors and allow the applicability of most commercial products.

5.5 Verification of the q-factor via incremental dynamic analysis (IDA)

The non-linear static analyses (NLSA) performed in the previous section provided the q-factor contributions of several 2D configurations through a parametric approach. This section investigates those contributions based on more advanced analysis. The non-linear dynamic analysis allows the practitioners to figure out the non-linear behaviour of a structure, taking into account the hysteretic response under earthquake ground motions.

An incremental dynamic analysis (IDA) was carried out to investigate the complete non-linear behaviour of CLT structures for two geometrical configurations in terms of shearwalls and number of storeys. The two configurations, representative of low- and mid-rise buildings, were designed in the two dissipative classes (moderate ductility DC2 and high ductility DC3) in order to compare the performances. In particular, the following aspects were investigated:

1. Verification of the q_0 component via IDA;
2. Verification of the performance via reliability-analysis;
3. Estimation of the inter-storey drift limits for CLT buildings.

5.5.1 Case study configurations

Two 2D building configurations were considered for the IDA analyses due to the computational effort required. A three and five storeys configurations designed in DC2 and DC3 class were taken into account (Figure 5.25) to compare the performances of different ductility classes.

The design approach was the same as the parametric NLSA (section 5.4.1) however, a hand design was carried out to reduce the overstrength effect. The skeleton curves of hold-downs have a strength/stiffness 0.5 times the experimental one for the DC3 class whereas for DC2 the experimental values were implemented with Pinching4 material. A q-factors equal to 2.0 and 3.0 were adopted for the DC2 and DC3, respectively. The details of each structural configurations are reported in Tables 5.20-5.22-5.21-5.23.

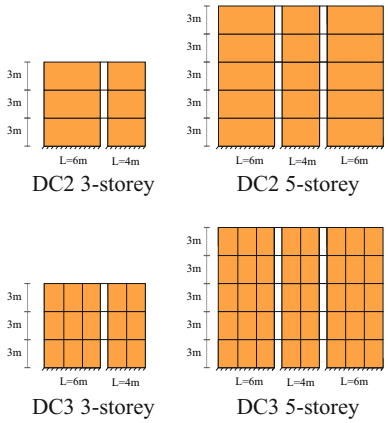

Figure 5.25. Configurations analyzed for NLDA: DC2 and DC3.

Storey	Vertical load	Shearwall 1	Shearwall 2
	kN/m	L=6m	L=4m
3	6.0	1 AB + 2 HD	1 AB + 2 HD
2	18.0	3 AB + 2 HD	2 AB + 2 HD
1	18.0	4 AB + 2 HD	3 AB + 2 HD

Table 5.20. DC2 3-storey details.

Storey	Vertical load	Shearwall 1	Shearwall 2
	kN/m	L=6m, 3-panels	L=4m, 2-panels
3	6.0	3 AB + 2 HD + 5 SC	2 AB + 2 HD + 5 SC
2	18.0	4* AB + 2 HD + 5 SC	(2*+1) AB + 2 HD + 5 SC
1	18.0	5* AB + 2 HD + 5 SC	(3*+1) AB + 2 HD + 5 SC

Table 5.21. DC3 3-storey details (*double strength of the standard connection; screws for each vertical joint).

Storey	Vertical load	Shearwall 1	Shearwall 2	Shearwall 3
	kN/m	L=6m	L=4m	L=6m
5	6.0	1 AB + 2 HD	1 AB + 2 HD	1 AB + 2 HD
4	18.0	3 AB + 2 HD	2 AB + 2 HD	3 AB + 2 HD
3	18.0	4 AB + 2 HD	3 AB + 2 HD	4 AB + 2 HD
2	18.0	5 AB + 2 HD	3 AB + 2 HD	5 AB + 2 HD
1	18.0	5 AB + 2 HD	4 AB + 2 HD	5 AB + 2 HD

Table 5.22. DC2 5-storey details.

Storey	Vertical load	Shearwall 1	Shearwall 2	Shearwall 3
	kN/m	L=6m, 3-panels	L=4m, 2-panels	L=6m, 3-panels
5	6.0	2 AB + 2 HD + 5 SC	2 AB + 2 HD + 5 SC	2 AB + 2 HD + 5 SC
4	18.0	7 AB + 2 HD + 5 SC	5 AB + 2 HD + 5 SC	7 AB + 2 HD + 5 SC
3	18.0	(5*+1) AB + 2 HD + 5 SC	(3*+1) AB + 2 HD + 5 SC	(5*+1) AB + 2 HD + 5 SC
2	18.0	(6*+1) AB + 2 HD + 5 SC	(4*+1) AB + 2 HD + 5 SC	(6*+1) AB + 2 HD + 5 SC
1	18.0	7* AB + 2 HD + 5 SC	(4*+1) AB + 2 HD + 5 SC	7* AB + 2 HD + 5 SC

Table 5.23. DC3 5-storey details (*double strength of the standard connection; screws for each vertical joint).

5.5.2 IDA concepts and fragility curves

The Incremental Dynamic Analysis (IDA) is a parametric analysis which can be used to estimate the structural performance under seismic loads (Vamvatsikos and Allin Cornell, 2002) via time-history analysis.
IDA consists of applying a suite of ground motions to a numerical model with an increasing level of intensity until the structure reaches a particular level of damage. IDA are useful to built the seismic fragility functions (also called fragility curves) of a particular structure describing the performance in probabilistic terms (Figure 5.26).

The seismic fragility function allows estimating the vulnerability of a structure under telluric events through a probabilistic approach. The functions correlate the probability (y-axis in Figure 5.26) of achieving a particular level of damage D (or other limit states of interest) to an intensity measure $IM = im$ (x-axis in Figure 5.26) of a ground motion event GM. Spectral acceleration, peak-ground acceleration PGA, peak-ground velocity PGV or peak-ground displacement PGD are the most widespread intensity measure used for seismic design while the D is often associated to the inter-storey drift limits or the chord rotation for frame structures.

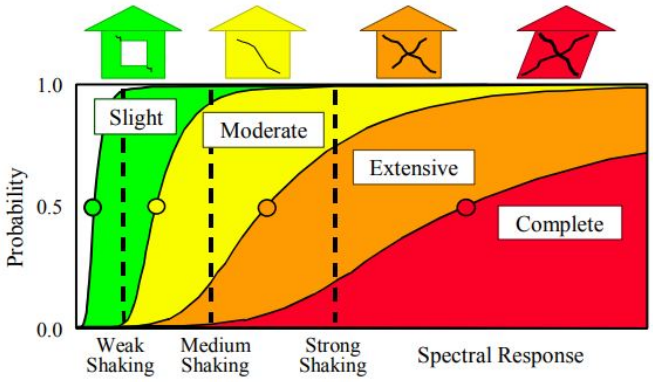

Figure 5.26. Example fragility curves for slight, moderate, extensive and complete damage (Kircher et al., 2006).

Several approaches can be adopt to define the fragility function based on the type of method and the data obtained ((Baker, 2015), (Baraschino et al., 2020)). In this work, the fragility functions are estimated by fitting the cumulative distribution function (CDF) of the lognormal distribution

((Ibarra and Krawinkler, 2005), (Eads et al., 2013)):

$$P(D|IM = im) = \Phi\left(\frac{ln(im) - \hat{\mu}}{\hat{\sigma}}\right) \tag{5.16}$$

where $\Phi(\cdot)$ is the CDF of the normal distribution and $\hat{\mu}$ and $\hat{\sigma}$ are respectively the mean and the lognormal standard deviation of the given N outcomes of the intensity measure IM associate to the damage D. In probabilistic terms, $P(D|IM = im)$ is the probability of a ground motion with intensity im will leads the structure to a level of damage D. The parameters of the CDF ($\hat{\mu}$ and $\hat{\sigma}$) are estimated via the method of moments estimator (Equations 5.17-5.18). It is worth mentioning that the method of the moments estimator is equivalent to the method of maximum likelihood if the data are representative of the full distribution.

$$\hat{\mu} = \frac{1}{N}\sum_{n=1}^{N} ln(im) \tag{5.17}$$

$$\hat{\sigma} = \sqrt{\frac{1}{N-1}\sum_{n=1}^{N}[ln(im) - \hat{\mu}]^2} \tag{5.18}$$

5.5.3 Ground motions selection

The reference site was L'Aquila (Italy) a high-seismic risk area in Italy and Europe. A return period of $T_R = 475$ years, with a probability of exceeding 10% in 50 years was used as design ground motion. Soil type B and topography class T1 with 5% of critical damping defined the elastic pseudo-acceleration spectrum. The design PGA is equal to 0.30g.

A set of un-scaled 14 real ground-motions spectrum compatible was obtained from Rexel (Iervolino et al., 2010) (Figure 5.27b) by adopting a disaggregation analysis[5] (Figure 5.27a). The moment magnitude was selected between 4.5 and 6.5, with a maximum epicentral distance of 30km. The lower and upper tolerance was fixed respectively equal to 10% and 30%. The period of interest was between 0.15sec and 1.5sec. The ground motion records were selected from SIMBAD database (Smerzini and Paolucci, 2013).

[5]The disaggregation analysis is a process that allows calculating the contribution of different scenario $M - R$ of the seismic hazard (McGuire, 1995).

Table 5.24 and Figure 5.27b summarize the ground motion events and the pseudo-acceleration response spectrum. In Annex B the ground motions time-histories are reported.

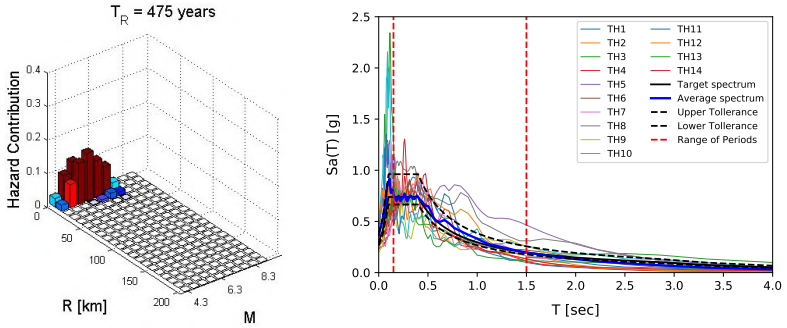

(a) (b)

Figure 5.27. Ground motion selection: disaggregation analysis (Iervolino et al., 2010) (a), elastic response spectrum (b).

TH	Location	Date	Mw	Epicentral D. [km]	PGA_{gm} [g]	Length [sec]
1	Parkfield	28/09/2004	6.0	12.49	0.51	20.96
2	Mid Niigata Prefecture	23/10/2004	6.3	16.53	0.23	81.85
3	South Iceland	21/06/2000	6.4	11.1	0.44	24.55
4	S. Suruga Bay	10/08/2009	6.2	28.13	0.23	93.31
5	Olfus	29/05/2008	6.3	8.89	0.48	20.35
6	Emilia	20/05/2012	6.1	13.36	0.26	34.78
7	Christchurch	21/02/2011	6.2	13.73	0.25	38.15
8	Imperial Valley	15/10/1979	6.5	27.03	0.49	39.00
9	N. Miyagi Prefecture	25/07/2003	6.1	9.93	0.20	78.89
10	Honshu	10/08/1996	5.9	13.89	0.46	128.14
11	NW Kagoshima Prefecture	26/03/1997	6.1	12.15	0.43	38.44
12	L'Aquila	06/04/2009	6.3	4.39	0.49	100.00
13	Bingol	01/05/2003	6.3	11.79	0.29	34.86
14	Friuli	06/06/1976	6.4	21.72	0.35	36.39

Table 5.24. Ground motions records.

5.5.4 Intensity and damage measures

The intensity measure (IM) adopted in the IDA analyses was the Peak Ground Acceleration (PGA [g]) to compare the performances of the two configurations designed for different ductility classes.
Each ground motion was linearly scaled from a PGA of 0.00g to 1.50g with an increment step of 0.02g by using a scale factor λ_i

$$PGA_i = PGA_{gm} \cdot \lambda_i \tag{5.19}$$

where PGA_i is the $i-th$ peak-ground acceleration and PGA_{gm} is the real peak-ground acceleration.
The Damage measure (DM) was the local deformation attained at the connections level as implemented in the pushover analyses. The connections deformability were monitored at each time-step with the displacement domains (described in section §) through ad-hoc dedicated tool.
The attainment of the DM was used to find the corresponding inter-storey drift limits.

5.5.5 Solution of the dynamic problem

The numerical model strategy adopted for the dynamic analyses is described in section 5.4.2. Pinching4 material was implemented in the model to account the hysteretic response of the CLT shearwalls. The storeys masses are lumped in the same nodes in which the vertical loads are applied. The gravity loads were applied before the dynamic analysis and maintained constant during the ground motion. A Rayleigh damping formulation was adopted to define the damping matrix $\boldsymbol{C}$. Equivalent viscous damping $\xi_{eq} = 5\%$, as included in the ground motion and the elastic response spectrum was applied to the entire model proportional to the mass matrix $\boldsymbol{M}$. The factor α_M was calibrated on the first circular frequency ω_1.

$$\mathbf{C} = \alpha_M \cdot \mathbf{M} = 2 \cdot \xi_{eq} \cdot \omega_1 \cdot \mathbf{M} \tag{5.20}$$

The Hilber-Hughes-Taylor Method (HHT) (Hilber et al., 1977) was adopt to solve the dynamic problem with an α factor equal to 0.1.

An integration time step $\Delta T = 0.005s$ was adopted while in case of a convergency problem, a dedicated algorithm was developed to reduce the time-step during the analysis.

Krylov-Newton (Scott and Fenves, 2020) algorithm was used as a solution strategy.

The energy increment test was implemented to check the convergence with a tolerance equal to 1.0^{-5}.

Class	**Configuration**	$T_1\,[sec]$	$\omega_1\,[rad/sec]$
DC2	3-storey	0.29	21.66
	5-storey	0.51	12.34
DC3	3-storey	0.24	25.65
	5-storey	0.40	15.78

Table 5.25. Periods and circular frequency of the FE models.

5.5.6 Analyses and results

Pushover analyses were carried out on each model before the IDAs to compare the two types of methods. Table 5.26 reports the q-factor components estimated with the pushover approach. Tables 5.27-5.28-5.29-5.30 summarize the output data of parameters of interest for each of the ground motions obtained from the IDA analyses. The PGA_Y, PGA_{SD}, PGA_{NC} correspond respectively to the peak-ground acceleration at the first connection's yield (Y), the attainment of the significant damage limit state (SD) on the first connection and the attainment of the near-collapse limit state (NC) on the first connection. The same definition is for the inter-storey drifts, defined as the maximum values attained during each time-history in all storeys. The intrinsic component of the q-factor, q_0 ($q_R \cdot q_D$) was calculated as the ratio between PGA_{SD} and PGA_Y as later described.

Class	**Configuration**	**Load Path**	q_S	q_R	q_D	q_0
DC2	3-storey	Modal	1.65	1.37	1.15	1.58
		Masses	1.74	1.37	1.08	1.48
	5-storey	Modal	1.28	1.36	1.25	1.70
		Masses	1.42	1.35	1.17	1.58
DC3	3-storey	Modal	2.54	1.44	1.63	2.35
		Masses	2.57	1.43	1.45	2.07
	5-storey	Modal	3.14	1.45	1.67	2.42
		Masses	3.31	1.45	1.61	2.33

Table 5.26. q-factor contributions of the four configurations.

TH	PGA_Y [g]	PGA_{SD} [g]	PGA_{NC} [g]	$drift_Y$ [%]	$drift_{SD}$ [%]	$drift_{NC}$ [%]	q_0 [−]
1	0.46	0.66	0.84	0.51	0.84	1.16	1.43
2	0.32	0.56	0.70	0.48	0.77	1.05	1.75
3	0.56	0.82	1.08	0.52	0.85	1.20	1.46
4	0.28	0.38	0.48	0.50	0.77	1.06	1.36
5	0.60	0.74	0.88	0.52	0.84	1.15	1.23
6	0.32	0.42	0.58	0.49	0.75	1.01	1.31
7	0.28	0.46	0.60	0.49	0.77	1.06	1.64
8	0.52	0.74	0.90	0.54	0.85	1.17	1.42
9	0.36	0.54	0.68	0.50	0.76	1.12	1.50
10	0.82	1.32	-	0.53	0.89	-	1.61
11	0.48	0.66	0.82	0.53	0.85	1.16	1.38
12	0.56	0.78	1.02	0.53	0.85	1.17	1.39
13	0.46	0.66	0.90	0.48	0.74	1.01	1.43
14	0.52	0.76	0.96	0.49	0.78	1.03	1.46
Mean	0.47	0.68	0.80	0.51	0.81	1.10	1.46
Median	0.47	0.66	0.84	0.51	0.81	1.12	1.43
St. dev.	0.15	0.23	0.18	0.02	0.05	0.07	0.14

Table 5.27. IDA result: DC2 3-storey.

Figures 5.28 show the overlaps of the capacity curves obtained from the

TH	PGA_Y [g]	PGA_{SD} [g]	PGA_{NC} [g]	$drift_Y$ [%]	$drift_{SD}$ [%]	$drift_{NC}$ [%]	q_0 [−]
1	0.48	0.72	0.90	0.63	1.06	1.42	1.50
2	0.36	0.52	0.70	0.67	0.97	1.21	1.44
3	0.52	0.78	0.96	0.54	0.88	1.35	1.50
4	0.28	0.40	0.46	0.67	0.81	1.40	1.43
5	0.34	0.44	0.52	0.56	0.89	1.19	1.29
6	0.38	0.52	0.60	0.64	0.88	1.19	1.37
7	0.34	0.44	0.50	0.67	1.01	1.28	1.29
8	0.40	0.60	0.72	0.58	0.89	1.47	1.50
9	0.30	0.40	0.64	0.55	0.87	1.41	1.33
10	0.78	1.02	1.18	0.56	0.89	1.22	1.31
11	0.36	0.54	0.72	0.56	0.90	1.20	1.50
12	0.48	0.72	0.90	0.56	0.89	1.20	1.50
13	0.50	0.68	0.76	0.54	0.84	1.25	1.36
14	0.46	0.68	0.88	0.53	0.80	1.24	1.48
Mean	0.43	0.60	0.75	0.59	0.90	1.29	1.41
Median	0.39	0.57	0.72	0.56	0.89	1.25	1.44
St. dev.	0.13	0.17	0.20	0.05	0.07	0.10	0.08

Table 5.28. IDA result: DC2 5-storey.

TH	PGA_Y [g]	PGA_{SD} [g]	PGA_{NC} [g]	$drift_Y$ [%]	$drift_{SD}$ [%]	$drift_{NC}$ [%]	q_0 [−]
1	0.46	0.78	1.00	0.36	0.91	1.42	1.70
2	0.26	0.56	0.92	0.31	0.88	1.38	2.15
3	0.42	0.88	1.26	0.32	0.86	1.34	2.10
4	0.24	0.44	0.58	0.34	0.84	1.40	1.83
5	0.58	0.74	0.92	0.34	0.85	1.36	1.28
6	0.26	0.50	0.70	0.34	0.90	1.43	1.92
7	0.26	0.40	0.62	0.32	0.83	1.39	1.54
8	0.32	0.60	0.82	0.32	0.87	1.38	1.88
9	0.34	0.50	0.66	0.34	0.88	1.41	1.47
10	0.68	1.16	-	0.34	0.88	-	1.71
11	0.48	0.68	0.82	0.32	0.86	1.38	1.42
12	0.54	0.78	1.00	0.31	0.85	1.35	1.44
13	0.34	0.70	1.36	0.32	0.86	1.40	2.06
14	0.36	0.74	1.00	0.34	0.88	1.42	2.06
Mean	0.40	0.68	0.90	0.33	0.87	1.39	1.75
Median	0.35	0.69	0.92	0.33	0.86	1.39	1.77
St. dev.	0.14	0.20	0.24	0.01	0.02	0.03	0.29

Table 5.29. IDA result: DC3 3-storey.

NLSA and the IDA in top-displacement/base-shear plots. The IDA curves are defined as the maximum base-shear and the associated top-displacement leading to an irregular shape even if in good agreement with the pushover curves.

Figures 5.29 report the maximum inter-storey/PGA curves with the Y, SD, and NC limit states highlighted in green, blue and red respectively. Time history 10 (TH 10) is neglected at the NC since it does not lead to the collapse of all configurations except DC2 5-storey.

TH	PGA_Y [g]	PGA_{SD} [g]	PGA_{NC} [g]	$drift_Y$ [%]	$drift_{SD}$ [%]	$drift_{NC}$ [%]	q_0 [–]
1	0.36	0.72	1.06	0.37	0.91	1.45	2.00
2	0.32	0.58	0.78	0.35	0.90	1.39	1.81
3	0.48	0.92	1.22	0.35	0.92	1.39	1.92
4	0.22	0.42	0.58	0.34	0.87	1.48	1.91
5	0.36	0.60	0.70	0.37	0.89	1.40	1.67
6	0.28	0.64	0.74	0.33	0.88	1.44	2.29
7	0.24	0.54	0.64	0.34	0.87	1.46	2.25
8	0.40	0.64	0.82	0.35	0.89	1.39	1.60
9	0.24	0.48	0.78	0.36	0.88	1.43	2.00
10	0.54	1.38	-	0.34	0.88	-	2.56
11	0.32	0.62	0.90	0.36	0.88	1.38	1.94
12	0.38	0.78	1.00	0.36	0.88	1.45	2.05
13	0.42	0.84	1.18	0.34	0.91	1.43	2.00
14	0.40	0.76	1.00	0.34	0.89	1.42	1.90
Mean	0.35	0.71	0.88	0.35	0.89	1.42	1.99
Median	0.36	0.64	0.82	0.35	0.88	1.43	1.97
St. dev.	0.09	0.24	0.20	0.01	0.02	0.03	0.25

Table 5.30. IDA result: DC3 5-storey.

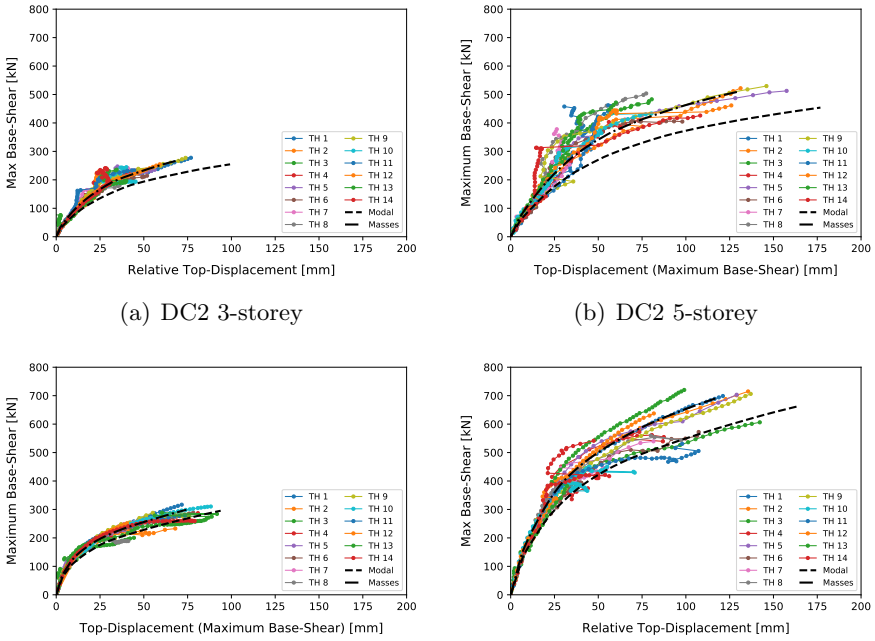

(a) DC2 3-storey

(b) DC2 5-storey

(c) DC3 3-storey

(d) DC3 5-storey

Figure 5.28. Comparison between pushover and IDA curves.

5.5.6.1 Verification of q_0

The intrinsic component of the q-factor, q_0 ($q_R \cdot q_D$), for the two ductility classes was evaluated by implementing the PGA approach. The original method adopted in (Ceccotti, 2008)-(Ceccotti et al., 2010) defines the q-factor as the ratio between the design PGA_d and the PGA_{NC} which leads to the failure one connection (hold-down in tension). Pozza et al. (2017)

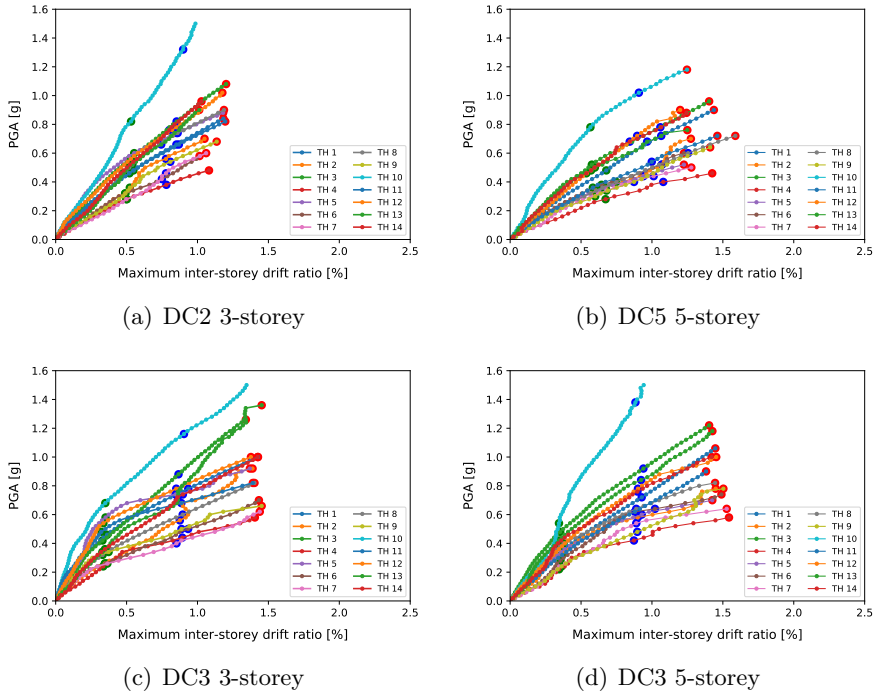

(a) DC2 3-storey

(b) DC5 5-storey

(c) DC3 3-storey

(d) DC3 5-storey

Figure 5.29. IDA results: PGA vs maximum inter-storey drift ratio.

used the same method by assuming unitary overstrength-factors to obtain the intrinsic q_0 component. The PGA_{NC} was defined when one connection (angle-bracket or hold-down) attains the ultimate displacement in the two orthogonal directions (shear and tension).

In this work, to disaggregate the intrinsic component q_0 from the over-design and code dependent part, the intrinsic component q_0 was calculated according to Equation 5.21:

$$q_0 = \frac{PGA_{SD}}{PGA_Y} \tag{5.21}$$

where:

PGA_Y is the peak-ground acceleration which is associated with the yield of the first connection Y;

PGA_{SD} is the peak-ground acceleration which is associated with the attainment of the SD deformation in the first connection.

Table 5.31 and Figure 5.30 summarize the results for the four configurations. The mean values of the intrinsic component q_0 obtained from the IDA

analysis are in agreement with the result obtained from the NLSA. A general underestimation of the q_0 was obtained for all configurations. A low value of the q_0 was founded in the DC3 3-storey configuration, especially for a particular ground motion (i.e. TH5). Future analyses are scheduled to investigate in more details the dynamic behaviour of DC3. Several aspects may affect the results, such as:

- The method adopted to estimate the q-factor;
- The hysteretic energy understimation of the FE model;
- The friction effect;
- The selection of the earthquake ground motions;
- The number of the earthquake ground motions;
- The ground motions scaling effect;
- The choice of the elastic viscous damping;
- The limited number of analyzed structures.

Class	**Configuration**	**NLSA** $q_{0,mean}$	**IDA** $q_{0,mean}$
DC2	3-storey	$(1.58 + 1.48)/2 = 1.53$	1.46
	5-storey	$(1.70 + 1.58)/2 = 1.64$	1.41
DC3	3-storey	$(2.35 + 2.07)/2 = 2.21$	1.75
	5-storey	$(2.42 + 2.33)/2 = 2.38$	1.99

Table 5.31. Intrinsic component q_0 of the behaviour factor.

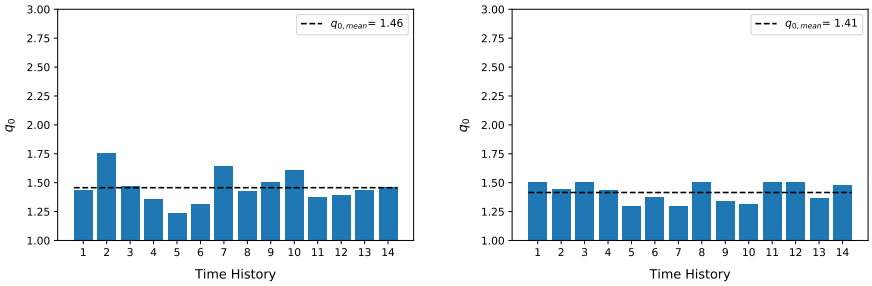

(a) DC2 3-storey

(b) DC5 5-storey

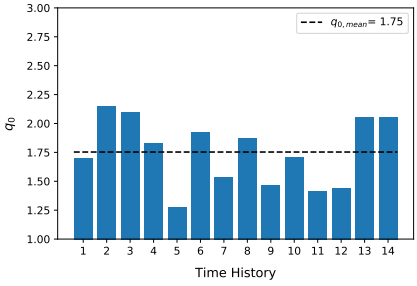

(c) DC3 3-storey

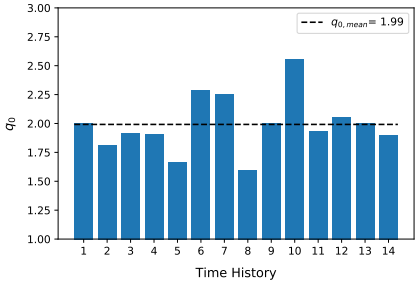

(d) DC3 5-storey

Figure 5.30. Intrinsic component of the q-factor q_0.

5.5.6.2 Performance verification

5.5.6.2.1 Fragility curves

Figures 5.31 show the fragility curves of the four configurations defined with Equation 5.16. The use of the PGA, instead of the spectral acceleration at the fundamental period, allows a direct comparison since all configurations were designed with the same pseudo-elastic spectrum with different q-factors (2.0 for DC2 and 3.0 for DC3). The scatter of the results is related to record-to-record uncertainty. Table 5.32 reports the median PGA_{LS} and the standard deviation of the lognormal distribution β_{LS}. Both ductility classes show around the same β_{LS} of 0.30 for all limit states.

For the designed ground motion with a 10% of the probability of exceedance in 50 years, the probability of reaching the first connection's yield is less for the DC2 class than the DC3 class. In particular, the values of 10.66% and 11.65% were founded for DC2 3-storey and DC2 5-storey respectively, whereas 25.00% for DC3 3-storey and DC3 30.79% DC3 5-storey, respectively. The estimated probability of reaching the SD limit state was 0.76% and

0.86% for the 3-storey and 5-storey configurations designed in DC2, while the values of 0.29% and 0.38% were found for the 3-storey and 5-storey configurations in DC3, respectively.

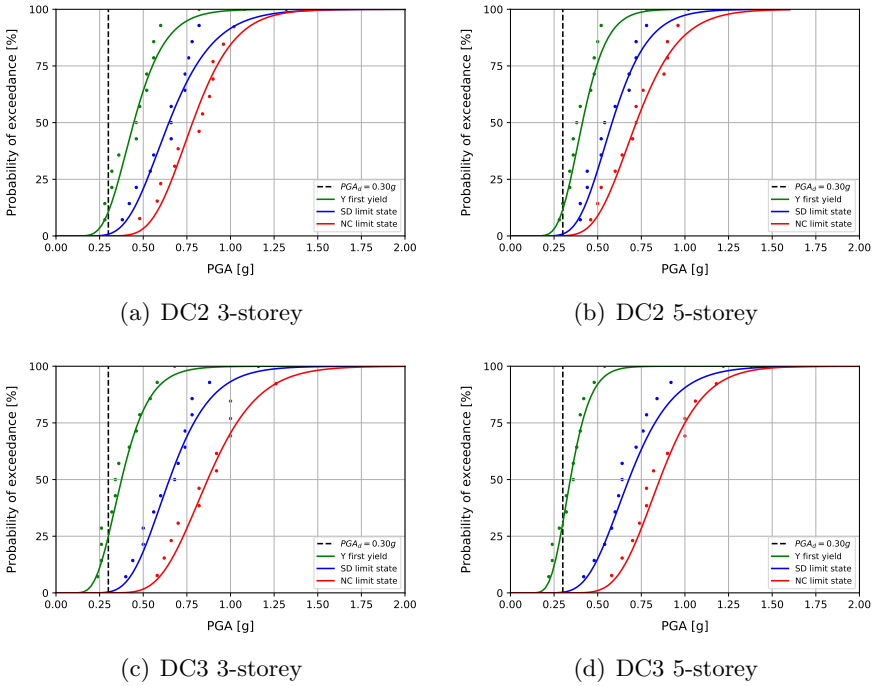

(a) DC2 3-storey (b) DC2 5-storey

(c) DC3 3-storey (d) DC3 5-storey

Figure 5.31. Fragility curves with record-to-record uncertainties.

Class	Configuration	$PGA_Y\,[g]$	β_Y	$PGA_{SD}\,[g]$	β_{SD}	$PGA_{NC}\,[g]$	β_{NC}
DC2	3-storey	0.47	0.32	0.66	0.32	0.84	0.24
	5-storey	0.39	0.27	0.57	0.27	0.72	0.27
DC3	3-storey	0.35	0.33	0.69	0.29	0.92	0.26
	5-storey	0.36	0.27	0.64	0.30	0.82	0.23

Table 5.32. Median and scatter of the results.

Although the results show a proper safety margin, a reliability verification was carried out including all uncertainties (modelling, material, data) and the design reference site (L'Aquila). The next section reports a simplified reliability verification based on the prEC8-1-1.

5.5.6.2.2 Reliability-based analysis according to the EC8 draft

The "Annex E" of the prEC8-1-1 was implemented to verify the structure performance in probabilistic terms accounting for the seismic hazard curve and the seismic vulnerability through the fragility functions. The verification is satisfied if the annual target probability of exceedance of a designed limit state for a given consequence class ($P_{t,LS}$) is greater than the annual probability of exceedance a designed limit state (P_{LS}).

$$P_{LS} \leq P_{t,LS} \tag{5.22}$$

A simplified formulation to assess the annual probability of exceedance of a designated limit-state is calculated using Equation 5.23 ((Cornell, 1996), (Fajfar and Dolšek, 2012)). The hazard function is assumed linear in the logarithmic domain in a close form solution (Equation 5.24).

$$P_{LS} = H(S_{e,LS}) \cdot e^{\left(0.5k^2 \cdot \beta^2_{Se,LS}\right)} \tag{5.23}$$

$$H(S_{e,LS}) = \frac{1}{T_{ref}} \left(\frac{S_{e,ref}}{S_{e,LS}} \right)^k \tag{5.24}$$

where:

$H(S_{e,LS})$	is the median of annual frequency of exceedance of $S_{e,LS}$;
$S_{e,ref}$	is the value of S_e corresponding to the reference return period T_{ref} of seismic action for SD limit state;
k	is the slope of the seismic hazard curve for $S_{e,ref}$ in logarithmic domain;
$\beta_{Se,LS}$	is the logarithmic standard deviation of spectral accelerations accounting for all uncertainties.

The $\beta_{Se,LS}$ coefficent takes into account the uncertainties related to record-to-record, desing requirements, test data and modelling parameters[6]. "Annex E" suggests a conservative values as a function of the limit state and the fundamental period of the structures. A conservative value of 0.6 was considered for all configurations at the ultimate limit states.

[6] In (FEMA et al., 2009) a detailed formulation is provided.

PGA was assumed as reference acceleration ($S_{e,T=0}$). Figure 5.32 shows the median seismic hazard curve for L'Aquila and the approximated linear hazard function in the logarithmic scale for the return periods of 475 and 975 years. The slope of the seismic hazard curve k is equal to 3.0. Table 5.33 reports the annual target probability for the ultimate limit states whereas the reliability verification is displayed in Table 5.34.

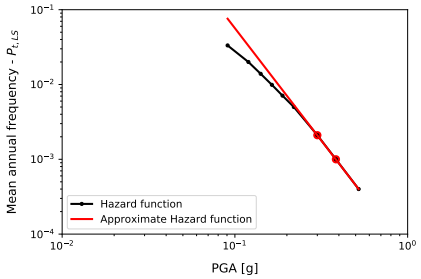

Figure 5.32. Seismic hazard function and the approximated linear hazard function in the logarithmic domain for $T_R = 475\,years$ and $T_R = 975\,years$.

LS	$t_l\,[years]$	$P_{t,l}$	$T_R\,[years]$	$P_{t,LS}$
SD	50	10%	475	2.11E-03
NC	50	5%	975	1.03E-03

Table 5.33. Annual target probability for SD and NC limit states.

Class	**Configuration**	$S_{SD}\,[g]$	$H(PGA_{SD})$	P_{SD}	$P_{t,SD}$	$P_{t,SD}/P_{SD}$
DC2	3-storey	0.66	1.95E-04	1.00E-03	2.11E-03	2.11
	5-storey	0.57	3.04E-04	1.56E-03	2.11E-03	1.35
DC3	3-storey	0.69	1.71E-04	8.75E-04	2.11E-03	2.41
	5-storey	0.64	2.14E-04	1.10E-03	2.11E-03	1.92

Table 5.34. Reliability verification for the SD LS.

The reliability verification shows that, for the examined configurations, the margin safety ratios $P_{t,SD}/P_{SD}$ are greater than one for all configurations. As a general trend, the safety ratio decreases with the number of storeys and DC2 class shows lower values than the DC3 class. The main reason for the last consideration is associated with the overstrength introduced in the design phases, mostly affecting the DC3 class.

5.5.6.3 Inter-storey drift limits

Inter-storey drift is defined as the ratio between the two adjacent storeys drift and the inter-storey height. Inter-storey drift could be adopted as a measure of global damage.
Inter-storey drift limits were estimated by monitoring the level of deformation at the connections level. The inter-storey drifts were taken as the absolute maximum values attained during each time-history along with all storeys. The mean values are reported in Table 5.35 whereas the proposed values for desing/verification are listed in Table 5.36.

DC2 shows inter-storey drifts at the first yielded connection of about 0.55% while DC3 shows values of about 0.34%. The SD limit state for both ductility class is about 0.85%. Values of the 1.10% and 1.40% can be considered as representative for the DC2 and DC3 classes, respectively.
The results are in good agreement with those reported by Sun et al. (2018) in which 0.30%-0.75%-1.40% and 0.25%-0.70%-1.30% were suggested for low and mid-high rise CLT buildings, respectively.

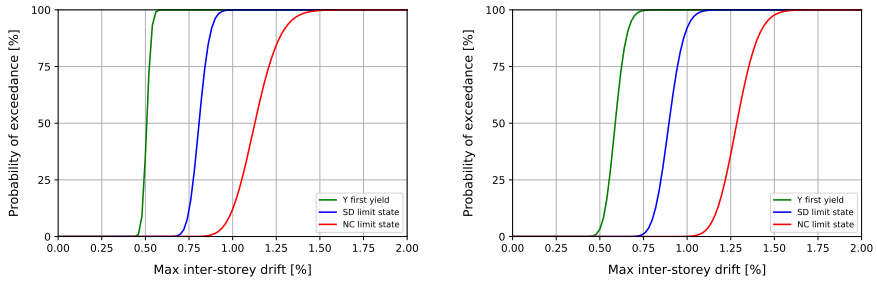

(a) DC2 3-storey

(b) DC2 5-storey

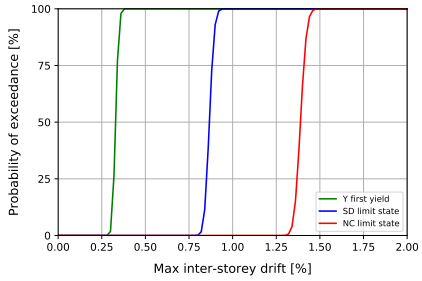

(c) DC3 3-storey

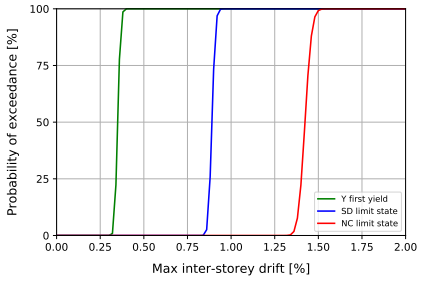

(d) DC3 5-storey

Figure 5.33. Distribution of the maximum inter-storey drift associated to the connections' damage.

Class	Configuration	$drift_Y$ [%]	$drift_{SD}$ [%]	$drift_{NC}$ [%]
DC2	3-storey	0.51	0.81	1.10
	5-storey	0.59	0.90	1.29
DC3	3-storey	0.33	0.87	1.39
	5-storey	0.35	0.89	1.42

Table 5.35. Mean values of the inter-storey drift limits.

Class	$drift_Y$ [%]	$drift_{SD}$ [%]	$drift_{NC}$ [%]
DC2	0.55	0.85	1.20
DC3	0.35	0.85	1.40

Table 5.36. Inter-storey drift limit proposed.

5.6 Conclusions and proposals

The chapter investigates the seismic behaviour of CLT structures designed following the EC8 draft for two ductility classes: moderate ductility DC2 and high ductility DC3. The DC1 low ductility class has not been considered as the dissipative capabilities are neglected and go beyond the scope of this work.

Parametric non-linear static and dynamics analyses were performed to evaluate the behaviour factors contributions: the q_R overstrength component and the q_D ductility capacity/energy dissipation component. The results obtained through non-linear static parametric analyses are in agreement with the values reported in the literature. CLT structures show high safety margins also due to the overstrength introduced at the design phase. Based on the results of the parametric studies, conservative values of 1.30 for q_R and 1.15 for q_D are recommended for DC2, whereas values of 1.50 for q_R and 1.40 for q_D are recommended for DC3. A further parametric analysis where the ductility of the connections was varied to verify the proposed values of the q-factors of 2.24 and 3.15 for DC2 and DC3 respectively: for hold-downs/angle-brackets a minimum ductility of 1.5 can be adopted, whereas screw wall panel-to-panel vertical joints, a ductility of 5.5 is required for the use of the proposed q-factors. Means values of the plastic deformation α_{SD} equal to 0.35 for DC2 and 0.50 for DC3 correlate the attainment of the SD LS at the connections level to the SD LS on the global capacity curves.

The non-linear dynamic analyses performed with an incremental dynamic analysis showed a general safety margin when using the proposed q-factors in design which increases with the number of storeys and ductility class. Inter-storey drift limits specific to the ductility class were found of the order of 0.55%-0.85%-1.2% (first yield-SD-NC) for DC2 and 0.35%-0.85%-1.4% (first yield-SD-NC) for DC3.

[Blank page]

Conclusions

Chapter abstract

The dissertation deals with the seismic behaviour of Cross-Laminated Timber (CLT) buildings to propose design values for the revision of the Eurocode 8. The present conclusion chapter summarizes all results and considerations of the previous chapters providing recommendations for future research. As for the introduction chapter, a bullet list resumes all outcomes based on the aims of this dissertation.

6.1 Conclusions and recommendations for future research

This dissertation deals with the seismic behaviour of Cross-Laminated Timber (CLT) buildings. The main objectives outlined in Chapter 1 are summarised and reported with the results, comments and recommendations for future research.

- *"Apply the EN 12512 draft in combination with EN 1998 draft."*

The revisions of EN 1998-1:2004 (EC8) and EN 12512:2001 are ongoing parallelly. The two norms are linked since EC8 defines the demand, while EN 12512 describe the methodology to estimate the properties of timber joints. The current EN 12512:2001 has few interpretative limits combined with the EN 1998-1:2004, especially regarding a unique definition of the minimum ductility and its limit.

As a proposal, the introduction of strength impairment factor φ_{imp}, joints the two norms guaranteeing a prefixed level of strength degradation due to the cycle loadings and the minimum ductility demand request for each connection and specific for the structural typology.
The approach was implemented on experimental test, collected by Gavrić et al. ((Gavric et al., 2015a), (Gavric et al., 2015b)), showing a reduction of the ultimate displacement (thus ductility) for all connection typologies, especially for the screws of the half-lap joint employed between adjacent wall panels. The results are suddenly used for the estimation of the q-factors for CLT buildings. The approach excludes low ductility connections in seismic design applications ensuring adequate hysteretic energy dissipation. In addition, the rules provided in prEN 1998-1-2:2020 for non-linear static analysis (NLSA) based on a tri-linearization of the capacity of the connections, are an excellent tool to perform NLSA for the first time.

Future investigations should be oriented on using the proposed revision of EN 12512 on more connections available in the global market to characterize a general behaviour of specific joints and provide data for engineers as soon

as possible.

- *"Develop a linear-elastic finite-element model strategy to improve the existing approaches."*

Although in the last decades' research has investigated the non-linear seismic behaviour of CLT buildings in more detail, practice-oriented finite element (FE) modelling strategies are still at an early stage.

Due to several non-linearities (e.g. contact between panels, contact with the foundation, friction, non-linear behaviour of connections, vertical loads) encounter in the seismic physical problem, the current practice-oriented methods are based on simplificative assumptions often too conservative.

A new modelling strategy based on the upgrade of the Christovasilis et al. (2020), was implemented to account for the non-linearities due to the effect of the vertical loads and the activation/non-activation of the rocking mechanism. The proposed model introduces the following advantages:

i) Use of only 2D area elements;

ii) Inclusion of the vertical load contribution;

iii) Inclusion of the floor compressibility;

iv) More refined loads distributions of the seismic actions along the shearwalls into for 3D FE structures;

v) Reduction of the scatter between a detailed non-linear model and the new proposal linear-elastic approach, especially for shearwalls with low aspect ratio L/H;

vi) Possible reduction of the seismic design force with a consequent reduction of the overdesigning phenomenon for mid/high-rise buildings.

The future steps will be a real application/comparison between the proposed and the existing practice-oriented strategies, and further investigations of the floor's effect on multi-panel structures.

- *"Estimate the behaviour factors for revising the Eurocode 8 for the two ductile classes designed in moderate (DC2) and high (DC3) respecting new design rules."*

The results obtained from the connections analyzed in the second chapter are used to estimate the behaviour factors for CLT buildings designed in moderate (DC2) and high (DC3) ductility classes.

New seismic design rules based on state-of-the-art knowledge are applied to get the q-factor contributions following the new material independent formulation. The behaviour factor q will be the product of three components. Specifically, the over-resistance due to the overstrength introduced in the design q_S (fixed to 1.5 and material independent), the component that takes into account the overstrength due to the redistribution of the seismic action in redundant structures q_R and the component that consider the dissipative capacity q_D.

The contributions are estimated by a parametric non-linear pushover analysis on several 2D configurations to get unique values of the q-factors valid for all scenarios in terms of shearwalls size/number of storeys. An additional parametric study is carried out to define the minimum connections ductility required to ensure the tabulated q-factors. Suddenly, the incremental dynamic analyses are performed on two configurations designed in DC2 and DC3 to investigate the safety margin in probabilistic terms and finding design/verification inter-storey drift limits.

The main results and remarks achieved at the end of this chapter are:

i) The proposal values of the q-factors for DC2 and DC3 classes are:

Structural type	**Ductility class**						
	DC1	**DC2**			**DC3**		
	q	q_D	q_R	q	q_D	q_R	q
Cross-Laminated Timber structures	1.50	1.15	1.30	2.24	1.40	1.50	3.15

ii) The proposal values of the mimimum connections' ductility are:

Structural type	**Dissipative sub-assembly/joint/2D or 3D-nailing plate/connection**	**Type of ductility**	μ **DC2**	μ **DC3**
a) Cross laminated timber structures	Hold-downs, tie-downs, foundation tie-downs, angle brackets, shear plate	Displacement	1.5	1.5
	Screwed wall panel-to-panel joints	Displacement	-	5.5

iii) The values of the plastic deformation α_{SD} at the SD LS was estimated equal to 0.35 and 0.50 for DC2 and DC3, respectively. It is emphasized that these values are valid for the same modelling strategy and the connections adopted. It is encouraged to monitor the deformation level of the connections;

iv) The proposal values for inter-storey drift limits are:

Class	$drift_Y$ [%]	$drift_{SD}$ [%]	$drift_{NC}$ [%]
DC2	0.55	0.85	1.20
DC3	0.35	0.85	1.40

v) The proposed values of the q-factors are conservative. Small increments can be acceptable even if the local ductility of the dissipative components is guaranteed;

vi) In DC2, the behaviour factor is higher in structures composed of shearwalls where the L/H ratio is small due to the predominant rocking mechanism. On the other hand, the q-factor decreses for high L/H ratios due to the less ductile sliding mechanism. Therefore, the behaviour factor q, in structures composed by shearwalls with both low and high L/H ratio, is governed by the collapse mechanism of the shearwalls with high L/H ratios;

vii) In DC3, the ductility of the building tends to increase by using segmented walls with short panel size;

viii) It is encouraged to use non-linear static analysis, through simplified/detailed FE models, by monitoring the limit state at the connections level.

ix) The non-linear dynamics analyses performed with increment dynamic (IDA) method show inline safety margin as required for new buildings with the probability of achieving the significant damage for the design earthquake (10% of the probability of exceedance in 50 years) between 0.29% and 0.86% for both ductility classes;

x) The q-factors estimated with the IDA analysis are in line with the values proposed obtained with pushover method.

xi) The reliability-based verifications, following prEN 1998-1-1:2020 Annex "E"), show conservative margin safety ratios $P_{t,SD}/P_{SD}$ (for the SD LS) greater than one for all configurations analyzed; as a general trend, the safety decrease with the number of storeys independently for the ductility class (mean values of 2.26 and 1.65 for 3-storey and 5-storey, respectively);

xii) It is advisable to develop shear anchoring systems that guarantee high

strength in shear and low strength/stiffness in tension for DC3 class to simplify the design process (reducing the iterations steps if tension is accounted in the design) and improve the energy dissipation with the couple-panel behaviour;

xiii) It could be advisable to reduce the overstrength storeys ratio γ_{Rd} at the wall/building levels (currently at 1.6) to simplify the design in DC3 class. Values lower than 1.6 should be proposed.

The following list suggests possible research which should be developed in the future in order of importance:

i) Even if the hierarchy rules at the connections level were not the subject of this work, it is advisable to review the values of the overstrength factors proposed in the prEN 1998-1-2:2020. Those rather high values may make the design of CLT structures fairly difficult to achieve.

ii) Modify the overstrength-factor γ_{Rd} at the global level for DC3 class to reduce the number of angle-brackets required to prevent the sliding mechanism. The overstrength could be reduced since the sliding mechanism is a "less-ductile" mechanism compared to the couple-panel behaviour and not a "brittle" mechanism;

iii) Develop innovative solutions for the wall-to-foundation connections to improve the design strength values of the concrete-side (e.g. generally, the timber-to-steel strength is much higher than the tensile strength of the anchoring system, under cyclic loads, leading to difficulties in respecting the hierarchy rules with traditional connectors);

iv) Modify or introduce a clause for the linearization of the structural capacity curve in case of marked non-linearities combined with low ductility structure as achievable for DC2 buildings;

v) Development of sliding anchoring systems able to develop high shear capacity and low tension strength/stiffness (especially for the DC3 class);

vi) Investigate via experimental/numerical the effect of the floor on the rocking mechanism (especially for the DC3 class).

References

Akima, H. (1970). A New Method of Interpolation and Smooth Curve Fitting Based on Local Procedures. *Journal of the ACM (JACM).*

Albanesi, T. and Nuti, C. (2007). Analisi statica non lineare (pushover). *Roma: Dipartimento di Strutture (DiS), Università degli Studi Roma*, 3.

Albanesi, T., Nuti, C., and Vanzi, I. (2000). A simplified procedure to assess the seismic response of nonlinear structures. *Earthquake Spectra.*

ANSI, A. (2010). Aisc 341-10 (2010). *Seismic provisions for structural steel buildings. Chicago: American Institute of Steel Construction.*

ASCE (2017). *Minimum design loads and associated criteria for buildings and other structures.*

ASTM (2019). Astm e2126 - 19 standard test methods for cyclic (reversed) load test for shear resistance of vertical elements of the lateral force resisting systems for buildings.

Baker, J. W. (2015). Efficient analytical fragility function fitting using dynamic structural analysis. *Earthquake Spectra.*

Baraschino, R., Baltzopoulos, G., and Iervolino, I. (2020). R2R-EU: Software for fragility fitting and evaluation of estimation uncertainty in seismic risk analysis. *Soil Dynamics and Earthquake Engineering.*

Blass, H. and Fellmoser, P. (2004). Design of solid wood panels with cross layers. In *8th World Conference on Timber Engineering.*

Blass, H. J., Ceccotti, A., Dyrbye, C., Gnuschke, M., Hansen, K. F., Nielsen, J., Ohlsson, S., Parche, M., Reyer, E., Stieda, C. K., Vergne, A.,

Vignoli, A., Yasumura, M., and Dolan, J. D. (1994). Timber structures in seismic regions RILEM state-of-the-art report. *Materials and Structures*.

Bogensperger, T., Moosbrugger, T., and Silly, G. (2010). Verification of CLT-plates under loads in plane. In *11th World Conference on Timber Engineering 2010, WCTE 2010*.

Brandner, R., Flatscher, G., Ringhofer, A., Schickhofer, G., and Thiel, A. (2016). Cross laminated timber (CLT): overview and development. *European Journal of Wood and Wood Products*.

Casagrande, D., Bezzi, S., D'Arenzo, G., Schwendner, S., Polastri, A., Seim, W., and Piazza, M. (2020). A methodology to determine the seismic low-cycle fatigue strength of timber connections. *Construction and Building Materials*, 231:117026.

Casagrande, D., Doudak, G., Mauro, L., and Polastri, A. (2018). Analytical Approach to Establishing the Elastic Behavior of Multipanel CLT Shear Walls Subjected to Lateral Loads. *Journal of Structural Engineering (United States)*.

Casagrande, D., Doudak, G., and Polastri, A. (2019). A proposal for the capacity-design at wall- and building-level in light-frame and cross-laminated timber buildings. *Bulletin of Earthquake Engineering*.

Casagrande, D., Pacchioli, S., Polastri, A., and Pozza, L. (2021). Influence of the rocking behavior of shearwalls on the fundamental period of clt structures. *Earthquake Engineering & Structural Dynamics*, 50(6):1734–1754.

Casagrande, D., Polastri, A., Sartori, T., Loss, C., and Chiodega, M. (2016a). Experimental campaign for the mechanical characterization of connection systems in the seismic design of timber buildings. In *WCTE 2016 - World Conference on Timber Engineering*.

Casagrande, D., Rossi, S., Sartori, T., and Tomasi, R. (2016b). Proposal of an analytical procedure and a simplified numerical model for elastic response of single-storey timber shear-walls. *Construction and Building Materials*.

Ceccotti, A. (2008). New technologies for construction of medium-rise buildings in seismic regions: The XLAM case. *Structural Engineering International: Journal of the International Association for Bridge and Structural Engineering (IABSE)*.

Ceccotti, A. and Follesa, M. (2006). Seismic behaviour of multi-storey x-lam buildings. In *COST E29 International Workshop on Earthquake Engineering on Timber Structures*, pages 81–95.

Ceccotti, A. and Follesa, M. (2015). Seismic Behaviour of Multi-Storey XLam Buildings. *COST E29: International Workshop on Earthquake Engineering on Timber Structures*.

Ceccotti, A., Follesa, M., Kawai, N., Lauriola, M. P., Minowa, C., Sandhaas, C., and Yasumura, M. (2006). Which seismic behaviour factor for multi-storey buildings made of cross-laminated wooden panels. *Proceedings of 39th CIB W18 Meeting, paper*.

Ceccotti, A., Follesa, M., and Lauriola, M. P. (2007). *Le strutture di legno in zona sismica: criteri e regole per la progettazione e il restauro*. Clut.

Ceccotti, A., Sandhaas, C., Okabe, M., Yasumura, M., Minowa, C., and Kawai, N. (2013). SOFIE project - 3D shaking table test on a seven-storey full-scale cross-laminated timber building. *Earthquake Engineering and Structural Dynamics*.

Ceccotti, A., Sandhaas, C., and Yasumura, M. (2010). Seismic behaviour of multistory cross-laminated timber buildings.

Ceccotti, A. and Vignoli, A. (1989). A hysteretic behavioral model for semi rigid joints. In *European Earthquake Engineering*, pages Vol. 3–3–9.

CEN, B. (2006). 14358: 2006.: Timber structures-calculation of characteristic 5-percentile values and acceptance criteria for a sample.

Chen, Z. and Popovski, M. (2020). Mechanics-based analytical models for balloon-type cross-laminated timber (CLT) shear walls under lateral loads. *Engineering Structures*.

Chisari, C., Francavilla, A. B., Latour, M., Piluso, V., Rizzano, G., and Amadio, C. (2017). Critical issues in parameter calibration of cyclic models for steel members. *Engineering Structures*, 132:123–138.

Christovasilis, I. P., Riparbelli, L., Rinaldin, G., and Tamagnone, G. (2020). Methods for practice-oriented linear analysis in seismic design of Cross Laminated Timber buildings. *Soil Dynamics and Earthquake Engineering*.

Code, P. (1995). Eurocode 5: design of timber structure. *Brussels: European Committee for Standardization*.

Code, P. (2004). Eurocode 8: Design of structures for earthquake resistance-part 1: general rules, seismic actions and rules for buildings. *Brussels: European Committee for Standardization*.

Cornell, C. A. (1996). Calculating building seismic performance reliability: a basis for multi-level design norms. In *Proceedings of the 11th world conference on earthquake engineering*, volume 10, pages 5707–5712.

CSIRO, C. S. and Organization, I. R. (1996). Timber evaluation of mechanical joint systems: Part 3. earthquake loading.

D'Arenzo, G., Rinaldin, G., Fossetti, M., and Fragiacomo, M. (2019). An innovative shear-tension angle bracket for Cross-Laminated Timber structures: Experimental tests and numerical modelling. *Engineering Structures*.

De Luca, F., Vamvatsikos, D., and Iervolino, I. (2013a). Improving static pushover analysis by optimal bilinear fitting of capacity curves. *Computational Methods in Applied Sciences*.

De Luca, F., Vamvatsikos, D., and Iervolino, I. (2013b). Near-optimal piecewise linear fits of static pushover capacity curves for equivalent SDOF analysis. *Earthquake Engineering and Structural Dynamics*.

Demirci, C., Málaga-Chuquitaype, C., and Macorini, L. (2018). Seismic drift demands in multi-storey cross-laminated timber buildings. *Earthquake Engineering and Structural Dynamics*.

Dolan, J. D. (1989). The Dynamic Response of Timber Shear Walls. *Thesis submitted in partial fulfillment of the requirements for the degree of Doctor of Philosophy.*

Eads, L., Miranda, E., Krawinkler, H., and Lignos, D. G. (2013). An efficient method for estimating the collapse risk of structures in seismic regions. *Earthquake Engineering and Structural Dynamics.*

Elnashai, A. S. and Mwafy, A. M. (2002). Overstrength and force reduction factors of multistorey reinforced-concrete buildings. *The Structural Design of Tall Buildings*, 11(5):329–351.

Elwood, K. J. and Moehle, J. P. (2006). Idealized backbone model for existing reinforced concrete columns and comparisons with FEMA 356 criteria. *Structural Design of Tall and Special Buildings.*

EOTA (2007). ETA-07/0055. Three-dimensional nailing plate European tecnical approval.

EOTA (2016). ETA-11/0030. Screws for use in timber construction.

EOTA (2018). ETA-13/0523. Nails and screws for use in nailing plates timber structures.

European Commitee for Standardization (2004). Eurocode 8: Design of structures for earthquake resistance - Part 1 : General rules, seismic actions and rules for buildings. *European Committee for Standardization.*

European Committee for Standardization, C. (2001). En 12512 - timber structures — test methods — cyclic testing of joints made with mechanical fasteners.

Fajfar, P. and Dolšek, M. (2012). A practice-oriented estimation of the failure probability of building structures. *Earthquake Engineering and Structural Dynamics.*

FEMA, P. . et al. (2009). Quantification of building seismic performance factors.

Flaig, M. and Blass, H. J. (2013). Shear strength and shear stiffness of CLT-beams loaded in plane. In *PROC-CIB.*

Flatscher, G., Bratulic, K., and Schickhofer, G. (2015). Experimental tests on cross-laminated timber joints and walls. *Proceedings of the Institution of Civil Engineers - Structures and Buildings*.

Follesa, M. (2018). Wg2 "solid timber construction – cross laminated timber" 5th workshop of "cost action fp1402". In *Properties, Testing and Design of Cross Laminated Timber*.

Follesa, M., Christovasilis, I., Vassallo, D., Fragiacomo, M., and Ceccotti, A. (2013). Seismic design of multi-storey cross laminated timber buildings according to eurocode 8. *Ingegneria Sismica*.

Follesa, M., Fragiacomo, M., Casagrande, D., Tomasi, R., Piazza, M., Vassallo, D., Canetti, D., and Rossi, S. (2018). The new provisions for the seismic design of timber buildings in Europe. *Engineering Structures*.

Follesa, M., Ni, C., Popovski, M., and Karacabeyli, E. (2010). Blind prediction of the seismic response of the NEESWood Capstone Building. In *11th World Conference on Timber Engineering 2010, WCTE 2010*.

Folz, B. and Filiatrault, A. (2004). Seismic analysis of woodframe structures. I: Model formulation. *Journal of Structural Engineering*.

Foschi, R. O. (1977). Analysis of wood diaphragms and trusses. part i: Diaphragms. *Canadian Journal of Civil Engineering*, 4(3):345–352.

Franco, L., Pozza, L., Saetta, A., Savoia, M., and Talledo, D. (2019). Strategies for structural modelling of CLT panels under cyclic loading conditions. *Engineering Structures*.

Gavric, I., Fragiacomo, M., and Ceccotti, A. (2015a). Cyclic behavior of CLT wall systems: Experimental tests and analytical prediction models. *Journal of Structural Engineering (United States)*.

Gavric, I., Fragiacomo, M., and Ceccotti, A. (2015b). Cyclic behavior of typical screwed connections for cross-laminated (CLT) structures. *European Journal of Wood and Wood Products*.

Gavric, I., Fragiacomo, M., and Ceccotti, A. (2015c). Cyclic behaviour of typical metal connectors for cross-laminated (CLT) structures. *Materials and Structures/Materiaux et Constructions*.

Gavric, I. and Popovski, M. (2014). Design models for CLT shearwalls and assemblies based on connection properties. *Proceedings of Meeting 47, INTER- International Network on Timber Engineering Research*.

Gerami, M., Siahpolo, N., and Vahdani, R. (2017). Effects of higher modes and mdof on strength reduction factor of elastoplastic structures under far and near-fault ground motions. *Ain Shams Engineering Journal*, 8(2):127–143.

Germano, F., Metelli, G., and Giuriani, E. (2015). Experimental results on the role of sheathing-to-frame and base connections of a European timber framed shear wall. *Construction and Building Materials*.

Ghobarah, A. (2001). Performance-based design in earthquake engineering: State of development. *Engineering Structures*, 23:878–884.

Granello, G., Palermo, A., Pampanin, S., Pei, S., and van de Lindt, J. (2020). Pres-lam buildings: State-of-the-art. *Journal of Structural Engineering*, 146(6):04020085.

Gulkan, P. and Sozen, M. A. (1974). Inelastic responses of reinforced concrete structures to earthquake motions. *J Am Concr Inst*.

He, M., Lam, F., and Foschi, R. O. (2000). Numerical analysis of statically loaded three-dimensional timber light-frame buildings. *America*.

Hilber, H. M., Hughes, T. J. R., and Taylor, R. L. (1977). Improved numerical dissipation for time integration algorithms in structural dynamics. *Earthquake Engineering & Structural Dynamics*, 5(3):283–292.

Hildebrandt, J., Hagemann, N., and Thrän, D. (2017). The contribution of wood-based construction materials for leveraging a low carbon building sector in europe. *Sustainable Cities and Society*.

Hummel, J. and Seim, W. (2019a). Displacement-based design approach to evaluate the behaviour factor for multi-storey CLT buildings.

Hummel, J. and Seim, W. (2019b). Displacement-based design approach to evaluate the behaviour factor for multi-storey clt buildings. *Engineering Structures*, 201:109711.

Ibarra, L. F. and Krawinkler, H. (2005). Global Collapse of Frame Structures under Seismic Excitations. Technical report.

Iervolino, I., Galasso, C., and Cosenza, E. (2010). REXEL: Computer aided record selection for code-based seismic structural analysis. *Bulletin of Earthquake Engineering*.

International, A. (1995). Standard test method for evaluation dowel-bearing strength of wood and woodbased products.

ISO/TC 165, T. s. (2003). *Timber Structures: Joints Made with Mechanical Fasteners: Quasi-static Reversed-cyclic Test Method*. ISO.

Izzi, M., Casagrande, D., Bezzi, S., Pasca, D., Follesa, M., and Tomasi, R. (2018a). Seismic behaviour of Cross-Laminated Timber structures: A state-of-the-art review.

Izzi, M., Flatscher, G., Fragiacomo, M., and Schickhofer, G. (2016). Experimental investigations and design provisions of steel-to-timber joints with annular-ringed shank nails for Cross-Laminated Timber structures. *Construction and Building Materials*, 122:446–457.

Izzi, M., Polastri, A., and Fragiacomo, M. (2018b). Modelling the mechanical behaviour of typical wall-to-floor connection systems for cross-laminated timber structures. *Engineering Structures*.

Jockwer, R. and Jorissen, A. (2018). Load-deformation behaviour and stiffness of lateral connections with multiple dowel type fasteners. *INTER Proceedings: 2018 Tallinn, Estonia*, 51:141–158.

Johansen, K. (1949). Theory of timber connections. In *International Association for Bridge and Structural Engineering*, volume 9, pages 249–262.

Jorissen, A. and Fragiacomo, M. (2011). General notes on ductility in timber structures. *Engineering Structures*.

Karacabeyli, E. and Ceccotti, A. (1996). Quasi-static reversed-cyclic testing of nailed joints. In *Proc. Int. Council for Build. Res. Studies and Documentation, Working Commission W18-Timber Structure, Meetings*, volume 29.

Kircher, C. A., Whitman, R. V., and Holmes, W. T. (2006). HAZUS Earthquake Loss Estimation Methods. *Natural Hazards Review*.

Kivell, B. T., Moss, P. J., and Carr, A. J. (1981). Hysteretic modelling of moment-resisting nailed timber joints. *Bulletin of the New Zealand National Society for Earthquake Engineering*.

Larasatie, P., Albee, R., Muszynski, L., Guerrero, J., and Hansen, E. (2020). Global clt industry survey: The 2020 updates.

Lukacs, I., Björnfot, A., and Tomasi, R. (2019). Strength and stiffness of cross-laminated timber (CLT) shear walls: State-of-the-art of analytical approaches. *Engineering Structures*.

Masroor, M., Doudak, G., and Casagrande, D. (2020). The effect of bi-axial behaviour of mechanical anchors on the lateral response of multi-panel CLT shearwalls. *Engineering Structures*.

Mazzoni, S., McKenna, F., Scott, M. H., and Fenves, G. L. (2006). OpenSees command language manual. *Pacific Earthquake Engineering Research Center*.

McGuire, R. K. (1995). Probabilistic seismic hazard analysis and design earthquakes: closing the loop. *Bulletin - Seismological Society of America*.

McKenna, F. (2011). OpenSees: A framework for earthquake engineering simulation. *Computing in Science and Engineering*.

Mestar, M., Doudak, G., Caola, M., and Casagrande, D. (2020). Equivalent-frame model for elastic behaviour of cross-laminated timber walls with openings. *Proceedings of the Institution of Civil Engineers - Structures and Buildings*, 173(5):363–378.

Miranda, E. and Bertero, V. V. (1994). Evaluation of Strength Reduction Factors for Earthquake-Resistant Design. *Earthquake Spectra*.

Mitchell, D., Tremblay, R., Karacabeyli, E., Paultre, P., Saatcioglu, M., and Anderson, D. L. (2003). Seismic force modification factors for the proposed 2005 edition of the national building code of canada. *Canadian Journal of Civil Engineering*, 30(2):308–327.

Muñoz, W., Salenikovich, A., Mohammad, M., and Quenneville, P. (2008). Determination of yield point and ductility of timber assemblies: In search for a harmonised approach. In *10th World Conference on Timber Engineering 2008*.

NBCC (2015). National building code of canada 2015. *National Research Council of Canada*.

Newmark, N. M. and Hall, W. J. (1982). Earthquake spectra and design. *esd*.

Nolet, V., Casagrande, D., and Doudak, G. (2019). Multipanel CLT shearwalls: an analytical methodology to predict the elastic-plastic behaviour. *Engineering Structures*.

Norme Tecniche, p. l. C. (2018). Aggiornamento delle norme tecniche per le costruzioni. *Gazzetta Ufficiale Serie Generale*, (42).

Pei, S., van de Lindt, J. W., and Popovski, M. (2013). Approximate R-Factor for Cross-Laminated Timber Walls in Multistory Buildings. *Journal of Architectural Engineering*.

Pei, S., van de Lindt, J. W., Popovski, M., Berman, J. W., Dolan, J. D., Ricles, J., Sause, R., Blomgren, H., and Rammer, D. R. (2016). Cross-Laminated Timber for Seismic Regions: Progress and Challenges for Research and Implementation. *Journal of Structural Engineering*.

Petersen, C. (2013). *Dynamik der Baukonstruktionen*. Springer-Verlag.

Piazza, M., Polastri, A., and Tomasi, R. (2011). Ductility of timber joints under static and cyclic loads. *Proceedings of the Institution of Civil Engineers: Structures and Buildings*, 164(2):79–90.

Polastri, A., Izzi, M., Pozza, L., Loss, C., and Smith, I. (2019). Seismic analysis of multi-storey timber buildings braced with a CLT core and perimeter shear-walls. *Bulletin of Earthquake Engineering*.

Popovski, M. and Gavric, I. (2016). Performance of a 2-story clt house subjected to lateral loads. *Journal of Structural Engineering*, 142(4):E4015006.

Popovski, M. and Karacabeyli, E. (2011). Seismic Performance of Cross-Laminated Wood Panels. In *44th CIB-W18 meeting*.

Popovski, M., Pei, S., van de Lindt, J. W., and Karacabeyli, E. (2014). Force Modification Factors for CLT Structures for NBCC. *RILEM Bookseries*.

Popovski, M., Schneider, J., and Schweinsteiger, M. (2010). Lateral load resistance of cross-laminated wood panels. In *11th World Conference on Timber Engineering 2010, WCTE 2010*.

Pozza, L. (2013a). *Ductility and behaviour factor of wood structural systems - Theoretical and experimental development of a high ductility wood-concrete shearwall system.* PhD thesis, University of Padova.

Pozza, L. (2013b). Ductility and behaviour factor of wood structural systems-theoretical and experimental development of a high ductility wood-concrete shearwall system.

Pozza, L., Savoia, M., Franco, L., Saetta, A., and Talledo, D. (2017). Effect of different modelling approaches on the prediction of the seismic response of multi-storey CLT buildings. *International Journal of Computational Methods and Experimental Measurements*.

Pozza, L., Scotta, R., Trutalli, D., Pinna, M., Polastri, A., and Bertoni, P. (2014). Experimental and Numerical Analyses of New Massive Wooden Shear-Wall Systems. *Buildings*.

Pozza, L., Scotta, R., Trutalli, D., and Polastri, A. (2015). Behaviour factor for innovative massive timber shear walls. *Bulletin of Earthquake Engineering*.

Rahgozar, M. and Humar, J. (1998). Accounting for overstrength in seismic design of steel structures. *Canadian journal of civil engineering*, 25(1):1–15.

Rahmanishamsi, E., Soroushian, S., Maragakis, E. M., and Sarraf Shirazi, R. (2017). Analytical Model to Capture the In-Plane and Out-of-Plane Seismic Behavior of Nonstructural Partition Walls with Returns. *Journal of Structural Engineering*.

Reitherman, R. and Hall, J. (2002). The CUREE-Caltech Woodframe Project. In *Structural Engineers World Conference*.

Richard, N., Yasumura, M., and Davenne, L. (2003). Prediction of seismic behavior of wood-framed shear walls with openings by pseudodynamic test and FE model. *Journal of Wood Science*.

Rinaldin, G., Amadio, C., and Fragiacomo, M. (2013). A component approach for the hysteretic behaviour of connections in cross-laminated wooden structures. *Earthquake Engineering and Structural Dynamics*.

Rinaldin, G. and Fragiacomo, M. (2016). Non-linear simulation of shaking-table tests on 3- and 7-storey X-Lam timber buildings. *Engineering Structures*.

Rossi, S., Casagrande, D., Tomasi, R., and Piazza, M. (2016). Seismic elastic analysis of light timber-frame multi-storey buildings: Proposal of an iterative approach. *Construction and Building Materials*.

Rossi, S., Giongo, I., Casagrande, D., Tomasi, R., and Piazza, M. (2019). Evaluation of the displacement ductility for the seismic design of light-frame wood buildings. *Bulletin of Earthquake Engineering*, 17(9):5313–5338.

Rossum, G. (1995). Python reference manual.

Sanchez-Ricart, L. and Plumier, A. (2008). Parametric study of ductile moment-resisting steel frames: A first step towards Eurocode 8 calibration. *Earthquake Engineering & Structural Dynamics*, 37(7):1135–1155.

Schickhofer, G. and Ringhofer, A. (2012). *The seismic behaviour of buildings erected in Solid Timber Construction - Seismic design according to EN 1998 for a 5-storey reference building in CLT*.

Schneider, J., Shen, Y., Stiemer, S., and Tesfamariam, S. (2015). Assessment and comparison of experimental and numerical model studies of cross-laminated timber mechanical connections under cyclic loading. *Construction and Building Materials*, 77:197 – 212.

Sciomenta, M., Rinaldi, V., Follesa, M., and Fragiacomo, M. (2019). Seismically resistant timber buildings: how a supply chain of wood may help south asia achieve a resilient society?

Scott, M. H. and Fenves, G. L. (2020). Erratum: Krylov subspace accelerated newton algorithm: Application to dynamic progressive collapse simulation of frames (Journal of Structural Engineering (United States) DOI: 10.1061/(ASCE)ST.1943-541X.0000143). *Journal of Structural Engineering-asce*.

Shahnewaz, M., Alam, S., and Tannert, T. (2018). In-plane strength and stiffness of cross-laminated timber shear walls. *Buildings*, 8(8).

Shahnewaz, M., Pan, Y., Shahria Alam, M., and Tannert, T. (2020). Seismic Fragility Estimates for Cross-Laminated Timber Platform Building. *Journal of Structural Engineering*.

Sigrist, C., Casagrande, D., and Piazza, M. (2020). Revision of testing standards to determine the seismic capacity of timber connections according to eurocode 8.

Smerzini, C. and Paolucci, R. (2013). SIMBAD: a database with Selected Input Motions for displacementBased Assessment and Design – 3rd release. Technical report, Research Project DPC - RELUIS 2010-2013.

Smith, I., Asiz, A., Snow, M., and Chui, Y. (2006). Possible canadian/iso approach to deriving design values from test data. In *CIB-W18 Meeting in Florence*.

Stewart, W. (1987). *The seismic design of plywood sheathed shearwalls*. PhD thesis, University of Canterbury.

Sun, X., He, M., Li, Z., and Shu, Z. (2018). Performance evaluation of multi-storey cross-laminated timber structures under different earthquake hazard levels. *Journal of Wood Science*.

Sustersic, I. and Dujic, B. (2012). Simplified cross-laminated timber wall modelling for linear-elastic seismic analysis. *International Council for Research and Innovation in Building and Construction, CIB-W18*.

Sustersic, I., Fragiacomo, M., and Dujic, B. (2016). Seismic Analysis of Cross-Laminated Multistory Timber Buildings Using Code-Prescribed Methods: Influence of Panel Size, Connection Ductility, and Schematization. *Journal of Structural Engineering (United States)*.

Tamagnone, G. and Fragiacomo, M. (2018). On the rocking behavior of CLT wall assemblies. In *WCTE 2018 - World Conference on Timber Engineering*.

Tamagnone, G., Rinaldin, G., and Fragiacomo, M. (2020). Influence of the Floor Diaphragm on the Rocking Behavior of CLT Walls. *Journal of Structural Engineering (United States)*.

Tannert, T., Follesa, M., Fragiacomo, M., González, P., Isoda, H., Moroder, D., Xiong, H., and Van De Lindt, J. (2018). Seismic design of cross-laminated timber buildings. *Wood and Fiber Science*.

Tomasi, R. and Sartori, T. (2013). Mechanical behaviour of connections between wood framed shear walls and foundations under monotonic and cyclic load. *Construction and Building Materials*, 44:682 – 690.

Tomasi, R. and Smith, I. (2015). Experimental characterization of monotonic and cyclic loading responses of CLT Panel-To-Foundation Angle Bracket Connections. *Journal of Materials in Civil Engineering*.

Turesson, J., Berg, S., and Ekevad, M. (2019). Impact of board width on in-plane shear stiffness of cross-laminated timber. *Engineering Structures*, 196:109249.

Uang, C. (1991). Establishing r (or rw) and cd factors for building seismic provisions. *Journal of Structural Engineering*, 117(1):19–28.

Vamvatsikos, D. and Allin Cornell, C. (2002). Incremental dynamic analysis. *Earthquake Engineering and Structural Dynamics*.

van de Lindt, J. W., Amini, M. O., Rammer, D., Line, P., Pei, S., and Popovski, M. (2020). Seismic performance factors for cross-laminated timber shear wall systems in the united states. *Journal of Structural Engineering*, 146(9):04020172.

White, M. W. and Dolan, J. D. (1995). Nonlinear Shear-Wall Analysis. *Journal of Structural Engineering*.

Yasumura, M. and Kawai, N. (1998). Estimating seismic performance of wood-framed structures. *Proceedings of 5th WCTE*, 2:564–571.

Yasumura, M., Kobayashi, K., Okabe, M., Miyake, T., and Matsumoto, K. (2016). Full-scale tests and numerical analysis of low-rise clt structures under lateral loading. *Journal of Structural Engineering*, 142(4):E4015007.

Žižmond, J. and Dolšek, M. (2019). Formulation of risk-targeted seismic action for the force-based seismic design of structures. *Earthquake Engineering and Structural Dynamics*.

List of Publications

The following papers are indexed on Scopus

- Sciomenta, M., **Rinaldi, V.**, Bedon, C., Fragiacomo, M. (2020) "*Application of Modal-Displacement Based Design Method to Multi-Story Timber Blockhaus Structures*". Applied Sciences , Vol. 10, No. 11. 2020

- Sciomenta, M., Spera, L., Bedon, C., **Rinaldi, V.**, Fragiacomo, M., Romagnoli, M. (2021) "*Mechanical characterization of novel Homogeneous Beech and hybrid Beech-Corsican Pine thin Cross-Laminated timber panels*". Construction and Building Materials, Vol. 271, No. 11. 2020

- **Rinaldi, V.**, Casagrande, D., Cimini, D., Follesa, M., Fragiacomo, M., (2021) "*An upgrade of existing practice-oriented FE design models for the seismic analysis of CLT buildings*". Soil Dynamics and Earthquake Engineering 2021 [in-press]

International and national conference papers

- Sciomenta, M., **Rinaldi, V.**, Fragiacomo, M., Follesa, M. (2019). "*Seismic Resistant Timber Buildings: How a supply chain of wood may help south Asia achieve a resilient society?*". South Asia Conference on Earthquake Engineering (SACEE). 2019, Karachi (Pakistan)

- **Rinaldi, V.**, Sciomenta, M., Angiolilli, M., Fragiacomo, M., (2019). "*Numerical evaluation of the carbonation effect on the seismic vulnerability of a RC plane frame*". Conference proceedings ANIDIS. 2019, SG05-53, Ascoli Piceno (Italy)

- **Rinaldi, V.**, Casagrande, D., Cimini, D., Follesa, M., Sciomenta, M., Spera, L., Fragiacomo, M., (2021). "*Simplified strategies for the numerical modelling of CLT buildings subjected to lateral loads*". Proceedings of the WCTE 2021

Appendix A

Appendix A reports the configurations details in terms of baseshear associated with the limit states and the q-factor contributions. The findings are referred to section §5.4 for DC2 and DC3 ductility classes. Reading key:

- Configurations (column index "Conf.") from 1 to 180 are analyses with modal load-path whereas from 181 to 360 are analyses with masses load-path;
- The column index "N.Sto." defines the number of the storeys of the configuration.
- The column index "Shearwalls" describes the number of the shearwalls (length of the list) and the corresponding length. For example, [4,6] is a configuration with two shearwalls with length 4m and 6m;
- The column index "Soil" specifies the soil type condition;
- The baseshear values V_x, at the corresponding limit states, are in kN;
- The q_x are the q-factor contributions.

Table A.1. DC2 outcomes of the parametric analysis.

Conf.	N.Sto.	Shearwalls	Soil	V_d	V_1	V_{SD}	V_E	q_S	q_R	q_D	$q_{1.5}$
1	1	[4]	A	7.39	32.17	42.20	49.51	4.35	1.31	1.17	2.31
2	2	[4]	A	21.59	38.80	53.45	59.26	1.80	1.38	1.11	2.29
3	3	[4]	A	28.79	70.50	99.47	130.18	2.45	1.41	1.31	2.77
4	4	[4]	A	32.28	71.65	95.34	146.75	2.22	1.33	1.54	3.07
5	5	[4]	A	37.38	76.72	98.31	172.23	2.05	1.28	1.75	3.37
6	6	[4]	A	39.33	75.51	94.50	174.26	1.92	1.25	1.84	3.46
7	1	[6]	A	11.09	30.70	39.70	52.45	2.77	1.29	1.32	2.56
8	2	[6]	A	26.44	71.63	94.26	114.52	2.71	1.32	1.21	2.40
9	3	[6]	A	41.09	95.97	124.40	146.74	2.34	1.30	1.18	2.29
10	4	[6]	A	48.07	101.67	132.25	145.94	2.12	1.30	1.10	2.15
11	5	[6]	A	52.06	118.18	153.65	188.80	2.27	1.30	1.23	2.40
12	6	[6]	A	51.02	116.66	154.94	186.77	2.29	1.33	1.21	2.40
13	1	[4, 4]	A	14.79	64.21	84.50	99.23	4.34	1.32	1.17	2.32
14	2	[4, 4]	A	43.17	77.59	106.89	118.51	1.80	1.38	1.11	2.29
15	3	[4, 4]	A	57.58	141.01	198.95	260.36	2.45	1.41	1.31	2.77
16	4	[4, 4]	A	64.56	143.92	191.33	291.01	2.23	1.33	1.52	3.03
17	5	[4, 4]	A	74.77	153.10	196.61	344.49	2.05	1.28	1.75	3.38
18	6	[4, 4]	A	78.66	151.80	189.95	353.36	1.93	1.25	1.86	3.49
19	1	[6, 6]	A	22.18	61.21	79.50	104.73	2.76	1.30	1.32	2.57
20	2	[6, 6]	A	52.88	143.11	188.51	229.04	2.71	1.32	1.21	2.40
21	3	[6, 6]	A	82.18	191.71	248.80	294.69	2.33	1.30	1.18	2.31
22	4	[6, 6]	A	96.14	202.96	264.49	291.88	2.11	1.30	1.10	2.16
23	5	[6, 6]	A	104.13	235.86	307.30	377.61	2.27	1.30	1.23	2.40
24	6	[6, 6]	A	102.05	238.25	309.88	373.56	2.33	1.30	1.21	2.35
25	1	[4, 6]	A	18.49	61.27	81.00	98.56	3.31	1.32	1.22	2.41
26	2	[4, 6]	A	48.27	108.74	149.07	168.80	2.25	1.37	1.13	2.33
27	3	[4, 6]	A	70.04	133.72	180.11	208.10	1.91	1.35	1.16	2.33
28	4	[4, 6]	A	78.30	157.46	208.34	240.11	2.01	1.32	1.15	2.29
29	5	[4, 6]	A	88.06	160.75	211.92	236.46	1.83	1.32	1.12	2.21
30	6	[4, 6]	A	91.85	189.56	245.62	322.11	2.06	1.30	1.31	2.55
31	1	[3, 6, 6]	A	27.73	89.39	122.20	145.04	3.22	1.37	1.19	2.43
32	2	[3, 6, 6]	A	67.23	172.95	235.85	277.52	2.57	1.36	1.18	2.41
33	3	[3, 6, 6]	A	105.02	228.31	305.86	364.69	2.17	1.34	1.19	2.40
34	4	[3, 6, 6]	A	122.48	244.15	324.14	384.09	1.99	1.33	1.18	2.36
35	5	[3, 6, 6]	A	135.68	263.84	351.75	415.25	1.94	1.33	1.18	2.36
36	6	[3, 6, 6]	A	129.67	279.65	364.04	480.41	2.16	1.30	1.32	2.58
37	1	[4, 5, 6]	A	27.73	91.71	121.20	147.95	3.31	1.32	1.22	2.42
38	2	[4, 5, 6]	A	72.41	171.57	232.90	265.89	2.37	1.36	1.14	2.32
39	3	[4, 5, 6]	A	96.38	209.75	273.51	310.29	2.18	1.30	1.13	2.22
40	4	[4, 5, 6]	A	116.85	226.56	303.00	349.30	1.94	1.34	1.15	2.31
41	5	[4, 5, 6]	A	126.62	233.10	310.03	353.21	1.84	1.33	1.14	2.27
42	6	[4, 5, 6]	A	130.97	233.99	312.20	352.28	1.79	1.33	1.13	2.26
43	1	[4, 5, 5, 6]	A	36.97	122.14	161.40	197.01	3.30	1.32	1.22	2.42
44	2	[4, 5, 5, 6]	A	96.54	234.14	316.52	362.74	2.43	1.35	1.15	2.32
45	3	[4, 5, 5, 6]	A	128.79	271.12	361.95	415.51	2.11	1.34	1.15	2.30
46	4	[4, 5, 5, 6]	A	155.22	330.69	430.34	513.12	2.13	1.30	1.19	2.33
47	5	[4, 5, 5, 6]	A	168.55	305.53	408.61	467.33	1.81	1.34	1.14	2.29
48	6	[4, 5, 5, 6]	A	175.04	313.90	410.98	470.20	1.79	1.31	1.14	2.25
49	1	[3, 4, 5, 6]	A	33.28	124.74	163.90	188.71	3.75	1.31	1.15	2.27
50	2	[3, 4, 5, 6]	A	86.78	203.74	279.59	318.10	2.35	1.37	1.14	2.34
51	3	[3, 4, 5, 6]	A	118.89	235.90	317.96	370.15	1.98	1.35	1.16	2.35
52	4	[3, 4, 5, 6]	A	141.05	279.49	365.39	429.83	1.98	1.31	1.18	2.31
53	5	[3, 4, 5, 6]	A	156.75	277.08	368.70	435.00	1.77	1.33	1.18	2.35
54	6	[3, 4, 5, 6]	A	158.68	279.04	369.03	433.32	1.76	1.32	1.17	2.33
55	1	[4, 5, 6, 3, 4.5, 5, 6]	A	61.93	208.24	284.50	337.76	3.36	1.37	1.19	2.43
56	2	[4, 5, 6, 3, 4.5, 5, 6]	A	160.46	378.67	513.95	591.02	2.36	1.36	1.15	2.34
57	3	[4, 5, 6, 3, 4.5, 5, 6]	A	220.33	443.77	598.99	688.46	2.01	1.35	1.15	2.33
58	4	[4, 5, 6, 3, 4.5, 5, 6]	A	259.90	504.11	677.49	786.90	1.94	1.34	1.16	2.34
59	5	[4, 5, 6, 3, 4.5, 5, 6]	A	290.46	514.57	689.71	794.42	1.77	1.34	1.15	2.32
60	6	[4, 5, 6, 3, 4.5, 5, 6]	A	294.52	517.90	692.71	798.72	1.76	1.34	1.15	2.31

Continued on next page

Table A.1. DC2 outcomes of the parametric analysis.

Conf.	N.Sto.	Shearwalls	Soil	V_d	V_1	V_{SD}	V_E	q_S	q_R	q_D	$q_{1.5}$
61	1	[4]	B	8.87	32.17	42.20	49.51	3.63	1.31	1.17	2.31
62	2	[4]	B	30.17	53.28	77.62	90.89	1.77	1.46	1.17	2.56
63	3	[4]	B	46.07	70.50	99.47	130.18	1.53	1.41	1.31	2.77
64	4	[4]	B	54.66	71.23	94.78	141.16	1.30	1.33	1.49	2.97
65	5	[4]	B	68.01	76.77	99.15	168.41	1.13	1.29	1.70	3.29
66	6	[4]	B	74.70	83.02	109.27	190.65	1.11	1.32	1.74	3.44
67	1	[6]	B	13.31	30.70	39.70	52.45	2.31	1.29	1.32	2.56
68	2	[6]	B	42.30	71.63	94.26	112.71	1.69	1.32	1.20	2.36
69	3	[6]	B	65.74	109.01	142.00	187.09	1.66	1.30	1.32	2.57
70	4	[6]	B	79.74	127.24	168.34	212.98	1.60	1.32	1.27	2.51
71	5	[6]	B	96.36	127.22	167.94	221.68	1.32	1.32	1.32	2.61
72	6	[6]	B	100.46	128.39	167.26	231.66	1.28	1.30	1.38	2.71
73	1	[4, 4]	B	17.75	64.21	84.50	99.23	3.62	1.32	1.17	2.32
74	2	[4, 4]	B	60.34	106.55	155.30	182.39	1.77	1.46	1.17	2.57
75	3	[4, 4]	B	92.13	141.01	198.95	260.36	1.53	1.41	1.31	2.77
76	4	[4, 4]	B	109.32	143.04	190.42	283.05	1.31	1.33	1.49	2.97
77	5	[4, 4]	B	136.03	153.22	198.31	342.85	1.13	1.29	1.73	3.36
78	6	[4, 4]	B	149.39	165.68	218.54	381.34	1.11	1.32	1.74	3.45
79	1	[6, 6]	B	26.62	61.21	79.50	104.73	2.30	1.30	1.32	2.57
80	2	[6, 6]	B	84.60	143.11	188.51	225.42	1.69	1.32	1.20	2.36
81	3	[6, 6]	B	131.49	217.80	284.00	376.16	1.66	1.30	1.32	2.59
82	4	[6, 6]	B	159.48	254.17	336.67	425.97	1.59	1.32	1.27	2.51
83	5	[6, 6]	B	192.72	253.33	336.58	445.58	1.31	1.33	1.32	2.64
84	6	[6, 6]	B	200.92	255.41	335.38	466.23	1.27	1.31	1.39	2.74
85	1	[4, 6]	B	22.18	61.27	81.00	98.56	2.76	1.32	1.22	2.41
86	2	[4, 6]	B	75.43	122.12	169.72	195.31	1.62	1.39	1.15	2.40
87	3	[4, 6]	B	112.07	180.52	239.12	299.31	1.61	1.32	1.25	2.49
88	4	[4, 6]	B	134.80	185.46	241.64	308.87	1.38	1.30	1.28	2.50
89	5	[4, 6]	B	164.57	209.55	276.50	361.31	1.27	1.32	1.31	2.59
90	6	[4, 6]	B	168.86	209.76	272.38	368.83	1.24	1.30	1.35	2.64
91	1	[3, 6, 6]	B	33.28	89.39	122.20	145.04	2.69	1.37	1.19	2.43
92	2	[3, 6, 6]	B	107.57	172.95	235.85	274.28	1.61	1.36	1.16	2.38
93	3	[3, 6, 6]	B	168.04	255.99	346.92	451.59	1.52	1.36	1.30	2.65
94	4	[3, 6, 6]	B	204.75	304.50	399.22	525.93	1.49	1.31	1.32	2.59
95	5	[3, 6, 6]	B	244.97	337.91	447.14	597.26	1.38	1.32	1.34	2.65
96	6	[3, 6, 6]	B	254.22	319.91	421.51	555.66	1.26	1.32	1.32	2.61
97	1	[4, 5, 6]	B	33.28	91.71	121.20	147.95	2.76	1.32	1.22	2.42
98	2	[4, 5, 6]	B	113.14	184.69	253.69	290.94	1.63	1.37	1.15	2.36
99	3	[4, 5, 6]	B	168.04	235.97	312.61	369.51	1.40	1.32	1.18	2.35
100	4	[4, 5, 6]	B	205.18	286.03	372.35	464.53	1.39	1.30	1.25	2.44
101	5	[4, 5, 6]	B	244.97	299.24	393.43	511.48	1.22	1.31	1.30	2.56
102	6	[4, 5, 6]	B	254.22	302.03	390.81	531.84	1.19	1.29	1.36	2.64
103	1	[4, 5, 5, 6]	B	44.37	122.14	161.40	197.01	2.75	1.32	1.22	2.42
104	2	[4, 5, 5, 6]	B	150.85	247.25	337.68	385.66	1.64	1.37	1.14	2.34
105	3	[4, 5, 5, 6]	B	223.74	328.42	422.23	499.60	1.47	1.29	1.18	2.28
106	4	[4, 5, 5, 6]	B	275.46	383.26	504.69	621.74	1.39	1.32	1.23	2.43
107	5	[4, 5, 5, 6]	B	316.98	402.35	525.45	673.36	1.27	1.31	1.28	2.51
108	6	[4, 5, 5, 6]	B	339.48	405.97	519.66	702.13	1.20	1.28	1.35	2.59
109	1	[3, 4, 5, 6]	B	39.93	124.74	163.90	188.71	3.12	1.31	1.15	2.27
110	2	[3, 4, 5, 6]	B	135.77	216.62	300.07	342.67	1.60	1.39	1.14	2.37
111	3	[3, 4, 5, 6]	B	204.14	285.44	376.33	448.67	1.40	1.32	1.19	2.36
112	4	[3, 4, 5, 6]	B	250.30	334.80	433.00	548.89	1.34	1.29	1.27	2.46
113	5	[3, 4, 5, 6]	B	297.00	361.97	477.87	622.02	1.22	1.32	1.30	2.58
114	6	[3, 4, 5, 6]	B	307.31	365.35	468.00	646.42	1.19	1.28	1.38	2.65
115	1	[4, 5, 6, 3, 4.5, 5, 6]	B	74.32	208.24	284.50	337.76	2.80	1.37	1.19	2.43
116	2	[4, 5, 6, 3, 4.5, 5, 6]	B	252.68	406.72	558.43	638.26	1.61	1.37	1.14	2.35
117	3	[4, 5, 6, 3, 4.5, 5, 6]	B	375.05	537.24	714.43	851.14	1.43	1.33	1.19	2.38
118	4	[4, 5, 6, 3, 4.5, 5, 6]	B	464.54	630.56	816.70	1019.67	1.36	1.30	1.25	2.43
119	5	[4, 5, 6, 3, 4.5, 5, 6]	B	533.58	683.70	902.82	1152.45	1.28	1.32	1.28	2.53
120	6	[4, 5, 6, 3, 4.5, 5, 6]	B	572.57	697.42	895.30	1231.04	1.22	1.28	1.38	2.65

Continued on next page

Table A.1. DC2 outcomes of the parametric analysis.

Conf.	N.Sto.	Shearwalls	Soil	V_d	V_1	V_{SD}	V_E	q_S	q_R	q_D	$q_{1.5}$
121	1	[4]	C	9.98	32.17	42.20	49.51	3.22	1.31	1.17	2.31
122	2	[4]	C	33.94	53.28	77.62	90.89	1.57	1.46	1.17	2.56
123	3	[4]	C	59.40	70.50	99.47	126.26	1.19	1.41	1.27	2.69
124	4	[4]	C	84.85	94.84	131.68	192.50	1.12	1.39	1.46	3.04
125	5	[4]	C	95.65	111.41	155.16	219.83	1.16	1.39	1.42	2.96
126	6	[4]	C	105.04	100.09	134.76	223.41	0.95	1.35	1.66	3.35
127	1	[6]	C	14.97	30.70	39.70	52.45	2.05	1.29	1.32	2.56
128	2	[6]	C	50.91	68.78	87.05	108.63	1.35	1.27	1.25	2.37
129	3	[6]	C	89.10	109.01	142.00	181.58	1.22	1.30	1.28	2.50
130	4	[6]	C	121.99	143.77	192.09	229.94	1.18	1.34	1.20	2.40
131	5	[6]	C	142.95	153.90	204.98	265.92	1.08	1.33	1.30	2.59
132	6	[6]	C	158.16	153.27	199.97	272.65	0.97	1.30	1.36	2.67
133	1	[4, 4]	C	19.97	64.21	84.50	99.23	3.22	1.32	1.17	2.32
134	2	[4, 4]	C	67.88	106.55	155.30	182.39	1.57	1.46	1.17	2.57
135	3	[4, 4]	C	118.80	141.01	198.95	252.53	1.19	1.41	1.27	2.69
136	4	[4, 4]	C	169.71	193.16	263.93	386.39	1.14	1.37	1.46	3.00
137	5	[4, 4]	C	191.29	225.06	311.08	441.50	1.18	1.38	1.42	2.94
138	6	[4, 4]	C	210.08	201.10	270.44	443.45	0.96	1.34	1.64	3.31
139	1	[6, 6]	C	29.95	61.21	79.50	104.73	2.04	1.30	1.32	2.57
140	2	[6, 6]	C	101.82	137.43	174.09	218.02	1.35	1.27	1.25	2.38
141	3	[6, 6]	C	178.19	217.80	284.00	364.70	1.22	1.30	1.28	2.51
142	4	[6, 6]	C	243.98	286.51	384.80	458.75	1.17	1.34	1.19	2.40
143	5	[6, 6]	C	285.90	307.40	409.97	531.86	1.08	1.33	1.30	2.60
144	6	[6, 6]	C	316.32	306.04	399.95	545.33	0.97	1.31	1.36	2.67
145	1	[4, 6]	C	24.96	61.27	81.00	98.56	2.46	1.32	1.22	2.41
146	2	[4, 6]	C	84.85	137.71	186.50	228.58	1.62	1.35	1.23	2.49
147	3	[4, 6]	C	148.49	180.52	239.12	293.20	1.22	1.32	1.23	2.44
148	4	[4, 6]	C	206.71	237.21	322.40	401.31	1.15	1.36	1.24	2.54
149	5	[4, 6]	C	238.80	259.34	346.06	478.75	1.09	1.33	1.38	2.77
150	6	[4, 6]	C	263.32	254.65	336.54	506.51	0.97	1.32	1.51	2.98
151	1	[3, 6, 6]	C	37.44	89.39	122.20	145.04	2.39	1.37	1.19	2.43
152	2	[3, 6, 6]	C	127.28	200.82	263.95	317.66	1.58	1.31	1.20	2.37
153	3	[3, 6, 6]	C	222.74	255.99	346.92	439.29	1.15	1.36	1.27	2.57
154	4	[3, 6, 6]	C	307.11	359.43	474.41	585.72	1.17	1.32	1.23	2.44
155	5	[3, 6, 6]	C	358.87	380.60	512.00	697.77	1.06	1.35	1.36	2.75
156	6	[3, 6, 6]	C	397.62	379.04	498.93	708.44	0.95	1.32	1.42	2.80
157	1	[4, 5, 6]	C	37.44	91.71	121.20	147.95	2.45	1.32	1.22	2.42
158	2	[4, 5, 6]	C	127.28	201.50	276.61	317.59	1.58	1.37	1.15	2.36
159	3	[4, 5, 6]	C	222.74	274.52	371.21	447.50	1.23	1.35	1.21	2.45
160	4	[4, 5, 6]	C	309.71	348.23	469.69	595.77	1.12	1.35	1.27	2.57
161	5	[4, 5, 6]	C	357.89	383.12	516.76	720.10	1.07	1.35	1.39	2.82
162	6	[4, 5, 6]	C	398.70	382.19	510.86	757.27	0.96	1.34	1.48	2.97
163	1	[4, 5, 5, 6]	C	49.91	122.14	161.40	197.01	2.45	1.32	1.22	2.42
164	2	[4, 5, 5, 6]	C	169.71	264.03	362.25	410.81	1.56	1.37	1.13	2.33
165	3	[4, 5, 5, 6]	C	296.99	368.31	502.95	601.62	1.24	1.37	1.20	2.45
166	4	[4, 5, 5, 6]	C	412.42	459.46	617.41	784.41	1.11	1.34	1.27	2.56
167	5	[4, 5, 5, 6]	C	476.77	505.17	678.34	869.03	1.06	1.34	1.28	2.58
168	6	[4, 5, 5, 6]	C	533.96	513.81	675.75	1003.90	0.96	1.32	1.49	2.93
169	1	[3, 4, 5, 6]	C	44.92	124.74	163.90	188.71	2.78	1.31	1.15	2.27
170	2	[3, 4, 5, 6]	C	152.74	244.44	339.88	386.68	1.60	1.39	1.14	2.37
171	3	[3, 4, 5, 6]	C	267.29	322.67	432.49	524.54	1.21	1.34	1.21	2.44
172	4	[3, 4, 5, 6]	C	372.69	408.18	552.55	688.04	1.10	1.35	1.25	2.53
173	5	[3, 4, 5, 6]	C	430.84	451.71	613.39	860.69	1.05	1.36	1.40	2.86
174	6	[3, 4, 5, 6]	C	480.04	453.27	604.04	897.74	0.94	1.33	1.49	2.97
175	1	[4, 5, 6, 3, 4.5, 5, 6]	C	83.61	208.24	284.50	337.76	2.49	1.37	1.19	2.43
176	2	[4, 5, 6, 3, 4.5, 5, 6]	C	284.26	449.99	621.66	709.53	1.58	1.38	1.14	2.37
177	3	[4, 5, 6, 3, 4.5, 5, 6]	C	497.45	600.77	812.77	981.22	1.21	1.35	1.21	2.45
178	4	[4, 5, 6, 3, 4.5, 5, 6]	C	691.86	777.59	1033.91	1288.18	1.12	1.33	1.25	2.48
179	5	[4, 5, 6, 3, 4.5, 5, 6]	C	800.17	838.09	1127.96	1468.52	1.05	1.35	1.30	2.63
180	6	[4, 5, 6, 3, 4.5, 5, 6]	C	894.12	843.88	1131.29	1690.00	0.94	1.34	1.49	3.00

Continued on next page

Table A.1. DC2 outcomes of the parametric analysis.

Conf.	N.Sto.	Shearwalls	Soil	V_d	V_1	V_{SD}	V_E	q_S	q_R	q_D	$q_{1.5}$
181	1	[4]	A	7.39	32.17	42.20	49.51	4.35	1.31	1.17	2.31
182	2	[4]	A	21.59	40.00	54.02	62.95	1.85	1.35	1.17	2.36
183	3	[4]	A	28.79	72.80	100.52	141.02	2.53	1.38	1.40	2.91
184	4	[4]	A	32.28	76.00	100.18	139.57	2.35	1.32	1.39	2.75
185	5	[4]	A	37.38	89.70	116.84	172.14	2.40	1.30	1.47	2.88
186	6	[4]	A	39.33	89.60	114.44	182.47	2.28	1.28	1.59	3.05
187	1	[6]	A	11.09	30.70	39.70	52.45	2.77	1.29	1.32	2.56
188	2	[6]	A	26.44	75.14	97.20	110.20	2.84	1.29	1.13	2.20
189	3	[6]	A	41.09	101.24	133.00	148.28	2.46	1.31	1.11	2.20
190	4	[6]	A	48.07	102.00	136.34	152.71	2.12	1.34	1.12	2.25
191	5	[6]	A	52.06	123.50	163.66	178.23	2.37	1.33	1.09	2.16
192	6	[6]	A	51.02	124.80	165.68	183.03	2.45	1.33	1.10	2.20
193	1	[4, 4]	A	14.79	64.21	84.50	99.23	4.34	1.32	1.17	2.32
194	2	[4, 4]	A	43.17	80.00	107.94	125.90	1.85	1.35	1.17	2.36
195	3	[4, 4]	A	57.58	146.30	201.60	280.37	2.54	1.38	1.39	2.87
196	4	[4, 4]	A	64.56	153.00	201.96	280.20	2.37	1.32	1.39	2.75
197	5	[4, 4]	A	74.77	180.70	235.49	347.08	2.42	1.30	1.47	2.88
198	6	[4, 4]	A	78.66	182.15	230.40	359.40	2.32	1.26	1.56	2.96
199	1	[6, 6]	A	22.18	61.21	79.50	104.73	2.76	1.30	1.32	2.57
200	2	[6, 6]	A	52.88	150.02	194.40	221.65	2.84	1.30	1.14	2.22
201	3	[6, 6]	A	82.18	201.50	266.70	297.73	2.45	1.32	1.12	2.22
202	4	[6, 6]	A	96.14	205.00	274.16	304.32	2.13	1.34	1.11	2.23
203	5	[6, 6]	A	104.13	247.00	327.73	360.35	2.37	1.33	1.10	2.19
204	6	[6, 6]	A	102.05	251.20	334.36	364.21	2.46	1.33	1.09	2.17
205	1	[4, 6]	A	18.49	61.27	81.00	98.56	3.31	1.32	1.22	2.41
206	2	[4, 6]	A	48.27	111.60	151.10	172.76	2.31	1.35	1.14	2.32
207	3	[4, 6]	A	70.04	141.40	185.71	212.21	2.02	1.31	1.14	2.25
208	4	[4, 6]	A	78.30	168.00	223.33	242.03	2.15	1.33	1.08	2.16
209	5	[4, 6]	A	88.06	173.21	227.50	250.19	1.97	1.31	1.10	2.17
210	6	[4, 6]	A	91.85	204.80	269.51	298.34	2.23	1.32	1.11	2.19
211	1	[3, 6, 6]	A	27.73	89.39	122.20	145.04	3.22	1.37	1.19	2.43
212	2	[3, 6, 6]	A	67.23	176.00	241.21	276.30	2.62	1.37	1.15	2.35
213	3	[3, 6, 6]	A	105.02	245.70	331.67	381.92	2.34	1.35	1.15	2.33
214	4	[3, 6, 6]	A	122.48	253.00	339.68	389.46	2.07	1.34	1.15	2.31
215	5	[3, 6, 6]	A	135.68	293.80	390.43	447.25	2.17	1.33	1.15	2.28
216	6	[3, 6, 6]	A	129.67	300.80	396.05	454.33	2.32	1.32	1.15	2.27
217	1	[4, 5, 6]	A	27.73	91.71	121.20	147.95	3.31	1.32	1.22	2.42
218	2	[4, 5, 6]	A	72.41	176.40	237.15	272.86	2.44	1.34	1.15	2.32
219	3	[4, 5, 6]	A	96.38	212.10	282.58	318.41	2.20	1.33	1.13	2.25
220	4	[4, 5, 6]	A	116.85	242.00	323.60	357.57	2.07	1.34	1.10	2.22
221	5	[4, 5, 6]	A	126.62	248.30	329.04	360.85	1.96	1.33	1.10	2.18
222	6	[4, 5, 6]	A	130.97	252.80	335.69	367.12	1.93	1.33	1.09	2.18
223	1	[4, 5, 5, 6]	A	36.97	122.14	161.40	197.01	3.30	1.32	1.22	2.42
224	2	[4, 5, 5, 6]	A	96.54	241.20	323.18	371.75	2.50	1.34	1.15	2.31
225	3	[4, 5, 5, 6]	A	128.79	282.80	379.28	426.95	2.20	1.34	1.13	2.26
226	4	[4, 5, 5, 6]	A	155.22	356.37	464.00	521.41	2.30	1.30	1.12	2.19
227	5	[4, 5, 5, 6]	A	168.55	327.60	432.65	470.76	1.94	1.32	1.09	2.16
228	6	[4, 5, 5, 6]	A	175.04	332.80	439.31	472.32	1.90	1.32	1.08	2.13
229	1	[3, 4, 5, 6]	A	33.28	124.74	163.90	188.71	3.75	1.31	1.15	2.27
230	2	[3, 4, 5, 6]	A	86.78	208.40	283.30	326.92	2.40	1.36	1.15	2.35
231	3	[3, 4, 5, 6]	A	118.89	247.10	329.48	378.28	2.08	1.33	1.15	2.30
232	4	[3, 4, 5, 6]	A	141.05	289.00	386.92	442.79	2.05	1.34	1.14	2.30
233	5	[3, 4, 5, 6]	A	156.75	297.70	394.36	444.34	1.90	1.32	1.13	2.24
234	6	[3, 4, 5, 6]	A	158.68	300.80	398.52	450.93	1.90	1.32	1.13	2.25
235	1	[4, 5, 6, 3, 4.5, 5, 6]	A	61.93	208.24	284.50	337.76	3.36	1.37	1.19	2.43
236	2	[4, 5, 6, 3, 4.5, 5, 6]	A	160.46	388.40	522.90	606.05	2.42	1.35	1.16	2.34
237	3	[4, 5, 6, 3, 4.5, 5, 6]	A	220.33	463.40	621.81	706.35	2.10	1.34	1.14	2.29
238	4	[4, 5, 6, 3, 4.5, 5, 6]	A	259.90	535.00	718.67	819.41	2.06	1.34	1.14	2.30
239	5	[4, 5, 6, 3, 4.5, 5, 6]	A	290.46	552.50	734.95	823.19	1.90	1.33	1.12	2.23
240	6	[4, 5, 6, 3, 4.5, 5, 6]	A	294.52	563.20	746.96	837.85	1.91	1.33	1.12	2.23

Continued on next page

Table A.1. DC2 outcomes of the parametric analysis.

Conf.	N.Sto.	Shearwalls	Soil	V_d	V_1	V_{SD}	V_E	q_S	q_R	q_D	$q_{1.5}$
241	1	[4]	B	8.87	32.17	42.20	49.51	3.63	1.31	1.17	2.31
242	2	[4]	B	30.17	53.60	78.06	91.38	1.78	1.46	1.17	2.56
243	3	[4]	B	46.07	72.80	100.52	134.15	1.58	1.38	1.33	2.76
244	4	[4]	B	54.66	76.00	100.18	139.57	1.39	1.32	1.39	2.75
245	5	[4]	B	68.01	89.70	116.84	172.14	1.32	1.30	1.47	2.88
246	6	[4]	B	74.70	99.20	131.16	199.18	1.33	1.32	1.52	3.01
247	1	[6]	B	13.31	30.70	39.70	52.45	2.31	1.29	1.32	2.56
248	2	[6]	B	42.30	75.14	97.20	109.43	1.78	1.29	1.13	2.18
249	3	[6]	B	65.74	120.01	152.60	179.66	1.83	1.27	1.18	2.25
250	4	[6]	B	79.74	138.75	181.00	216.29	1.74	1.30	1.19	2.34
251	5	[6]	B	96.36	139.10	186.67	210.25	1.44	1.34	1.13	2.27
252	6	[6]	B	100.46	140.80	186.25	206.41	1.40	1.32	1.11	2.20
253	1	[4, 4]	B	17.75	64.21	84.50	99.23	3.62	1.32	1.17	2.32
254	2	[4, 4]	B	60.34	107.20	156.21	183.60	1.78	1.46	1.18	2.57
255	3	[4, 4]	B	92.13	146.30	201.60	280.37	1.59	1.38	1.39	2.87
256	4	[4, 4]	B	109.32	153.00	201.96	280.20	1.40	1.32	1.39	2.75
257	5	[4, 4]	B	136.03	180.70	235.49	347.08	1.33	1.30	1.47	2.88
258	6	[4, 4]	B	149.39	200.00	264.60	400.94	1.34	1.32	1.52	3.01
259	1	[6, 6]	B	26.62	61.21	79.50	104.73	2.30	1.30	1.32	2.57
260	2	[6, 6]	B	84.60	150.02	194.40	219.97	1.77	1.30	1.13	2.20
261	3	[6, 6]	B	131.49	239.56	305.20	359.32	1.82	1.27	1.18	2.25
262	4	[6, 6]	B	159.48	276.83	362.00	435.54	1.74	1.31	1.20	2.36
263	5	[6, 6]	B	192.72	279.50	374.67	419.07	1.45	1.34	1.12	2.25
264	6	[6, 6]	B	200.92	281.60	372.03	412.81	1.40	1.32	1.11	2.20
265	1	[4, 6]	B	22.18	61.27	81.00	98.56	2.76	1.32	1.22	2.41
266	2	[4, 6]	B	75.43	124.80	173.81	196.85	1.65	1.39	1.13	2.37
267	3	[4, 6]	B	112.07	194.87	254.10	297.50	1.74	1.30	1.17	2.29
268	4	[4, 6]	B	134.80	196.00	261.67	298.91	1.45	1.34	1.14	2.29
269	5	[4, 6]	B	164.57	232.66	302.90	374.11	1.41	1.30	1.24	2.41
270	6	[4, 6]	B	168.86	236.93	305.60	369.33	1.40	1.29	1.21	2.34
271	1	[3, 6, 6]	B	33.28	89.39	122.20	145.04	2.69	1.37	1.19	2.43
272	2	[3, 6, 6]	B	107.57	176.00	241.21	273.99	1.64	1.37	1.14	2.34
273	3	[3, 6, 6]	B	168.04	290.42	372.40	443.53	1.73	1.28	1.19	2.29
274	4	[3, 6, 6]	B	204.75	336.39	441.00	558.11	1.64	1.31	1.27	2.49
275	5	[3, 6, 6]	B	244.97	376.10	501.80	658.36	1.54	1.33	1.31	2.63
276	6	[3, 6, 6]	B	254.22	350.40	468.12	566.49	1.38	1.34	1.21	2.43
277	1	[4, 5, 6]	B	33.28	91.71	121.20	147.95	2.76	1.32	1.22	2.42
278	2	[4, 5, 6]	B	113.14	189.60	259.51	293.94	1.68	1.37	1.13	2.33
279	3	[4, 5, 6]	B	168.04	254.34	326.90	372.69	1.51	1.29	1.14	2.20
280	4	[4, 5, 6]	B	205.18	301.45	401.00	467.99	1.47	1.33	1.17	2.33
281	5	[4, 5, 6]	B	244.97	332.60	430.30	502.23	1.36	1.29	1.17	2.27
282	6	[4, 5, 6]	B	254.22	335.52	436.80	501.51	1.32	1.30	1.15	2.24
283	1	[4, 5, 5, 6]	B	44.37	122.14	161.40	197.01	2.75	1.32	1.22	2.42
284	2	[4, 5, 5, 6]	B	150.85	254.40	345.46	392.10	1.69	1.36	1.14	2.31
285	3	[4, 5, 5, 6]	B	223.74	339.07	439.60	507.00	1.52	1.30	1.15	2.24
286	4	[4, 5, 5, 6]	B	275.46	418.35	538.00	633.28	1.52	1.29	1.18	2.27
287	5	[4, 5, 5, 6]	B	316.98	439.01	570.70	675.87	1.38	1.30	1.18	2.31
288	6	[4, 5, 5, 6]	B	339.48	438.67	579.20	679.07	1.29	1.32	1.17	2.32
289	1	[3, 4, 5, 6]	B	39.93	124.74	163.90	188.71	3.12	1.31	1.15	2.27
290	2	[3, 4, 5, 6]	B	135.77	221.60	305.56	348.28	1.63	1.38	1.14	2.36
291	3	[3, 4, 5, 6]	B	204.14	306.09	395.50	453.72	1.50	1.29	1.15	2.22
292	4	[3, 4, 5, 6]	B	250.30	356.07	468.00	554.93	1.42	1.31	1.19	2.34
293	5	[3, 4, 5, 6]	B	297.00	393.90	525.15	645.10	1.33	1.33	1.23	2.46
294	6	[3, 4, 5, 6]	B	307.31	398.40	526.47	637.62	1.30	1.32	1.21	2.40
295	1	[4, 5, 6, 3, 4.5, 5, 6]	B	74.32	208.24	284.50	337.76	2.80	1.37	1.19	2.43
296	2	[4, 5, 6, 3, 4.5, 5, 6]	B	252.68	417.20	569.18	647.62	1.65	1.36	1.14	2.33
297	3	[4, 5, 6, 3, 4.5, 5, 6]	B	375.05	586.70	747.60	856.28	1.56	1.27	1.15	2.19
298	4	[4, 5, 6, 3, 4.5, 5, 6]	B	464.54	656.54	878.00	1024.01	1.41	1.34	1.17	2.34
299	5	[4, 5, 6, 3, 4.5, 5, 6]	B	533.58	747.23	984.10	1187.24	1.40	1.32	1.21	2.38
300	6	[4, 5, 6, 3, 4.5, 5, 6]	B	572.57	775.87	1006.40	1202.75	1.36	1.30	1.20	2.33

Continued on next page

Table A.1. DC2 outcomes of the parametric analysis.

Conf.	N.Sto.	Shearwalls	Soil	V_d	V_1	V_{SD}	V_E	q_S	q_R	q_D	$q_{1.5}$
301	1	[4]	C	9.98	32.17	42.20	49.51	3.22	1.31	1.17	2.31
302	2	[4]	C	33.94	53.60	78.06	91.38	1.58	1.46	1.17	2.56
303	3	[4]	C	59.40	72.80	100.52	134.15	1.23	1.38	1.33	2.76
304	4	[4]	C	84.85	111.00	153.70	208.79	1.31	1.38	1.36	2.82
305	5	[4]	C	95.65	130.00	180.85	247.44	1.36	1.39	1.37	2.86
306	6	[4]	C	105.04	126.40	171.72	249.04	1.20	1.36	1.45	2.96
307	1	[6]	C	14.97	30.70	39.70	52.45	2.05	1.29	1.32	2.56
308	2	[6]	C	50.91	91.20	117.60	141.04	1.79	1.29	1.20	2.32
309	3	[6]	C	89.10	120.01	152.60	179.66	1.35	1.27	1.18	2.25
310	4	[6]	C	121.99	151.99	199.00	245.86	1.25	1.31	1.24	2.43
311	5	[6]	C	142.95	167.33	221.00	292.25	1.17	1.32	1.32	2.62
312	6	[6]	C	158.16	170.92	222.40	305.64	1.08	1.30	1.37	2.68
313	1	[4, 4]	C	19.97	64.21	84.50	99.23	3.22	1.32	1.17	2.32
314	2	[4, 4]	C	67.88	107.20	156.21	183.60	1.58	1.46	1.18	2.57
315	3	[4, 4]	C	118.80	146.30	201.60	267.38	1.23	1.38	1.33	2.74
316	4	[4, 4]	C	169.71	223.00	308.69	419.22	1.31	1.38	1.36	2.82
317	5	[4, 4]	C	191.29	260.00	361.71	494.89	1.36	1.39	1.37	2.86
318	6	[4, 4]	C	210.08	252.80	343.67	507.29	1.20	1.36	1.48	3.01
319	1	[6, 6]	C	29.95	61.21	79.50	104.73	2.04	1.30	1.32	2.57
320	2	[6, 6]	C	101.82	181.76	235.60	282.99	1.79	1.30	1.20	2.34
321	3	[6, 6]	C	178.19	239.56	305.20	359.32	1.34	1.27	1.18	2.25
322	4	[6, 6]	C	243.98	303.34	398.00	491.73	1.24	1.31	1.24	2.43
323	5	[6, 6]	C	285.90	343.66	443.30	582.32	1.20	1.29	1.31	2.54
324	6	[6, 6]	C	316.32	340.83	444.80	611.32	1.08	1.31	1.37	2.69
325	1	[4, 6]	C	24.96	61.27	81.00	98.56	2.46	1.32	1.22	2.41
326	2	[4, 6]	C	84.85	146.54	198.40	225.36	1.73	1.35	1.14	2.31
327	3	[4, 6]	C	148.49	194.87	254.10	297.50	1.31	1.30	1.17	2.29
328	4	[4, 6]	C	206.71	248.00	338.58	411.67	1.20	1.37	1.22	2.49
329	5	[4, 6]	C	238.80	286.00	387.77	499.78	1.20	1.36	1.29	2.62
330	6	[4, 6]	C	263.32	296.00	397.64	526.71	1.12	1.34	1.32	2.67
331	1	[3, 6, 6]	C	37.44	89.39	122.20	145.04	2.39	1.37	1.19	2.43
332	2	[3, 6, 6]	C	127.28	235.04	303.20	356.18	1.85	1.29	1.17	2.27
333	3	[3, 6, 6]	C	222.74	290.42	372.40	443.53	1.30	1.28	1.19	2.29
334	4	[3, 6, 6]	C	307.11	380.03	503.00	607.26	1.24	1.32	1.21	2.40
335	5	[3, 6, 6]	C	358.87	426.67	578.50	726.72	1.19	1.36	1.26	2.55
336	6	[3, 6, 6]	C	397.62	436.75	579.20	758.82	1.10	1.33	1.31	2.61
337	1	[4, 5, 6]	C	37.44	91.71	121.20	147.95	2.45	1.32	1.22	2.42
338	2	[4, 5, 6]	C	127.28	214.40	284.00	322.45	1.68	1.32	1.14	2.26
339	3	[4, 5, 6]	C	222.74	301.97	390.60	450.41	1.36	1.29	1.15	2.24
340	4	[4, 5, 6]	C	309.71	370.00	500.96	598.08	1.19	1.35	1.19	2.42
341	5	[4, 5, 6]	C	357.89	429.00	581.25	759.61	1.20	1.35	1.31	2.66
342	6	[4, 5, 6]	C	398.70	454.94	604.80	818.92	1.14	1.33	1.35	2.70
343	1	[4, 5, 5, 6]	C	49.91	122.14	161.40	197.01	2.45	1.32	1.22	2.42
344	2	[4, 5, 5, 6]	C	169.71	281.79	370.00	419.82	1.66	1.31	1.13	2.23
345	3	[4, 5, 5, 6]	C	296.99	409.06	527.10	603.28	1.38	1.29	1.14	2.21
346	4	[4, 5, 5, 6]	C	412.42	492.00	663.75	784.03	1.19	1.35	1.18	2.39
347	5	[4, 5, 5, 6]	C	476.77	572.00	772.06	1017.10	1.20	1.35	1.32	2.67
348	6	[4, 5, 5, 6]	C	533.96	595.20	796.00	1090.36	1.11	1.34	1.37	2.75
349	1	[3, 4, 5, 6]	C	44.92	124.74	163.90	188.71	2.78	1.31	1.15	2.27
350	2	[3, 4, 5, 6]	C	152.74	252.40	349.73	397.76	1.65	1.39	1.14	2.36
351	3	[3, 4, 5, 6]	C	267.29	337.40	456.91	533.30	1.26	1.35	1.17	2.37
352	4	[3, 4, 5, 6]	C	372.69	437.00	592.85	723.93	1.17	1.36	1.22	2.48
353	5	[3, 4, 5, 6]	C	430.84	518.70	709.64	913.26	1.20	1.37	1.29	2.64
354	6	[3, 4, 5, 6]	C	480.04	545.42	723.20	986.87	1.14	1.33	1.36	2.71
355	1	[4, 5, 6, 3, 4.5, 5, 6]	C	83.61	208.24	284.50	337.76	2.49	1.37	1.19	2.43
356	2	[4, 5, 6, 3, 4.5, 5, 6]	C	284.26	465.60	638.01	724.83	1.64	1.37	1.14	2.34
357	3	[4, 5, 6, 3, 4.5, 5, 6]	C	497.45	663.24	857.50	988.63	1.33	1.29	1.15	2.24
358	4	[4, 5, 6, 3, 4.5, 5, 6]	C	691.86	819.00	1107.47	1336.47	1.18	1.35	1.21	2.45
359	5	[4, 5, 6, 3, 4.5, 5, 6]	C	800.17	951.60	1286.09	1682.05	1.19	1.35	1.31	2.65
360	6	[4, 5, 6, 3, 4.5, 5, 6]	C	894.12	1005.84	1350.40	1827.44	1.12	1.34	1.35	2.73

Table A.2. DC3 outcomes of the parametric analysis.

Conf.	N.Sto.	Shearwalls	Soil	V_d	V_1	V_{SD}	V_E	q_S	q_R	q_D	$q_{1.5}$
1	1	[4]	A	4.93	27.00	45.65	70.01	5.48	1.69	1.53	3.89
2	2	[4]	A	16.76	59.63	94.60	134.01	3.56	1.59	1.42	3.37
3	3	[4]	A	23.35	100.27	165.46	248.67	4.29	1.65	1.50	3.72
4	4	[4]	A	24.78	118.52	189.94	289.48	4.78	1.60	1.52	3.66
5	5	[4]	A	25.61	136.09	210.91	315.74	5.31	1.55	1.50	3.48
6	6	[4]	A	27.87	166.85	257.88	394.28	5.99	1.55	1.53	3.54
7	1	[6]	A	7.39	42.20	68.06	105.66	5.71	1.61	1.55	3.76
8	2	[6]	A	25.14	88.19	134.41	192.71	3.51	1.52	1.43	3.28
9	3	[6]	A	33.62	139.97	217.14	329.48	4.16	1.55	1.52	3.53
10	4	[6]	A	35.68	165.25	255.31	408.34	4.63	1.55	1.60	3.71
11	5	[6]	A	36.88	196.17	291.70	450.62	5.32	1.49	1.54	3.45
12	6	[6]	A	38.05	225.88	331.48	511.89	5.94	1.47	1.54	3.40
13	1	[4, 4]	A	9.86	53.70	91.21	140.42	5.45	1.70	1.54	3.92
14	2	[4, 4]	A	33.52	117.71	188.38	267.90	3.51	1.60	1.42	3.41
15	3	[4, 4]	A	46.70	193.17	324.33	488.77	4.14	1.68	1.51	3.80
16	4	[4, 4]	A	49.56	223.62	362.63	543.06	4.51	1.62	1.50	3.64
17	5	[4, 4]	A	51.21	240.12	400.73	643.98	4.69	1.67	1.61	4.02
18	6	[4, 4]	A	55.74	253.38	427.39	683.96	4.55	1.69	1.60	4.05
19	1	[6, 6]	A	14.79	84.00	136.00	211.91	5.68	1.62	1.56	3.78
20	2	[6, 6]	A	50.28	174.52	267.83	386.05	3.47	1.53	1.44	3.32
21	3	[6, 6]	A	67.25	270.29	426.32	655.09	4.02	1.58	1.54	3.64
22	4	[6, 6]	A	71.37	320.38	502.76	804.18	4.49	1.57	1.60	3.77
23	5	[6, 6]	A	73.75	367.94	564.73	875.68	4.99	1.53	1.55	3.57
24	6	[6, 6]	A	76.10	394.69	619.94	997.97	5.19	1.57	1.61	3.79
25	1	[4, 6]	A	12.32	68.30	113.35	176.55	5.54	1.66	1.56	3.88
26	2	[4, 6]	A	41.90	145.69	227.72	326.82	3.48	1.56	1.44	3.36
27	3	[4, 6]	A	56.99	228.67	367.15	558.18	4.01	1.61	1.52	3.66
28	4	[4, 6]	A	60.47	270.83	432.69	678.87	4.48	1.60	1.57	3.76
29	5	[4, 6]	A	62.50	299.12	491.37	799.47	4.79	1.64	1.63	4.01
30	6	[4, 6]	A	64.92	317.62	531.47	885.79	4.89	1.67	1.67	4.18
31	1	[3, 6, 6]	A	18.49	103.00	165.74	253.02	5.57	1.61	1.53	3.68
32	2	[3, 6, 6]	A	62.69	212.60	327.72	468.20	3.39	1.54	1.43	3.30
33	3	[3, 6, 6]	A	82.48	336.05	538.69	836.01	4.07	1.60	1.55	3.73
34	4	[3, 6, 6]	A	87.53	398.04	631.63	1010.93	4.55	1.59	1.60	3.81
35	5	[3, 6, 6]	A	90.46	452.22	714.67	1152.91	5.00	1.58	1.61	3.82
36	6	[3, 6, 6]	A	93.60	505.64	789.74	1244.92	5.40	1.56	1.58	3.69
37	1	[4, 5, 6]	A	18.49	100.70	167.72	264.50	5.45	1.67	1.58	3.94
38	2	[4, 5, 6]	A	62.38	209.34	329.35	482.25	3.36	1.57	1.46	3.46
39	3	[4, 5, 6]	A	82.67	328.34	528.65	824.89	3.97	1.61	1.56	3.77
40	4	[4, 5, 6]	A	87.73	388.61	620.21	998.20	4.43	1.60	1.61	3.85
41	5	[4, 5, 6]	A	90.66	442.46	691.49	1099.69	4.88	1.56	1.59	3.73
42	6	[4, 5, 6]	A	94.36	494.04	768.25	1214.74	5.24	1.56	1.58	3.69
43	1	[4, 5, 5, 6]	A	24.65	133.10	220.74	349.74	5.40	1.66	1.58	3.94
44	2	[4, 5, 5, 6]	A	82.03	273.96	430.27	634.95	3.34	1.57	1.48	3.48
45	3	[4, 5, 5, 6]	A	108.30	430.06	690.59	1088.03	3.97	1.61	1.58	3.79
46	4	[4, 5, 5, 6]	A	114.93	508.78	810.15	1321.97	4.43	1.59	1.63	3.90
47	5	[4, 5, 5, 6]	A	118.77	582.78	904.45	1468.32	4.91	1.55	1.62	3.78
48	6	[4, 5, 5, 6]	A	124.30	663.90	1014.43	1611.24	5.34	1.53	1.59	3.64
49	1	[3, 4, 5, 6]	A	22.18	120.20	196.81	304.23	5.42	1.64	1.55	3.80
50	2	[3, 4, 5, 6]	A	73.43	248.74	388.66	561.89	3.39	1.56	1.45	3.39
51	3	[3, 4, 5, 6]	A	97.88	395.47	635.79	983.93	4.04	1.61	1.55	3.73
52	4	[3, 4, 5, 6]	A	103.87	467.58	745.66	1193.06	4.50	1.59	1.60	3.83
53	5	[3, 4, 5, 6]	A	107.35	531.67	844.07	1384.76	4.95	1.59	1.64	3.91
54	6	[3, 4, 5, 6]	A	113.72	617.79	966.87	1550.28	5.43	1.57	1.60	3.76
55	1	[4, 5, 6, 3, 4.5, 5, 6]	A	41.29	224.80	376.69	589.91	5.44	1.68	1.57	3.94
56	2	[4, 5, 6, 3, 4.5, 5, 6]	A	139.14	472.52	747.56	1091.46	3.40	1.58	1.46	3.46
57	3	[4, 5, 6, 3, 4.5, 5, 6]	A	185.22	747.69	1207.30	1870.25	4.04	1.61	1.55	3.75
58	4	[4, 5, 6, 3, 4.5, 5, 6]	A	196.56	888.20	1411.75	2259.26	4.52	1.59	1.60	3.82
59	5	[4, 5, 6, 3, 4.5, 5, 6]	A	203.13	1022.64	1589.55	2539.12	5.03	1.55	1.60	3.72
60	6	[4, 5, 6, 3, 4.5, 5, 6]	A	212.91	1195.68	1823.67	2872.92	5.62	1.53	1.58	3.60

Continued on next page

Table A.2. DC3 outcomes of the parametric analysis.

Conf.	N.Sto.	Shearwalls	Soil	V_d	V_1	V_{SD}	V_E	q_S	q_R	q_D	$q_{1.5}$
61	1	[4]	B	5.92	27.80	47.94	73.72	4.70	1.72	1.54	3.98
62	2	[4]	B	20.11	59.63	94.60	134.01	2.96	1.59	1.42	3.37
63	3	[4]	B	35.20	100.27	165.46	229.45	2.85	1.65	1.39	3.43
64	4	[4]	B	39.65	118.52	189.94	289.48	2.99	1.60	1.52	3.66
65	5	[4]	B	40.97	136.09	210.91	315.74	3.32	1.55	1.50	3.48
66	6	[4]	B	44.59	166.85	257.88	394.28	3.74	1.55	1.53	3.54
67	1	[6]	B	8.87	41.30	65.64	101.34	4.65	1.59	1.54	3.68
68	2	[6]	B	30.17	88.19	134.41	192.71	2.92	1.52	1.43	3.28
69	3	[6]	B	52.80	139.97	217.14	304.22	2.65	1.55	1.40	3.26
70	4	[6]	B	57.09	165.25	255.31	408.34	2.89	1.55	1.60	3.71
71	5	[6]	B	59.00	196.17	291.70	450.62	3.32	1.49	1.54	3.45
72	6	[6]	B	60.88	225.88	331.48	511.89	3.71	1.47	1.54	3.40
73	1	[4, 4]	B	11.83	51.80	86.37	132.41	4.38	1.67	1.53	3.83
74	2	[4, 4]	B	40.23	117.71	188.38	267.90	2.93	1.60	1.42	3.41
75	3	[4, 4]	B	70.40	193.17	324.33	449.88	2.74	1.68	1.39	3.49
76	4	[4, 4]	B	79.29	223.62	362.63	543.06	2.82	1.62	1.50	3.64
77	5	[4, 4]	B	81.94	240.12	400.73	643.98	2.93	1.67	1.61	4.02
78	6	[4, 4]	B	89.19	253.38	427.39	683.96	2.84	1.69	1.60	4.05
79	1	[6, 6]	B	17.75	82.10	131.14	203.40	4.63	1.60	1.55	3.72
80	2	[6, 6]	B	60.34	174.52	267.83	386.05	2.89	1.53	1.44	3.32
81	3	[6, 6]	B	105.60	270.29	426.32	601.76	2.56	1.58	1.41	3.34
82	4	[6, 6]	B	114.19	320.38	502.76	804.18	2.81	1.57	1.60	3.77
83	5	[6, 6]	B	118.01	367.94	564.73	875.68	3.12	1.53	1.55	3.57
84	6	[6, 6]	B	121.77	394.69	619.94	997.97	3.24	1.57	1.61	3.79
85	1	[4, 6]	B	14.79	65.10	106.06	163.16	4.40	1.63	1.54	3.76
86	2	[4, 6]	B	50.28	145.69	227.72	326.82	2.90	1.56	1.44	3.36
87	3	[4, 6]	B	88.00	228.67	367.15	513.85	2.60	1.61	1.40	3.37
88	4	[4, 6]	B	96.76	270.83	432.69	678.87	2.80	1.60	1.57	3.76
89	5	[4, 6]	B	99.99	299.12	491.37	799.47	2.99	1.64	1.63	4.01
90	6	[4, 6]	B	103.87	317.62	531.47	885.79	3.06	1.67	1.67	4.18
91	1	[3, 6, 6]	B	22.18	100.60	159.89	243.54	4.53	1.59	1.52	3.63
92	2	[3, 6, 6]	B	75.43	212.60	327.72	468.20	2.82	1.54	1.43	3.30
93	3	[3, 6, 6]	B	131.97	336.05	538.69	764.95	2.55	1.60	1.42	3.41
94	4	[3, 6, 6]	B	140.05	398.04	631.63	1010.93	2.84	1.59	1.60	3.81
95	5	[3, 6, 6]	B	144.73	452.22	714.67	1152.91	3.12	1.58	1.61	3.82
96	6	[3, 6, 6]	B	149.76	505.64	789.74	1244.92	3.38	1.56	1.58	3.69
97	1	[4, 5, 6]	B	22.18	96.50	158.54	250.07	4.35	1.64	1.58	3.89
98	2	[4, 5, 6]	B	75.43	209.34	329.35	482.25	2.78	1.57	1.46	3.46
99	3	[4, 5, 6]	B	131.99	328.34	528.65	753.45	2.49	1.61	1.43	3.44
100	4	[4, 5, 6]	B	140.37	388.61	620.21	998.20	2.77	1.60	1.61	3.85
101	5	[4, 5, 6]	B	145.06	442.46	691.49	1099.69	3.05	1.56	1.59	3.73
102	6	[4, 5, 6]	B	150.98	494.04	768.25	1214.74	3.27	1.56	1.58	3.69
103	1	[4, 5, 5, 6]	B	29.58	128.00	209.65	332.09	4.33	1.64	1.58	3.89
104	2	[4, 5, 5, 6]	B	100.57	273.96	430.27	634.95	2.72	1.57	1.48	3.48
105	3	[4, 5, 5, 6]	B	173.28	430.06	690.59	991.10	2.48	1.61	1.44	3.46
106	4	[4, 5, 5, 6]	B	183.89	508.78	810.15	1321.97	2.77	1.59	1.63	3.90
107	5	[4, 5, 5, 6]	B	190.04	582.78	904.45	1468.32	3.07	1.55	1.62	3.78
108	6	[4, 5, 5, 6]	B	198.88	663.90	1014.43	1611.24	3.34	1.53	1.59	3.64
109	1	[3, 4, 5, 6]	B	26.62	115.30	186.98	290.09	4.33	1.62	1.55	3.77
110	2	[3, 4, 5, 6]	B	90.51	248.74	388.66	561.89	2.75	1.56	1.45	3.39
111	3	[3, 4, 5, 6]	B	156.61	395.47	635.79	901.18	2.53	1.61	1.42	3.42
112	4	[3, 4, 5, 6]	B	166.20	467.58	745.66	1193.06	2.81	1.59	1.60	3.83
113	5	[3, 4, 5, 6]	B	171.76	531.67	844.07	1384.76	3.10	1.59	1.64	3.91
114	6	[3, 4, 5, 6]	B	181.95	617.79	966.87	1550.28	3.40	1.57	1.60	3.76
115	1	[4, 5, 6, 3, 4.5, 5, 6]	B	49.54	216.10	356.42	557.25	4.36	1.65	1.56	3.87
116	2	[4, 5, 6, 3, 4.5, 5, 6]	B	168.45	472.52	747.56	1091.46	2.81	1.58	1.46	3.46
117	3	[4, 5, 6, 3, 4.5, 5, 6]	B	294.79	747.69	1207.30	1711.78	2.54	1.61	1.42	3.43
118	4	[4, 5, 6, 3, 4.5, 5, 6]	B	314.49	888.20	1411.75	2259.26	2.82	1.59	1.60	3.82
119	5	[4, 5, 6, 3, 4.5, 5, 6]	B	325.01	1022.64	1589.55	2539.12	3.15	1.55	1.60	3.72
120	6	[4, 5, 6, 3, 4.5, 5, 6]	B	340.66	1195.69	1823.67	2872.42	3.51	1.53	1.58	3.60

Continued on next page

Table A.2. DC3 outcomes of the parametric analysis.

Conf.	N.Sto.	Shearwalls	Soil	V_d	V_1	V_{SD}	V_E	q_S	q_R	q_D	$q_{1.5}$
121	1	[4]	C	6.66	26.10	43.24	65.97	3.92	1.66	1.53	3.79
122	2	[4]	C	22.63	59.63	94.60	134.01	2.64	1.59	1.42	3.37
123	3	[4]	C	39.60	100.27	165.46	229.45	2.53	1.65	1.39	3.43
124	4	[4]	C	55.75	118.52	189.94	266.40	2.13	1.60	1.40	3.37
125	5	[4]	C	57.62	136.09	210.91	315.74	2.36	1.55	1.50	3.48
126	6	[4]	C	62.71	166.85	257.88	394.28	2.66	1.55	1.53	3.54
127	1	[6]	C	9.98	40.60	63.65	97.39	4.07	1.57	1.53	3.60
128	2	[6]	C	33.94	88.19	134.41	192.71	2.60	1.52	1.43	3.28
129	3	[6]	C	59.40	139.97	217.14	304.22	2.36	1.55	1.40	3.26
130	4	[6]	C	80.29	165.25	255.31	371.10	2.06	1.55	1.45	3.37
131	5	[6]	C	82.97	196.17	291.70	450.62	2.36	1.49	1.54	3.45
132	6	[6]	C	85.62	225.88	331.48	511.89	2.64	1.47	1.54	3.40
133	1	[4, 4]	C	13.31	50.40	82.41	124.95	3.79	1.64	1.52	3.72
134	2	[4, 4]	C	45.26	117.71	188.38	267.90	2.60	1.60	1.42	3.41
135	3	[4, 4]	C	79.20	193.17	324.33	449.88	2.44	1.68	1.39	3.49
136	4	[4, 4]	C	111.50	223.62	362.63	501.63	2.01	1.62	1.38	3.36
137	5	[4, 4]	C	115.23	240.12	400.73	643.98	2.08	1.67	1.61	4.02
138	6	[4, 4]	C	125.42	253.38	427.39	683.96	2.02	1.69	1.60	4.05
139	1	[6, 6]	C	19.97	80.80	127.19	195.27	4.05	1.57	1.54	3.62
140	2	[6, 6]	C	67.88	174.52	267.83	386.05	2.57	1.53	1.44	3.32
141	3	[6, 6]	C	118.80	270.29	426.32	601.76	2.28	1.58	1.41	3.34
142	4	[6, 6]	C	160.58	320.38	502.76	729.99	2.00	1.57	1.45	3.42
143	5	[6, 6]	C	165.95	367.94	564.73	875.68	2.22	1.53	1.55	3.57
144	6	[6, 6]	C	171.23	394.69	619.94	997.97	2.30	1.57	1.61	3.79
145	1	[4, 6]	C	16.64	63.50	102.14	155.02	3.82	1.61	1.52	3.66
146	2	[4, 6]	C	56.57	145.69	227.72	326.82	2.58	1.56	1.44	3.36
147	3	[4, 6]	C	99.00	228.67	367.15	513.85	2.31	1.61	1.40	3.37
148	4	[4, 6]	C	136.07	270.83	432.69	619.17	1.99	1.60	1.43	3.43
149	5	[4, 6]	C	140.62	299.12	491.37	799.47	2.13	1.64	1.63	4.01
150	6	[4, 6]	C	146.06	317.62	531.47	885.79	2.17	1.67	1.67	4.18
151	1	[3, 6, 6]	C	24.96	97.90	155.48	237.82	3.92	1.59	1.53	3.64
152	2	[3, 6, 6]	C	84.85	212.60	327.72	468.20	2.51	1.54	1.43	3.30
153	3	[3, 6, 6]	C	148.49	336.05	538.69	764.95	2.26	1.60	1.42	3.41
154	4	[3, 6, 6]	C	196.94	398.04	631.63	916.97	2.02	1.59	1.45	3.46
155	5	[3, 6, 6]	C	203.53	452.22	714.67	1152.91	2.22	1.58	1.61	3.82
156	6	[3, 6, 6]	C	210.60	505.64	789.74	1244.92	2.40	1.56	1.58	3.69
157	1	[4, 5, 6]	C	24.96	93.60	152.33	237.17	3.75	1.63	1.56	3.80
158	2	[4, 5, 6]	C	84.85	209.34	329.35	482.25	2.47	1.57	1.46	3.46
159	3	[4, 5, 6]	C	148.49	328.34	528.65	753.45	2.21	1.61	1.43	3.44
160	4	[4, 5, 6]	C	197.39	388.61	620.21	903.31	1.97	1.60	1.46	3.49
161	5	[4, 5, 6]	C	203.99	442.46	691.49	1099.69	2.17	1.56	1.59	3.73
162	6	[4, 5, 6]	C	212.31	494.04	768.25	1214.74	2.33	1.56	1.58	3.69
163	1	[4, 5, 5, 6]	C	33.28	124.70	201.83	317.02	3.75	1.62	1.57	3.81
164	2	[4, 5, 5, 6]	C	113.14	273.96	430.27	634.95	2.42	1.57	1.48	3.48
165	3	[4, 5, 5, 6]	C	197.99	430.06	690.59	991.10	2.17	1.61	1.44	3.46
166	4	[4, 5, 5, 6]	C	258.60	508.78	810.15	1191.37	1.97	1.59	1.47	3.51
167	5	[4, 5, 5, 6]	C	267.24	582.78	904.45	1468.32	2.18	1.55	1.62	3.78
168	6	[4, 5, 5, 6]	C	279.68	663.90	1014.43	1611.24	2.37	1.53	1.59	3.64
169	1	[3, 4, 5, 6]	C	29.95	112.70	179.30	274.86	3.76	1.59	1.53	3.66
170	2	[3, 4, 5, 6]	C	101.82	248.74	388.66	561.89	2.44	1.56	1.45	3.39
171	3	[3, 4, 5, 6]	C	178.19	395.47	635.79	901.18	2.22	1.61	1.42	3.42
172	4	[3, 4, 5, 6]	C	233.72	467.58	745.66	1082.20	2.00	1.59	1.45	3.47
173	5	[3, 4, 5, 6]	C	241.53	531.67	844.07	1384.76	2.20	1.59	1.64	3.91
174	6	[3, 4, 5, 6]	C	255.87	617.79	966.87	1550.28	2.41	1.57	1.60	3.76
176	2	[4, 5, 6, 3, 4.5, 5, 6]	C	189.51	472.52	747.56	1091.46	2.49	1.58	1.46	3.46
177	3	[4, 5, 6, 3, 4.5, 5, 6]	C	331.64	747.69	1207.30	1711.78	2.25	1.61	1.42	3.43
178	4	[4, 5, 6, 3, 4.5, 5, 6]	C	442.25	888.20	1411.75	2048.86	2.01	1.59	1.45	3.46
179	5	[4, 5, 6, 3, 4.5, 5, 6]	C	457.04	1022.64	1589.55	2539.12	2.24	1.55	1.60	3.72
180	6	[4, 5, 6, 3, 4.5, 5, 6]	C	479.05	1195.69	1823.67	2872.42	2.50	1.53	1.58	3.60
181	1	[4]	A	4.93	27	45.65	70.01	5.48	1.69	1.53	3.89

Continued on next page

Table A.2. DC3 outcomes of the parametric analysis.

Conf.	N.Sto.	Shearwalls	Soil	V_d	V_1	V_{SD}	V_E	q_S	q_R	q_D	$q_{1.5}$
182	2	[4]	A	16.76	59.6	94.64	136.09	3.56	1.59	1.44	3.43
183	3	[4]	A	23.35	100.1	165.44	250.12	4.29	1.65	1.51	3.75
184	4	[4]	A	24.78	123	191.01	278.6	4.96	1.55	1.46	3.4
185	5	[4]	A	25.61	148.2	224.9	329.52	5.79	1.52	1.47	3.34
186	6	[4]	A	27.87	174.4	259.42	369.82	6.26	1.49	1.43	3.18
187	1	[6]	A	7.39	42.2	68.06	105.66	5.71	1.61	1.55	3.76
188	2	[6]	A	25.14	88	134.09	194.5	3.5	1.52	1.45	3.32
189	3	[6]	A	33.62	140	216.98	330.68	4.16	1.55	1.52	3.54
190	4	[6]	A	35.68	178	265.1	396.43	4.99	1.49	1.5	3.34
191	5	[6]	A	36.88	214.5	312.17	464.22	5.82	1.46	1.49	3.25
192	6	[6]	A	38.05	252.8	359.83	521.13	6.64	1.42	1.45	3.09
193	1	[4, 4]	A	9.86	53.7	91.21	140.42	5.45	1.7	1.54	3.92
194	2	[4, 4]	A	33.52	118	188.58	271.79	3.52	1.6	1.44	3.45
195	3	[4, 4]	A	46.7	195.3	326.76	493.73	4.18	1.67	1.51	3.79
196	4	[4, 4]	A	49.56	232	369.65	540.1	4.68	1.59	1.46	3.49
197	5	[4, 4]	A	51.21	258.7	417.79	646.92	5.05	1.61	1.55	3.75
198	6	[4, 4]	A	55.74	276.8	461.09	737.94	4.97	1.67	1.6	4
199	1	[6, 6]	A	14.79	84	136	211.91	5.68	1.62	1.56	3.78
200	2	[6, 6]	A	50.28	175.2	268.17	390.57	3.48	1.53	1.46	3.34
201	3	[6, 6]	A	67.25	273	428.82	660.3	4.06	1.57	1.54	3.63
202	4	[6, 6]	A	71.37	338	514.7	777.96	4.74	1.52	1.51	3.45
203	5	[6, 6]	A	73.75	388.7	590.24	903.97	5.27	1.52	1.53	3.49
204	6	[6, 6]	A	76.1	422.4	654.48	1023.87	5.55	1.55	1.56	3.64
205	1	[4, 6]	A	12.32	68.3	113.35	176.55	5.54	1.66	1.56	3.88
206	2	[4, 6]	A	41.9	146	228.12	331.79	3.48	1.56	1.45	3.41
207	3	[4, 6]	A	56.99	231.7	369.78	561.75	4.07	1.6	1.52	3.64
208	4	[4, 6]	A	60.47	284	442.73	663.79	4.7	1.56	1.5	3.51
209	5	[4, 6]	A	62.5	318.5	504.87	778.53	5.1	1.59	1.54	3.67
210	6	[4, 6]	A	64.92	344	552.21	866.59	5.3	1.61	1.57	3.78
211	1	[3, 6, 6]	A	18.49	103	165.74	253.02	5.57	1.61	1.53	3.68
212	2	[3, 6, 6]	A	62.69	213.2	327.23	471.06	3.4	1.53	1.44	3.31
213	3	[3, 6, 6]	A	82.48	339.5	535.36	814.65	4.12	1.58	1.52	3.6
214	4	[3, 6, 6]	A	87.53	413	649.87	1024.56	4.72	1.57	1.58	3.72
215	5	[3, 6, 6]	A	90.46	482.3	744.54	1160.88	5.33	1.54	1.56	3.61
216	6	[3, 6, 6]	A	93.6	536	834.47	1301.86	5.73	1.56	1.56	3.64
217	1	[4, 5, 6]	A	18.49	100.7	167.72	264.5	5.45	1.67	1.58	3.94
218	2	[4, 5, 6]	A	62.38	210	329.71	488.47	3.37	1.57	1.48	3.49
219	3	[4, 5, 6]	A	82.67	331.8	532.16	832.32	4.01	1.6	1.56	3.76
220	4	[4, 5, 6]	A	87.73	405	630.86	974.89	4.62	1.56	1.55	3.61
221	5	[4, 5, 6]	A	90.66	473.2	719.96	1103.05	5.22	1.52	1.53	3.5
222	6	[4, 5, 6]	A	94.36	528	801.99	1220.9	5.6	1.52	1.52	3.47
223	1	[4, 5, 5, 6]	A	24.65	133.1	220.74	349.74	5.4	1.66	1.58	3.94
224	2	[4, 5, 5, 6]	A	82.03	274.8	429.87	640.17	3.35	1.56	1.49	3.49
225	3	[4, 5, 5, 6]	A	108.3	434	694.54	1097.44	4.01	1.6	1.58	3.79
226	4	[4, 5, 5, 6]	A	114.93	531	823.25	1285.19	4.62	1.55	1.56	3.63
227	5	[4, 5, 5, 6]	A	118.77	621.4	931.63	1427.28	5.23	1.5	1.53	3.45
228	6	[4, 5, 5, 6]	A	124.3	707.2	1048.99	1591.22	5.69	1.48	1.52	3.38
229	1	[3, 4, 5, 6]	A	22.18	120.2	196.81	304.23	5.42	1.64	1.55	3.8
230	2	[3, 4, 5, 6]	A	73.43	249.6	387.87	564.45	3.4	1.55	1.46	3.39
231	3	[3, 4, 5, 6]	A	97.88	399	632.7	963.68	4.08	1.59	1.52	3.62
232	4	[3, 4, 5, 6]	A	103.87	485	767.92	1217.55	4.67	1.58	1.59	3.77
233	5	[3, 4, 5, 6]	A	107.35	568.1	874.67	1367.48	5.29	1.54	1.56	3.61
234	6	[3, 4, 5, 6]	A	113.72	643.2	985.58	1521.61	5.66	1.53	1.54	3.55
235	1	[4, 5, 6, 3, 4.5, 5, 6]	A	41.29	224.8	376.69	589.91	5.44	1.68	1.57	3.94
236	2	[4, 5, 6, 3, 4.5, 5, 6]	A	139.14	473.6	746.94	1100.75	3.4	1.58	1.47	3.49
237	3	[4, 5, 6, 3, 4.5, 5, 6]	A	185.22	752.5	1212.44	1888.04	4.06	1.61	1.56	3.76
238	4	[4, 5, 6, 3, 4.5, 5, 6]	A	196.56	921	1429.26	2198.7	4.69	1.55	1.54	3.58
239	5	[4, 5, 6, 3, 4.5, 5, 6]	A	203.13	1098.5	1654.9	2520.51	5.41	1.51	1.52	3.44
240	6	[4, 5, 6, 3, 4.5, 5, 6]	A	212.91	1259.2	1871.39	2821.66	5.91	1.49	1.51	3.36
241	1	[4]	B	5.92	27.8	47.94	73.72	4.7	1.72	1.54	3.98

Continued on next page

Table A.2. DC3 outcomes of the parametric analysis.

Conf.	N.Sto.	Shearwalls	Soil	V_d	V_1	V_{SD}	V_E	q_S	q_R	q_D	$q_{1.5}$
242	2	[4]	B	20.11	59.6	94.64	136.09	2.96	1.59	1.44	3.43
243	3	[4]	B	35.2	100.1	165.44	230.23	2.84	1.65	1.39	3.45
244	4	[4]	B	39.65	123	191.01	260.1	3.1	1.55	1.36	3.17
245	5	[4]	B	40.97	148.2	224.9	329.52	3.62	1.52	1.47	3.34
246	6	[4]	B	44.59	174.4	259.42	369.82	3.91	1.49	1.43	3.18
247	1	[6]	B	8.87	41.3	65.64	101.34	4.65	1.59	1.54	3.68
248	2	[6]	B	30.17	88	134.09	194.5	2.92	1.52	1.45	3.32
249	3	[6]	B	52.8	140	216.98	304.85	2.65	1.55	1.4	3.27
250	4	[6]	B	57.09	178	265.1	396.43	3.12	1.49	1.5	3.34
251	5	[6]	B	59	214.5	312.17	464.22	3.64	1.46	1.49	3.25
252	6	[6]	B	60.88	252.8	359.83	521.13	4.15	1.42	1.45	3.09
253	1	[4, 4]	B	11.83	51.8	86.37	132.41	4.38	1.67	1.53	3.83
254	2	[4, 4]	B	40.23	118	188.58	271.79	2.93	1.6	1.44	3.45
255	3	[4, 4]	B	70.4	195.3	326.76	454.08	2.77	1.67	1.39	3.49
256	4	[4, 4]	B	79.29	232	369.65	503.16	2.93	1.59	1.36	3.25
257	5	[4, 4]	B	81.94	258.7	417.79	646.92	3.16	1.61	1.55	3.75
258	6	[4, 4]	B	89.19	276.8	461.09	737.94	3.1	1.67	1.6	4
259	1	[6, 6]	B	17.75	82.1	131.14	203.4	4.63	1.6	1.55	3.72
260	2	[6, 6]	B	60.34	175.2	268.17	390.57	2.9	1.53	1.46	3.34
261	3	[6, 6]	B	105.6	273	428.82	606.21	2.59	1.57	1.41	3.33
262	4	[6, 6]	B	114.19	338	514.7	719.66	2.96	1.52	1.4	3.19
263	5	[6, 6]	B	118.01	388.7	590.24	903.97	3.29	1.52	1.53	3.49
264	6	[6, 6]	B	121.77	422.4	654.48	1023.87	3.47	1.55	1.56	3.64
265	1	[4, 6]	B	14.79	65.1	106.06	163.16	4.4	1.63	1.54	3.76
266	2	[4, 6]	B	50.28	146	228.12	331.79	2.9	1.56	1.45	3.41
267	3	[4, 6]	B	88	231.7	369.78	517.38	2.63	1.6	1.4	3.35
268	4	[4, 6]	B	96.76	284	442.73	614.8	2.94	1.56	1.39	3.25
269	5	[4, 6]	B	99.99	318.5	504.87	778.53	3.19	1.59	1.54	3.67
270	6	[4, 6]	B	103.87	344	552.21	866.59	3.31	1.61	1.57	3.78
271	1	[3, 6, 6]	B	22.18	100.6	159.89	243.54	4.53	1.59	1.52	3.63
272	2	[3, 6, 6]	B	75.43	213.2	327.23	471.06	2.83	1.53	1.44	3.31
273	3	[3, 6, 6]	B	131.97	339.5	535.36	750.57	2.57	1.58	1.4	3.32
274	4	[3, 6, 6]	B	140.05	413	649.87	1024.56	2.95	1.57	1.58	3.72
275	5	[3, 6, 6]	B	144.73	482.3	744.54	1160.88	3.33	1.54	1.56	3.61
276	6	[3, 6, 6]	B	149.76	536	834.47	1301.86	3.58	1.56	1.56	3.64
277	1	[4, 5, 6]	B	22.18	96.5	158.54	250.07	4.35	1.64	1.58	3.89
278	2	[4, 5, 6]	B	75.43	210	329.71	488.47	2.78	1.57	1.48	3.49
279	3	[4, 5, 6]	B	131.99	331.8	532.16	759.73	2.51	1.6	1.43	3.43
280	4	[4, 5, 6]	B	140.37	405	630.86	894.35	2.89	1.56	1.42	3.31
281	5	[4, 5, 6]	B	145.06	473.2	719.96	1103.05	3.26	1.52	1.53	3.5
282	6	[4, 5, 6]	B	150.98	528	801.99	1220.9	3.5	1.52	1.52	3.47
283	1	[4, 5, 5, 6]	B	29.58	128	209.65	332.09	4.33	1.64	1.58	3.89
284	2	[4, 5, 5, 6]	B	100.57	274.8	429.87	640.17	2.73	1.56	1.49	3.49
285	3	[4, 5, 5, 6]	B	173.28	434	694.54	998.62	2.5	1.6	1.44	3.45
286	4	[4, 5, 5, 6]	B	183.89	531	823.25	1285.19	2.89	1.55	1.56	3.63
287	5	[4, 5, 5, 6]	B	190.04	621.4	931.63	1427.28	3.27	1.5	1.53	3.45
288	6	[4, 5, 5, 6]	B	198.88	707.2	1048.99	1591.22	3.56	1.48	1.52	3.38
289	1	[3, 4, 5, 6]	B	26.62	115.3	186.98	290.09	4.33	1.62	1.55	3.77
290	2	[3, 4, 5, 6]	B	90.51	249.6	387.87	564.45	2.76	1.55	1.46	3.39
291	3	[3, 4, 5, 6]	B	156.61	399	632.7	887.52	2.55	1.59	1.4	3.34
292	4	[3, 4, 5, 6]	B	166.2	485	767.92	1217.55	2.92	1.58	1.59	3.77
293	5	[3, 4, 5, 6]	B	171.76	568.1	874.67	1367.48	3.31	1.54	1.56	3.61
294	6	[3, 4, 5, 6]	B	181.95	643.2	985.58	1521.61	3.53	1.53	1.54	3.55
295	1	[4, 5, 6, 3, 4.5, 5, 6]	B	49.54	216.1	356.42	557.25	4.36	1.65	1.56	3.87
296	2	[4, 5, 6, 3, 4.5, 5, 6]	B	168.45	473.6	746.94	1100.75	2.81	1.58	1.47	3.49
297	3	[4, 5, 6, 3, 4.5, 5, 6]	B	294.79	752.5	1212.44	1725.02	2.55	1.61	1.42	3.44
298	4	[4, 5, 6, 3, 4.5, 5, 6]	B	314.49	921	1429.26	2020.2	2.93	1.55	1.41	3.29
299	5	[4, 5, 6, 3, 4.5, 5, 6]	B	325.01	1098.5	1654.9	2520.51	3.38	1.51	1.52	3.44
300	6	[4, 5, 6, 3, 4.5, 5, 6]	B	340.66	1259.2	1871.38	2821.09	3.7	1.49	1.51	3.36
301	1	[4]	C	6.66	26.1	43.24	65.97	3.92	1.66	1.53	3.79

Continued on next page

Table A.2. DC3 outcomes of the parametric analysis.

Conf.	N.Sto.	Shearwalls	Soil	V_d	V_1	V_{SD}	V_E	q_S	q_R	q_D	$q_{1.5}$
302	2	[4]	C	22.63	59.6	94.64	136.09	2.63	1.59	1.44	3.43
303	3	[4]	C	39.6	100.1	165.44	230.23	2.53	1.65	1.39	3.45
304	4	[4]	C	55.75	123	191.01	260.1	2.21	1.55	1.36	3.17
305	5	[4]	C	57.62	148.2	224.9	307.62	2.57	1.52	1.37	3.11
306	6	[4]	C	62.71	174.4	259.42	369.82	2.78	1.49	1.43	3.18
307	1	[6]	C	9.98	40.6	63.65	97.39	4.07	1.57	1.53	3.6
308	2	[6]	C	33.94	88	134.09	194.5	2.59	1.52	1.45	3.32
309	3	[6]	C	59.4	140	216.98	304.85	2.36	1.55	1.4	3.27
310	4	[6]	C	80.29	178	265.1	368.49	2.22	1.49	1.39	3.11
311	5	[6]	C	82.97	214.5	312.17	432.8	2.59	1.46	1.39	3.03
312	6	[6]	C	85.62	252.8	359.83	521.13	2.95	1.42	1.45	3.09
313	1	[4, 4]	C	13.31	50.4	82.41	124.95	3.79	1.64	1.52	3.72
314	2	[4, 4]	C	45.26	118	188.58	271.79	2.61	1.6	1.44	3.45
315	3	[4, 4]	C	79.2	195.3	326.76	454.08	2.47	1.67	1.39	3.49
316	4	[4, 4]	C	111.5	232	369.65	503.16	2.08	1.59	1.36	3.25
317	5	[4, 4]	C	115.23	258.7	417.79	590.68	2.25	1.61	1.41	3.42
318	6	[4, 4]	C	125.42	276.8	461.09	737.94	2.21	1.67	1.6	4
319	1	[6, 6]	C	19.97	80.8	127.19	195.27	4.05	1.57	1.54	3.62
320	2	[6, 6]	C	67.88	175.2	268.17	390.57	2.58	1.53	1.46	3.34
321	3	[6, 6]	C	118.8	273	428.82	606.21	2.3	1.57	1.41	3.33
322	4	[6, 6]	C	160.58	338	514.7	719.66	2.1	1.52	1.4	3.19
323	5	[6, 6]	C	165.95	388.7	590.24	832.52	2.34	1.52	1.41	3.21
324	6	[6, 6]	C	171.23	422.4	654.48	1023.87	2.47	1.55	1.56	3.64
325	1	[4, 6]	C	16.64	63.5	102.14	155.02	3.82	1.61	1.52	3.66
326	2	[4, 6]	C	56.57	146	228.12	331.79	2.58	1.56	1.45	3.41
327	3	[4, 6]	C	99	231.7	369.78	517.38	2.34	1.6	1.4	3.35
328	4	[4, 6]	C	136.07	284	442.73	614.8	2.09	1.56	1.39	3.25
329	5	[4, 6]	C	140.62	318.5	504.87	713.29	2.27	1.59	1.41	3.36
330	6	[4, 6]	C	146.06	344	552.21	866.59	2.36	1.61	1.57	3.78
331	1	[3, 6, 6]	C	24.96	97.9	155.48	237.82	3.92	1.59	1.53	3.64
332	2	[3, 6, 6]	C	84.85	213.2	327.23	471.06	2.51	1.53	1.44	3.31
333	3	[3, 6, 6]	C	148.49	339.5	535.36	750.57	2.29	1.58	1.4	3.32
334	4	[3, 6, 6]	C	196.94	413	649.87	933.38	2.1	1.57	1.44	3.39
335	5	[3, 6, 6]	C	203.53	482.3	744.54	1062.1	2.37	1.54	1.43	3.3
336	6	[3, 6, 6]	C	210.6	536	834.47	1301.86	2.55	1.56	1.56	3.64
337	1	[4, 5, 6]	C	24.96	93.6	152.33	237.17	3.75	1.63	1.56	3.8
338	2	[4, 5, 6]	C	84.85	210	329.71	488.47	2.47	1.57	1.48	3.49
339	3	[4, 5, 6]	C	148.49	331.8	532.16	759.73	2.23	1.6	1.43	3.43
340	4	[4, 5, 6]	C	197.39	405	630.86	894.35	2.05	1.56	1.42	3.31
341	5	[4, 5, 6]	C	203.99	473.2	719.96	1015.58	2.32	1.52	1.41	3.22
342	6	[4, 5, 6]	C	212.31	528	801.99	1220.9	2.49	1.52	1.52	3.47
343	1	[4, 5, 5, 6]	C	33.28	124.7	201.83	317.02	3.75	1.62	1.57	3.81
344	2	[4, 5, 5, 6]	C	113.14	274.8	429.87	640.17	2.43	1.56	1.49	3.49
345	3	[4, 5, 5, 6]	C	197.99	434	694.54	998.62	2.19	1.6	1.44	3.45
346	4	[4, 5, 5, 6]	C	258.6	531	823.25	1175.83	2.05	1.55	1.43	3.32
347	5	[4, 5, 5, 6]	C	267.24	621.4	931.63	1315.59	2.33	1.5	1.41	3.18
348	6	[4, 5, 5, 6]	C	279.68	707.2	1048.99	1591.22	2.53	1.48	1.52	3.38
349	1	[3, 4, 5, 6]	C	29.95	112.7	179.3	274.86	3.76	1.59	1.53	3.66
350	2	[3, 4, 5, 6]	C	101.82	249.6	387.87	564.45	2.45	1.55	1.46	3.39
351	3	[3, 4, 5, 6]	C	178.19	399	632.7	887.52	2.24	1.59	1.4	3.34
352	4	[3, 4, 5, 6]	C	233.72	485	767.92	1106.98	2.08	1.58	1.44	3.42
353	5	[3, 4, 5, 6]	C	241.53	568.1	874.67	1250.48	2.35	1.54	1.43	3.3
354	6	[3, 4, 5, 6]	C	255.87	643.2	985.58	1521.61	2.51	1.53	1.54	3.55
356	2	[4, 5, 6, 3, 4.5, 5, 6]	C	189.51	473.6	746.94	1100.75	2.5	1.58	1.47	3.49
357	3	[4, 5, 6, 3, 4.5, 5, 6]	C	331.64	752.50	1212.44	1725.02	2.27	1.61	1.42	3.44
358	4	[4, 5, 6, 3, 4.5, 5, 6]	C	442.25	921	1429.26	2020.2	2.08	1.55	1.41	3.29
359	5	[4, 5, 6, 3, 4.5, 5, 6]	C	457.04	1098.5	1654.9	2326.32	2.4	1.51	1.41	3.18
360	6	[4, 5, 6, 3, 4.5, 5, 6]	C	479.05	1259.2	1871.38	2821.09	2.63	1.49	1.51	3.36

Appendix B

Appendix B reports the accelerograms implemented in the dynamic analyses.

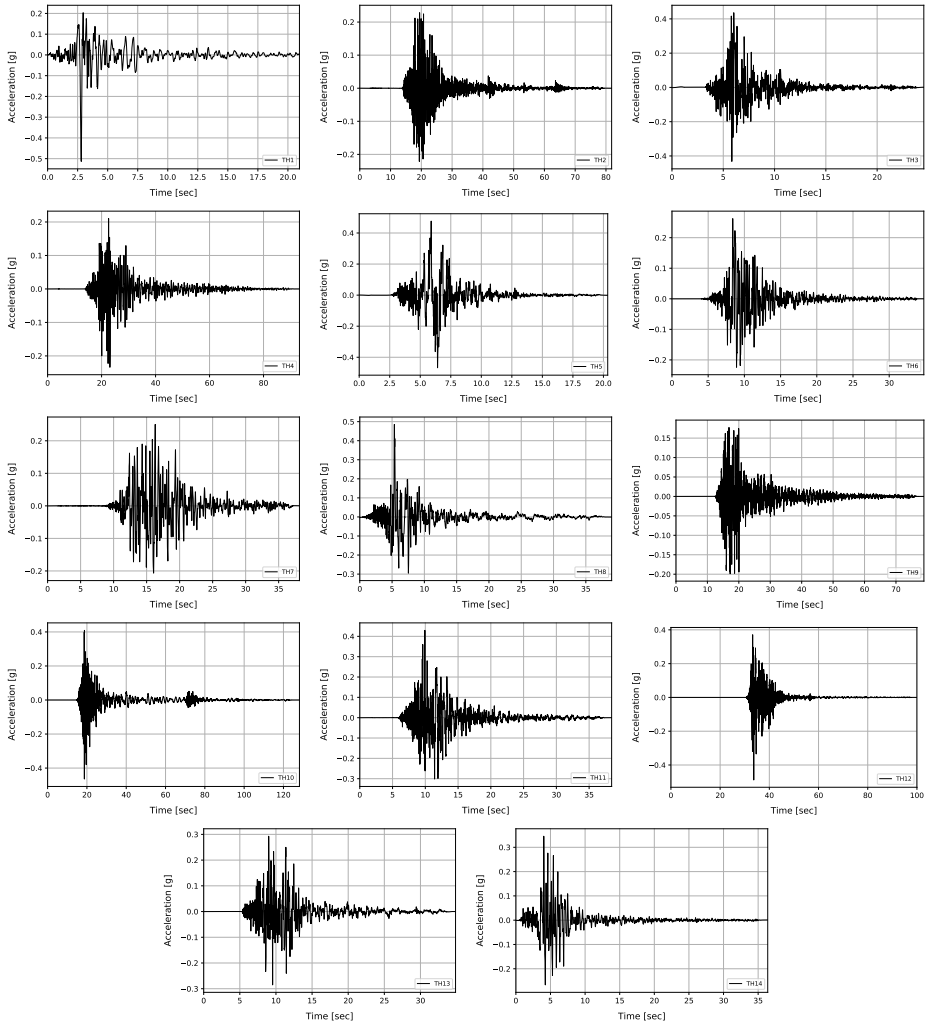

Figure B.1. Ground motions for IDA analyses.